Bioanalytical Capillary Electrophoresis

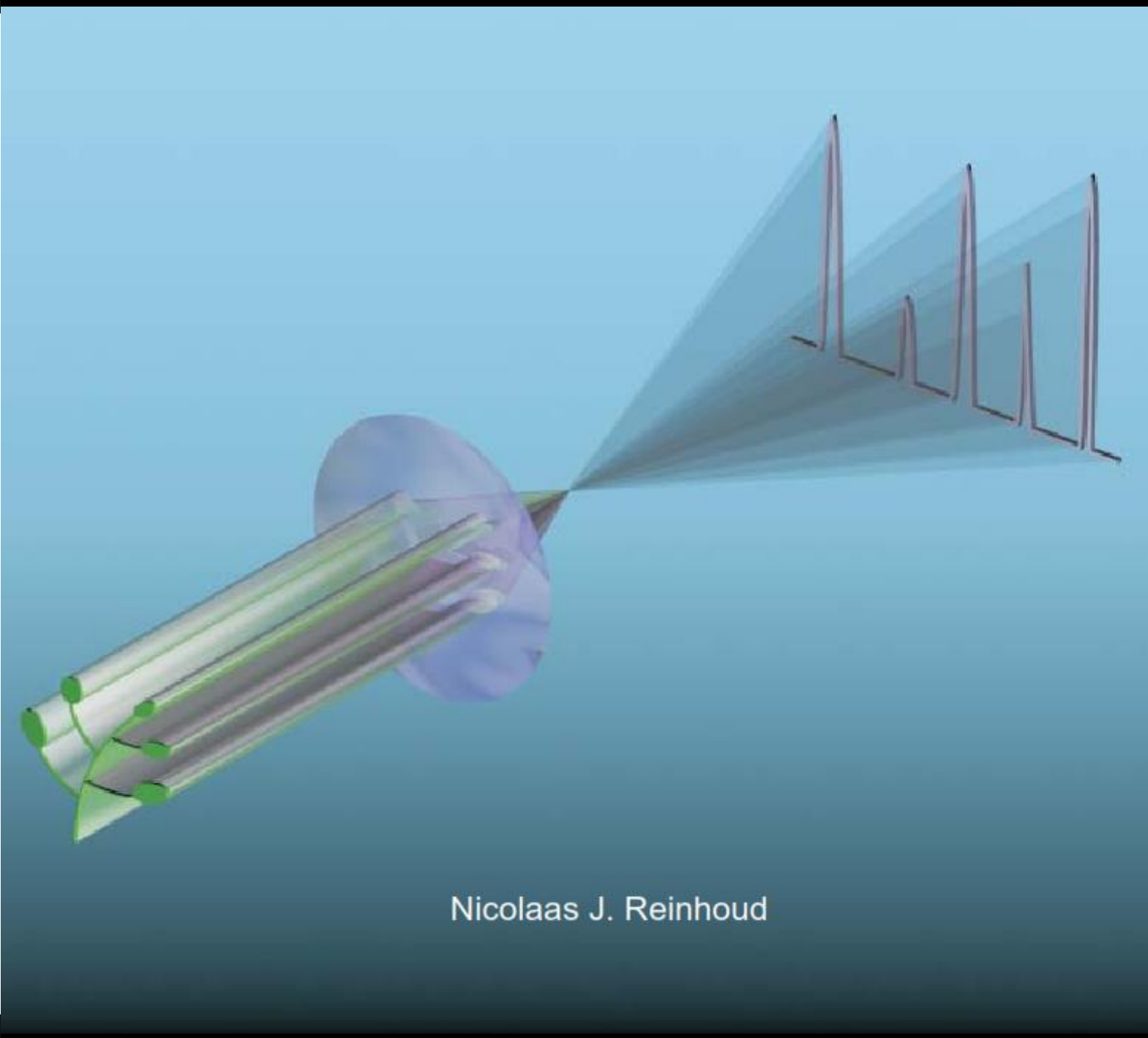

Nicolaas J. Reinhoud

Bioanalytical Capillary Electrophoresis

PROEFSCHRIFT

ter verkrijging van de graad van Doctor
aan de Rijksuniversiteit te Leiden,
op gezag van de Rector Magnificus Dr. L. Leertouwer,
hoogleraar in de faculteit der Godgeleerdheid,
volgens het besluit van het College van Dekanen
te verdedigen op donderdag 7 september 1995
te klokke 14.15 uur

door

Nicolaas Jan Reinhoud

geboren te Woerden in 1963

Promotiecommissie

Promotor:	Prof. dr. J. van der Greef
Co-promotor:	Dr. U.R. Tjaden
Referent:	Prof. dr. H. Poppe, Universiteit van Amsterdam
Overige leden:	Prof. dr. D.D. Breimer
	Prof. dr. H.E. Junginger
	Prof. dr. R. Verpoorte

Printed by Grafisch bedrijf Ponsen en Looijen B.V., Wageningen.
Printing of this thesis was supported by a grant from ANTEC Leyden B.V., The Netherlands.
Cover design: Ubbo R. Tjaden.

Aan Greet en Anne

Contents

Part 1

Capillary Electrophoresis

1.1

Introduction

Abstract

The basic principles of electrophoresis and parameters affecting electrophoretic separations are described. The equipment that is needed for CE separations is described and the several separation modes with different application areas are discussed. The potential of the technique is discussed by considering some bioanalytical applications from literature. Attention is paid to sample handling, buffer systems, capillary dimensions, detection and assay validation.

Introduction

Electrophoresis is defined as the migration of charged species in an electric field. This phenomenon has been studied for more then one century. The definition of cathode and anode was already introduced by Michael Faraday (1791-1867). Conductivity measurements led to a better understanding of the behaviour of weak and strong electrolytes in a solution. Important contributions were made by well known scientists like Friedrich Wilhelm Georg Kohlrausch (1840-1910), Svante August Arrhenius (1859-1927), Friedrich Wilhelm Ostwald (1853-1932), Lars Onsager (1903-1976) and many others. In the beginning of the twentiest century electrophoresis found its way in analytical applications. Separation and characterisation of different biomacromolecules based on differences in electrophoretic mobilities was possible. In biochemical research techniques like gel electrophoresis and isoelectric focusing are still important analytical tools.

Experiments of free zone electrophoresis in capillaries were reported by Hjerten in 1967 applying a rotating quartz tube of 1-3 mm inner diameter (ID) and Virtanen in 1974 who used 0.2-0.5 mm ID capillaries [1, 2]. Everaerts et al. developed in the 70's a capillary isotachophoresis apparatus suitable for routine analysis [3]. The first demonstration of the amazing separation power of capillary zone electrophoresis was done by Jörgenson and Lukacs in 1981 [4, 5]. Highly efficient separations in narrow bore capillaries (< 100μm ID) have been obtained using a high electric field strength [6]. A few years later Terabe et al. introduced micellar electrokinetic capillary chromatography extending the capillary electrophoretic separations from

ionic species to neutrals [7, 8]. These experiments, together with the development of new sensitive detection systems, were the beginning of a new direction in micro-scale separation methods, the capillary electrophoretic separations [9-18] (Fig. 1).

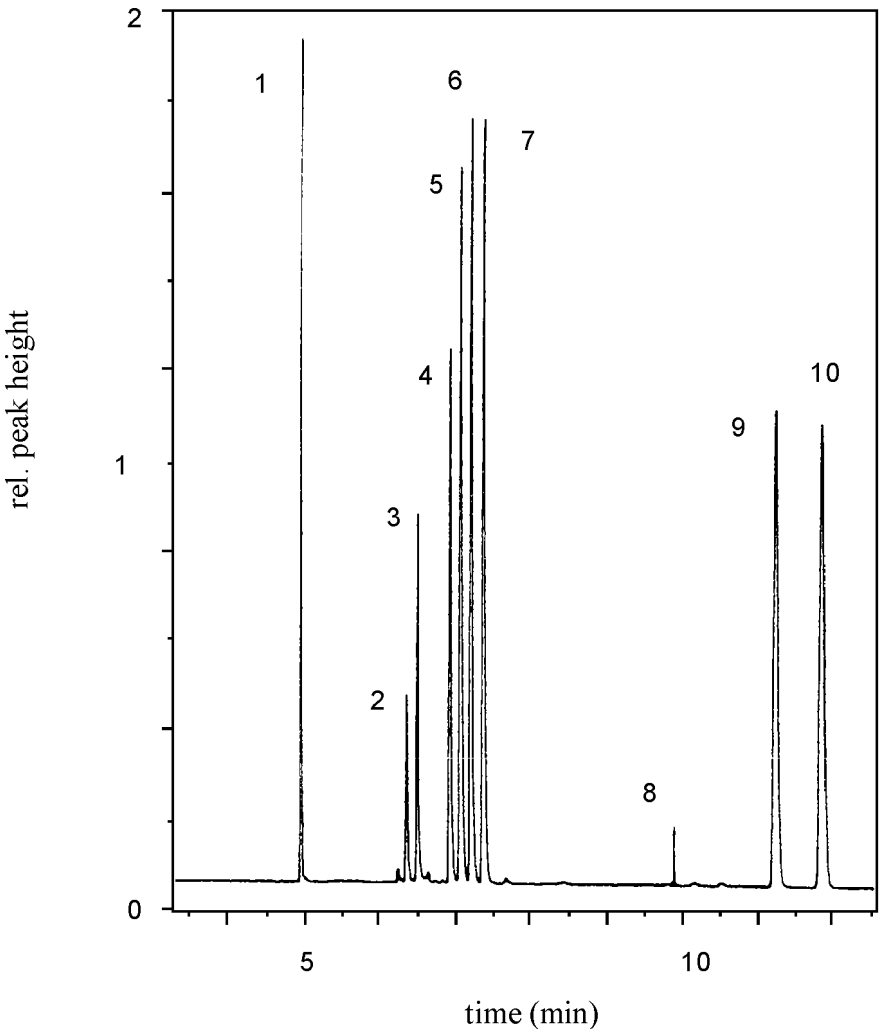

Fig. 1 Capillary zone electrophoresis attracted a lot of attention by highly efficient separations of standard mixtures. The potential of the technique is demonstrated by analysis of a mixture of amino acids, Arg (1), Lys (2, 3), Trp (4), Phe (5), Thr (6), Ser (7), L-Dopa (8), Glu (9) and Asp (10). Plate numbers vary from 3.5 10^5 (1) to 2.0 10^5 (9, 10). Detection of the derivatised amino acids took place with laser-induced fluorescence detection (LIF).

Theory

Electrophoresis

Electrophoresis is the migration of charged particles in an electric field. When an electric field is applied to an electrolyte solution the ions will migrate with an electrophoretic velocity (v_i) given by

$$v_i = m_i E \qquad (1)$$

where E is the electric field strength and m_i the electrophoretic mobility of ion i. A charged particle in an electrolyte solution is accelerated in a constant electric field by an electric force $F_{el}=qE$ where q is the charge on the particle. As the velocity of the particle increases, the electric force is counterbalanced by the frictional force given by Stoke's law, $F_{fr}= -6\pi r\eta v$ where r is the particle radius and η the dynamic viscosity of the medium.

Two other effects should be taken into account, the electrophoretic effect and the relaxation effect. The electrophoretic effect is caused by the oppositely charged ions that are surrounding a particle. In an electric field these ions move in the opposite direction which means that the particle is moving against a stream of solvent which reduces the particle velocity. The relaxation effect is also a result of the ionic atmosphere around the particle. When a particle moves into the direction of the electrode, it moves out of centre of its ionic atmosphere. Therefore, the symmetrically distributed ionic atmosphere around the ion is disturbed, resulting in an electrostatic drag on the moving particle. This also reduces the electrophoretic velocity of the particle.

Electrophoretic separation of different analytes is based upon differences in electrophoretic mobilities. The electrophoretic mobility is given by

$$m_i = C_i \zeta_i \varepsilon/\eta \qquad (2)$$

where ζ_i is the zeta potential of ion i, ε is the permittivity of the electrolyte and C_i is a constant depending on the size of the ion i and on the thickness of the electric layer surrounding it. The zeta potential of a particle reduces when the ionic strength of the electrolyte is increased resulting in a decrease of the electrophoretic mobility. To enable exchange of data it is convenient

to describe electrophoretic mobilities independently from the ionic strength. The electrophoretic mobilities of ions are often tabulated as the limiting ionic mobilities, i.e. the mobilities of the ionised particles at infinite dilution. The electrophoretic mobility at finite dilution can be calculated using the Debye-Hückel-Onsager equation, which is for electrolytes at 298K [19]

$$m_i = m^0_i - [\ (0.23\ |m^0_i z_i\ z_R\ | + 31.3\ 10^{-9}\ |z_i\ |)\ \sqrt{\mu}/(1+\sqrt{\mu}\ )\ ] \quad (3)$$

where μ is the ionic strength of the electrolyte solution (mol l^{-1}), m^0_i the limiting electrophoretic mobility and z_i the ionic charge of i. The subscript R refers to the counter ion. The ionic strength is given by $\mu=0.5\ \Sigma(\alpha_i \bar{c}_i z^2_i)$, where α_i is the degree of dissociation and $\bar{c}_i$ is the molar analytical concentration of i. A complete treatise on the Debye-Hückel-Onsager theory can be found in a textbook on physical chemistry.

As an example, the ionic mobility of acetate in 10 mmol/l sodium acetate at 298 K is calculated as -38.7 10^{-9} $m^2V^{-1}s^{-1}$ (limiting ionic mobility -42.4 10^{-9} $m^2V^{-1}s^{-1}$, μ=0.010 mol/l). For 1 mmol/l the ionic mobility of acetate is -41.1 10^{-9} $m^2V^{-1}s^{-1}$. Tabulated data on electrophoretic mobilities are often obtained using moving boundary electrophoresis or conductivity measurements for several concentrations of strong electrolytes. The limiting electrophoretic mobility is obtained by extrapolation to infinite dilution.

So far, only fully dissociated ions are considered. However, for weak ions the degree of dissociation is of much more importance for the electrophoretic mobility than the electrolyte ionic strength. The actual electrophoretic mobility for weak ions is given by the sum of the product of the ionic mobilities of the subspecies and the degrees of dissociation

$$\bar{m}_i = \Sigma(\alpha_i\ m_i) \quad (4)$$

where α_i is the degree of dissociation, m_i the ionic electrophoretic mobility of the fully dissociated subspecies and $\bar{m}_i$ the effective electrophoretic mobility of ion i.

For the calculation of the effective mobility, the ionic mobility is calculated from the limiting mobility and used in eqn. (3). As an example, the effective electrophoretic mobility of acetate in a 10 mmol/l Tris-acetate buffer at pH 4.8 is calculated as -19.8 10^{-9} $m^2V^{-1}s^{-1}$ (pK_a = 4.8, α_{Ac} = 0.5, μ = 0.005 mol l^{-1}, m^0_{Ac} = -42.4 10^{-9} $m^2V^{-1}s^{-1}$, m_{Ac} = -39.7 10^{-9} $m^2V^{-1}s^{-1}$). In practice, several other factors such as temperature inside the capillary, applied electric field and buffer

ionic strength are determined with a certain imprecision. Furthermore, at concentrations below 10 mmol/l the difference between m^0_i and m_i is small. Therefore, often the limiting ionic mobilities are used in eqn. (4). For the example of acetate this gives an effective mobility of -21.2 10^{-9} $m^2V^{-1}s^{-1}$. The effective electrophoretic mobilities of several buffer ions as a function of pH are shown in Fig. 2.

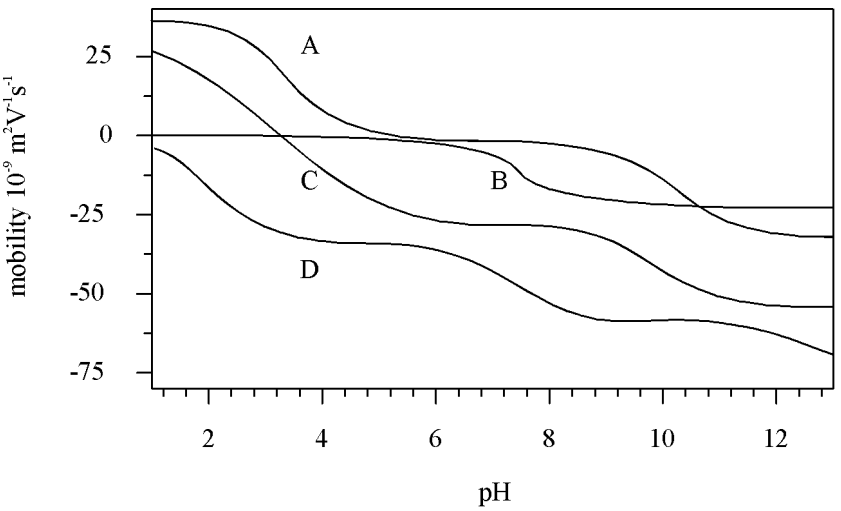

Fig. 2. Effective electrophoretic mobilities of some weak buffer ions vs. pH. The mobility of β-alanine (A) is low between pH 4-10 and reverses at the pI (pH 6.9). Line (B) is HEPES (4-(2-hydroxyethyl)-1-piperazine ethanesulphonic acid), (C) is glutamic acid and (D) is phosphoric acid.

Conductivity

The conductivity of an electrolyte solution depends on the concentration, charge and electrophoretic mobilities of the ionic constituents. The molar conductivity is defined as the specific conductivity divided by the concentration

$$\Lambda = \kappa/c \qquad (5)$$

The specific conductivity κ is can be determined in a conductometric cell as $\kappa=L/(AR)$, where L is the distance between the electrodes, A is the cross sectional area of the electrodes and R is the electric resistance. For accurate determination an alternating current (1-4 MHz) is used, so that polarisation effects are eliminated. In an electrolyte solution all ionic constituents

contribute to the specific conductivity which is given by

$$\kappa = F \Sigma(z_i \alpha_i \bar{c}_i m_i) \quad (6)$$

where F is Faraday's constant, z_i is the ionic charge, $\bar{c}_i$ is the analytical concentration and m_i the ionic electrophoretic mobility of i. For anions both z_i and m_i have negative values. In case of strong electrolytes α_i is 1. The sign ($^-$) on the concentration is often used in literature to refer to the analytical concentration. In case of weak acids this is $\bar{c}_A=[A^-]+[HA]$.

When the conductivity of an electrolyte is measured the value of κ refers to the contribution of all ionic species. Kohlrausch found already a century ago that at infinite dilution the contribution of a certain cation to the total conductivity is always the same, irrespective of the anion that is used. This is the law of independent migration of ions

$$\Lambda = \lambda_+ + \lambda_- \quad (7)$$

where λ_+ and λ_- are the ionic conductivities of the cation and the anion. Equation (7) enables the determination of weak electrolytes using several solutions of strong electrolytes. In practice it is easier to determine the limiting ionic conductivities of strong electrolytes than of weak electrolytes.

For example the conductivity of a weak acid such as acetic acid can be calculated using strong electrolyte solutions of sodium acetate, sodium chloride and hydrochloric acid as

$$\Lambda^0_{HAc} = \lambda^0_{Na+} + \lambda^0_{Ac-} + \lambda^0_{H+} + \lambda^0_{Cl-} - \lambda^0_{Na+} - \lambda^0_{Cl-} \quad (8)$$

Conductivity measurements can be used in calculation of electrophoretic mobilities. The limiting electrophoretic mobility can be calculated from the limiting conductivity using

$$m_0 = \lambda_0/(F\ z) \quad (9)$$

Equations 3, 4, 6 and 9 are particularly useful for calculation of the electrolyte conductivity and analyte mobilities from tabulated values of limiting mobilities and conductivities [3, 19-21]. Data on mobilities and conductivities are required in optimisation of CE procedures. However, tabulated data for a given electrophoresis buffer are not always available, especially when

certain additives such as organic modifiers or complex forming agents are used. In such cases mobilities and conductivities can be determined experimentally using CZE with indirect detection (see Chapter 3.2).

Electroosmosis

The velocity of an ion in CE is not only determined by the electrophoretic velocity. When an electric field is applied over a fused silica capillary the bulk solution moves into the direction of the cathode. This phenomenon is called the electroosmotic flow (EOF) (Fig. 3).

The fused silica capillary that is used in CE separations contains silanol groups. Under most operating conditions the silanol groups are negatively charged. Cations in the electrolyte are arranged as an ionic layer to the silanol groups at the capillary surface. The cations close to the surface are constrained in a rigid plane, the so-called Stern layer. Further away from the capillary surface the cations are freely moving and the ionic atmosphere becomes more diffuse. Under the influence of an electric field these cations move into the direction of the cathode and drag the inner bulk liquid along.

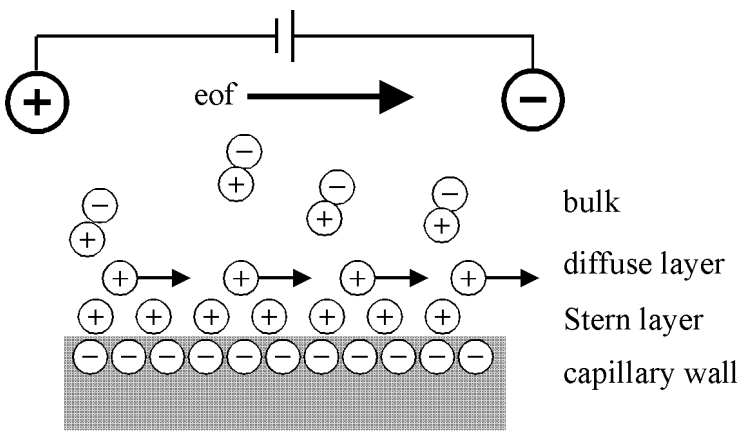

Fig. 3. Schematic representation of the EOF induced by charge differences in the double layer. The total number of positive and negative charges is exactly the same (electroneutrality). Because of freely moving cations in the diffuse layer the bulk is moving towards the cathode.

Characteristic of the EOF is the plug flow profile. In principle, all ions outside the double layer are affected the same way by electroosmosis irrespective of the radial position of the ion. Therefore, the EOF does not contribute to zone broadening in CZE. This is in contrast to a pressure-induced flow profile as seen in liquid chromatography. A so-called Poiseuille flow,

results in a parabolic flow profile that contributes to band broadening.

The electric potential at the boundary of the fixed and freely moving cations is the zeta potential. The velocity of the EOF is given by

$$v_{eof} = m_{eof}E \qquad (10)$$

and the electroosmotic mobility is defined as

$$m_{eof} = -\varepsilon\zeta/\eta \qquad (11)$$

Because the EOF is generated at the capillary wall, η is the viscosity at the wall. This is important in case additives are used that adsorb to the wall. These additives such as cellulose polymers change the local viscosity and reduce the EOF. The viscosity of the bulk liquid is hardly affected, which means that the electrophoretic mobility remains the same.

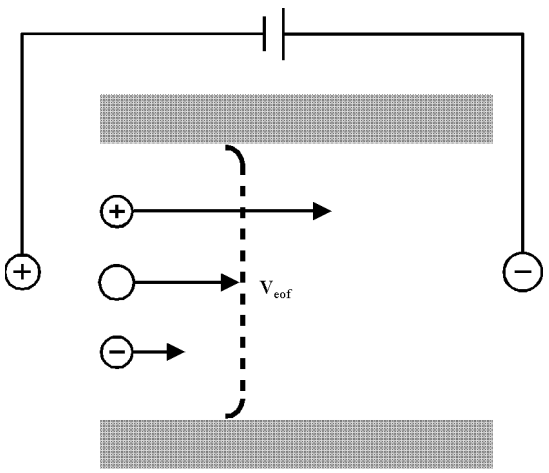

Fig. 4. The net velocities of anions, neutrals and cations in capillary electrophoresis in presence of an EOF.

In CZE the magnitude of the zeta potential is in the order of -0.1V for fused silica capillaries at neutral pH. For a buffer viscosity of 10^{-3}Nsm^{-2} and a dielectric constant of 7.08 10^{-10}CV^{-1}m^{-1} the electroosmotic mobility is 7.1 10^{-8}m^{2}V^{-1}s^{-1}, which is higher than the absolute mobility of most anions. The electrophoretic velocity is superimposed on the electroosmotic velocity. As a result cations, neutrals and anions are all moving in the same direction. The neutrals are

carried with the EOF and migrate together in one zone (Fig. 4).

Temperature and efficiency

A characteristic of C(Z)E is the application of a high electric field strength, typically 50 kV/m. A high electric field strength is favourable with respect to migration time and efficiency. Dissipation of the Joule heat resulting from the electrical current is possible by the use of narrow bore capillaries with inner diameters of 100 μm or smaller. The application of high electric field strengths is limited by thermal dispersion. An optimum exists in the applied electric field strength with respect to plate height and separation efficiency.

The migration time (t) is given by the capillary length and the sum of the electrophoretic and electroosmotic velocities as

$$t = l/v \qquad (13)$$

where l is the effective capillary length and v the migration rate of the analyte. In a CZE system the detection often takes place at a short distance from the capillary end. Therefore, the length from injection to detection is the effective capillary length l and the total capillary length is L. Substituting (1), (10) in (13) and defining the electric field strength as the voltage divided by the total capillary length gives

$$t_i = \left[\frac{L\, l}{\overline{m}_i + m_{eof}} \right] \cdot \frac{1}{V} \qquad (14)$$

where V is the running voltage.

In an optimised CZE system the longitudinal diffusion is considered the only factor that contributes to zone broadening. The longitudinal variance is given by the Einstein equation $\sigma_d^2=2Dt$ where D is the molecular diffusion coefficient and t is the CZE migration time. Substitution in the well known efficiency equation $N=l^2/\sigma^2$ results in $N=l^2/(2Dt)$. Substitution with (14) gives

$$N = \left[\frac{(\overline{m}_i + m_{eof})\, l}{2DL} \right] \cdot V \qquad (15)$$

Equation (14) and (15) clearly demonstrate the importance of the high voltage for a high efficiency and a short migration time. It should be kept in mind that eqn. (15) is based on the assumption that thermal dispersion is negligible which is not the case when the electric field strength becomes too high.

The contribution of Joule heat to zone broadening has been described by several authors. The theoretical model assumes that the Joule heat is dissipated through the capillary wall. The temperature varies with the radial position in the capillary and result in a radial parabolic temperature profile (Fig. 5). The lowest temperature is near the wall, the highest in the axis of the capillary. Under optimised conditions the temperature difference is less than 0.1 K.

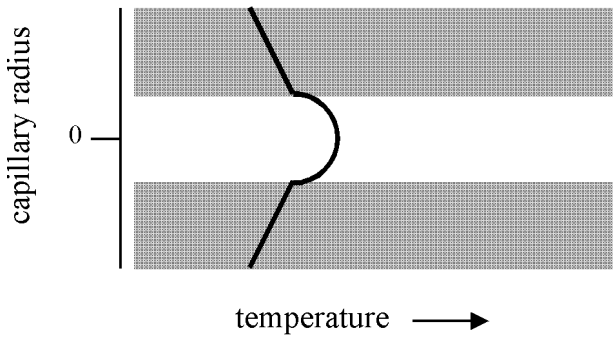

Fig. 5. The heat generated under influence of an electric field is dissipated through the wall. As a result a radial parabolic temperature profile exists in the capillary.

The viscosity of the buffer changes with temperature which results in a parabolic viscosity profile in the capillary. Because of the inversely dependence on the electrophoretic mobility to the viscosity (eqn. 2), the analyte velocity changes with its radial position and zone broadening occurs. Knox et al. [22, 23] derived an equation for the thermal contribution to the plate height as

$$H_T = \frac{d^2 v}{96\ D} \cdot (0.013\theta)^2 \qquad (16)$$

where d is the capillary diameter and with

$$\theta = \frac{r^2 E^2 \kappa}{4\lambda_T} \qquad (17)$$

where κ is the conductivity of the background electrolyte, r is the capillary radius and λ_T is the thermal conductivity. Writing the thermal variance as $\sigma_T^2 = H_T L$, using (1) and (13) and replacing the constant 0.013 for 0.5 δ results in

$$\sigma^2 = \frac{t\kappa^2\delta^2 m^2 E^6 r^6}{1536 D\lambda_T^2} \qquad (18)$$

where δ is the velocity spread factor which gives the relative change in mobility as a function of temperature. Equation (18) is the same equation as used by Foret et al. [17, 24]. A somewhat different result is obtained by Hjerten [1, 25] who derived

$$4\sigma_T = \frac{BLr^2 E^2 \kappa}{4\lambda_T T^2} \qquad (19)$$

where $4\sigma_T$ is the zone width at the baseline, B is a constant (2400 K), T is the temperature and L is the electrophoretic migration distance. Grushka et al. [26] confirmed these findings and concluded that the Knox approach is in fact a limiting case of equation (19).

For example, when an analyte is detected after 10 min (EOF marker at 5 min) at a voltage of 20 kV (10.1 μA) and a capillary of 700x0.075 mm (600 mm effective length) is used, then the variance (σ^2_T) calculated with eqn. (18) is 1.48 10^{-11} m^2 (t=600 s, κ=0.080 Sm^{-1}, δ=0.024 K^{-1}, E=28570 Vm^{-1}, $\overline{m}_i$=-35 10^{-9} $m^2V^{-1}s^{-1}$, m_{eof}=70 10^{-9} $m^2V^{-1}s^{-1}$, D=0.5 10^{-9} m^2s^{-1}, λ_T=0.6 $Wm^{-1}K^{-1}$, T=293 K). Using the same values in eqn. (19) and writing L as the electrophoretic migration distance $L_{el}=\overline{m}_i Et$ (eqn. 13 and 1) the thermal variance is calculated as 2.57 10^{-8} m^2. The thermal contribution to the total variance using (19) is approximately a factor 1700 higher than calculated with (18). However, in both cases the thermal variance is almost negligible with respect to the longitudinal diffusion calculated using $\sigma_d^2=2Dt$=6.0 10^{-7} m^2. When in equation (19) L is written as a function of E then in both equations the variance increases with E^6, κ^2 and (in eqn. 19 only) with r^4. These three parameters are often varied in CE optimisation procedures.

In practise, efficient heat dissipation to the environment appears to be of major importance for temperature control and stability. Therefore, often a CE system is equipped with an air or liquid capillary-cooling device. In Chapter 3.3 (eqn. 31) the contribution of heat dissipation to the temperature inside the capillary is described.

It should be noted that the electroosmotic plug flow profile is not affected by Joule heat [25]. The dependence of the EOF velocity on the viscosity (and temperature) is referring to the viscosity at the capillary wall (eqn. 11). The contribution of Joule heat to zone broadening is small in most cases where capillaries with inner diameters <100 μm are used. Other factors such as the injection zone length, longitudinal diffusion and the composition of the sample buffer are predominantly influencing the zone width. A more detailed discussion on zone broadening is given in Chapter 1.3.

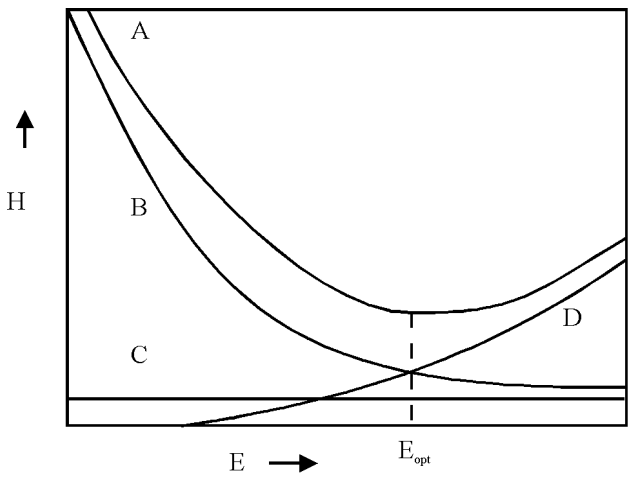

Fig. 6. An optimum electric field strength (E_{opt}) exists with respect to plate height (H). At higher electric field strengths the thermal contribution to plate height (D) increases. The longitudinal contribution (B) decreases due to a decrease in migration time. The contribution of injection and detection (C) is constant. As a result a minimum exists in the total plate height (A) at $E=E_{opt}$.

When the contributions of Joule heat and longitudinal diffusion to zone broadening in CZE are given as a function of the electric field strength, then it is possible to derive an equation for the optimum electric field strength (Fig. 6). The optimum is given by solving the equation $\delta H/\delta E=0$. Obviously, such an equation is of great practical value in an optimisation procedure of a CZE analysis. Foret et al. derived [17, 24]

$$E_{opt} = \frac{2.92}{r} \cdot \left[\frac{D\lambda_T}{\delta \kappa (\overline{m}_i + m_{eof})} \right]^{\frac{1}{3}} \qquad (20)$$

Hjerten derived a different equation for the optimum electric field strength [25]

$$E_{opt} = 2 \cdot \left[\frac{3D (|\overline{m}_i| + m_{eof}) \lambda_T^2 T^4}{\overline{m}_i^2 B^2 \kappa^2 r^4 l} \right]^{\frac{1}{5}} \qquad (21)$$

where B is a constant (2400 K) and T the temperature.

For the same example and the same constants as used with eqn. (18) and (19) an optimum electric field strength of 128 kV/m is calculated using eqn. (20) and 38.4 kV/m using eqn. (21). Although both equations describe qualitatively the parameters that affect the optimum electric field strength, in our experience the result of eqn. (21) is more realistic than eqn. (20). One of the factors that causes the difference is the contribution of thermal zone broadening, which is considerably lower in the Foret approach (eqn. 18, 20).

For calculation of the optimum electric field strength the electroosmotic and the electrophoretic mobility is needed. The electroosmotic mobility is determined by adding a detectable neutral marker such as mesityloxide or methanol to the sample. The electroosmotic mobility is then calculated from the migration time of the neutral marker using eqn. (10). When the electroosmotic migration time is known the effective electrophoretic mobility can be calculated from the CZE migration time using

$$\overline{m}_i = \left[\frac{1}{t_{tot}} - \frac{1}{t_{eof}} \right] \cdot \frac{L\, l}{V} \qquad (22)$$

where t_{tot} is the CZE migration time of analyte i and t_{eof} is the electroosmotic migration time.

Another important parameter in optimisation procedures is the resolution. The resolution is determined by the efficiency and the selectivity as

$$R = \frac{\sqrt{N}}{4} \cdot \frac{\Delta v}{v_{1,2}} \qquad (23)$$

where $v_{1,2}$ is the mean velocity of both analytes and $\Delta v/v_{1,2}$ the relative velocity difference between the two analytes which is the selectivity. The velocity is the sum of the electroosmotic and the electrophoretic velocity. Using eqn. (1) and (10) the difference in velocity can be written as $\Delta v = (\overline{m}_1 - \overline{m}_2)E$. Using the same equations the mean velocity can be written as $v_{1,2} = (\overline{m}_{1,2} + m_{eof})E$, where $\overline{m}_{1,2}$ is the mean effective electrophoretic mobility of both analytes. Combining this with eqn. (15) and (23) gives

$$R = (\overline{m}_1 - \overline{m}_2) \cdot \sqrt{\frac{2Vl}{64DL(\overline{m}_{1,2} + m_{eof})}} \qquad (24)$$

Equation (24) shows that a high voltage is favourable for the resolution.

It should be kept in mind that this equation is derived from (15) which is only valid when the longitudinal diffusion is the predominant source of zone broadening. Changing one of the parameters in eqn. (24) may also affect the heat development and thermal dispersion. This may even lead to a situation where eqn. (24) is no longer valid and a decrease of resolution is obtained. Therefore, the resolution is often optimised by improving the selectivity ($\Delta v/v_{1,2}$). This can be done by changing the electrophoresis buffer, changing the pH or using additives.

Instrumentation

A schematic representation of equipment used in CZE experiments is given in Fig. 7. The capillary is filled with background electrolyte (BGE) and placed into an anode and a cathode buffer vial filled with the same BGE. The fused silica capillary (F) is placed in the 4 ml buffer vials (V1 and V2). The power supply (P) is connected to the electrode in V1 which is placed in a safety box (B). This electrode is used as cathode or anode depending on the polarity of the power supply.

The high voltage unit is usually in the range of 15-60 kV with a maximum current of ca. 0.3 mA. In most equipment a bi-polar power supply is used. This is convenient in case polarity

switching is applied. The other electrode is positioned outside the safety box and close to the detector (D) and is therefore grounded. The current is measured via an amperometer (A) at the grounded electrode. The sample vial (S) is kept at an adjustable level with respect to the electrode buffer level to enable hydrodynamic sample injection. All vials are septum closed to prevent evaporation.

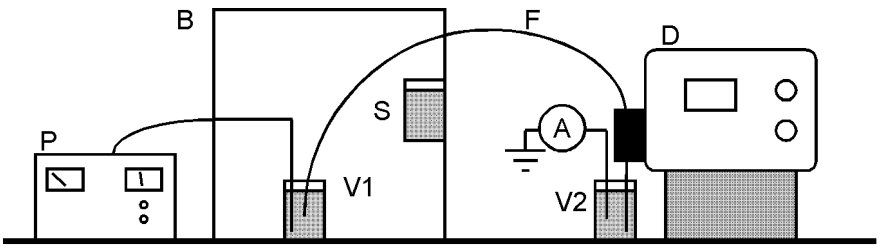

Fig. 7. Schematic representation of a typical custom-made CZE system. For explanation see text.

In most CE systems injection takes place either electrokinetically or hydrodynamically. An injection zone length that is smaller than 1% of the effective capillary length is favourable with respect to efficiency and resolution (Fig. 8). Regardless of all other contributions to zone broadening, the maximum separation efficiency that can be achieved for an effective capillary length l is given by $N = 12\ l^2/L^2_{inj}$, where L_{inj} is the injection zone length [17]. Injection volumes are therefore usually in the range of 0.1-20 nl. For electrokinetic injection the capillary inlet and the electrode are placed in the sample vial. The analyte ions migrate into the capillary by applying a certain voltage for a certain period of time. The injection volume (Q_{inj}) is then given by

$$Q_{inj} = \left[\frac{l\ \pi r^2}{t_{tot} V} \right] \cdot t_{inj} V_{inj} \qquad (25)$$

where l, t_{tot}, t_{inj} and V_{inj} are the effective capillary length, the CZE migration time, and the duration and voltage of injection, respectively. Each different analyte migrates with its unique velocity into the capillary which means that each different analyte is injected with a different zone length and volume.

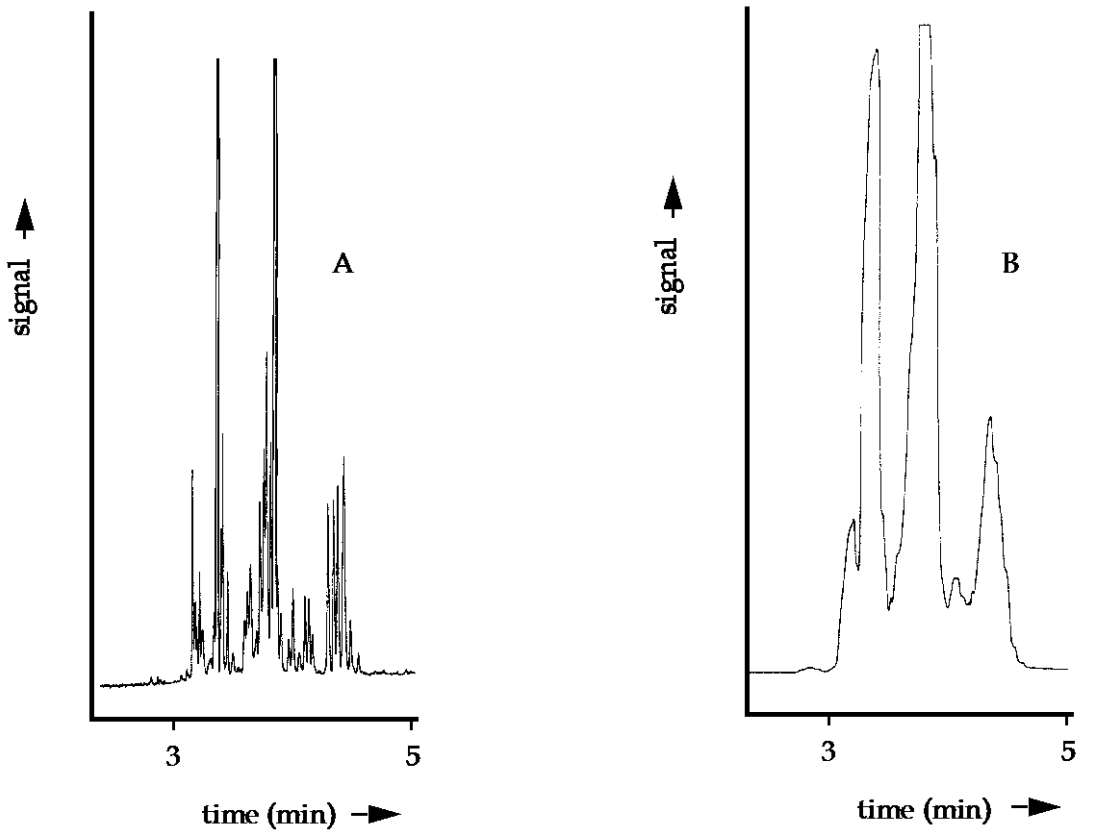

Fig. 8. High resolution separations are possible when the injected sample volume is smaller than 1% of the effective capillary length. Separation of a mixture of fluorescently labelled amino acids at an injection volume of 12 nl (A, 0.1%) and 1.0 μl (B, 8.5%). A capillary of 1000x0.15 mm with 700 mm effective length is used.

Characteristic for CZE separations is the possibility of improving the loadability of the system by electrophoretic analyte focusing [27]. This can be done by using a sample buffer with a lower conductivity than the BGE. This phenomenon is called stacking, zone sharpening or field amplified injection. When a sample buffer is used at a specific conductivity that is a factor Y lower than the specific conductivity of the BGE then the injected sample concentration increases a factor Y [28]. As a result the injected sample zone length is reduced with a factor 1/Y. In practice this means that when the sample is dissolved in water and electrokinetic injection is applied, the sample concentration detection limit improves by a factor 10-1000 depending on the BGE.

In Fig. 9A an electropherogram is given obtained after electrokinetic injection for 5s at 5 kV of a 1 mg/ml solution of the drug suramin in 1 mol/l phosphate buffer. The same sample solution was diluted with water to (B) 100µg/ml in 100 mmol/l buffer (C) 10µg/ml in 10 mmol/l buffer and (D) 1µg/ml in 1 mmol/l buffer. The detector settings and the injection voltage and time were the same. The electrophoresis buffer consisted of 50 mmol/l phosphate buffer at pH 4.5. In case (A) zone broadening due to concentration overloading occurs, in case (C) and (D) the analyte is concentrated during injection (stacking).

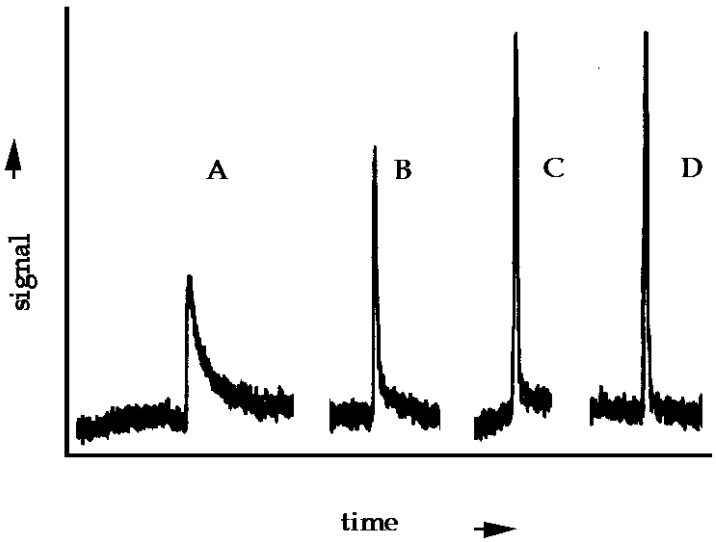

Fig. 9. The performance in CZE can be manipulated by using a sample buffer concentration differing from the BGE. For further explanation see text.

Hydrodynamic injection procedures are performed by placing the capillary inlet in the sample vial and applying a pressure or height difference. The injection volume is given by

$$Q_{inj} = \left[\frac{\pi d^4}{128\ \eta L}\right] \cdot t_i\ \Delta p_i \qquad (26)$$

The pressure difference can be converted to a height difference using $\Delta h = \Delta p/\rho g$ where Δp is the pressure difference (bar), ρ is the buffer density (kgm^{-3}), and g is the gravitational force ($9.8\ ms^{-2}$). For water a pressure difference of 20 mbar corresponds to a height difference of

approximately 20 cm. This conversion is independent of the capillary diameter. Using a hydrodynamic injection results in equal zone lengths and volumes for different analytes. However, when the sample buffer is different from the BGE with respect to concentration, pH or additives, different changes in zone length and in analyte concentration may occur for different analytes after starting the CZE analysis. When sample matrix effects are not wanted, the analyte should be dissolved in BGE and the sample concentration should be at least a factor of 100 below the BGE concentration.

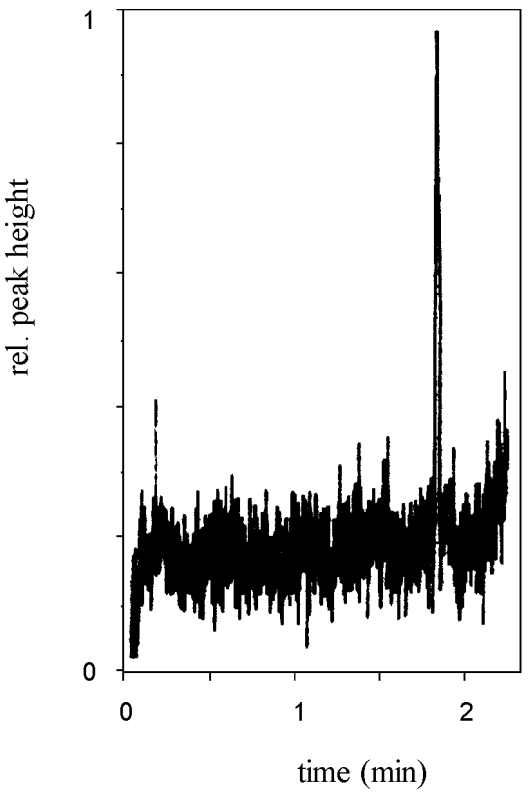

Fig. 10. LIF detection of 120 pmol/l fluorescein. Minimum detectable concentration based on $3x\sigma_{noise}$ is 17 pmol/l which corresponds to a minimum detectable amount of 0.3 attomol.

Several detection systems have been reported in literature [10, 11]. Highest sensitivities are obtained with laser induced fluorescence (LIF) and electrochemical detection, provided that the compound of interest has the suitable detection properties (Fig. 10). In most commercially available systems absorbance detection is applied. Absorbance detection is easy and more

widely applicable. Optical detection takes place close to the capillary end using a small part of the capillary as detection cell. The detection cell is made by burning off a small part of the protective outer polyimide coating. In capillaries with an UV transparent (outer)coating the detection takes place without any modification of the capillary.

For a cylindrical on-capillary detection cell the optical path length is dependent on the radial position of incidence. Therefore, a modification on Beer's law is applied. Foret et al. derived for absorbance detection [17]

$$A = -\log [1-2.303 (\varepsilon\, c\, 0.67\, d)] \qquad (27)$$

where A is the absorbance, ε is the molar absorptivity, c the analyte concentration and d the capillary diameter. Bruin also took the aperture width in consideration and derived [29]

$$A = \varepsilon c \cdot \left[\sqrt{r^2 - s^2} + \frac{r^2}{s} \arcsin \frac{s}{r} \right] \qquad (28)$$

where s is half the aperture width. Both equations can be used in the absorbance range below 0.1 AU.

As an example the limit of detection for a highly UV absorbing compound in a capillary with an inner diameter of 75 μm filled with BGE is calculated. For a molar absorptivity of 10000 l mol^{-1} cm^{-1}, a concentration of 10^{-6} mol l^{-1} and a width of the slit which is the same as the capillary diameter (s=r=37.5 μm), the absorbance is calculated as 5.9 10^{-5} AU (eqn. 27) or 5.0 10^{-5} AU (eqn. 28). When a noise level of 1 10^{-5} AU is assumed (peak-to-peak) then the detection limit is 120 nmol/l for this particular compound. The detection limit is here defined as the concentration that gives a signal equal to 3 times the standard deviation of the noise (σ_{noise} ~ 0.2 x peak-to-peak noise). Favourable conditions are used in this calculation, for most compounds the absorbance detection limits in CE are higher.

In CE absorbance detectors the light is directed on the capillary by means of a slit or a focusing lens. In practice the width of the slit between the light source and the capillary is kept approximately similar to the capillary inner diameter. When a larger aperture width is used, the light that reaches the photomultiplier without striking the liquid only contributes to the noise. When a smaller aperture width is used the number of photons that reach the photomultiplier decreases. This results in a relative increase of the shot noise. Bruin [29] compared various

designs of absorbance detection cells and concluded that using a slit results in a similar sensitivity compared with a absorbance detector using a focusing lens, but the linear dynamic range was a factor 2 larger in the latter case.

Capillary electrophoresis

Several capillary electrophoretic separation modes can be distinguished [9-18]. Techniques like capillary zone electrophoresis (CZE), micellar electrokinetic capillary chromatography (MECC), capillary isotachophoresis (CITP), capillary gel electrophoresis (CGE) and capillary isoelectric focusing (CIEF) have in common that the separation can be performed using the same equipment. The different modes are mainly specified by the buffer system that is used. In practice it is easy to switch between these modes, in most cases only the buffers have to be changed.

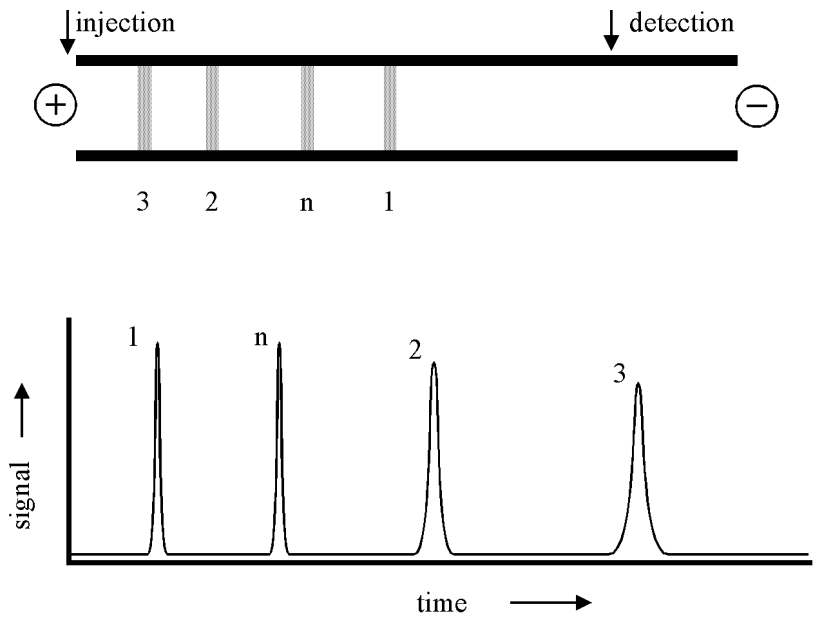

Fig. 11. Schematic representation of a CZE separation. The cationic analyte (1) has the highest mobility followed by the neutrals (n) and two anionic analytes (2,3).

Capillary zone electrophoresis

CZE is performed in a capillary filled with a continuous buffer i.e. the cathode and anode

buffer is the same [9]. After injection the electric field is applied and the different analytes migrate with different velocities in the direction of the detector. The EOF velocity in untreated fused silica capillaries is higher than the velocity of most ions. As a result anions, cations and neutrals migrate in the direction of the cathode.

In Fig. 11 the schematic representation of a CZE separation is given. Zone 1 are cations migrating with the highest velocity. The neutrals (zone n) are migrating with the same velocity, the velocity of the EOF. Sometimes, at high sensitivity, non-absorbing neutrals are seen as a small dip in the baseline. The peak width of zone 1 is smaller than 2 and 3. Most factors that contribute to zone broadening are a function of time. As a result of the short migration times the zone broadening is less in case of zone 1. Furthermore, the velocity at which the zone migrates through the detector is higher for zone 1 than for 2 and 3. This also results in a smaller zone width for zone 1 (see also Fig. 1).

Micellar electrokinetic capillary chromatography

In MECC separations a surfactant at a concentration above its critical micelle concentration (cmc) is added to the BGE [7, 8, 30, 31]. The surfactant contains a charged group which gives the micelle an electrophoretic velocity that is close, but oppositely, to the velocity of the EOF. As a result the total velocity of the surfactants is low and the micellar phase is moving slowly as a semi-stationary phase through the capillary.

Neutrals that are carried along with the EOF, are solubilised by the semi-stationary micelles. As a result the velocity of the neutrals is reduced. Because not all neutrals are solubilised to the same extent separation takes place. A MECC separation window can be defined. The neutrals that are completely solubilised are migrating with the velocity of the micelles, neutrals that are not at all solubilised are migrating with the velocity of the EOF.

This is illustrated in Fig. 12. Cationic analyte (1) is unaffected by the semi-stationary micellar phase and migrates zone-electrophoretically outside the MECC window. Analyte (3) is a neutral that is completely solubilised in the micellar phase and migrates with the velocity of the micellar phase. The dye sudan III is often used as such a neutral marker. Neutral analyte (2) is partly solubilised and migrates with a lower velocity than the EOF velocity.

Micelles are dynamic structures with a limited lifetime, which are in equilibrium with the surfactant monomers in solution. Solubilisation is therefore a dynamic process. The dynamic equilibrium in electrokinetic capillary chromatography can be influenced by using additives such as organic modifiers. Organic modifiers may also enhance the solubility of neutrals in the

BGE.

Sometimes surfactants are added to the BGE to enhance the CZE performance without utilising micellar solubilisation. Cationic surfactants such as hexadecyl-, cetyl- and dodecyltrimethylammoniumbromide (resp. HTAB, CTAB and DTAB) adsorb to the capillary wall and change the ζ-potential. They can be used to manipulate the EOF. Anionic surfactants such as sodium dodecylsulphate (SDS) are occasionally applied to prevent adsorption of proteins to the capillary wall.

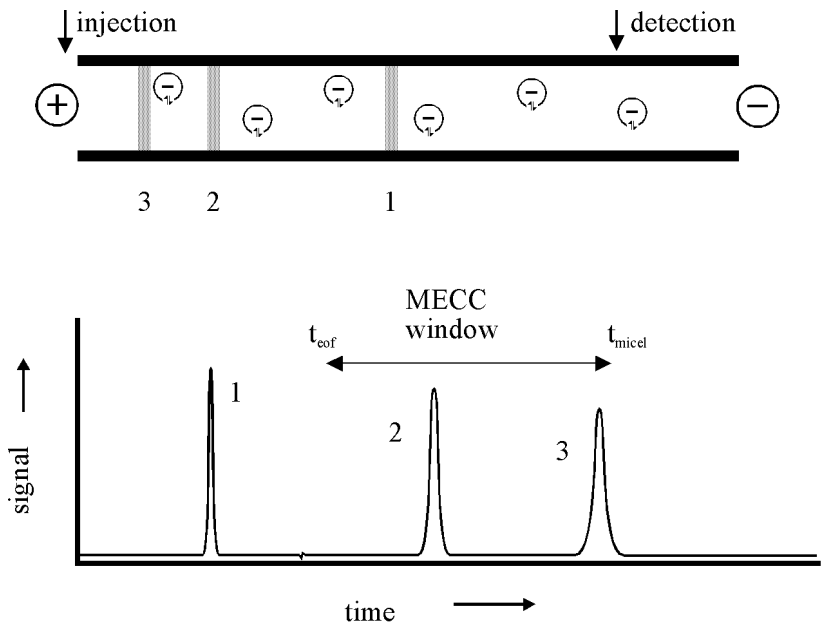

Fig. 12. Schematic representation of a MECC separation.

Enantiomer separations in CZE are based on the same principle as electrokinetic capillary chromatography [31-33]. The enantiomers are complexating with a chiral selector which is added to the BGE. When the equilibrium constant of this dynamic process is different for the enantiomers separation takes place. In most applications cyclodextrines are used as chiral selector.

Capillary isotachophoresis

In CITP a discontinuous buffer is used and only anions or cations are analysed in one run [3, 19, 34]. In most cases modified capillaries are used without EOF. In anionic separations the

capillary and the anode vial is filled with leading buffer. The leading buffer contains anions with a mobility higher than the mobility of the analyte ions. The cathode vial is filled with terminating ions which have the lowest mobility. The pH is set with the buffering counterions. In the steady state, when the analytes are separated, they migrate as consecutive zones ordered by their electrophoretic mobilities (Fig. 13).

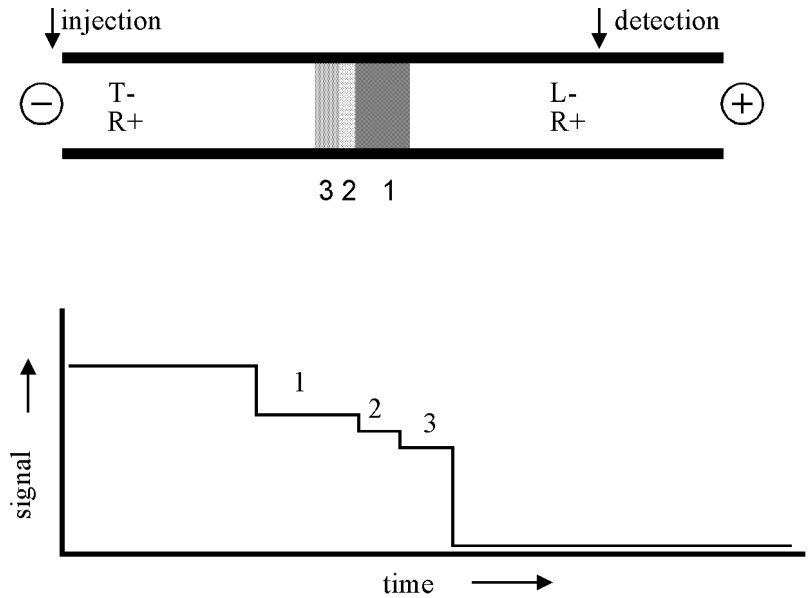

Fig. 13. Schematic representation of a CITP separation using conductometric detection. The separated anions migrate in consecutive zones. The analyte zone length is correlated with concentration and is used in quantitative analysis. The EOF is suppressed and anions move to the anode.

Characteristic for CITP is its concentration regulating property. The concentrations of analyte ions are adapted to the concentration of the leading ions according to the Kohlrausch regulation function. The adjusted isotachophoretic concentration is given by

$$\bar{c}_i = \frac{m_i}{m_i + m_R} \cdot \frac{m_L + m_R}{m_L} \cdot \frac{z_L}{z_i} \cdot \bar{c}_L \qquad (29)$$

where $\bar{c}_i$ is the adjusted analytical concentration of analyte i, $\bar{c}_L$ is the leading ion concentration, z is the charge on the ion and m is the ionic mobility. In eqn. (29) the absolute values of

z and m are used. For any combination of weak and strong electrolytes (R, i and L) the *ionic* mobilities are used.

The concentration is proportional to the leading buffer concentration (eqn. 29), i.e. the concentration in the analyte zone in independent from the concentration in the sample. For quantitation the zone length is used. Often the differential of the signal as shown in Fig. 13 is used which makes it easier to mark different zones.

In most CITP equipment as developed by Everaerts et al. polytetrafluoroethylene (PTFE) capillaries with inner diameters ranging from 200-500 μm were used. PTFE is not UV transparent and thus not suitable for on-capillary absorbance detection. Therefore, the capillary is connected to a quartz detection cell or conductometric detection is applied. A typical ITP electropherogram is shown in Fig. 13. The leading buffer with the highest mobility has the highest conductivity (eqn. 9). Isotachophoresis has been used in many applications such as analysis of drugs in plasma, inorganic ions, nucleotides etc. The technique has never been utilised to the same extent as CZE nowadays. Recently, the technique has gained a lot of interest as concentrating pretreatment for CZE. On-line combination of CITP with CZE enables highly efficient separations at low analyte concentration levels [27, Chapter 2 and 3].

Capillary gel electrophoresis

Another application area of CE separations is found in the field of biopolymer analysis [35-38] (Fig. 14). Electrophoretic separations are already for many decades an important tool in biochemistry. Proteins are analysed on polyacrylamide gels on a routine basis. DNA fragments are analysed on large slab gels. Large biopolymers of a similar structure such as DNA fragments usually have approximately the same electrophoretic mobility.

In free zone electrophoresis mixtures of these biomolecules are difficult to separate. However, in gel electrophoresis the separation is mainly based on differences in size. Small molecules are moving freely while large molecules are hindered by the gel network which functions as a molecular sieve. In polyacrylamide filled capillaries the size of the pores can be manipulated by varying the percentage of monomers in the gel. Resolution in CGE is similar as in slab gels however, the migration times are shorter (factor 2-4). Furthermore, gel-filled capillaries can be used repeatedly in contrast to slab gels.

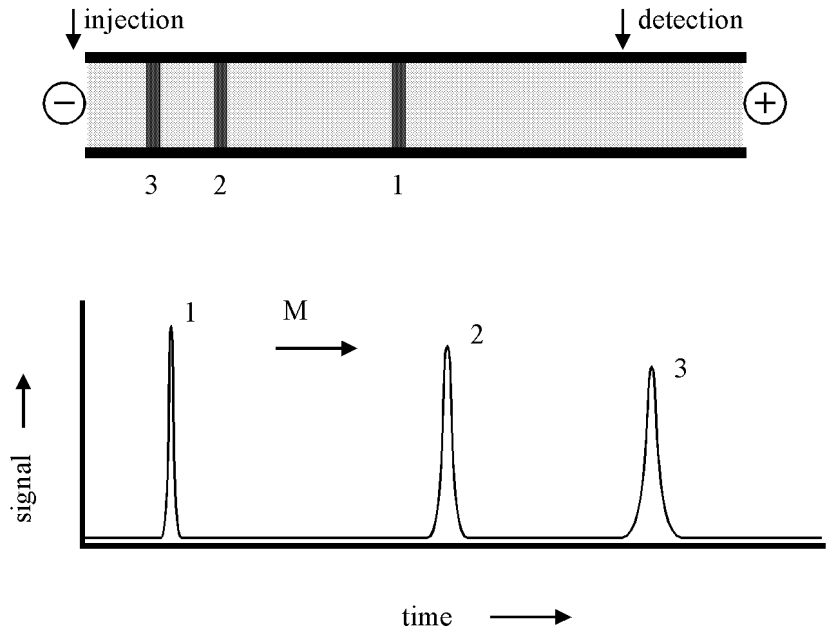

Fig. 14. Schematic representation of a CGE separation. The capillary is filled with a gel and separation is mainly based on differences in molecular mass (M). In CGE the EOF is suppressed.

A great deal of work has been done on the development of a method for production of reproducible and stable gel-filled capillaries, which appears to be difficult. During polymerisation of acrylamide gas bubbles may appear that make a gel unusable. After several runs bubbles may appear at the in- and outlet which can only be removed by cutting off a piece of the capillary. A gel-filled capillary can not be flushed, changing buffer solutions can only be done by electromigration. In practice this means that the lifetime of gel-filled capillaries is limited to several days.

An alternative is the use of soluble polymers which are added to the BGE. A dynamic molecular sieve is formed by entanglement of these linear non-cross-linked polymers. These polymers can be used in untreated fused silica capillaries with similar results as the gel-filled capillaries. The molecular sieving effect can be manipulated by the polymer concentration.

Capillary isoelectric focusing

In CIEF separations are based on differences in isoelectric point (pI) of biomacromolecules [39-41] (Fig. 15). Ampholytes which individual isoelectric points cover the desired pH range

are used to generate a stable pH gradient in the capillary. The analytes are added to this ampholyte mixture and loaded on the capillary. The anode vial contains the acidic buffer and the cathode vial the alkaline buffer. When the analysis is started the ampholytes migrate to the position where the pH is the same as there pI. At that point they will remain thus stabilising the pH gradient. At the same time the biomacromolecules migrate to the position where the pH equals their pI.

To enable the formation of a stable pH gradient the EOF is reduced or eliminated. After the focusing step the liquid in the capillary is mobilised and detection takes place. Mobilisation is done either by pressure or by the addition of salts in one of the vials which results in an EOF. The high loadability and the concentrating properties of the CIEF make the technique suitable for the analysis of low concentrations of proteins.

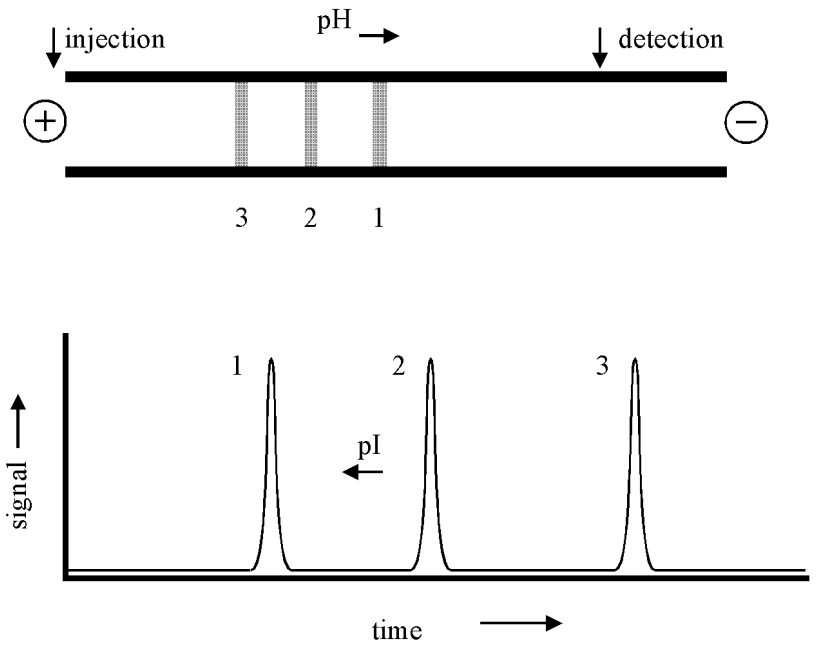

Fig. 15. Schematic representation of a CIEF separation. In the focusing step the pH gradient is formed and the separation takes place based on pI. In the second step the bulk is mobilised and detection takes place. The EOF is usually suppressed during the focusing step.

Applications of CZE in bioanalysis

One way of demonstrating the potential of an analytical method is considering its applications. Therefore, in this paragraph 16 applications are evaluated with regard to method and validation. A selection from literature based on papers concerning drug analysis in complex matrices using CZE or MECC is made (Table I). Papers without assay validation are not included. Most papers have been found in Journal of Chromatography and deal with the analysis of plasma or serum samples. Although the overview is certainly not complete, it gives an impression of the current applicability of CZE and MECC. With respect to method a difference can be made between those applications dealing with trace analysis (< 1 μmol/l) and those concerning higher determination limits.

Table I. Some selected applications of CZE or MECC in drug analysis in complex matrix.

nr	analyte	matrix	ref.
1	retinol	blood, serum	42
2	cytosine-β-D-arabinoside	plasma	43
3	glyphosate, aminomethyl-phosphonic acid	serum	44
4	warfarin	plasma	45
5	aspoxicillin	plasma	46
6	bilirubin	plasma	47
7	caffeine, theophylline, theobromine, uric acid, xanthine, paraxanthine	plasma	48
8	primidone, phenobarbital, phenythoin, carbamazepine	plasma	49
9	fosfomycin	serum	50
10	bupivacaine, fluoxetine, verapamil, carvedilol, pindolol	serum	51
11	hippuric acid, p-hydroxyhippuric acid, uric acid	serum	52
12	doxorubicin, epirubicin, daunorubicin	plasma	53
13	cicletanine	plasma (urine)	54
14	methotrexate, 7-hydroxymethotrexate	serum	55
15	desipramine, nortriptyline, doxepin, imipramine, amitriptilyne	plasma	56
16	cicletanine	plasma	57

In assays concerning the higher determination limits (Table II, case 1-11), the sample pretreatment varies from solid phase isolation (SPI) or liquid-liquid extraction (LLE) to no pretreatment at all. If the plasma sample is injected without a desalting sample pretreatment step precautions are taken to prevent overloading of the capillary with matrix ions. The sample is diluted before injection (case 6, 11) or the buffer concentration of the background electrolyte is increased (case 9). To prevent adsorption of the plasma proteins to the capillary wall a surfactant is added to the BGE (case 5, 6).

In trace analysis (Table II, case 12-16) the method usually includes a pretreatment step where the analyte is separated from the main matrix constituents before the analytical separation takes place. A SPI or LLE is followed by an evaporation step resulting in a concentration of the analyte ions.

Table II. Overview of methods and separation conditions.

nr	pretreatment	BGE			L	ID	V	detection
		buffer (mM)	additive (mM)	pH	(cm)	(μm)	(kV)	
1	CTF	Phos 50	NaCl 10	7.8	60	50	24	LIF
2	SPE	Citrate 40		2.5	26	50	8	Abs
3	DPR, DER, LLE, EV	Bor 100	MeOH 10%	9.6	72	50	30	Abs
4	LLE, EV	Phos 100	Me-βCD 8, MeOH 2%	8.4	72	50	20	Abs
5	none	Phos/Bor 20	SDS 50	8.5	65	50	20	Abs
6	DIL	Phos/Bor 20	SDS 25, MeOH 3%	8.5	50	75	16	Abs
7	LLE, EV	Phos 25	SDS 80	8.0	72	50	21	Abs
8	LLE, EV	Phos 25	SDS 50	8.0	72	50	30	Abs
9	DPR, EV, FLT	Bor 200	phenylphosphonicacid 10	8.2	57	75	30	I-Abs
10	LLE, EV	Tris-Phos 18	dMe-βCD 10, HTAB 0.03, MHEC 0.1%	2.9	64	50	24	Abs
11	FLT, DIL	βAla/Ac10	MES/His 10, MHEC 0.05 %	6.8	15	200	10	Abs
12	LLE	Phos 100	ACN 70%	3.0	70	75	25	LIF
13	LLE, EV	Bor 100	SDS 100, γCD 25, ACN 10%	8.6	57	75	15	Abs
14	SPE, EV, DER	Mes 5	Na_2SO_4 16, MeOH 30%	6.7	100	75	25	LIF
15	LLE, EV	Phos 37.5	DTAB 25, urea 2000	8.0	71	50	25	Abs
16	LLE, EV	Bor 100	SDS 25, ACN 10%	8.6	57	75	20	Abs

Abbreviations: none: no pretreatment, CTF: centrifugation, DPR: deproteination, DER: derivatisation, EV: evaporation, DIL: dilution, FLT: filtration, Phos: phosphate buffer, Bor: borate buffer, Ac: acetate, MES: 2-(N-morpholino)ethanesulphonic acid, MHEC: methylhydroxyethylcellulose, SDS: sodium dodecylsulphate, ACN: acetonitrile, MeOH: methanol, (d)Me-βCD: (di)methyl-β-cyclodextrine, γCD: γ-cyclodextrine, Abs: absorbance detection, I-Abs: indirect absorbance detection. For references, see Table I.

Detection limits are improved by reconstituting the analyte in a buffer with a lower conductivity than the BGE or in water. The injection is then performed under stacking conditions (case 2, 7-10, 12, 13, 15, 16). Another possibility of improving determination limits is using a sensitive detection system such as LIF (case 1, 12, 14). However, because of the limited number of different detection systems that are commercially available and capable of trace analysis, most applications are based on absorbance detection.

In most cases (Table II) the BGE consists of a phosphate buffer. An advantage is its wide buffering pH range. With respect to heat development during the analysis low conductivity buffers such as MES, TRIS and β-Ala are an alternative. In several applications (case 3, 4, 6, 12, 13, 14, 16) organic modifiers are used. Organic modifiers decrease the current and heat development in the separation system, they may improve the resolution and may prevent analyte adsorption to the capillary wall. The addition of polymers such as MHEC is usually applied to reduce the EOF (case 10, 11). The cellulose polymers adsorb to the capillary wall and increase the local viscosity which may result in an almost complete suppression of the EOF. In membrane-closed capillaries (case 11) this is necessary to prevent zone broadening because of electroosmotically induced convection. In case 15 an improved resolution is reported after addition of 2 mol/l urea. Urea increases the solubility of the tricyclic compounds in BGE and affects the partitioning in the DTAB micelles. This resulted in an improved resolution without increasing the MECC migration time. In some cases (case 1 and 14) salts are added to the buffer to improve the separation performance. Unless there is a specific interaction of the added ions with the analyte or the capillary wall, increasing the buffer concentration may have the same result.

A characteristic of CZE is the ease of switching from one BGE to another. By simply adding a surfactant to the BGE above its cmc, the CZE system is converted into a MECC system (case 5-8, 15, 16). Addition of a chiral selector such as a cyclodextrine to the BGE may enable enantiomer separations (case 4, 10, 13). Switching buffers usually requires only a few minutes equilibration by flushing the capillary with the new BGE. An exception is the addition of cellulose polymers where the equilibration takes place overnight. In several applications a combination of additives is used. Micellar separations may be improved by addition of organic modifiers (case 6, 16). Chiral separations are performed in combination with organic modifiers (case 4) or surfactants (case 10) or both (case 13). Surfactants and organic modifiers may interact with the cyclodextrin-analyte equilibrium, organic modifiers may interact with the micellar solubility of the analytes. Optimisation of an enantiomer separation usually includes a study of the effect of additives on resolution and efficiency.

The pH is an important parameter in the optimisation procedure. It does not only affect the charge on the analyte and buffer ions in case of weak acids or bases, but also the EOF velocity. In some cases it also influences the detectability. When closely related analytes are to be separated it can be shown that the best resolution is obtained at a pH close to the pK_a.

The capillary diameter is in all considered cases 75 or 50 μm, with exception of case 11.

With respect to loadability and optical path length, large diameters are favourable. However, the thermal variance increases with the r^4 resulting in a decrease of efficiency and peak height. The capillary length is in all cases smaller than 1 meter, longer capillaries result in most cases in unacceptable migration times. The minimum length is determined by hardware restrictions, in most commercially available CZE systems a minimum capillary length of 25-50 cm is applied.

Table III. Overview of the assay validation parameters. Most applications (1-11) are in the micromolar range. Highest sensitivities have been obtained with LIF detection (1, 12, 14). Abbreviations: IS = use of internal standard, t (min) = run time, range = concentration range investigated, t RSD (%) = relative standard deviation in migration time.

nr	IS	t (min)	range (µmol/l)	LOD (µmol/l)	t RSD (%)	in-accuracy (%)	im-pre-cesion (%)
1	yes	5	140 - 830	0.014	-	-	7.5
2	no	5	1 - 10	0.5	4	7	12
3	no	15	2.5 - 500	0.5	2	-	5.5
4	yes	12	3 - 10	0.65	0.3	-	5
5	yes	20	50 - 600	2.6	1	-	4
6	no	20	6 - 160	6	0.4	-	3.5
7	no	12	27 - 330	15	1	-	5
8	yes	17	25 - 200	-	0.5	-	2
9	yes	10	55 - 550	33	2	-	1
10	yes	15	0.6 - 13.2	-	-	-	1.5
11	no	8	12.5 - 125	-	0.9	-	6
			(nmol/l)	(nmol/l)			
12	yes	9	0.6 - 600	0.4	0.5	2	4.5
13	yes	15	40 - 2000	40	-	1.6	7.5
14	no	20	5 - 10000	0.5	-	-	10
15	yes	15	200 - 1000	20	2	-	7
16	yes	12	80 - 4000	80	-	1.5	9.5

The validation of the considered applications is given in Table III. The reproducibility in migration times varies from 0.3 to 4%. The values given in Table III are the maximum standard deviations that were reported. In our experience a standard deviation in migration time of 1-2% in a manually operated system and of less than 1% in an automated system is usually obtained. Causes of irreproducibility in migration times are irreproducibility in switching on the voltage (ramping from zero to running voltage), the manual start of the run timer in case of

non-automated systems, evaporation of organic modifier or buffer, or differences in sample conductivity. Other possible causes of especially inter-day variability are changes in the capillary condition, temperature, BGE composition or buffer pH.

The imprecision is determined by the standard deviation in peak height, in peak area or, if used, in the peak height or area ratios with the internal standard. Mean values of the reported imprecision over the total concentration range are used in Table III. In some cases a large imprecision was reported at a concentration near the detection limit. These values were not included. The imprecision varies strongly from 1-12%. In our experience the use of an internal standard reduces the imprecision with a factor 2-3. This is confirmed by case 9 where a factor 2 improvement is reported. Other factors such as the concentration range, the pretreatment and the complexity of the total method also play a role.

The inaccuracy is characterised as the difference between the real and measured concentration devided by the real concentration of a calibration standard. The mean value of the inaccuracy is in most cases, if reported, smaller than 3%. Some authors report the standard deviation in the recovery as inaccuracy. These data are not used in Table III.

The migration times vary from 5 to 20 minutes. The washing step between runs that is needed in some cases is not included. When the migration time was not mentioned the run time from a published electropherogram was used. The limit of determination (LOD, concentration detection limit in matrix) is given as reported by the author. This may be the concentration analyte that results in a signal that is 2, 3, 5 or 10 times the noise. None of the authors describes how the noise is defined (i.e. RMS noise, standard deviation of the noise or peak-to-peak noise). Comparison of sensitivities is therefore not relevant under these circumstances. Together with the concentration range the LOD gives a rough impression of the sensitivity of the method.

In some cases (1, 11, 16) a comparison was made with HPLC by linear regression of the obtained data by both methods. In all three cases the slope was not significantly differing from unity and the intercept was not significantly differing from zero. A comparison of a CZE and an EMIT method (enzyme multiplied immunoassay technique) for methotrexate (case 14) resulted in 50% lower concentrations determined by CZE. Cross reactivity of metabolites in the EMIT method is given as a possible explanation for these findings.

Conclusions

Capillary electrophoretic separations are widely applied in analytical procedures. The technique is capable of highly efficient separations which has been demonstrated for standard mixtures of carbohydrates, amino acids, catecholamines, polymers, proteins, peptides, DNA and RNA fragments, inorganic ions etc. Micellar systems have widened the applicability from separations of anions and cations to neutrals. Gel-filled capillaries and the use of entangled polymers in the BGE enabled high resolution separations of (bio-)polymers based upon differences in molecular mass. CIEF is suitable for separations of proteins with different isoelectric points. CITP is a powerful separation technique that has been used in many analytical methods. Recently, the technique has gained a lot of interest as concentrating pretreatment for CZE. The commercial availability of several automated systems makes CE in principle suitable for routine analysis. Especially in quality control such as determination of drugs in pharmaceutical preparations, CZE is already applied on a routine basis.

The limited loadability, the small optical path length and the resulting lack of sensitivity form one of the problem areas of the technique. Most applications of CE methods in bioanalysis concern the micromolar concentration range. The commercial availability of sensitive detection systems is limited. In most cases absorbance detection is used. Also the availability of complete analytical methods for determinations in complex matrix, including derivatisation procedures for LIF or ECD that are compatible with the small sample volumes in CE, are limited. A detector with zeptomol (zepto = 10^{-21}) sensitivity for derivatized amino acid standards can only be applied if a derivatisation procedure is available for the corresponding sample concentration levels.

Applications of CE in complex matrix that are using a concentrating sample pretreatment method or a derivatisation procedure are all based on off-line methods. For routine applications automated pretreatment procedures are required that can be combined on-line with CZE equipment. It is peculiar that although several automated pretreatment systems are available for HPLC, to our knowledge none of these systems has been utilised in combination with CE. Combining automated pretreatment and derivatisation methods with sensitive detection systems will make the potential of capillary electrophoretic separation methods available for trace analysis.

References

1. S. Hjerten, Chrom. Rev., 9 (1967) 122
2. R. Virtanen, Acta Polytech. Scand., 123 (1974) 1
3. F.M. Everaerts, J.L. Beckers and T.P.E.M. Verheggen, *Isotachophoresis: Theory, Instrumentation and Practice*, Elsevier, Amsterdam, 1976.
4. J.W. Jörgenson and K.D. Lukacs, Anal. Chem., 53 (1981) 1298
5. J.W. Jörgenson and K.D. Lukacs, J. Chromatogr., 218 (1981) 209
6. J.W. Jörgenson and K.D. Lukacs, Science, 222 (1983) 266
7. S. Terabe, K. Otsuka, K. Ichikawa, A. Tsuchiya and T. Ando, Anal. Chem., 56 (1984) 111
8. S. Terabe, K. Otsuka and T. Ando, Anal. Chem., 57 (1985) 834
9. R.A. Wallingford and A.G. Ewing, Adv. Chromatogr., 29 (1989) 1
10. W.G. Kuhr, Anal. Chem., 62 (1990) 403R
11. W.G. Kuhr and C.A. Monnig, Anal. Chem., 64 (1992) 389R
12. C.C. Campos and C.F. Simpson, J. Chromatogr. Sci., 30 (1992) 53
13. J.W. Jörgenson, Anal. Chem., 58 (1986) 743A
14. B. Karger, A.S. Cohen, and A. Guttman, J. Chromatogr., 492 (1989) 585
15. A.G. Ewing, R.A. Wallingford and T.M. Olefirowics, Anal. Chem., 61 (1989) 292A
16. M.J. Gordon, X. Huang, S.L. Pentoney and R.N. Zare, Science, 242 (1988) 224
17. F. Foret and P. Bocek, in A. Chrambach, M.J. Dunn, B.J.Radola (editors) *Advances in Electrophoresis*, Vol. 3, VCH Weinheim, 1989, p. 271-347
18. Z. Deyl and R. Struzinsky, J. Chromatogr., 569 (1991) 63
19. P. Bocek, M. Deml, P. Gebauer and V. Dolnik, *Analytical Isotachophoresis*, Electrophoresis Library 1, Ed. B.J. Radola, 1988, VCH, Weinheim, Switzerland.
20. J. Pospichal, P. Gebauer and P. Bocek, Chem. Rev., 89 (1989) 419
21. Hirokawa, M. Nishino, N. Aoki, Y. Kiso, Y. Sawamoto, T. Yagi and J.I. Akiyama, J. Chromatogr., 271 (1983) D1-D106
22. J.H. Knox and I.H. Grant, Chromatographia, 24 (1987) 135
23. J.H. Knox, Chromatographia, 26 (1988) 329
24. F. Foret, M. Deml and P. Bocek, J. Chromatogr., 452 (1988) 601
25. S. Hjerten, Electrophoresis, 11 (1990) 665
26. E. Grushka, R.M. McCormick and J.J. Kirkland, Anal. Chem., 61 (1989) 241
27. M. Albin, P.D. Grossman and S.E. Moring, Anal. Chem., 65 (1993) A489
28. R.L. Chien and D.S. Burgi, Anal. Chem., 64 (1992) 489A
29. G.J.M. Bruin, Thesis, 1992
30. S. Terabe, K. Otsuka and T. Ando, Anal. Chem., 61 (1989) 251
31. S. Terabe, H. Ozaki, K. Otsuka and T. Ando, J. Chromatogr., 332 (1985) 211
32. E. Gassmann, J.E. Kuo and R.N. Zare, Science, 230 (1985) 813
33. J. Snopek, I . Jelinek and E. Smolkova-Keulemansova, J. Chromatogr., 452 (1988) 571
34. V. Kasicka and Z. Prusik, J. Chromatogr., 569 (1991) 123
35. A.S. Cohen and B.L. Karger, J. Chromatogr., 397 (1987) 409
36. A.S. Cohen, A. Paulus and B.L. Karger, Chromatographia, 24 (1987) 15
37. Y. Baba, T. Matsuura, K. Wakamoto, Y. Morita, Y. Nishitsu, M. Tsuhako, Anal.Chem., 64 (1992) 1221

38. L.M. Smith, Nature, 349 (1991) 812
39. S. Compton and R. Brownlee, Biotechniques, 6 (1988) 432
40. J.R. Mezzeo and I.S. Krull, Biotechniques, 10 (1991) 638
41. M.D. Zhu, R. Rodriguez and T. Wehr, J. Chromatogr., 559 (1991) 479
42. Y.F. Ma, Z.K. Wu, H.C. Furr, C. Lammikeefe and N.E. Craft, J. Chromatogr., 616 (1993) 31
43. D.K. Lloyd, A.M. Cypess and I.W. Wainer, J. Chromatogr., 568 (1991) 117
44. M. Tomita, T. Okuyama, Y. Nigo, B. Uno and S. Kawai, J. Chromatogr., 571 (1991) 324
45. P. Gareil, J.P. Gramond and F. Guyon, J. Chromatogr., 615 (1993) 317
46. H. Nishi, T. Fukuyama and M. Matsuo, J. Chromatogr., 515 (1990) 245
47. N. Wu, T.S. Wang, R.A. Hartwick and C.W. Huie, J. Chromatogr., 582 (1992) 77
48. K.J. Lee, G.S. Heo, N.J. Kim and D.C. Moon, J. Chromatogr., 577 (1992) 135
49. K.J. Lee, G.S. Heo, N.J. Kim and D.C. Moon, J. Chromatogr., 608 (1992) 243
50. A. Baillet, G.A. Pianetti, M. Taverna, G. Mahuzier and D. Baylocqferrier, J. Chromatogr., 616 (1993) 311
51. H. Soini, M.L. Riekkola and M.V. Novotny, J. Chromatogr., 608 (1992) 265
52. A.C. Schoots, T.P.E.M. Verheggen, P.M.J.M. de Vries and F.M. Everaerts, Clin. Chem., 36 (1990) 435
53. N.J. Reinhoud, U.R. Tjaden, H. Irth and J. van der Greef, J. Chromatogr., 574 (1992) 327
54. J. Prunonosa, R. Obach, A. Diezcascon and L. Gouesclou, J. Chromatogr., 574 (1992) 127
55. M.C. Roach, P. Gozel and R.N. Zare, J. Chromatogr., 426 (1988) 129
56. K.J. Lee, J.J. Lee and D.C. Moon, J. Chromatogr., 616 (1993) 135
57. J. Prunonosa, R. Obach, A. Diezcascon and L. Gouesclou, J. Chromatogr., 581 (1992) 219

Table IV. Ionic mobilities m (10^{-9} $m^2V^{-1}s^{-1}$) of frequently used electrolytes. The mobilities are given at zero ionic strength (I in mmol/l) in water, at a temperature of 298 K [19] or not specified [3, 20] (ambient) unless otherwise specified.

ion	m	pK_a	I	ref.
ACES	-31.3	6.8	5	20
acetate	-42.4	4.8		19
acetylsalicylate	-26.7	3.5	10	20
α-alanine	-32.2	9.9		20
β-alanine	36.7	3.6		19
β-alanine	-30.8	10.2		20
ε-aminocaproate	29.8	4.4		20
ammediol	29.5	8.8		19
ammonium	76.1	9.2		19
aniline	38.7	4.7		20
arginine	26.9	8.9		20
asparagine	-31.6	9.0		20
aspartate(1-)	-30.1	3.9		20
aspartate(2-)	-55.4	10.0		20
benzoate	-32.9	4.2		20

ion	m	pK_a	I	ref.
BES	-24.0	7.2	6	20
bromide	-78.4			3
cacodylate	-29.9	6.2		20
carbonate(1-)	-46.1	6.4		19
carbonate(2-)	-71.8	10.3		19
chlorate	-66.6			20
chloride	-79.1			19
chloroacetate	-41.9	2.9		20
chromate(1-)	-59.3	0.7		20
chromate(2-)	-81.1	6.5		20
citrate(1-)	-31.0	3.1		20
citrate(2-)	-53.4	4.8		20
citrate(3-)	-70.8	6.4		20
creatinine	36.8	4.8		20
cyanide	-78.0	9.5		3

ion	m	pK_a	I	ref.
diethanolamine	30.6	8.9	10	20
ethanolamine	44.3	9.5		20
formate	-56.6	3.8		19
fumarate(1-)	-35.1	3.0		20
fumarate(2-)	-60.5	4.4		20
glucuronate	-26.6	3.5		20
glutamate (1+)	28.7	2.2		20
glutamate (1-)	-28.7	4.3		20
glutamate(2-)	-54.3	10.0		20
glutamine	-28.8	9.2		20
glycine	-37.4	9.8		20
glycylglycine	-31.5	8.4		20
HEPES	-21.8	7.5	5	20
HEPPSO	-22.0	7.5	5	20
hippurate(1-)	-25.9	2.5		20
hippurate(2-)	-55.3	7.3		20
histidine	29.6	6.0		20
histidine	-28.3	9.3		20
hydrogen	362.5			19
hydroxide	-205.5			19
imidazole	52.0	7.2		20
isoleucine	-26.7	9.8		20
leucine	-26.4	9.7		20
lithium	38.7			3
lysine	26.4	9.1		20
lysine	-26.4	10.8		20
malate(1-)	-34.9	3.5		20
malate(2-)	-58.5	5.1		20
maleate(1-)	-42.5	1.9		20
maleate(2-)	-62.0	6.2		20
malonate(1-)	-42.4	2.8		20
malonate(2-)	-65.4	5.7		20
MES(1-)	-26.8	6.1		20
methionine	-29.3	9.3		20
4-methyl-pyri-dinium	42.8	6.1		20
MOPS	-24.4	7.2	6	20

ion	m	pK_a	I	ref.
MOPSO	-23.8	6.8	6	20
oxalate(1-)	-44.9	1.3		20
oxalate(2-)	-74.6	4.3		20
perchlorate	-70.0			20
phosphate(1-)	-35.1	2.1		19
phosphate(2-)	-61.5	7.5		19
phosphate(3-)	-71.5	12.4		19
pimelate(1-)	-27.6	4.5		20
pimelate(2-)	-48.4	5.3		20
potassium	76.2			19
proline	-25.4	10.6		20
propionate	-36.9	4.8		20
pyridinium	51.1	5.1		20
pyruvate	-42.3	2.5		20
salicylate	-35.3	2.9		20
serine	-33.6	9.3		20
sodium	51.9			19
sorbate	-27.3	4.8	10	20
succinate(1-)	-35.2	4.2		20
succinate(2-)	-57.5	5.6		20
sulfate(1-)	-52.0			19
sulfate(2-)	-82.9	1.9		19
TAPS	-25.0	8.3		20
TES	-22.4	7.4		20
threonine	-30.9	9.2		20
trichloroacetate	-36.2	0.6		20
triethanolamine	30.0	7.8		20
triethyl-ammonium	33.8	10.7		20
TRIS	29.5	8.1		20
tryptophane	-25.4	9.6		20
tyrosine(1-)	-20.0	9.0		20
tyrosine(2-)	-40.0	10.2		20
valine	-28.4	9.7		20

1.2

Bioanalysis of some Anthracyclines in Human Plasma by Capillary Zone Electrophoresis with Laser-induced Fluorescence Detection

Abstract

A rapid method for the determination of daunorubicin, doxorubicin and epirubicin in human plasma is described. Samples are pretreated and concentrated by a liquid-liquid extraction with chloroform and a back extraction into phosphoric acid, respectively. This pretreatment results in a sample matrix of low ionic strength in comparison with the electrophoresis buffer enabling a 20 - 30 fold increase of the injected amount by zone sharpening when electrokinetic injection is applied. Analyte interaction with the capillary wall is prevented by using high acetonitrile contents in the electrophoresis buffer, which results in reproducible migration times and highly efficient separations. Laser-induced fluorescence detection provides an extremely sensitive and selective method without detectable biological interferences. The limit of quantification of daunorubicin, epirubicin and doxorubicin in plasma ranges from 125 - 250 pg/ml.

Introduction

The drug doxorubicin (DOX) and its epimer epirubicin (EPI) are two of the most frequently used anthracycline antibiotics in the treatment of a wide variety of cancers. Because of the serious side effects of chemotherapy, there is a continuous search for analogues with better therapeutic characteristics. As a result numerous analytical procedures have been developed for anthracyclines and several reviews have been published. The analytical aspects of cytostatic drug analysis have recently been reviewed [1]. High-performance liquid chromatography (HPLC) is frequently used for the quantitative analysis of anthracyclines and, especially in combination with fluorescence detection, low detection limits can be achieved. Under acidic conditions the anthracyclines show native fluorescence [1-3].

Capillary zone electrophoresis (CZE) is a separation technique that is characterised by its extremely high efficiencies and short analysis times [4,5], recently reviewed by Kuhr [6]. However, although plate numbers of more than one million have been reported these efficiencies are not always obtained in bioanalytical applications. A biological matrix, especially plasma,

contains high concentrations of interfering compounds such as proteins and salts. Therefore, a sample pretreatment resulting in a matrix that is compatible with the CZE buffer (i.e. deproteinated, same ionic strength) is of extreme importance for reproducible analysis.

The injection volumes in CZE are in the order of 0.1 - 10 nl. This implicates that only a few microlitres of sample have to be pretreated of which only a fraction will be analysed. In this assay the sample volume to be pretreated is only limited by the amount of analyte that can be handled without decrease of reproducibility and sensitivity due to aspecific adsorption onto the surface of sample vials and other laboratory materials.

As a consequence of the small optical path length of narrow bore capillaries the concentration detection limits in CZE are relatively high. Highly sensitive detectors such as systems based on laser-induced fluorescence (LIF) are mandatory and several publications appeared in literature showing very low detection limits [7].

Literature on the application of CZE in the bioanalysis of drugs in plasma samples is limited demonstrating the difficulties of working with biological matrices. Roach et al. [8] presented a method for the bioanalysis of methotrexate in plasma using solid phase isolation, followed by a concentration step before CZE analysis. Nishi et al. [9] described the analysis of aspoxicillin in plasma with direct sample injection using micellar electrokinetic capillary chromatography (MECC). Sodium dodecylsulphate (SDS) in the electrophoresis buffer complexates with the plasma proteins and prevents protein adsorption onto the capillary wall.

In this Chapter a bioanalysis of some anthracyclines is described using CZE in combination with LIF. For the optimisation of the CZE analysis a test mixture of DOX and EPI is used, which are stereoisomers only differing in that the hydroxyl group at C-4' of the daunosamine is inverted. For calibration plots of both drugs daunorubicin (DAU) is used as internal standard, which differs from DOX in that an extra hydroxyl group is present on the adriamycinone [1,3]. The applicability of the method is demonstrated with the analysis of samples from cancer patients treated with EPI.

Experimental

Equipment

CZE was carried out in a 700 x 0.075 mm ID fused silica capillary (SGE, Ringwood, Victoria, Australia) using an electrophoresis buffer composed of acetonitrile (ACN) in 100 mM, pH 4.2 sodium phosphate buffer (PB) (7:3, v/v). The voltage (20 - 25 kV) was supplied by a

model RR100-1.5P power supply (Gamma High Voltage Research, Mt. Vernon, NY, USA) operating in the constant current mode at 35 μA. The current was measured in series between the cathode and earth using a micro-amperometer (#134312, Goerz, Vienna, Switzerland). Samples were electrokinetically injected applying 12 kV for 5 s.

On-capillary LIF detection took place at 650 mm from the anodic end, using a water-cooled argon-ion laser (2025-03, Spectra-Physics Inc., Mt. View, CA, USA) lasing at a wavelength of 476.5 nm at 80 mW for excitation. For comparison of detection limits an air-cooled argon-ion laser (#162D07, Spectra-Physics Inc.) operating at 5 mW at a wavelength of 488 nm has been used.

The laser beam was focused on the capillary from which the polyimide coating over a length of several mm was removed. Fluorescence light was transported to the photomultiplier tube (PMT) through a liquid light guide (1000 x 5.0 mm ID, #77556 Oriel, Stratford, C.T., USA) equipped with a plano convex fused silica lens (D 11 mm, focal length 19 mm, Model 41210) at each end. The fluorescence light was directed onto a 595 nm band pass interference filter (10 nm bandwidth, type 53920 Oriel). The PMT (model RFIB235F, Thorn EMI, Ruislip, Middlesex, UK) was operated at 800 V (power supply model PM28B, Thorn EMI).

The signal was amplified by a current amplifier (model 427, Keithley Instruments Inc., Cleveland, Ohio, USA) and digitised using a custom-made 12-bit A/D converter operating at a frequency of 20 Hz. The A/D converter was connected to a computer (Atari Mega ST4, Atari Corp., Sunnyvale, CA, USA) which controlled the operating voltage, the injection voltage and injection time, the sampling frequency of the converter and the data handling.

Chemicals

Doxorubicin (Adriblastina) and epirubicin (Farmorubicine) were both available as 1 mg/ml chlorohydrate solutions containing 5 mg/ml lactose and were purchased from Farmitalia, Carlo Erba S.A., Belgium. Daunorubicin (Cerubidine) was purchased from Rhône-Poulenc (France). Chloroform (J.T. Baker, Deventer, The Netherlands) and phosphoric acid 85% (Merck, Darmstadt, FRG) were of analytical grade. Acetonitrile (Rathburn, Walkerburn, Scotland) was HPLC grade and degassed and sucked through a 0.2 μm membrane filter (type SM 11606, Sartorius, Breukelen, The Netherlands) after mixing with 100 mM sodium dihydrogenphosphate (Merck, Darmstadt, FRG) buffer. Throughout all experiments demineralised water was used.

Calibration curves and extraction

Plasma samples were spiked with EPI and DOX at a concentration range of 0.3 - 300 ng/ml by adding 100 μl EPI and DOX (in PB 10 mM pH 4.2 containing 10% ACN) to 900 μl plasma in 10 ml polyethylene vials. A final DAU concentration of 100 ng/ml was used as internal standard (IS) for analysis of patient samples. For assay validation 5 ng/ml DAU was used. A 1-ml volume of spiked plasma was extracted by adding 2 ml of chloroform, vortex mixing for 1 min and centrifuging for 10 min at 1000 g. A volume of 1.6 ml of the lower organic layer was removed, extracted with 100 μl of 5 mM phosphoric acid at pH 2.3, vortex mixed and centrifuged in the same way. A 50-μl volume of the upper layer was removed and used for CZE analysis after addition of 150 μl of ACN, resulting in a final ACN concentration of 75%. Patient samples were treated the same way except that, instead of adding EPI or DOX, 100 μl of DAU (1.0 μg/ml) was added to 900 μl of serum as IS.

Results and discussion

Development of the CZE system

In preliminary experiments with a phosphate buffer DAU, DOX and EPI are not separated. Such conditions resulted in a poor performance due to interactions with the capillary wall (Fig. 1a). By modifying the electrophoresis buffer with 70% ACN the interaction of analyte with the capillary wall decreased and the peak shape and the resolution of DAU, DOX and EPI improved dramatically (Fig. 1b).

The field strength is optimised to 33 kV/m. Higher field strengths resulted in loss of efficiency and resolution because of the increased heat generation in the capillary. Early reports on CZE described a linear relationship between the efficiency an the applied voltage when diffusion is the major contribution to peak broadening [5]. However, when capillaries with diameters above 50 μm are used the Joule heat becomes an important source of peak broadening and an optimum in the applied voltage exists with respect to efficiency [10].

In the present assay relative peak heights and areas are calculated using an internal standard for quantification, implying that it is not necessary to know the exact sample volume injected. This also implicates that, assuming that the total electrophoretic mobilities do not change during analyses, it is not necessary to make corrections for the discrimination of analytes which is

in principle the case when electrokinetic injection applied [11]. However, for optimisation purposes it is interesting to have some insight in the injection volume. In terms of detectability high injection volumes are favourable but the efficiency decreases as a result of the broader zones (Fig. 2).

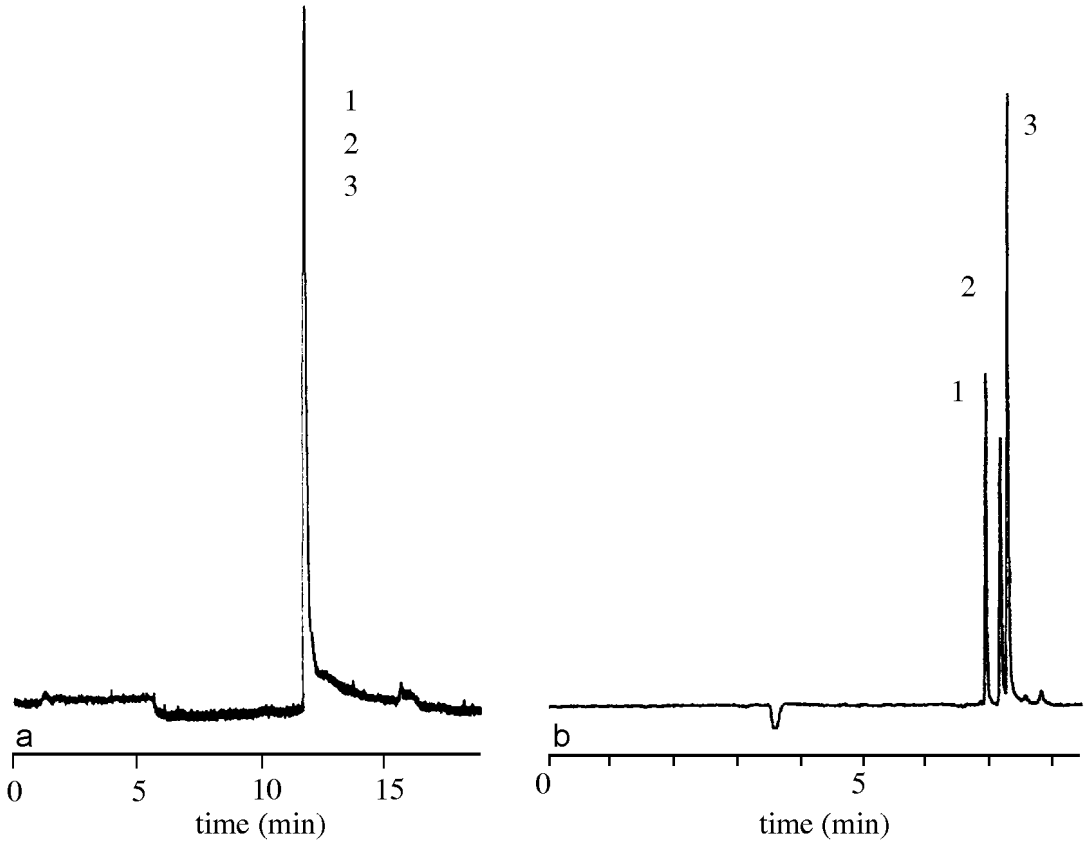

Fig. 1. Effect of the addition of acetonitrile to the electrophoresis buffer on the separation of anthracyclines. (a) CZE analysis of a mixture of 1 μg/ml DAU (1), EPI (2) and DOX (3) in 20 mM PB pH 4.2, using a voltage of 20 kV over a 75 μm x 70 cm capillary (65 cm to detection). The injection is made electrokinetically at 10 kV for 5 s. (b) The separation of 100 ng/ml DAU (1), EPI (2) and DOX (3) in 100 mM PB (pH 4.2), diluted 3:7 with ACN. The injection is made electrokinetically at 12 kV for 5 s, other conditions as in (a).

Some authors describe the maximum loadability of the capillary without considerable loss of efficiency to be at 1% of the total capillary volume [10]. The injection volume in case of

electrokinetic injection for a certain compound is determined by both the injection voltage and the duration of the pulse. Therefore we characterised the injection volume as a block (voltage x duration). The injection block is increased from 4kV x 4s to 15kV x 7s. Injection blocks larger than 12kV x 5s resulted in broader peaks, not in a higher fluorescence signal (Fig. 2).

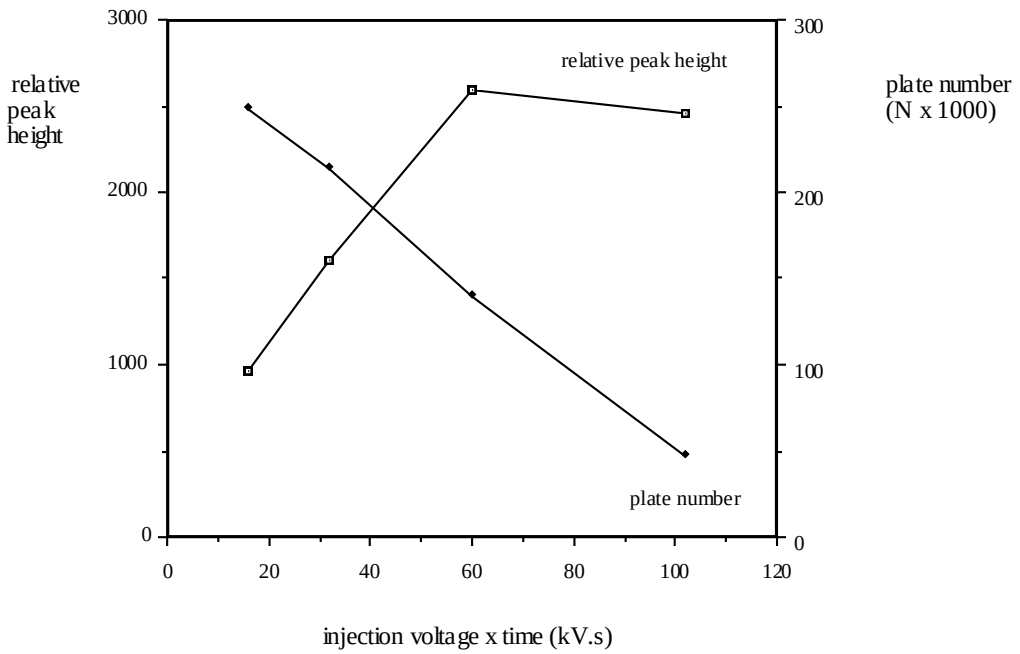

Fig. 2. Effect of injection volume on the efficiency and the peak height for a 100 ng/ml solution of DOX in electrophoresis buffer. CZE conditions are the same as in Fig. 1b.

An injection of 12 kV during 5s is chosen corresponding to a plug length of 3.2 mm and a plug volume of 14 nl being 0.5% of the total volume and resulting in plate numbers of approximately 170000 for DOX. The injection volume and plug length are calculated from the total electrophoretic mobility of DOX ($3.24\ 10^{-4}$ $cm^2\ V^{-1}s^{-1}$). This calculation is only relevant when the mobility in the sample matrix is the same as in the electrophoresis buffer i.e. same pH, ionic strength, viscosity etc. Therefore the optimisation is done with a mixture of 100 ng/ml DOX and 500 ng/ml EPI in electrophoresis buffer. This also implicates that no zone sharpening took place.

Laser induced fluorescence detection

The influence of the laser power of the water-cooled argon-ion laser on the signal and noise level for DOX is investigated. An optimum appeared in the minimum detectable concentration (MDC), calculated as the concentration which results in a signal-to-noise ratio of 3, at 100 mW (Fig. 3A).

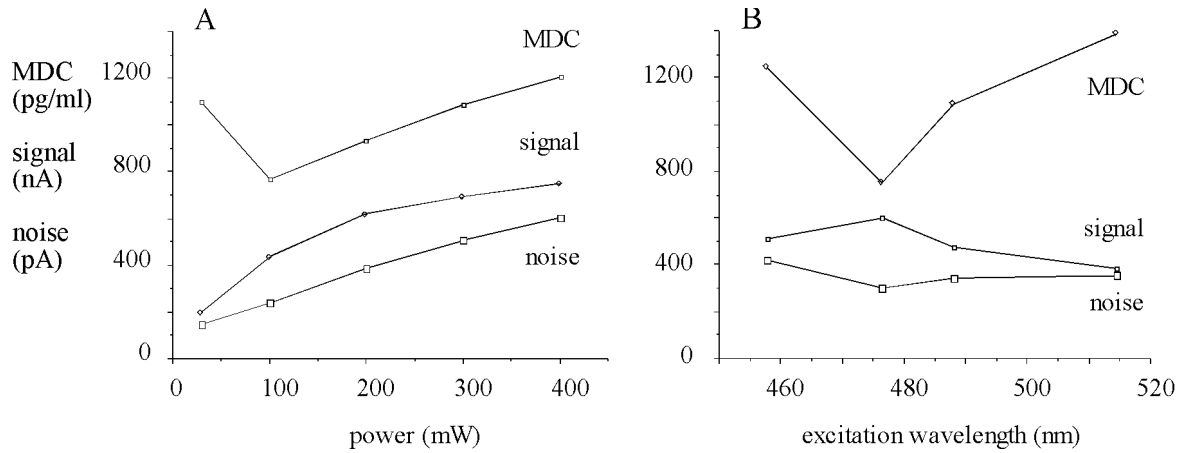

Fig. 3. Effect of the power (A) at 488 nm and the wavelength (B) at 100 mW of the excitation laser beam on the fluorescence of a 500 ng/ml DOX solution in electrophoresis buffer and on the noise level. See text for further conditions.

Due to the photodegradation of DOX the fluorescence signal is not proportional to the laser power in contrast with the noise resulting in an increased MDC at higher laser powers. Since the excitation maximum of anthracyclines is between 450 and 520 nm and the laser can supply several lasing wavelengths between 457 and 515 nm, the MDC at different lasing lines is determined. The fluorescence signal (peak height) of a 500 ng/ml DOX solution in electrophoresis buffer after injection at 20 kV for 10 s, and the noise level are measured. The MDC for DOX is 1.24, 0.75, 1.09 and 1.39 ng/ml for excitation at 457.9, 476.5, 488.0 and 514.5 nm, respectively. Excitation at 476.5 nm resulted in a higher fluorescence signal and a lower noise in comparison with the other wavelengths (Fig. 3B).

The DOX is dissolved in electrophoresis buffer which means that no preconcentration by stacking during injection took place. The injection is done by overloading the capillary in order to get a maximum and reproducible fluorescence signal. As can be seen in Fig. 2 injection

blocks larger than 80 kVs give a maximum fluorescence and variations in injection volume do not affect peak heights, only the peak area.

Experiments with a low-cost air-cooled argon-ion laser operating at 5 mW and 488 nm showed a MDC for DOX in electrophoresis buffer (i.e. without zone sharpening) of 8 ng/ml. Although a factor of 9 higher in detection limit, this type of laser should be usable for the described anthracycline assay, in combination with a concentrating pretreatment.

Sample treatment

DOX and analogues are known to adsorb to glassware and laboratory materials [1] introducing a source of irreproducibility, especially at low concentrations. Therefore, care is taken that all anthracycline solutions contained at least 10% ACN. To demonstrate the necessity of ACN, a dilution is made of 100 ng/ml EPI in 10 mM phosphate buffer pH 4.2 in a 10 ml polyethylene vial. The fluorescence signal is measured and considered to be 100%. An aliquot is transferred from the 10 ml vial to a 1.5 ml polyethylene Eppendorf vial and the fluorescence is immediately measured. The fluorescence signal reduced to 30% and after vortex mixing the 1.5 ml vial for 5 s the signal reduced to 15%. However, when the same experiment is done in presence of 10% ACN no decrease of fluorescence is observed.

Determination in plasma

In preliminary experiments for the bioanalysis of anthracyclines, a sample pretreatment consisting of a deproteination step of spiked plasma samples by addition of 400 µl ACN to 200 µl plasma (66% ACN), resulted in a rapid and reproducible method. The deproteinated plasma samples are directly analysed without further pretreatment and no interferences from the plasma matrix could be observed. However, because of the diluting sample pretreatment the detection limit of DOX in plasma is 30 ng/ml, which is not low enough for analysis of plasma samples from cancer patients. Therefore a concentrating sample pretreatment using liquid-liquid extraction and back extraction is applied.

The MDC of DAU, EPI and DOX in plasma based on a signal-to-noise ratio of 3 is 50, 70 and 35 pg/ml respectively (Fig. 4). The limit of quantification (i.e. the determination limit) defined as the concentration of analyte in plasma resulting in a signal-to-noise ratio of 10, is 175, 250 and 125 pg/ml, respectively. The noise is defined as 0.2 times the peak-to-peak noise. The double liquid-liquid extraction which results in a sample matrix with a low ionic strength (5 mM phosphoric acid/75% ACN) appears to be very advantageous regarding the detection

limits because of a strong zone sharpening effect during electrokinetic injection. This zone sharpening results in a 20 - 30 fold increase of peak height. Also the efficiencies of the anthracyclines improved to plate numbers ranging from $3 \cdot 10^5$ to $5 \cdot 10^5$.

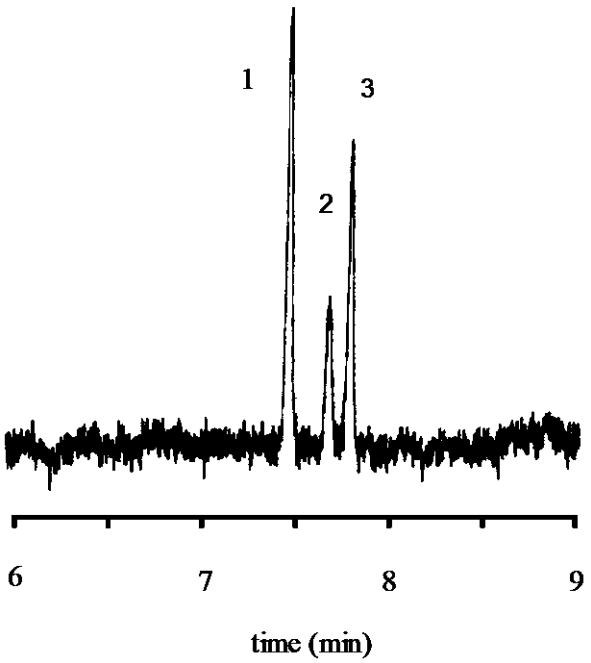

Fig. 4. Electropherogram of an extract of blank plasma spiked with 1 ng/ml DAU (1), 500 pg/ml EPI (2) and 500 pg/ml DOX (3). CZE conditions are the same as in Fig. 1b. See text for sample pretreatment procedure.

The peak concentrating effect is measured for a mixture of DAU, DOX and EPI with a concentration of 100 ng/ml after dilution. When the dilution is made in electrophoresis buffer the signals are 20 - 30 times lower compared to a dilution in 5 mM phosphoric acid to which 75% ACN is added. The MDC for DAU, EPI and DOX in electrophoresis buffer without zone sharpening, amounts to 1.4, 1.5 and 0.9 ng/ml, respectively. The overall improvement in detectability is realised by zone sharpening (factor 20-30). The concentrating pretreatment (factor 8) is counter balanced by the recovery (factor 0.4 - 0.7, see validation below) and a dilution (factor 0.25) because of addition of 75% ACN to the extraction buffer before CZE analysis.

An additional advantage of the extraction procedure in combination with the high ACN percentage in the electrophoresis buffer is that there is no need for cleaning steps between runs. The extraction procedure results in a clean and well defined sample matrix, while the high ACN content prevents interaction of the analytes with the capillary wall. This resulted in a relative standard deviation in migration times smaller than 0.5% (n=5), which corresponds to a standard deviation of 2 s at a migration time of approximately 8 min for the three anthracyclines.

Validation

A typical calibration plot of EPI in plasma, used for analysis of patient samples, corresponded to the calculated regression equation $Y = (8.66 \pm 0.08)\ 10^{-3}\ X + (0.017 \pm 0.017)$, ($r = 0.99997$) where Y is the ratio of the peak areas of EPI to DAU, X is the concentration of EPI (ng/ml) and r is the correlation coefficient.

Table 1. Validation of the anthracycline assay. Mean values and coefficients of variation are given for n=4 in all cases, except for inter-day variation where n=3.

Conc.	EPI				DOX			
	Mean	C.V.	Inaccuracy		Mean	C.V.	Inaccuracy	
(ng/ml)	(ng/ml)	(%)	(ng/ml)	(%)	(ng/ml)	(%)	(ng/ml)	(%)
Inter-day variability								
0.5	0.493	1.7	0.007	1.4	0.509	3.5	0.009	1.8
5	5.07	5.4	-0.07	-1.5	4.96	1.9	-0.04	-0.8
10	10.1	2.0	-0.1	-1.3	10.2	2.4	0.2	2.2
Intra-day variability								
0.5	0.486	3.0	0.014	2.9	0.501	6.9	0.001	0.2
5	4.91	1.0	0.09	1.9	4.90	1.9	-0.1	-2.1
10	10.2	3.3	0.2	1.9	10.2	2.0	0.2	2.1

The precision of the assay is measured as the inter-day and the intra-day variability for EPI and DOX in plasma (n=4) at concentrations of 0.5, 5 and 10 ng/ml. The intra-day precision is calculated as the coefficient of variation (CV) of the four determinations and varied from 1.0 - 6.9% (Table I). The inter-day precision is calculated as the CV of the mean of the measured concentrations on three different days (n=3) and varied from 1.7 - 5.4% (Table I). The inaccuracy of the assay is determined by calculating the difference between the measured and the real concentration (Table I).

The reproducibility of the CZE system only is determined for n=6 injections of a 1 μg/ml solution of DAU and DOX in electrophoresis buffer. The CV of the peak areas is 7% for DOX and 8% for DAU while the CV of the peak area ratios is 2.5%.

Table 2. Recoveries of doxorubicin and epirubicin. The mean values of n=4 determinations are given for each concentration.

Conc.	Recovery (mean ± C.V.) (%)	
(ng/ml)	EPI	DOX
0.5	55 ± 16	50 ± 15
5.0	55 ± 8	45 ± 8
50.0	70 ± 8	66 ± 8

The recovery is measured for different concentrations of EPI and DOX at 0.5, 5 and 50 ng/ml in plasma (n=4). A correction in the calculation is made for the 20% loss of chloroform where 1.6 ml of the total 2.0 ml is re-extracted and for the concentration factor of 10 (1 ml plasma to 100 μl phosphoric acid). This results in a theoretical concentrating factor of 8. Concentrating factors of 3.5 - 5.6 corresponding to recoveries of 45 - 70 % with CV's of 16 - 8% are measured (Table II).

The usefulness of the developed method is demonstrated with the analysis of plasma samples of a cancer patient treated with 50 mg/m^2 EPI. The CZE analysis of plasma samples shows a remarkably clean background, which is caused by the combination of the extraction procedure and the selective detection (Fig. 5). There are not many compounds in the biological matrix having native fluorescence in the visible part of the spectrum. Fig. 6 shows the plasma concentration time course for the same patient.

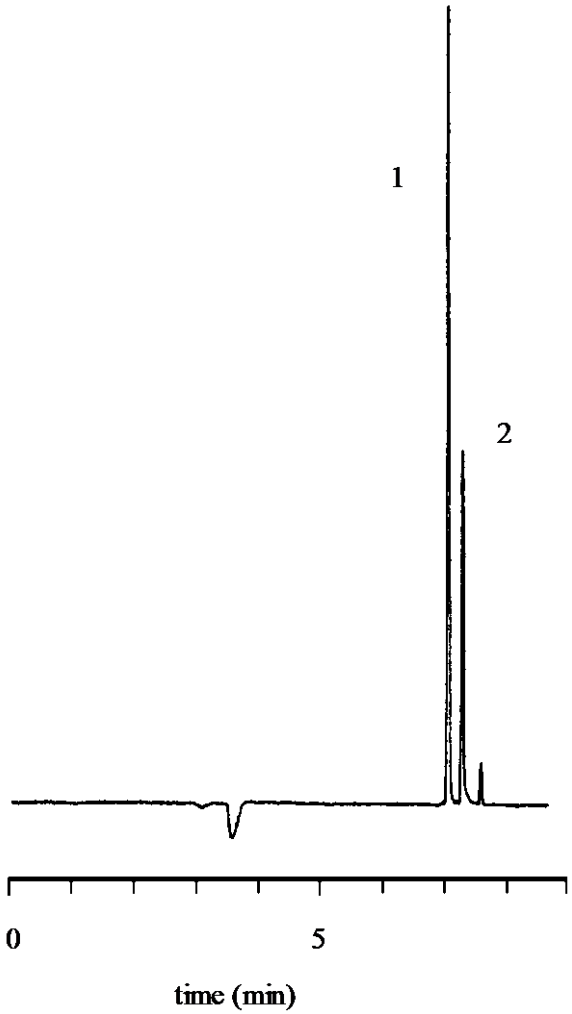

Fig. 5. Electropherogram of an extract of a plasma sample taken 120 min after administration from a patient treated intravenously with 50 mg/m^2 EPI (2) intravenously; 100 ng/ml of DAU (1) is used as internal standard. The EPI peak corresponds to 27 ng/ml. The small third peak could not be identified.

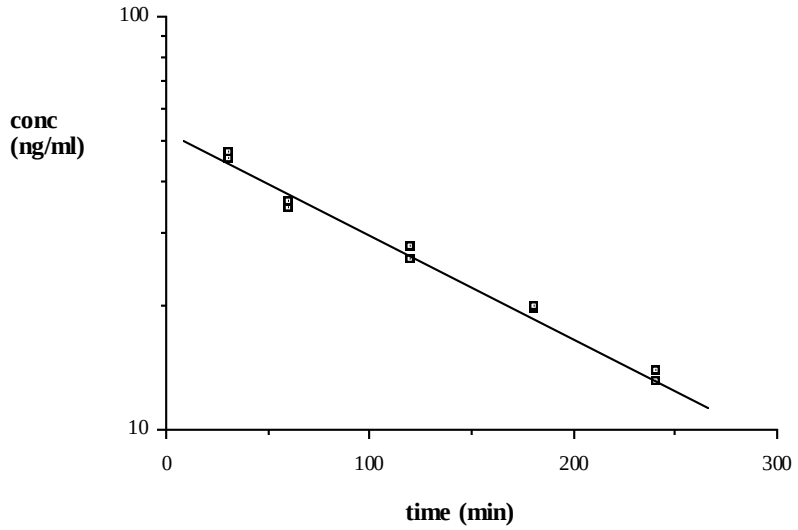

Fig. 6. Plasma concentration time course from the patient samples as described in Fig. 5.

Conclusion

A sensitive and selective assay for the determination of anthracyclines in plasma is presented. Detection limits in the pg/ml range have been obtained, resulting in an interesting alternative for HPLC methods where analyses may be disturbed by interferences originating from the biological matrix or where the selectivity and efficiency are not satisfactory.

References

1. U.R. Tjaden and E.A. de Bruijn, J. Chromatogr., 531 (1990) 235
2. P.A. Maessen, K.B. Mross, H.M. Pinedo and W.J.F. van der Vijgh, J. Chromatogr., 417 (1987) 339
3. A. Suarato in D.E.V. Wilman (Editor), *The Chemistry of Antitumour Agents*, Blackie, London, 1990, Chapter 2.
4. B. Nickerson and J.W. Jörgenson, J. High Resolut. Chromatogr. Chromatogr. Commun., 11 (1988) 533
5. J.W. Jörgenson and K.D. Lukacs, J. Chromatogr., 218 (1981) 209
6. W.G. Kuhr, Anal. Chem., 62 (1990) 403R
7. Y. Cheng and N.J. Dovichi, Science, 242 (1988) 562
8. M.C. Roach, P. Gozel and R.N. Zare, J. Chromatogr., 426 (1988) 129
9. H. Nishi, T. Fukuyama and M. Matsuo, J. Chromatogr., 515 (1990) 245
10. F. Foret, M. Deml and P. Bocek, J. Chromatogr., 452 (1988) 601
11. R.A. Wallingford and A.G. Ewing, Adv. Chromatogr., 29 (1989) 1

1.3

Manipulation of Anions in Capillary Zone Electrophoresis with Indirect Absorbance Detection

Abstract

In the first part of this Chapter different optimisation procedures are proposed for anionic systems with and without electroosmotic flow using indirect absorbance detection. Several factors contribute to zone broadening which are dependent on the configuration of the capillary zone electrophoresis (CZE) system. Therefore, all sources of zone broadening and the effect on the relative peak height in indirect detection are considered for several analyte and chromophore mobilities.

In the next part of this Chapter certain exceptional cases are considered where hydrodynamic manipulation improves the capillary electrophoretic analysis of anions with indirect absorbance detection. It can be used in cases where high efficiencies are not required such as a rapid screening of the migration order of anions as used in setting up ITP-CZE methods. Calculated zone widths are compared with experimental results for several test compounds.

Introduction

In CZE the high electric field strength facilitates highly efficient separations with plate numbers of 10^5 - 10^6. In an optimised CZE system longitudinal diffusion is the predominant source of zone broadening. However, at high field strength the heat development inside the capillary causes a radial temperature profile which results in thermal dispersion. Therefore, a high field strength is used in combination with narrow bore capillaries with good heat dissipating properties. An optimum electric field strength can be found with respect to the plate number [1, 2].

In practice several other factors may contribute to zone broadening in CZE such as adsorption to the capillary wall, the detection cell dimensions and the injection zone length. At high analyte concentrations or high sample buffer concentrations the conductivity difference between the sample zone and the CZE background electrolyte results in electromigration dispersion. Studies on these phenomena resulted in some practical rules for highly efficient separations. The injection zone length should be smaller than 1 % of the total capillary length and the sample should be dissolved in background electrolyte at a concentration below 1% of the buffer

concentration [2]. With respect to detection sensitivity it is not always possible to apply low sample concentrations. Especially in indirect detection systems electromigration dispersion due to a high analyte concentration may be a problem.

Indirect absorbance detection is based on the displacement of the chromophore by analyte ions [3]. The concentration of chromophore in the analyte zone is lower than in the background electrolyte and a negative signal is obtained. In an ideal situation the conductivity of the analyte zone is the same as the conductivity of the BGE and the homogeneity of the electric field is not disturbed. However, often poor concentration detection limits are obtained in indirect absorbance detection, reason why often high analyte concentrations are applied. This results in disturbances in the local electric field strength and in electromigration dispersion. Zone broadening and asymmetric peaks are therefore often characteristic for CZE with indirect detection. Choosing a chromophore with a mobility similar to that of the analyte ions is one of the possibilities in optimising an indirect detection system. Another option is to keep the analyte concentration as low as possible [3-5].

This Chapter deals with two aspects of CZE with indirect detection. First, a generally applicable optimisation is described. All contributions to zone broadening are considered in systems with and without electroosmotic flow. Optimum peak heights are calculated for several analyte and chromophore mobilities. Different optimisation procedures are proposed for anionic systems with or without electroosmotic flow.

The second aspect deals with certain exceptional situations where hydrodynamic manipulation improves the performance in CZE. A hydrodynamic flow is used to reduce the electrophoretic migration distance and the analysis time. In certain cases of CZE with indirect detection, where electromigration dispersion often occurs, this results in a decrease of zone broadening. Anions with an electrophoretic velocity similar to the electroosmotic flow velocity in the opposite direction, can be detected without modifications of the capillary or the buffer by the described method. In our experience, the method is conveniently used in cases where high efficiencies are not required such as a rapid screening of the migration order of anions as used in setting up ITP-CZE methods [20, 21, Chapter 3.2].

Experimental

CZE with indirect detection

Untreated fused silica (100 μm ID, SGE, Ringwood, Victoria, Australia) capillary was used. The diameter was verified by weighing the water filled capillary and was 95 μm ID. The capillary length was 50 cm, the effective length from injection to detection was 25 cm. On-capillary UV absorbance detection took place using a Spectra 100 UV/VIS detector (Spectra-Physics Inc., Mt. View, CA, USA) at a wavelength of 210 nm. The CZE background electrolyte consisted of 10 mmol/l benzoic acid set at pH 8.0 with triethanolamine (TEtOHA, pK_a 7.76). The mobility of fully ionised TEtOHA was experimentally verified at pH 5.0 and was 30 10^{-9} $m^2V^{-1}s^{-1}$. The ionic mobility of benzoate is -32.9 10^{-9} $m^2V^{-1}s^{-1}$ [6] (pK_a 4.2). The electroosmotic mobility was experimentally determined and was 54.4 10^{-9} $m^2V^{-1}s^{-1}$. The current at 15 kV amounted to 14 μA, which means that the measured conductivity of the background electrolyte was 0.066 S/m. All experiments were carried out at room temperature (293 K) without capillary cooling. Injections were performed manually at a height difference of 5 cm for 5 s which corresponds to a 10 nl injection and an injection zone length of 1.4 mm. The signal was registered on a chart recorder (BD 40, Kipp & Zn, Delft, The Netherlands). All CZE runs were made in triplicate.

Conditions used for calculations

The conditions used in calculations such as voltage, capillary length and diameter were similar to the experimental conditions. In all calculations a molecular diffusion coefficient of 0.5 $10^{-9}m^2s^{-1}$ was used.

Chemicals

Triethanolamine (TEtOHA) (97%) and 4-(2-Hydroxyethyl)-1-piperazine ethanesulphonic acid (HEPES) was from Janssen Chimica (Beerse, Belgium). Acetic acid, benzoic acid and hydrochloric acid was obtained from Merck (Darmstadt, FRG). In all experiments deionised water was used (Milli-Q system, Millipore, Bradford, MA, USA).

Theory

Several papers have described zone broadening in CZE in detail [1, 2, 13, 14]. The total

variance in CZE is given as the sum of all variances

$$\sigma^2 = \sigma_i^2 + \sigma_d^2 + \sigma_T^2 + \sigma_k^2 + \sigma_h^2 + \sigma_o^2 \quad (1)$$

where σ^2_i is the dispersion resulting from injection [15], σ^2_d longitudinal diffusion [16], σ^2_T dispersion due to Joule heat [11, 12, 17-19], σ^2_k electromigration dispersion [1, 3], σ^2_h hydrodynamic dispersion and σ^2_o other sources of zone broadening.

Dispersion from injection and longitudinal diffusion

The contribution of injection to the total variance is given by

$$\sigma^2_i = L^2_i/12 \quad (2)$$

where L_i is the injection zone length. The contribution due to the detection cell is considered negligible, while the contribution of the longitudinal diffusion [2] is given by

$$\sigma^2_d = 2Dt \quad (3)$$

where D is the molecular diffusion coefficient and t is the CZE analysis time. Equation (3) implies that reducing the CZE analysis time will reduce the longitudinal diffusion.

In the presence of an electroosmotic flow the total velocity is the sum of the electroosmotic and the electrophoretic velocity. Instead of migration time, migration distance may be used. The electrophoretic or electroosmotic migration distance is calculated from the electrophoretic or electroosmotic velocity and the CZE analysis time using $L_{el}=v_{el}t$ or $L_{eof}=v_{eof}t$, respectively.

Electromigration dispersion

The zone broadening caused by a difference in conductivity of the sample zone and the background electrolyte has been described as [1]

$$4\sigma = \frac{\Delta\kappa}{\kappa} L_{el} \quad (4)$$

where $\Delta\kappa$ is the conductivity difference, κ is the conductivity of the background electrolyte and L_{el} is the electrophoretic migration distance. The conductivity of the background electrolyte is calculated using [1, 4]

$$\kappa_1 = F\bar{c}_{A,1}(|\bar{m}_A| + \alpha_A m_R) \qquad (5)$$

where κ_1 is the conductivity of the background electrolyte, F the Faraday constant, $\bar{c}_{A,1}$ the analytical concentration of the chromophore, $\bar{m}_A$ the effective mobility of the chromophore, m_R the ionic mobility of the counter ion and α_A the molar fraction of chromophore that is in the ionic form. The subscripts 1 and 2 refer to the pure background electrolyte and the sample zone, respectively. The subscripts S, A and R refer to the sample ion, the chromophore and the counter ion, respectively. The conductivity of the sample zone is given by

$$\kappa_2 = F [\bar{c}_{A,2}(|\bar{m}_A| + \alpha_A m_R) + \bar{c}_{S,2}(|\bar{m}_S| + \alpha_S m_R)] \qquad (6)$$

The concentration of univalent chromophore ions in the sample zone ($\bar{c}_{A,2}$) is described by the equation for displacement electrophoresis [1]

$$\bar{c}_{A,2} = \bar{c}_{A,1} - \bar{c}_S K \qquad (7)$$

with

$$K = \frac{m_A}{m_S} \cdot \frac{(m_R + |m_S|)}{(m_R + |m_A|)} \qquad (8)$$

The mobilities in (8) are *ionic* mobilities. The displacement d can be expressed as a percentage of the total chromophore concentration in the background electrolyte by using $d = 100(\bar{c}_{A,1} - \bar{c}_{A,2})/\bar{c}_{A,1} = 100(\bar{c}_S K)/ \bar{c}_{A,1}$.

The relative conductivity difference between the sample zone and the background electrolyte is calculated using [1, 4]

$$\frac{\Delta\kappa}{\kappa} = \frac{\bar{c}_{S,2}}{\bar{c}_{A,1}} \cdot \frac{(|m_S| + m_R)(|\bar{m}_S| - |\bar{m}_A|)}{|m_S|(|\bar{m}_A| + \alpha_A m_R)} \qquad (9)$$

where $\Delta\kappa/\kappa$ is the relative conductivity difference and $\bar{c}_{S,2}$ is the analytical concentration of analyte in the sample zone which is assumed to be the same as the injected analyte concentration. This is an assumption which holds for low sample concentrations. For high sample concentrations the concentration in the sample zone is more or less independent of the initial concentration and is regulated by the Kohlrausch function [4, 7-9]. However, irrespective of concentration, the conclusions will be drawn from a model of electromigration dispersion based on a given conductivity difference.

All calculations are based on univalent buffer and analyte ions. In equations (5) - (9) the absolute values of mobilities are used and the effect of $[H_3O^+]$ and $[OH^-]$ on conductivity and electroneutrality is considered negligible.

Equation (9) shows that when the analyte has a concentration much lower than the BGE concentration ($\bar{c}_{S,2} << \bar{c}_{A,1}$), $\Delta\kappa/\kappa$ becomes zero and the electromigration dispersion is negligible.

Thermal dispersion

The calculation of thermal zone broadening is done using the equation derived by Hjerten [10, 1] and later by Grushka et al. [11, 12]

$$4\sigma_T = \frac{B\,\kappa\,L\,r^2\,E^2}{4\,\lambda_T\,T^2} \qquad (10)$$

where $4\sigma_T$ is the zone width at the baseline, B is a constant (2400 K), κ is the conductivity of the background electrolyte, λ_T is the thermal conductivity of the background electrolyte (λ_T=0.6 W m^{-1} K^{-1}), r is the capillary radius, E is the electric field strength, T is the working temperature (293 K) and L is the electrophoretic migration distance. When a neutral is carried with the electroosmotic flow only, the electrophoretic migration distance is zero which means that neutrals are not affected by thermal zone broadening as described by eqn. (10). For anions, the thermal dispersion will decrease with the electrophoretic migration distance.

Hydrodynamic dispersion

Shortening the electrophoretic migration distance of anions thus reduces the longitudinal, thermal and electromigration dispersion (eqn. 3, 4, 10). This can be done in several ways such as: by shortening the capillary, by placing the detector closer to the point of injection or by using a higher electroosmotic flow. All these options result in changes in the hardware or a change of the capillary length or condition. We considered another option, the application of a hydrodynamic flow. In case of highly efficient separations the hydrodynamic dispersion will reduce the separation efficiency considerably. However, in some cases only qualitative information is needed such as determination of the migration order of anions as used in setting up ITP-CZE systems [20, 21]. In such a case it is convenient to switch rapidly between buffers to obtain qualitative information using indirect detection.

When a hydrodynamic pressure is applied during electrophoresis, the velocities of all species will increase. The electroosmotic and electrophoretic migration distances are shortened and replaced by a hydrodynamic migration distance (L_{hd}). The hydrodynamic migration distance is calculated with the hydrodynamic velocity and the CZE analysis time, $L_{hd}=tv_{hd}$. The contribution of a hydrodynamic flow to the zone width is described by the well known convection term in open tubular chromatography

$$\sigma_{hd}^2 = \frac{L_{hd}\, v_{hd}\, d^2}{96\, D} \qquad (11)$$

where L_{hd} is the hydrodynamic migration distance, v_{hd} the hydrodynamic velocity, d the capillary diameter and D the molecular diffusion coefficient.

Particularly in the case of anions with a velocity close to the velocity of the electroosmotic flow, a decrease of analysis time will result in a decrease of the zone width and an increase of peak height. Obviously, it is not enough to consider only the electromigration dispersion in an optimisation procedure. Therefore, all contributions to zone broadening are considered.

Relative peak height in indirect detection

Equation (7) gives the displacement of chromophore ions for any given analyte concentration irrespective of zone broadening. When the peak area is considered to be constant, the peak height decreases with an increase of zone width. In indirect detection this means that the chromophore concentration in the analyte zone increases during the run. When the concentration chromophore calculated by (7) is considered the initial chromophore concentration in the sample zone $c_{A,2}(0)$, the concentration chromophore at time t is obtained by

$$c_{A,2}(t) = c_{A,2}(0)\ \sigma_t/\sigma_0 \qquad (12)$$

where σ_0 is the zone width at the start of the CZE analysis and σ_t is the zone width after time t. The chromophore concentration in the analyte zone increases linearly with the zone width. The initial chromophore concentration and the initial peak width ($c_{A,2}(0)$, σ_0) are constants and the peak height of the indirect signal decreases with the zone width given by

$$h(t) = C_S\ K/\sigma_t \qquad (13)$$

where C_S is an analyte dependent constant and K the displacement factor (eqn. 8). Equation (13) can be used in optimisation procedures of the indirect detection system. The change of peak height is given as a function of the zone width and the displacement (eqn. 7). The zone width is calculated as the zone width at the baseline (4σ) using eqn. (1) from all contributions given by equations (2), (3), (4), (10) and (11).

Results and discussion

In Figs. 1-3 the relative peak heights are calculated as described in theory. Conclusions are drawn for optimisation of indirect detection. A theoretical example is given in Table I. Optimisation via shorter electrophoretic migration distances is applied for some test compounds. The electrophoretic migration distance is shortened by applying a hydrodynamic flow.

In Fig. 1 the analyte effective mobility and ionic mobility is considered the same. In Fig. 2 and 3 for effective mobilities smaller than $-30\ 10^{-9}$ $m^2V^{-1}s^{-1}$ a weak electrolyte is assumed. In that case the ionic mobility is kept constant at $-30\ 10^{-9}$ $m^2V^{-1}s^{-1}$. In practice, small anions with an effective mobility below $-30\ 10^{-9}$ $m^2V^{-1}s^{-1}$ are often weak acids.

Optimisation in indirect detection

In Fig. 1 the relative peak height calculated for several analyte mobilities is plotted. The analyte and chromophore concentrations are 1.0 and 10 mmol/l, respectively. The displacement factor K (eqn. 8) is almost constant in the considered range. The total zone width (eqn. 1) is strongly influenced by the analyte mobility. At high mobilities the electromigration dispersion and the longitudinal diffusion term are the predominant contributions to the total variance. At low electrophoretic mobilities the electrophoretic migration distance is short and the resulting electromigration dispersion (eqn. 5) is small. The analyte is mainly carried with the electroosmotic flow. When the electrophoretic mobilities of the analyte and the chromophore are equal the electromigration dispersion is zero (eqn. (9), $\overline{m}_S = \overline{m}_A$, $\Delta\kappa/\kappa = 0$). At this point of minimum electromigration dispersion maximum peak heights will be obtained [3-5].

The relative peak height is calculated using eqn. (13) as the ratio of the displacement and the total zone width at the baseline (4σ). The displacement of chromophore in the analyte zone (d%) is given as the percentage of the buffer chromophore concentration.

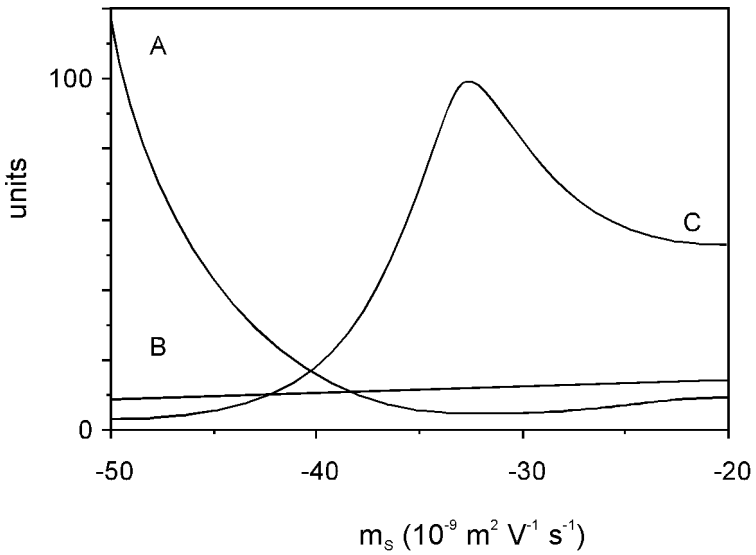

Fig. 1. The calculated zone width (A, 4σ in mm), displacement (B, d in %) and relative indirect peak height (C) for several analyte mobilities. Chromophore and counter ion mobility of benzoic acid and TEtOHA are used for calculation. Other parameters: see Experimental.

In Fig. 2A the calculated relative peak height is shown for several analyte mobilities in a

system with electroosmotic flow (54.4 $10^{-9}m^2V^{-1}s^{-1}$, see Experimental) and for an analyte concentration of 1 mmol/l. For chromophore mobility -30 10^{-9} $m^2V^{-1}s^{-1}$ the best results are obtained at analyte mobilities at or below the chromophore mobility. For chromophore mobility -60 10^{-9} $m^2V^{-1}s^{-1}$ there is not such an optimum. An analyte with a mobility close to the chromophore mobility will have a long migration time and a large longitudinal diffusion resulting in an increased zone width. Such a system is optimised by suppressing the electroosmotic flow or changing the BGE in a way that lower (anionic) electrophoretic analyte mobilities are obtained. Optimisation only with respect to similar mobilities of chromophore and analyte is in such a case not relevant. At low mobilities (-5 10^{-9} $m^2V^{-1}s^{-1}$) a second optimum appears. At these low mobilities the electrophoretic migration distance approaches zero (neutrals) and several dispersion factors become negligible.

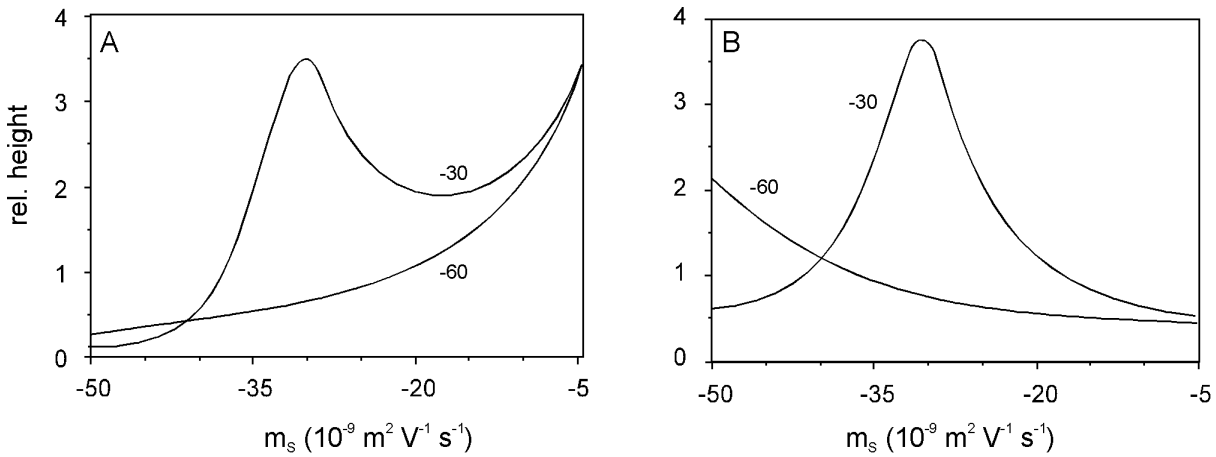

Fig. 2. The calculated relative peak height for several analyte mobilities in a system with (A) and without electroosmotic flow (B). Analyte and chromophore concentration is 1 and 10 mmol/l, respectively. TEtOHA is used as counter ion. Chromophore mobility is -30 or -60 $10^{-9}m^2V^{-1}s^{-1}$. For other conditions see Experimental.

In Fig. 2B the situation is shown for a system without electroosmotic flow. In such a case the migration times and longitudinal diffusion are reduced at high analyte mobilities. For both considered chromophore mobilities an optimum is found where analyte and chromophore mobilities are equal.

When both cases (with and without electroosmosis) are considered for analyte concentration 0.1 mmol/l the situation is completely different (Fig. 3A and B). Under these circumstances

the electromigration dispersion is almost negligible. Optimisation is done with respect to longitudinal diffusion. Best results are obtained at high analyte velocities with short CZE analysis times.

For systems with electroosmotic flow this means that low analyte mobilities are favourable (Fig. 3A). For a system without electroosmotic flow high analyte mobilities give the optimum peak heights (Fig. 3B). In both cases a high mobility of the chromophore results in (slightly) better peak heights. This is a result of the smaller $\Delta\kappa/\kappa$ (eqn. 9) and the lower electromigration dispersion at higher background conductivity. The concentration levels as used in Fig. 3 are at 1% of the BGE concentration. These concentrations are only detectable in an indirect detection system with a high signal-to-noise ratio.

In all considered cases (Fig. 1-3) the displacement factor K is more or less constant with the analyte mobility. For indirect detection systems the reduction of the zone broadening will improve the detection sensitivity. In cases where electromigration dispersion is predominantly contributing to zone broadening best results are obtained when the analyte and chromophore mobilities are the same ($\overline{m}_S = \overline{m}_A$).

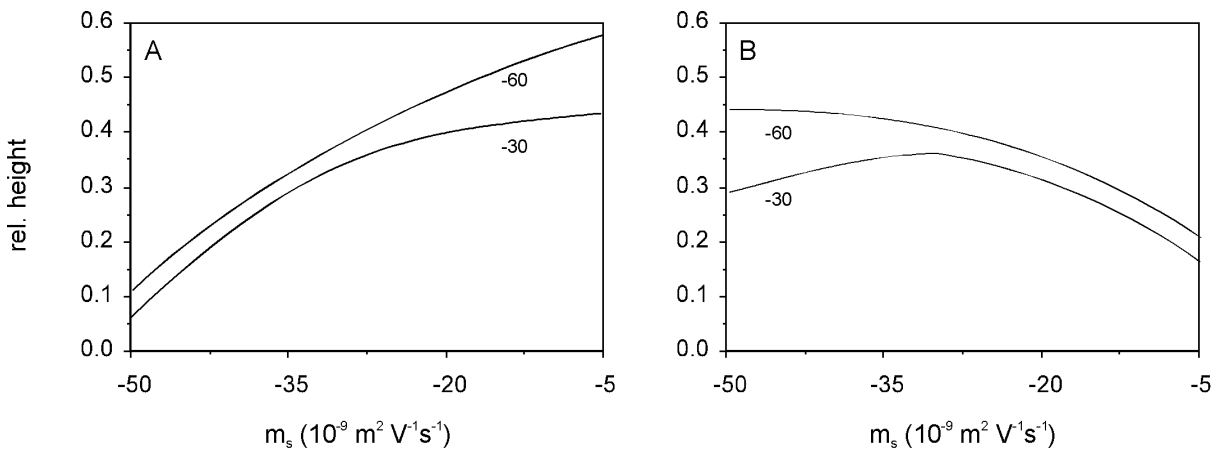

Fig. 3. The calculated relative peak height for several analyte mobilities in a system with (A) and without electroosmotic flow (B). Analyte concentration is 0.1 mmol/l. Chromophore mobility is -30 or -60 $10^{-9} m^2 V^{-1} s^{-1}$. Other conditions are the same as in Fig. 2.

One exception is the case where the chromophore mobility is almost as high as the mobility of the electroosmotic flow. In that case it is advisable to use a modified capillary without elec-

troosmotic flow. Another exception is at low analyte concentrations. Such a system is optimised by realising shorter analysis times.

An example of a calculated optimisation procedure with respect to peak height is given in Table I. The considered analyte and chromophore concentrations are 0.1 and 10 mmol/l, respectively. Choosing a chromophore with similar absorbance characteristics but with another mobility ($\overline{m}_S = \overline{m}_A$) improves the peak height with a factor 2 (case 1 *vs.* 2). Reducing the migration distance by using a capillary without electroosmotic flow results in approximately 4 times better peak height (case 1 *vs.* 3). In this case also the polarity of the voltage is switched because the analytes migrate in the opposite direction. Choosing both a different chromophore and a coated capillary gives the best result, a factor 5 (case 1 *vs.* 4). When the analyte is a weak acid, the effective mobility can be changed to $\overline{m}_S = \overline{m}_A$. When all other parameters are assumed independent of the pH (which is not the case) the peak height increases a factor 3 (case 1 *vs.* 5).

Table 3. Example of an optimisation procedure with respect to peak height. Case 1: starting situation. Case 2: alternative chromophore. Case 3: suppressed electroosmotic flow. Case 4: suppressed electroosmotic flow, alternative chromophore. Case 5: Change analyte mobility via pH (weak acid). All values are in mm except the mobilities (in $10^{-9}m^2V^{-1}s^{-1}$) or otherwise specified. The negative values of migration distance indicate that the direction is opposite to the direction of the electroosmotic flow. For other conditions see Experimental.

case	1	2	3	4	5
$\overline{m}_A$	-35	-50	-35	-50	-35
$\overline{m}_S$	-48.9	-48.9	-48.9	-48.9	-34.9
t(min)	25.0	25.0	2.84	2.84	7.10
L_{eof}	2451	2451	0	0	696.1
L_{el}	-2201	-2201	250	250	-446.1
$4\sigma_i$	1.60	1.60	1.60	1.60	1.60
$4\sigma_d$	4.90	4.90	1.65	1.65	2.61
$4\sigma_T$	3.27	4.02	0.37	0.46	0.66
$4\sigma_k$	7.60	0.48	0.86	0.05	0.01
$4\sigma_{tot}$	9.75	6.55	2.48	2.35	3.14
d (%)	0.87	1.0	0.87	1.0	0.87
h (rel.)	8.9	15.2	35.1	42.6	27.7

Application of a hydrodynamic flow

In the following paragraphs a situation is considered where hydrodynamic manipulation improves the performance in CZE with indirect absorbance detection. A hydrodynamic flow is

used to reduce the electrophoretic migration distance and the analysis time.

A mixture of chloride, acetate and HEPES is used as test compounds. Calculations are made for acetate and HEPES. Using the equations (5), (6) and (9) the background electrolyte conductivity is calculated at 0.061 S/m. The calculated sample zone conductivity differences ($\Delta\kappa$) are $1.13\ 10^{-2}$ and $1.13\ 10^{-3}$ S/m for 10 and 1 mmol/l acetate, respectively (limiting ionic mobility $-42\ 10^{-9}\ m^2V^{-1}s^{-1}$, measured effective mobility $-39.7\ 10^{-9}\ m^2V^{-1}s^{-1}$) and $-3.74\ 10^{-2}$ and $-3.74\ 10^{-3}$ S/m for 10 and 1 mmol/l HEPES, respectively (limiting ionic mobility $-22\ 10^{-9}\ m^2V^{-1}s^{-1}$, measured effective mobility $-16.5\ 10^{-9}\ m^2V^{-1}s^{-1}$) [6]. Other conditions are given in Experimental.

The measured migration times varied a few percent when analyte concentrations are increased from 1 to 10 mmol/l, for calculations the CZE analysis times are considered independent of concentration. Calculation of the CZE analysis times in presence of a hydrodynamic flow is done using the electrophoretic, electroosmotic and the hydrodynamic velocity. The hydrodynamic flow velocity is calculated in mm/s using Poiseuilles law

$v_{hd} = \Delta h\ d^2 / (32000\ \eta\ \rho\ g\ L)$, where Δh, d, η, ρ, g and L are the height difference between anode and cathode vial in mm, the capillary inner diameter in mm, the viscosity ($\eta=9.93\ 10^{-4}\ kgm^{-1}s^{-1}$), the background electrolyte density ($\rho=1000\ kgm^{-3}$), the gravitational force ($g=9.8\ ms^{-2}$) and the capillary length in mm, respectively.

In Fig. 4a the effect of a hydrodynamic flow on the total peak width at the baseline (4σ) is calculated using eqn. (1). The calculation included zone broadening due to injection, Joule heat, longitudinal diffusion, electromigration and hydrodynamic dispersion. Parameters used in this and other calculations are given in Experimental and Table II. For acetate concentrations above 1 mmol/l the conductivity difference is the major source of zone broadening and a reduction in zone width is shown when a hydrodynamic flow is applied. The contribution of injection, temperature and molecular diffusion is negligible for concentrations above 5 mmol/l. At higher flow rates (> 2 mm/s) the total variance approaches the variance caused by the hydrodynamic flow which is then the major source of zone broadening. However, at lower hydrodynamic velocities and high sample concentrations (> 1 mmol/l) a considerable decrease of zone width is calculated. For acetate concentrations below the 0.1 mmol/l the zone broadening only increases with a hydrodynamic flow.

In Fig. 4b the zone width calculated from the sum of all variances, except the hydrodynamic dispersion, is given as a function of the electrophoretic migration distance (line A-D). As mentioned in Theory the zone width decreases with the migration distance.

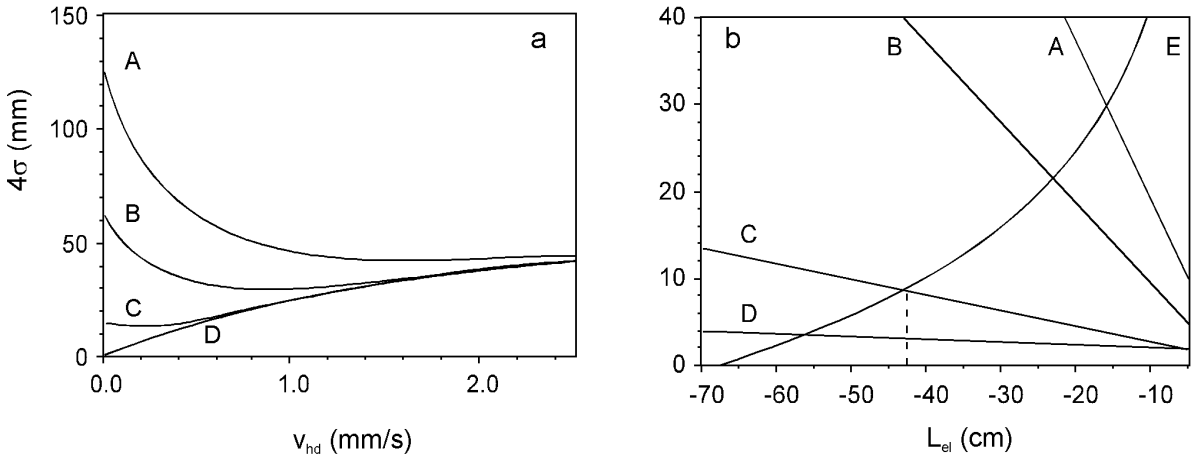

Fig. 4a. Calculated peak width at baseline for (A) 10.0, (B) 5.0 and (C) 1.0 mmol/l acetate. When the hydrodynamic flow rate increases hydrodynamic dispersion (D) becomes predominant for the total variance. The minimum zone width is found where electromigration dispersion equals hydrodynamic dispersion, i.e. $\sigma_{hd} = \sigma_k$.
Fig. 4b. The intersection of the lines for calculated hydrodynamic dispersion (E) and all other dispersion factors for (A) 10.0, (B) 5.0, (C) 1.0 and (D) 0.1 mmol/l acetate. The intersection corresponds to the minimum zone width in Fig. 4a. The intersection can be used for accurate calculation of the maximum allowed hydrodynamic flow (see text).

The intersection with the line of hydrodynamic dispersion (line E) gives the point where the variances are equal. A hydrodynamic flow will improve the zone width until the corresponding migration distance is reached.

For example the migration distance of 1 mmol/l acetate (line C) can be reduced from -67 to -43 cm resulting in a decrease of zone width. The CZE analysis time is linearly related to the electrophoretic migration distance. Therefore, the reduction in electrophoretic migration distance by the application of a hydrodynamic flow will be proportional to the reduction in CZE analysis time. The ratio is given by

$$t_1/t_2 = L_{el,1}/L_{el,2} \qquad (14)$$

where t is the CZE analysis time. For the example of 1 mmol/l acetate this means that a hydrodynamic flow is allowed that speeds up the CZE analysis time with a factor 67/43. Thus the CZE analysis time of acetate can be decreased hydrodynamically to 6.0 min (43/67 x 9.41 min) with a decrease of zone width.

Resolution

Changing the migration distance will also affect the resolution. The resolution is given by

$$R = \frac{\sqrt{N}}{4} \cdot \frac{\Delta v}{\bar{v}} \qquad (15)$$

where N is the efficiency. The selectivity is given as $\Delta v/\bar{v}$ which is the relative velocity difference and is equal to the relative CZE analysis time difference $\Delta t/\bar{t}$. When a hydrodynamic flow rate is applied the resolution is affected by the decreased efficiency.

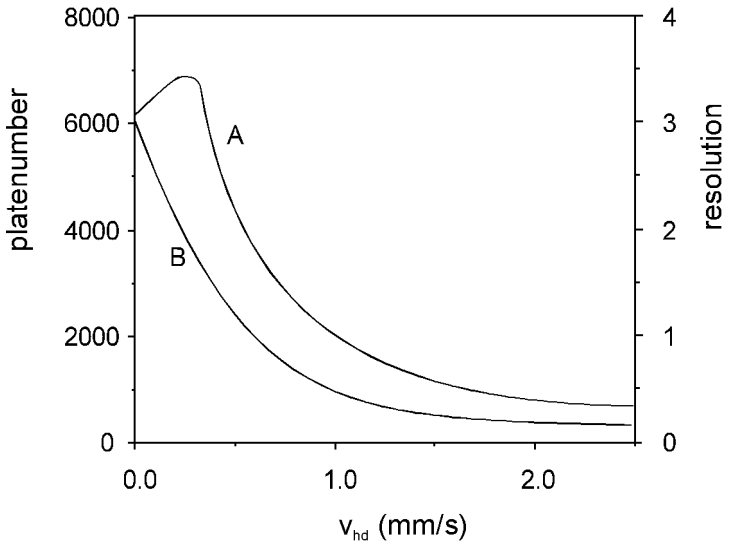

Fig. 5. The efficiency (A) and resolution (B) are both affected by the hydrodynamic flow. The optimum in the efficiency of 1.0 mmol/l acetate corresponds to the minimum zone width in Fig. 1, line C. The resolution is calculated for 1 mmol/l acetate and another analyte migrating at 9.4 an 8.0 min, respectively.

In Fig. 5 the calculated effect of a hydrodynamic flow on the efficiency is shown for 1 mmol/l acetate. The resolution is calculated using (15) for two analytes with a CZE analysis time of 9.4 (acetate) and 8.0 min. The efficiency first increases because of the reduction of the electromigration dispersion and then decreases as a result of hydrodynamic dispersion. The selectivity decreases proportionally to the electrophoretic migration distance as shown in Fig. 6.

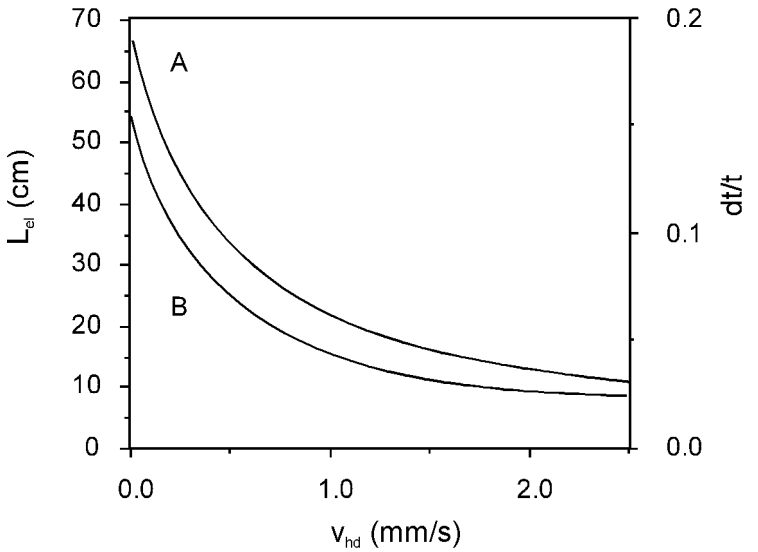

Fig. 6. Separation in CZE is based on differences in electrophoretic mobility. When the electrophoretic migration distance (A) is shortened by a hydrodynamic flow the selectivity (B) decreases proportionally.

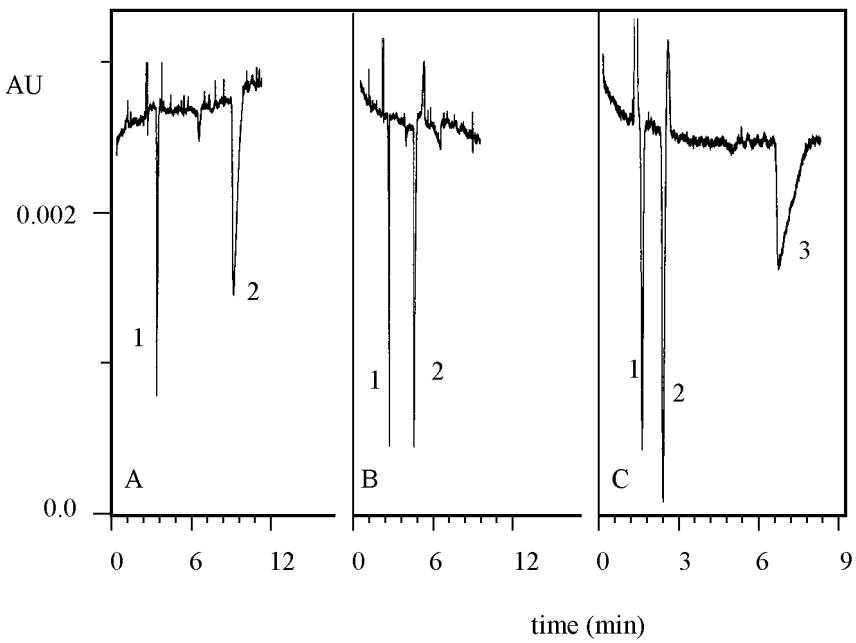

Fig. 7. Separation of 1.0 mmol/l HEPES (1), acetate (2) and chloride (3) without (A) and with (B) 0.56 mm/s and with (C) 1.11 mm/s hydrodynamic flow. For other settings and conditions see Experimental.

The effect of a hydrodynamic flow is demonstrated in Fig. 7. At zero hydrodynamic flow the chloride zone is never seen because the electroosmotic velocity is approximately the same as the electrophoretic velocity in the opposite direction. When the hydrodynamic flow velocity is increased to 0.56 and 1.11 mm/s by applying a height difference of 10 and 20 cm, respectively (corresponding to ca. 10 and 20 mbar pressure difference) the zones are still easily separated and the chloride zone appears at 6.5 min (Fig. 7C).

The peak heights and the peak height ratio of HEPES and acetate changes by applying the hydrodynamic flow. The peak height of acetate increases with the height difference, the peak height of HEPES increases after applying a hydrodynamic flow velocity of 0.56 mm/s. Increasing the flow to 1.11 mm/s does not increase the peak height of HEPES. This means that the minimum zone width for HEPES is reached at a lower hydrodynamic velocity than for acetate although HEPES has a higher conductivity difference with the background electrolyte than acetate at similar concentrations. This seems in contradiction with the conclusion drawn from Fig. 4 that at higher conductivity differences a higher hydrodynamic velocity is allowed. However, for HEPES the short electrophoretic migration distance should also be taken in account.

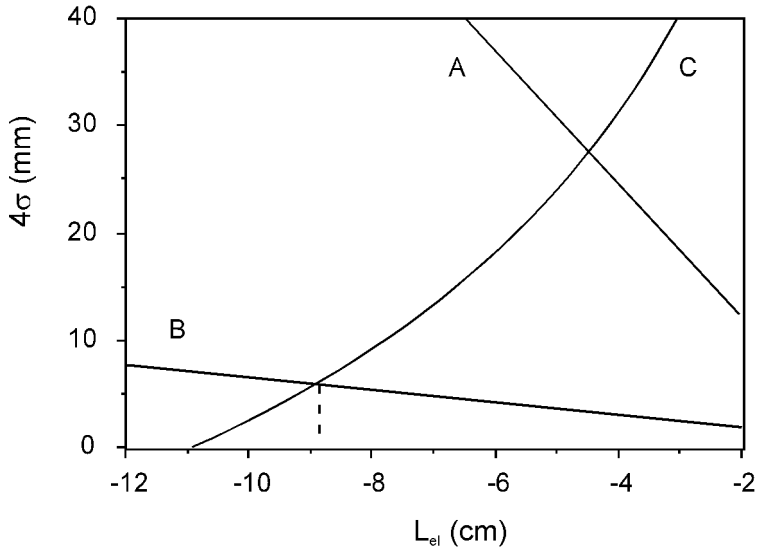

Fig. 8. The intersection of the lines for calculated hydrodynamic dispersion (C) and all other dispersion factors for (A) 10.0 and (B) 1.0 mmol/l HEPES.

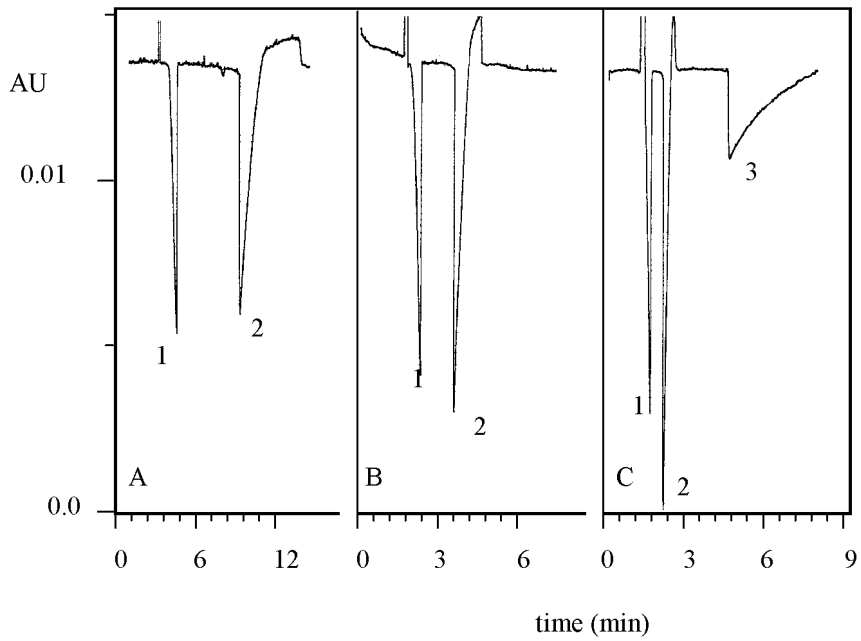

Fig. 9. Separation of 10.0 mmol/l HEPES (1), acetate (2) and chloride (3) without (A) and with 0.56 mm/s (B) and with 1.11 mm/s (C) hydrodynamic flow. See Experimental for conditions.

As can bee seen in Fig. 8 the intersection point for 1 mmol/l HEPES is at -8.8 cm electrophoretic migration distance. The migration distance at zero hydrodynamic flow is -10.9 cm. This means that a minimum in zone width is expected when the CZE analysis time of HEPES is hydrodynamically reduced to 2.95 min (8.8/10.9 x 3.66 min). In Fig. 7B the analysis time of HEPES is 2.3 min which is already beyond the optimum. As discussed before (example Fig. 4b), the acetate CZE analysis time can be decreased hydrodynamically to 6.0 min with a decrease of zone width. This is a decrease to 64% of the CZE analysis time at zero hydrodynamic flow, for HEPES a decrease to only 80% is allowed. The difference in conductivity is not only determined by concentration but also by electrophoretic mobility. Therefore, for similar concentrations and different mobilities, different optimum hydrodynamic flow velocities will be found.

The effect of a high analyte concentration (10 mmol/l) is shown in Fig. 9. Even at 20 cm height difference (v_{hd}=1.11 mm/s) an improvement in peak height (decrease of zone width) is seen for both acetate and HEPES. In Table II the measured and calculated zone widths are given.

Table 4. Calculated and measured zone width of HEPES and acetate. The various contributions to the total zone width are given as 4σ. All values are given in mm unless mentioned otherwise.

	HEPES			acetate		
v_{hd} (mm/s)	0	0.56	1.11	0	0.56	1.11
t (min)	3.66	2.46	1.85	9.41	4.17	2.68
L_{eof}	358.8	241.0	181.4	922.5	408.8	262.6
L_{el}	-108.8	-73.1	-55.0	-672.5	-298.0	-191.4
L_{hd}	0.0	82.1	123.6	0.0	139.2	178.8
$4\sigma_i$	1.61	1.61	1.61	1.61	1.61	1.61
$4\sigma_d$	1.87	1.54	1.33	3.01	2.00	1.60
$4\sigma_{hd}$	0.00	11.72	20.34	0.00	15.27	24.47
$4\sigma_T$	0.16	0.10	0.08	0.97	0.43	0.27
	$\bar{c}_S$ = 1 mmol/l					
$4\sigma_k$	6.70	4.50	3.39	12.48	5.53	3.55
$4\sigma_{tot}$	7.14	12.75	20.73	12.98	16.45	24.84
$4\sigma_{measured}$	15.85	12.96	18.45	21.09	11.42	16.21
ratio*	0.45	1.0	1.1	0.6	1.4	1.5
	$\bar{c}_S$ = 10 mmol/l					
$4\sigma_k$	66.99	45.00	33.88	124.76	55.29	35.51
$4\sigma_{tot}$	67.04	46.55	39.57	124.81	57.42	43.19
$4\sigma_{measured}$	39.68	36.76	36.20	41.87	34.63	29.07
ratio*	1.7	1.3	1.1	2.9	1.7	1.5

* Ratio of calculated and measured value: $4\sigma_{tot}/4\sigma_{measured}$.

In Fig. 10 the CZE separation window is widened to all anions. The voltage is changed from +15 kV to -5 kV and a height difference of 20 cm is applied. Reversal of the voltage results in reversal of the electrophoretic migration direction of the anions. However, the larger hydrodynamic flow moves the bulk liquid into the direction of the detector. The total separation is completed within 8 min. All zones are still easily separated and a considerable improvement of the chloride zone width is shown. Fig. 10B shows how the resolution can be manipulated by reducing the hydrodynamic flow. The chloride peak in Fig. 10B appears after the same CZE analysis time as in Fig. 7C. However, the zone width has been reduced a factor 1.9 by hydrodynamic manipulation. Fast and qualitative information on the ionic composition of the sample is obtained.

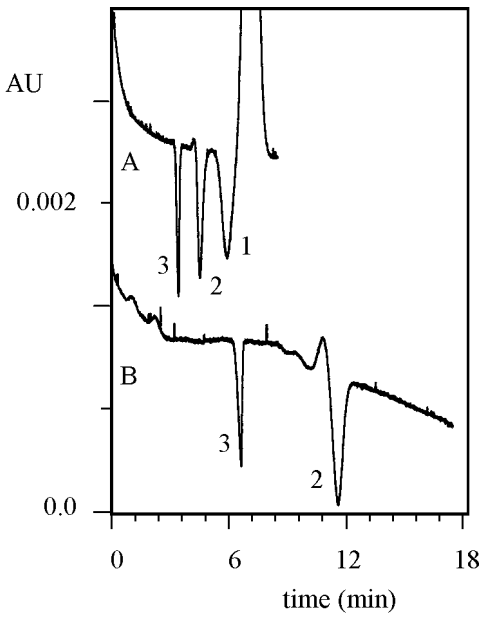

Fig. 10. Separation of 1.0 mmol/l HEPES (1), acetate (2) and chloride (3) with (A) 1.11 mm/s and with (B) 0.56 mm/s hydrodynamic flow. The running voltage is -5.0 kV. See Experimental for conditions.

Conclusions

Optimisation of indirect detection in CZE of anions depends on the several parameters. At analyte concentrations close to the CZE buffer concentration, best results are obtained when the analyte and chromophore mobilities are the same ($\overline{m}_S = \overline{m}_A$). If the analyte mobility is high it is advisable to use a chromophore with a similar mobility together with a modified capillary to eliminate electroosmotic flow.

At low analyte concentrations the indirect detection is optimised with shorter analysis times. It is unlikely that attempts to optimise a system by the displacement factor K will be successful, as in most cases K is more or less constant with analyte mobility.

In certain exceptional situations hydrodynamic manipulation improves the performance in CZE with indirect detection. Under conditions where the electromigration dispersion is larger than the hydrodynamic dispersion an improvement in efficiency is seen. The separation window is enlarged, analytes that migrates with the same (but opposite) velocity as the electroosmotic flow can be analysed. A hydrodynamic reversal of the bulk flow together with a reversal of the voltage widens the separation window to all anionic compounds. In cases where fast and

only qualitative data are required, application of a hydrodynamic flow offers an alternative to coated capillaries or buffer additives to change the electroosmotic flow.

References

1. S. Hjerten, Electrophoresis, 11 (1990) 665
2. F. Foret, M. Deml and P. Bocek, J. Chromatogr., 452 (1988) 601
3. E.S. Yeung and W.G. Kuhr, Anal. Chem., 63 (1991) A275
4. V. Sustacek, F. Foret and P. Bocek, J. Chromatogr., 545 (1991) 239
5. F. Foret, S. Fanali, L. Ossicini, P. Bocek, J. Chromatogr., 470 (1989) 299
6. J. Pospichal, P. Gebauer and P. Bocek, Chem. Rev., 89 (1989) 419
7. F.E.P. Mikkers, thesis 1980
8. F. Foret, P. Bocek, in A. Chrambach, M.J. Dunn, B.J.Radola (editors) *Advances in Electrophoresis*, Vol. 3, VCH Weinheim, 1989, p. 271-347
9. P. Gebauer, W. Thormann, P. Bocek, J. Chromatogr., 608 (1992) 47
10. S. Hjerten, Chromatogr. Rev., 9 (1967) 122
11. E. Grushka, R. McCormick and J. Kirkland, Anal. Chem., 61 (1989) 241
12. A.E. Jones and E. Grushka, J. Chromatogr., 466 (1989) 219
13. H. Poppe, Anal. Chem., 64 (1992) 1908
14. G.J.M. Bruin, A.C. van Asten, X.M. Xu and H. Poppe, J. Chromatogr., 608 (1992) 97
15. E. Grushka and R.M. McCormick, J. Chromatogr., 471 (1989) 421
16. E. Kenndler and C. Schwer, Anal. Chem., 63 (1991) 2499
17. J.H. Knox and I.H. Grant, Chromatographia, 24 (1987) 135
18. J.H. Knox, Chromatographia, 26 (1988) 329
19. W.A. Gobie and C.F. Ivory, J. Chromatogr., 516 (1990) 191
20. M.H. Lamoree, N.J. Reinhoud, U.R. Tjaden, W.M.A. Niessen and J. van der Greef, Biolog. Mass Spectrom., 23 (1994) 339
21. N.J. Reinhoud, U.R. Tjaden and J. van der Greef, J. Chromatogr. A, 653 (1993) 303
22. S. Terabe, K. Otsuka and T. Ando, Anal. Chem., 61 (1989) 251

Part 2

Capillary Electrophoresis - Mass Spectrometry

2.1

Liquid Junction Coupling of Capillary Zone Electrophoresis with Continuous-flow Fast Atom Bombardment Mass Spectrometry

Abstract

On-line capillary zone electrophoresis - continuous-flow fast atom bombardment mass spectrometry (CZE-CF-FAB-MS) is described. The effects of a liquid junction coupling (LJC) on the efficiency and resolution is investigated. A decreased efficiency of a factor 10 is seen which is in agreement with the calculated dispersion due to the hydrodynamic flow in the transport capillary.

A position and time resolved ion counting (PATRIC) array detector is compared with a conventional scanning electron multiplier detector. An increase in sensitivity of a factor 100 - 1000 is observed for the scanning array mode and the static array mode respectively. Absolute detection limits in the low femtomolar range are achievable, corresponding to the low micromolar concentration range.

Introduction

Capillary zone electrophoresis (CZE) coupled to mass spectrometry (MS) is an extremely powerful analytical tool. It combines a very efficient separation method with a selective detector that is capable of giving structural information that can be used for analyte identification. Interfacing CZE with MS has been reported using existing LC-MS interfaces such as electrospray [1-2], ionspray [3] or continuous-flow fast atom bombardment (CF-FAB) [4-7]. These approaches are attractive because the soft ionisation characteristics opens the possibility of analysing polar high molecular mass compounds.

The mentioned interfaces have their optimal flow rate in the lower µl/min range. Therefore, a make-up flow is mandatory to increase the flow rate from the nl/min range in CZE to 5-20 µl/min required for successful operation of these interfaces. The addition of a make-up flow is achieved either by a coaxial solvent flow [2, 7] or by means of a liquid junction coupling, which is in fact a low dead volume T-piece between the separation capillary and the transport capillary [3-6]. The latter approach may result in a considerable loss of efficiency [5].

When CZE-MS is used for identification purposes of unknown analytes, the detection must

be performed over a wide molecular mass range. Unfortunately, the sensitivity of the MS decreases with the scan time. In array detection the scan times are considerably lower and only limited by the time that is needed to read out the detection channels. The PATRIC detector can be used as an array detector in a fixed mass window of 8% around the central mass [8]. The m/z range can be increased by using the array in the scanning mode. An advantage over a conventional scanning electron multiplier is that scanning takes place with a mass window in stead of 1 mass at a time. This increases the scanning speed and the detection sensitivity substantially.

In this study the performance of a liquid junction coupling for CZE-CF-FAB-MS is investigated. Efficiencies in the MS are compared with CZE efficiencies measured before the LJC for dextromethorphan and some β-endorphin fragments. The detection sensitivity of an array detection system is compared with a conventional scanning electron multiplier.

Experimental

Efficiency study

The CZE system consisted of a Model RR100-1.5P high voltage power supply (Gamma High Voltage Research Inc., Mt. Vernon, NY, USA), a 700x0.075 mm fused silica capillary (SGE, Ringwood, Victoria, Australia) for electrophoresis, a custom-made liquid junction coupling, a 1000x0.075 mm fused silica transport capillary. On-capillary absorbance detection (Spectroflow 757, Kratos, Ramsey, NJ, USA) in CZE took place 150 mm before the LJC at 210 nm. The Finnigan MAT 90 (Bremen, FRG) double focusing mass spectrometer was equipped with a Finnigan MAT CF-FAB probe and a cryopump at the ion source housing. A stainless steel target was used in combination with a wick of compressed paper at the bottom of the ion volume to ascertain stable ionisation conditions in CF-FAB operation [9]. In MID mode a cycle time of 0.5 s was used. For sample introduction electrokinetic injection was applied.

The electrophoresis buffer consisted of a 20 mmol/l ammonium acetate at pH 8 and containing 3% of glycerol which was added to improve the post-capillary mixing with the CF-FAB make-up liquid. CZE was performed by applying a voltage of 20 kV between the injection point and the liquid junction interface. The make-up liquid added to the effluent of the electrophoretic capillary to obtain a total flow-rate of 5-8 μl/min to the CF-FAB probe consisted of 0.25% trifluoroacetic acid (TFA) and 10-16% of glycerol in water.

Trifluoroacetic acid and ammonium acetate were purchased from Merck (Darmstadt, FRG), 98% chemical pure glycerol from Lamers & Pleuger ('s-Hertogenbosch, The Netherlands). The mobile phase was freshly prepared each day using distilled water and filtered before use.

PATRIC detector

Capillary electrophoresis was performed with a 800x0.075 mm fused silica capillary, applying a potential of 20 kV. A volume of typically 20 nl was injected hydrodynamically. A custom-made liquid junction coupling, was used for the addition of the make-up fluid (0.025% trifluoroacetic acid and 16.6% glycerol in water) and for the coupling of the CZE capillary with the CF-FAB interface. The transport capillary between the liquid junction coupling and the CF-FAB probe tip was a 840x0.100 mm fused silica capillary, resulting in a flow rate of ca. 14 μl/min. A newly designed CF-FAB target was used with a gold plated channel [9] yielding an almost instant stability under the described conditions.

A Finnigan MAT 900 double focusing mass spectrometer equipped with both a normal secondary electron multiplier (SEM) and a PATRIC detector was used. The array detector was used in static and in scanning mode. For the experiments comparing the different detection modes in the analysis of three β-endorphin fragments the resolution was set at 1000. A resolution of 1000 and 2000 was used in the measurements of 15 pmol galanin and 2 pmol magainin, respectively. Galanin and magainin were purchased from Bachem Feinchemicalien AG (Bubendorf, Switzerland).

Theory

Several approaches have been described in coupling of CZE to the MS interface. Some approaches are based upon insertion of the CZE capillary in the interface, the so-called coaxial approach. Another approach is based upon the coupling of capillaries by means of a liquid junction. In principle, both coupling devices can be used for CZE CF-FAB-MS. Both the coaxial and the LJC approach have specific advantages.

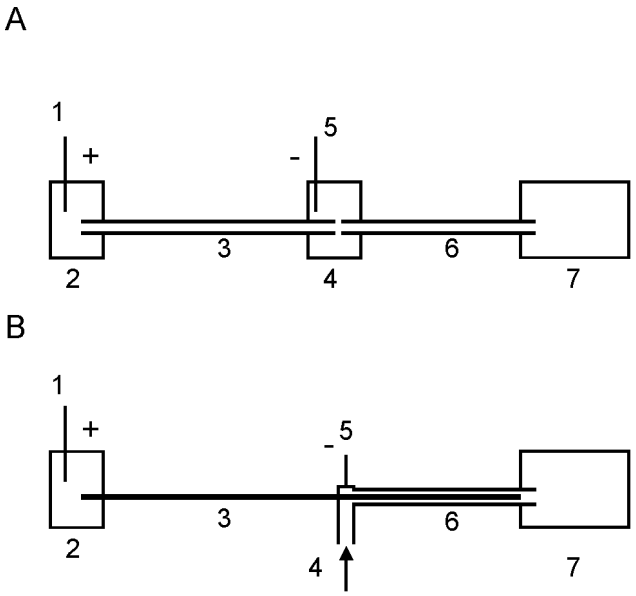

Fig. 1. Schematic representation of CZE-CF-FAB-MS with a liquid junction (A) and a coaxial coupling(B). Numbers are: high voltage anode (1), anode buffer vial (2), CZE capillary (3), addition of make up liquid (4), grounded cathode (5), transport capillary (6) and mass spectrometer (7). See text for further explanation.

In the coaxial approach the CZE capillary is inserted in the CF-FAB probe until a few millimetres before the end of the probe (Fig. 1). Capillaries with small inner diameters are used (< 15 μm ID) to suppress a hydrodynamic flow caused by the vacuum at the ion source. High separation efficiencies can be obtained, however, the limited loadability results in a poor detection sensitivity.

In a LJC the CZE capillary is placed oppositely to a transport capillary to the MS interface. The junction is immersed in a make-up liquid which is in contact with the counter electrode for CZE. The junction between the two capillaries is small, typically 20 μm. Analytes migrating out of the CZE capillary enter the transport capillary and are flushed towards the MS by means of a pressure induced flow caused by the vacuum in the ion source.

The LJC offers more flexibility than the coaxial approach. In an optimised situation the ionisation is not disturbed by the CZE voltage which may be the case in the coaxial approach. Another advantage is that the CZE capillary dimensions can be chosen independently from the MS interface. The loadability of the CZE-MS system can be increased by using larger ID CZE capillaries which is not the case in the coaxial approach. A possible disadvantage of the LJC is

that the pressure induced flow in the transport capillary contributes considerably to the zone broadening.

Zone broadening in the transport capillary

The maximum achievable plate number in the LJC approach can be calculated by considering all sources of zone broadening negligible, except for the hydrodynamic dispersion. The variance (in m^2) by a pressure induced flow in the transport capillary is given by (Chapter 1.3)

$$\sigma_{hd}^2 = \frac{L_{hd}\, v_{hd}\, d^2}{96\, D} \qquad (1)$$

where L_{hd} is the hydrodynamically covered distance, v_{hd} the hydrodynamic velocity, d the capillary diameter and D the molecular diffusion. The temporal variance (in s^2) is given by:

$$\sigma_{hd}^2 = \frac{L_{hd}\, \pi\, d^4}{6.4\, D\, F} \qquad (2)$$

where F is the flow rate in μl/min.

For a transport capillary of 840 x 0.100 mm the flow rate due to a pressure difference of 1 bar will be approximately 17.6 μl/min. The CZE-MS variance (eqn. 2) resulting from hydrodynamic transport is then $\sigma_h^2 = 4.67\ s^2$ (L_{hd} = 840 mm, $\eta = 9.93\ 10^{-4}$ kg m^{-1} s^{-1}, d = 0.1 mm, D = $0.5\ 10^{-3}$ $mm^2 s^{-1}$). Assuming a CZE-MS analysis time of 600 s, the maximum achievable efficiency is then calculated as $N=(t/\sigma)^2= 77000$, for an analysis time of 300 s the maximum efficiency is 19000.

One way to optimise CZE-MS is to use a smaller ID capillary and an increased pressure drop to keep the flow rate in the transport capillary constant. For CZE-MS a factor 2 smaller ID transport capillary, would result in a factor 16 decrease of the hydrodynamic variance (eqn. 2). A factor 16 higher pressure drop (Poiseuille) would be required to keep the flow rate constant.

Although under the experimental conditions with a LJC the loss in efficiency may be considerable, in practice separation efficiency is usually not a limiting factor in CZE-MS. The MS

is such a selective detection method that in most cases baseline separation is not required. Application of CZE-MS in analytical methods is often limited by the small sample loadability resulting in a poor detection sensitivity.

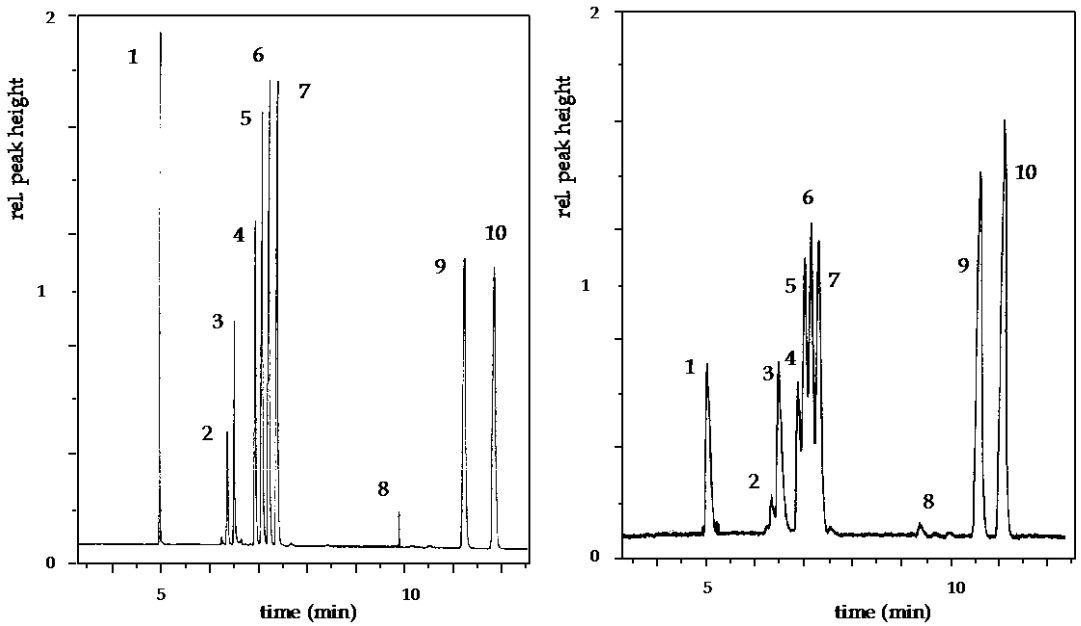

Fig. 2. Separation and LIF detection of fluorescently labelled amino acids. Arg (1), Lys (2, 3), Trp (4), Phe (5), Thr (6), Ser (7), L-Dopa (8), Glu (9) and Asp (10). Detection before (A) and after (B) a liquid junction coupling similar as used in CZE-MS. The efficiencies in (B) are a factor 10 lower, the resolution decreased with the square root of the efficiency.

In Fig. 2 the effect of a decrease of efficiency is illustrated for the separation of a number of amino acids detected with laser-induced fluorescence (LIF) detection. A similar two capillary system with an LJC is used in Fig. 2B. Detection before the LJC resulted in efficiencies varying from $2\ 10^5$ - $3\ 10^5$ and after the LJC the efficiencies are approximately a factor 10 lower. The resolution decreased by a factor of 3.

Results and discussion

CZE and CZE-MS efficiency

In Fig. 3A and B a CZE and a CZE-MS electropherogram of a peptide mixture is shown. The efficiency of peak 3 is in both cases the same, approximately 6000. The plate numbers are calculated as $N=(t/\sigma)^2$.

The low CZE performance is explained by the high sample concentrations (340 μmol/l) that are necessary to obtain a MS signal. Due to concentration overloading and the poor CZE performance the contribution of hydrodynamic dispersion in the transport capillary to the zone broadening is negligible. However, the resolution is not only determined by the efficiency but also by the selectivity. In both electropherograms the peaks are baseline separated which is more then enough for identification purposes. In Fig. 4 another peptide mixture is shown with similar concentrations, efficiencies and resolution. The total ion current in Fig. 4C shows overlap of peak 2 and 3, the selectivity of the MS is demonstrated by the individual traces in Fig. 4B.

A better efficiency and sensitivity is obtained in the analysis of dextromethorphan, a cationic drug. Dextromethorphan is dissolved in water (100 ng/ml), enabling electrokinetic injection under stacking conditions. In Fig. 5 the absorbance and MS electropherograms of dextromethorphan are shown with efficiencies of respectively 115000 and 9000, which is a factor of 13 decrease of efficiency.

Although the CZE performance for dextromethorphan is considerably better than for the peptides, the overall CZE-MS plate numbers are poor. The CZE-MS efficiencies are mainly determined by the dispersion in the LJC and the transport capillary. Under these circumstances the electromigration dispersion, due to overloading of the CZE capillary, hardly affects the overall separation efficiency. Optimisation should therefore start with a reduction of the excessive zone broadening in the transport capillary and LJC.

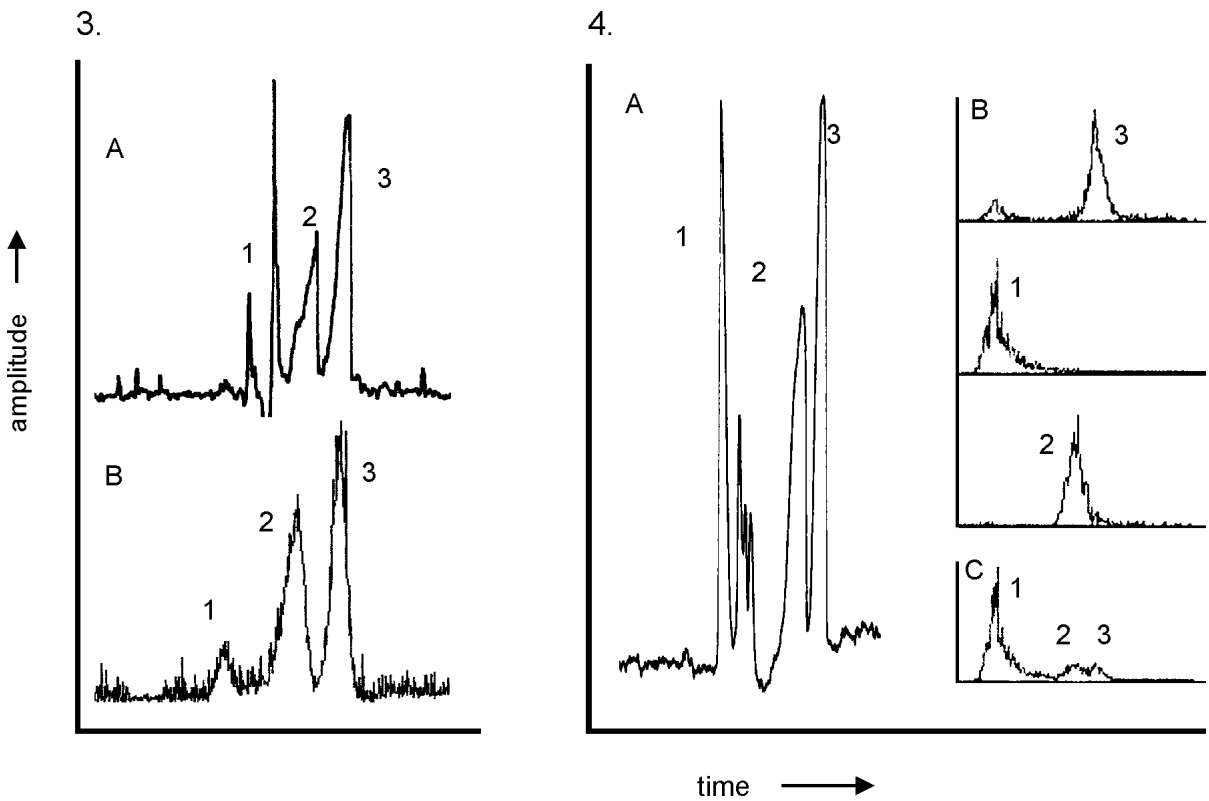

Fig. 3. On-capillary absorbance detection of β-endorphin fragment (1) 6-13, (2) 8-15 and (3) 10-17, before the LJC (A) and the corresponding CZE-MS reconstructed total ion electropherogram using CF-FAB (B). The MS is operated in the MID mode. The displayed time window is 5 min for both electropherograms, (A) 2.5-7.5 min and (B) 5.0-10.0 min. The peptides are dissolved in electrophoresis buffer at a concentration of 300 µmol/l.

Fig. 4. On-capillary absorbance detection of β-endorphin fragment (1) 9-17, (2) 8-17 and (3) 10-17, before the LJC (A) and the corresponding CZE-MS reconstructed total ion electropherogram using CF-FAB (C). In (B) the individual traces of the three peptides are shown. The MS is operated in the scan mode in m/z range 700-1350. The displayed time window is 3 min for both electropherograms, (A) 4.0-7.0 min and (B and C) 5.5-8.5 min. The peptides are dissolved in electrophoresis buffer at a concentration of 340 µmol/l.

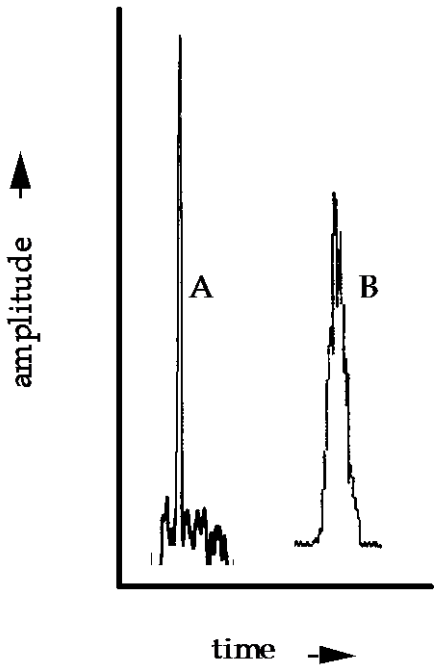

Fig. 5. (A) On-capillary absorbance detection of 100 ng/ml dextromethorphan before the LJC and the corresponding (B) CZE-MS MID electropherogram (m/z 272). The displayed time window is 30 s for both electropherograms, (A) 3.5-4.0 min and (B) 4.7-5.2 min. Injection is performed under stacking conditions.

Comparison of different detection modes

Three β-endorphin fragments 6-13, 8-15 and 10-17 with molecular masses of 857, 882 and 900, respectively, are selected for a comparative study of the different detection modes: i.e. conventional detection by means of a SEM, scanning array detection and static array detection by means of the PATRIC detector. In the latter case the ions in a fixed mass range of 8% around a centre mass, in this case a mass-to-charge ratio (m/z) of 875, are detected. The analysis is performed with 5 pmol of each β-endorphin fragment.

With the SEM detector scanning over a broad mass range (m/z 300-1000) at the 5 pmol level is not successful. Therefore, the mass range in this mode is reduced to m/z 840 - 910 using a cycle time of 1 second. The reconstructed mass electropherograms of the m/z values of the protonated molecules are given in Fig. 6A together with a spectrum of the fragment 8 -15 in Fig. 6B. Scanning array detection is performed over a much wider mass range, i.e. m/z 300 -

1000 with a cycle time of 1 second. The reconstructed mass electropherograms and the spectrum of the 8-15 fragment from this analysis are given in Fig. 6C and D. In Fig. 6E and F the results are given as obtained with the static array detection using the full 8% window, i.e. detecting over a mass range of m/z 840 - 910, and an accumulation time of 1 second.

When the reconstructed mass electropherograms in Fig. 6A, C and E are compared, a strong improvement in S/N ratio is observed going from scanning with SEM detection via scanning with array detection to the static array detection mode. In the latter case actually the three peaks are clearly observed in the trace of m/z 883. The last peak can be attributed to the 8 - 15 fragment; this protonated molecule of this peptide looses a molecule of water on FAB. One of the other peaks is the β-endorphin fragment 6-13, while the additional peak at this m/z ratio is probably due to an impurity in the sample.

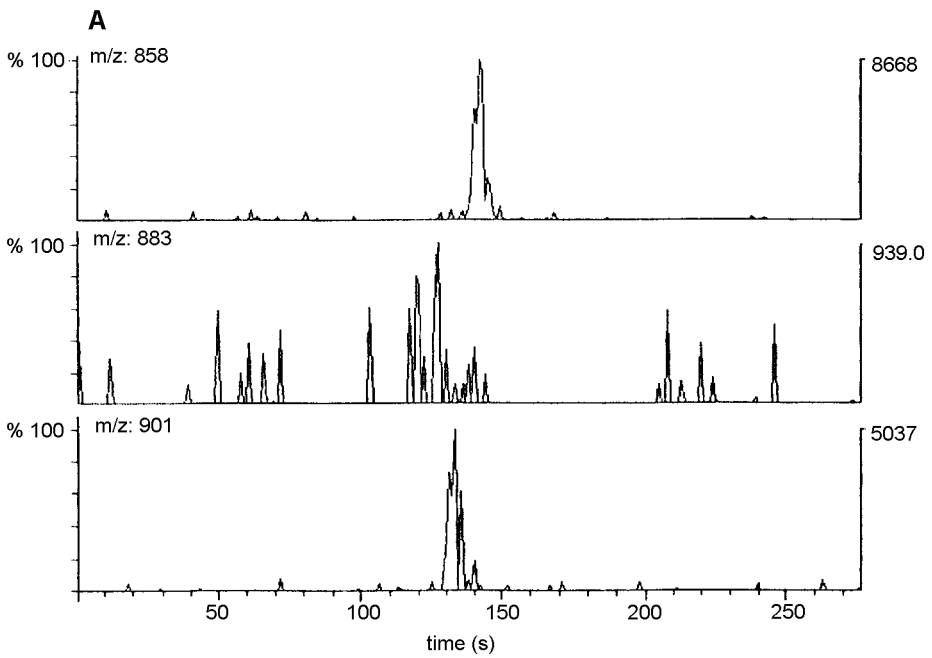

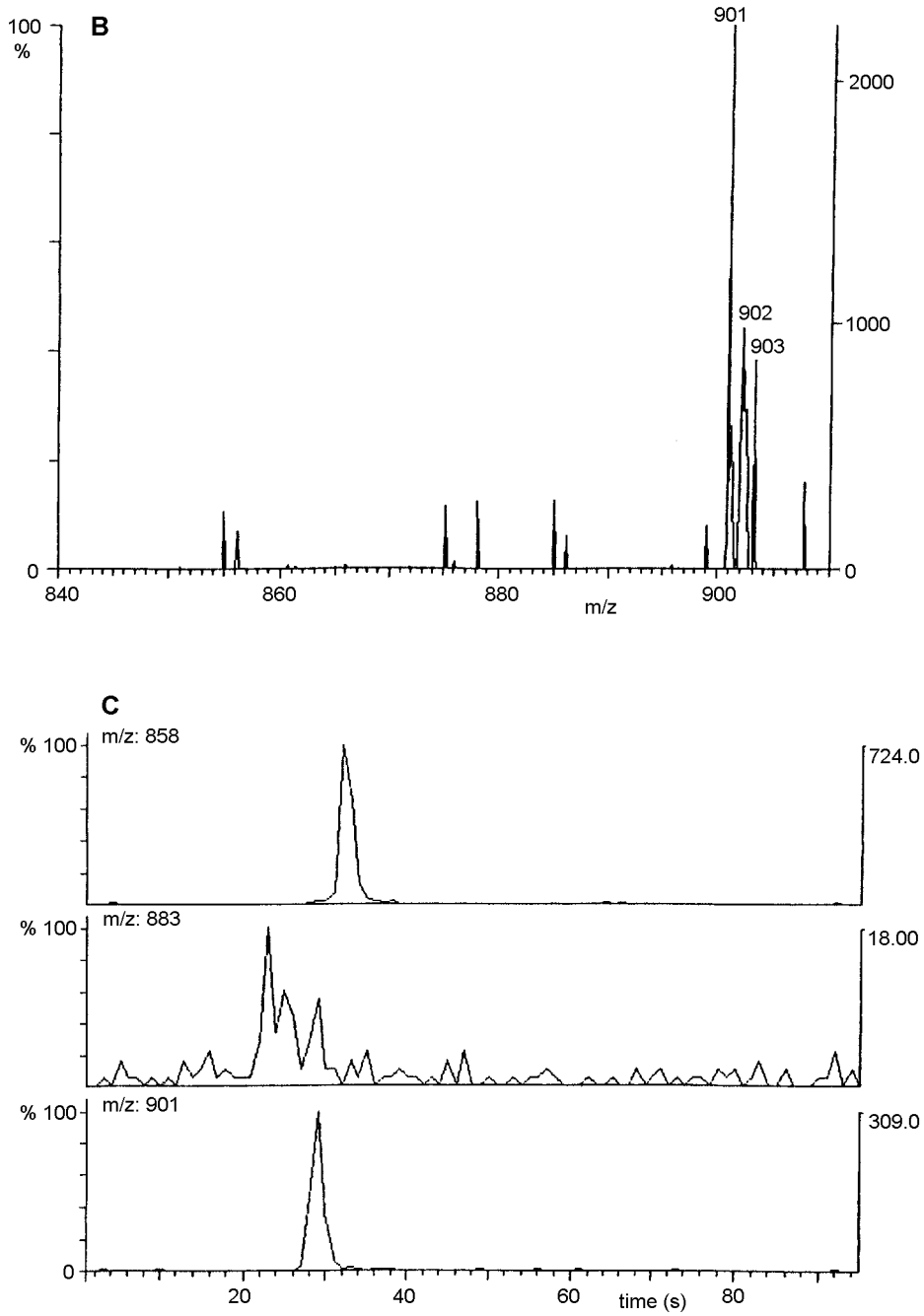
B
100
%
901
2000
902
1000
903
0
0
840
860
880
900
m/z
C
% 100
m/z: 858
724.0
% 100
m/z: 883
18.00
% 100
m/z: 901
309.0
0
20
40
60
time (s)
80

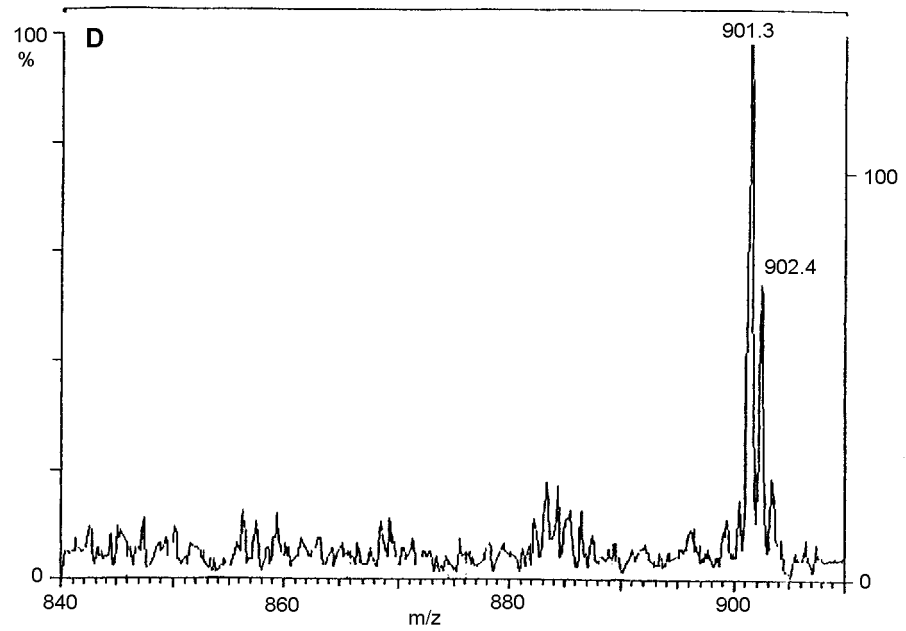
D
100
%
901.3
902.4
100
0
0
840
860
880
900
m/z

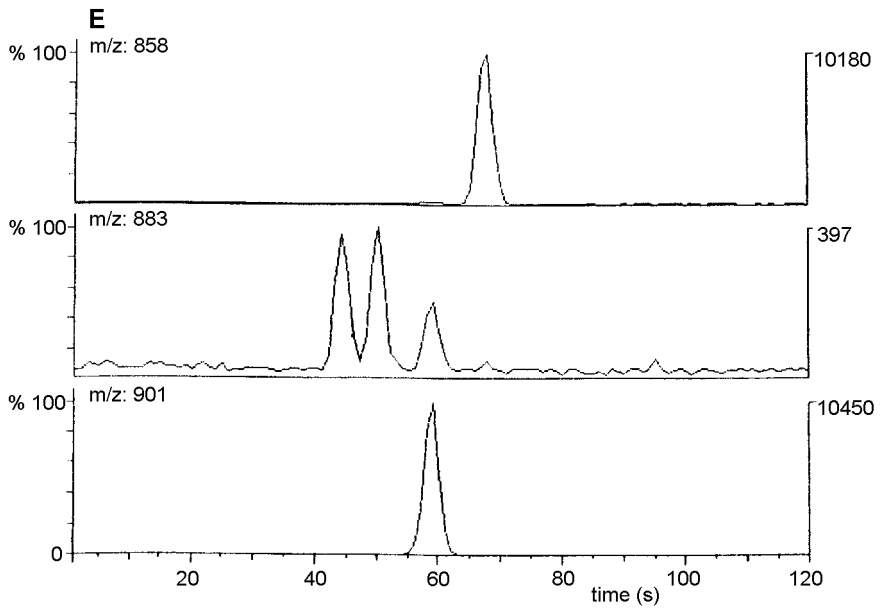
E
% 100
m/z: 858
10180
% 100
m/z: 883
397
% 100
m/z: 901
10450
0
20
40
60
80
100
120
time (s)

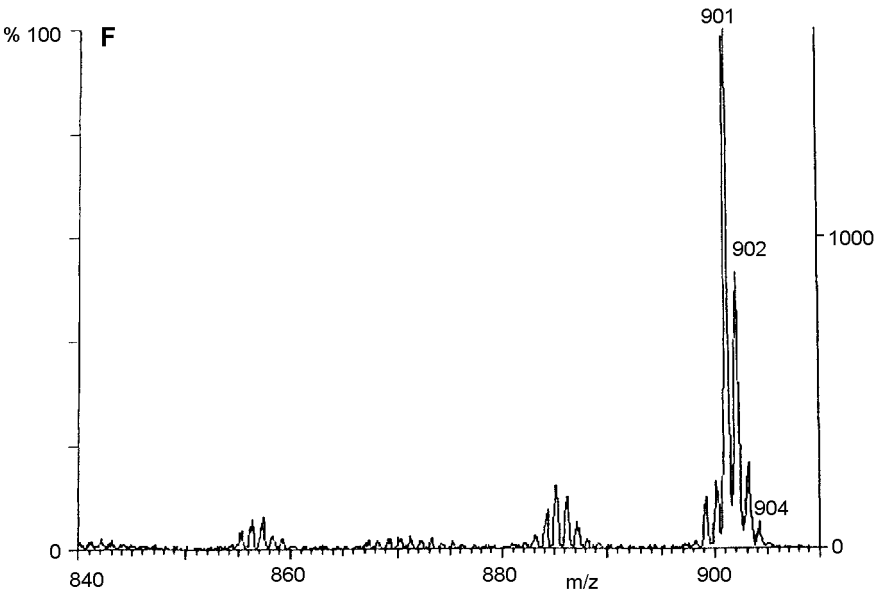

Fig. 6. (A, C and E) Reconstructed mass electropherograms (time in s) from the CZE-MS analysis of the β-endorphin fragments 6-13, 8-15 and 10-17 and (B, D and F) CF-FAB mass spectra of the β-endorphin fragment 8-15. Data acquired with 1s per scan. A and B, electron multiplier in scanning mode (m/z 840-910); C and D, scanning array detection (m/z 300-1000); E and F, static array detection with 8% window (m/z 840-910).

The improvement of the spectrum quality in the series Fig. 6B, D and F, which represent single spectra without averaging, is also evident from the S/N ratio and the isotope cluster. The numbers of ions detected for the peak at m/z 901 in a single spectrum of fragment 8 - 15 in the three different modes are 16, 480 and 16000, respectively. In evaluating these figures it must be kept in mind that for the scanning array detection mode a broader mass range is scanned (m/z 300-1000) than for the conventional detector (m/z 840-910). Taking this into account a 100-fold improvement for the scanning array mode and a 1000-fold improvement for the static array mode is observed. The data compared are all based on one spectrum and a cycle time of 1 second. This means for the static array mode that the absolute detection limit for the peptides investigated is in the 1-5 femtomolar range and even lower, if all spectra during a CZE peak are averaged.

Static array detection

Continuous-flow FAB has been successfully used in the detection of peptides in the m/z range below 2000. Above this range hardly any data are reported. From our own experiences the sensitivity at higher mass is lower than expected on the basis of comparing conventional FAB with CF-FAB at low mass. For this reason static array detection is used to measure the performance of CF-FAB in combination with CZE in the m/z range of 2000 - 3300.

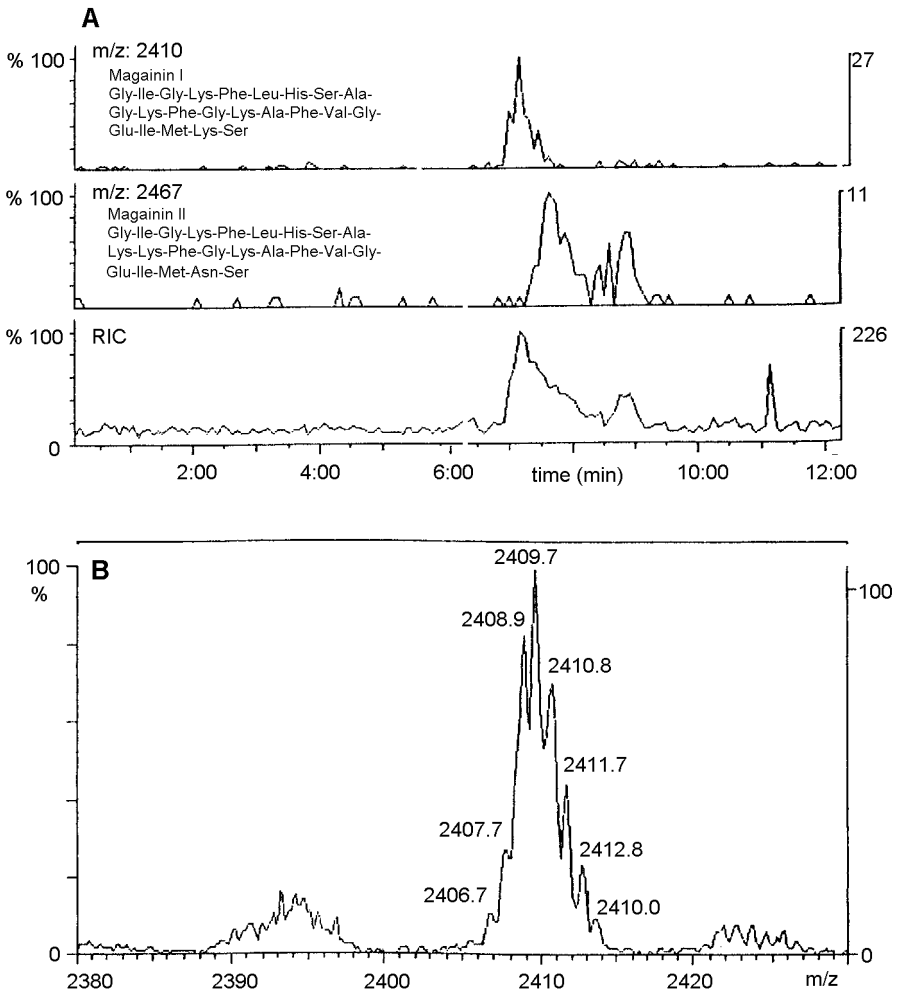

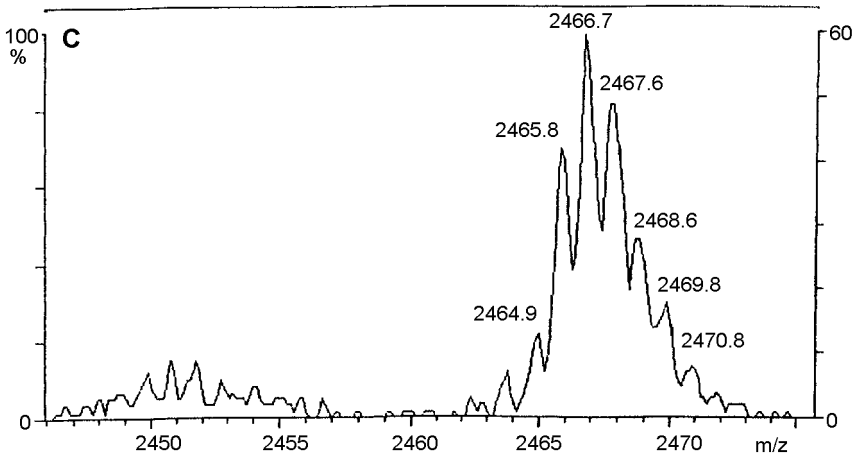

Fig. 7. (A) Reconstructed total ion and mass electropherograms (time in min) from CZE-MS analysis of magainin I and II (static array detection). Data acquired with 1s per scan. (B) CF-FAB mass spectrum of magainin I. Averaged molecular mass of the protonated molecule is 2410.9. (C) CF-FAB mass spectrum of magainin II. Averaged molecular mass of the protonated molecule is 2467.9.

The reconstructed total ion and the mass electropherograms for a CZE/MS analysis of the two peptides magainin I and II are given in Fig. 7A. The magainin I and II peptides, which originally are isolated from frog skin, have a molecular mass of 2408.3 and 2465.3, respectively. Although the peptides differ only in 2 of the 23 amino acids separation is achieved in CZE. The spectra obtained at the 2 pmol level with a resolution of 2000 are given in Fig. 7B and C and are of good quality; a well defined isotope envelope is obtained.

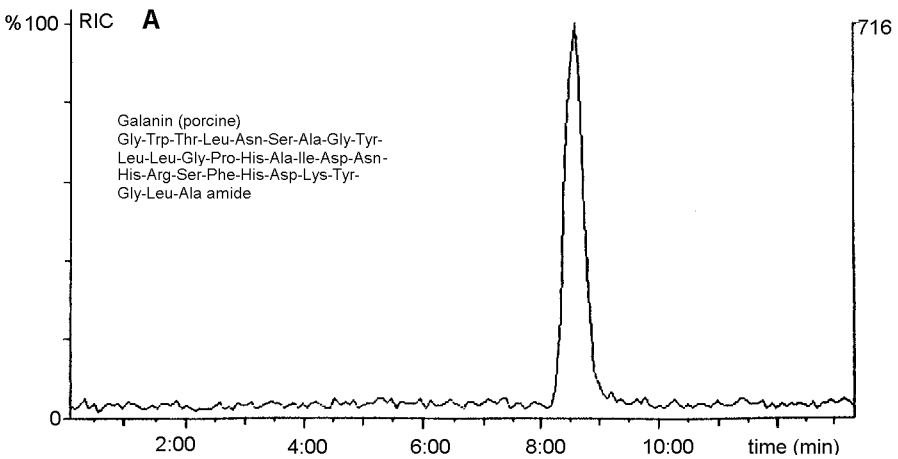

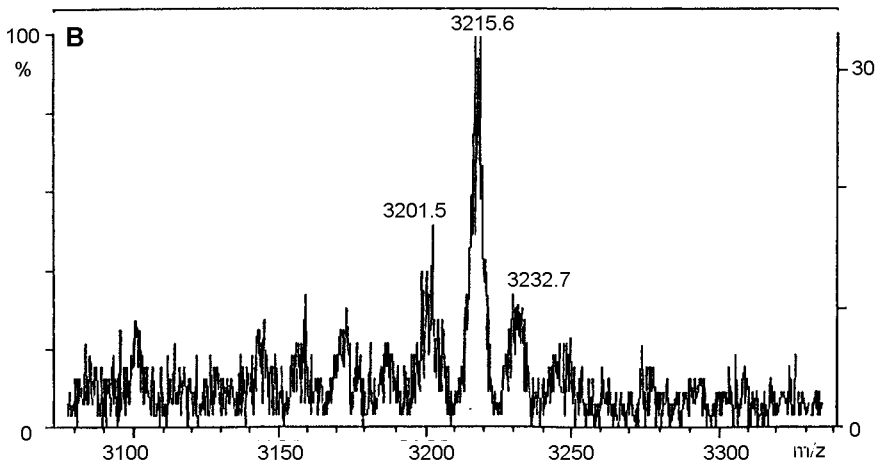

Fig. 8. (A) Reconstructed total ion electropherogram (time in min) and (B) CF-FAB mass spectrum of galanin. Averaged molecular mass of the protonated molecule is 3211.6. Data acquired with 1s per scan.

Fig. 8. shows the spectrum of 15 pmol Galanin (averaged molecular mass 3211.6) with a resolution of 1000. Although the sensitivity at higher mass decreases, a usable spectrum could be obtained.

Conclusions

The liquid junction coupling of CZE with CF-FAB-MS is successfully applied in the analysis of peptide mixtures. Due to hydrodynamic dispersion in the transport capillary the CZE efficiencies decreased to CZE-MS efficiencies of approximately 5000-10000. The CZE-MS efficiencies are mainly determined by the dispersion in the LJC and the transport capillary. Optimisation should therefore start with a reduction of the excessive zone broadening in the transport capillary.

Application of a PATRIC array detection system results in a considerable improvement of the sensitivity in mass spectrometric detection in CZE-MS. The static detection mode is useful in target compound analysis and results in sensitivities comparable with single ion monitoring, but information over a larger mass range of 8% around a centre mass is obtained. Scanning array detection is a universal detection approach of major importance, since the gain in sensitivity can be in the order of 10 - 100 as compared to a conventional SEM in combination with scanning.

References

1. J.A. Olivares, N.T. Nguyen, C.R. Yonker and R.D. Smith, Anal. Chem., 59 (1987) 1230.
2. R.D. Smith, C.J. Barinaga and H.R. Udseth, Anal. Chem., 60 (1988) 1948.
3. E.D. Lee, W.M. Mück, J.D. Henion and T.R. Covey, Biomed. Environ. Mass Spectrom., 18 (1989) 844.
4. R.D. Minard, D. Luckenbill, P. Curry, Jr. and A.G. Ewing, Adv. Mass Spectrom., 11 (1989) 436.
5. N.J. Reinhoud, W.M.A. Niessen, U.R. Tjaden, L.G. Gramberg, E.R. Verheij and J. van der Greef, Rapid Commun. Mass Spectrom., 3 (1989) 348.
6. R.M. Caprioli, W.T. Moore, M. Martin, B.B. DaGue, K. Wilson and S. Morning, J. Chromatogr., 480 (1989) 247.
7. M.A. Moseley, L.J. Deterding, K.B. Tomer and J.W. Jörgenson, Rapid Commun. Mass Spectrom., 3 (1989) 87.
8. C. Brunnee, R. Pesch and E. Schröder, Rapid Commun. Mass Spectrom., 4 (1990) 173
9. P. Kokkonen, E. Schröder, W.M.A. Niessen, U.R. Tjaden and J. van der Greef, Org. Mass Spectrom., 25 (1990) 566

2.2

Capillary Isotachophoretic Analyte Focusing for Capillary Zone Electrophoresis with Mass Spectrometric Detection using Electrospray Ionisation

Abstract

An improvement in detectability in capillary zone electrophoresis-mass spectrometry (CZE-MS) is realised using isotachophoretic (ITP) analyte focusing. The practical approach is described for the on-line coupling of ITP-CZE-MS using an electrospray (ESP) interface. An equation is derived for the calculation of the splitting ratio of ITP zones into the CZE system. The applicability of analyte focusing is demonstrated for the analysis of a mixture of anthracyclines. Initial experiments showed a 200-fold improvement in concentration detection limit for ITP-CZE-MS compared to CZE-MS.

Introduction

CZE in combination with MS can be a potentially powerful tool in the analysis of various compounds [1-9]. Especially in the area of protein and peptide analysis there is a growing interest for a highly efficient separation technique such as CZE in combination with the high selectivity of mass spectrometric detection. CZE-MS interfaces described in literature are continuous-flow fast atom bombardment (CF-FAB), electrospray (ESP) and ionspray (ISP).

The application of CF-FAB is realised by either a liquid junction coupling or a coaxial approach for addition of the necessary make-up fluid for this type of ionisation. In the coaxial approach [10] the separation capillary is inserted in the CF-FAB capillary and ends only a few millimetres before the tip of the CF-FAB probe. This minimises the dead volume and facilitates high efficient separations.

In the other approach of CZE-CF-FAB-MS a liquid junction coupling (LJC) for the electric uncoupling and for addition of make-up fluid is used [2, 11, 12]. This type of coupling utilises a transport capillary between the CZE capillary and the mass spectrometer. Transport of ions in this capillary is facilitated by means of a hydrodynamic flow generated by the vacuum in the ion source of the mass spectrometer. It is evident that this type of CZE-MS coupling results in considerably more peak broadening with respect to the coaxial approach.

On the other hand however, the coaxial approach necessitates the use of 10 μm ID capillaries in order to prevent a hydrodynamic flow in the CZE capillary because of the vacuum of the ion source at the CZE capillary outlet. This means a considerable drawback with respect to the loadability and the corresponding sample concentration detection limits in CZE-MS [9]. Although the use of a LJC results in band broadening the mass flow to the mass spectrometer will be superior to the LJC type of couplings where 75 μm capillaries are used with an approximately 50 times higher loadability than the 10 μm ID capillaries. Nevertheless, the loadability is limited to the nanolitre range resulting in relatively high minimum detectable concentrations. An important improvement in detectability is realised by using a PATRIC (Position And Time Resolved Ion Counting) array detector for CZE-CF-FAB-MS [3].

The ESP interface for CZE-MS described by Smith [13, 14] has several advantages over the CF-FAB interface. Firstly, the CZE capillary is inserted in the ion source and the migrating ions are electrosprayed from the capillary outlet directly into the mass spectrometer implying that no additional peak broadening after the CZE separation is introduced. Secondly, the use of a sheath flow with an approximately 10 times higher flow rate enables the use of CZE buffers with minor consideration of the ionisation compatibility. In peptide analysis CZE can be performed in buffers with high pH, while positive ions are detected in the mass spectrometer because of addition of acetic acid to the sheath flow. Thirdly, the ion source is at atmospheric pressure resulting in the absence of a hydrodynamic flow and 75 μm CZE capillaries can be used. Finally, the ESP interface enables the analysis of high molecular mass compounds such as proteins. Because of multiple charges on the large molecules the corresponding charge-to-mass ratios are within the detectable range of the mass spectrometer.

The coupling of CZE-MS using electrospray with pneumatically assisted nebulisation (ionspray) is described utilising either a LJC [15] or a coaxial approach [16]. In a recent investigation both approaches are compared [17].

ITP is a capillary separation technique which is capable of concentrating trace components and diluting of major constituents of the sample. The combination of these features makes ITP in principle an ideal technique for sample treatment. The use of ITP as sample pretreatment in CZE is described already in literature [18- 21].

Characteristic of CITP is its concentrating properties. The concentrations of analyte ions are adapted to the concentration of the leading ions according to the Kohlrausch regulation function. The adjusted isotachophoretic concentration is given by

$$\bar{c}_i = \frac{z_L\, m_i\, (m_L + m_R)}{z_i\, m_L (m_i + m_R)} \cdot \bar{c}_L \qquad (1)$$

where $\bar{c}_i$ is the analytical concentration of analyte i, $\bar{c}_L$ is the leading ion concentration, z is the charge on the ion and m is the ionic mobility. The absolute values of z and m are used in (1). For any combination of weak and strong electrolytes (R, i and L) the *ionic* mobilities are used in (1).

In this paper we describe the preliminary results of the on-line coupling of ITP-CZE-MS with an ESP interface. For the coupling of ITP with CZE we used the same set up as described previously [18, 19] where we demonstrated a decrease of the concentration detection limits with a factor of 100-1000. The CZE-MS coupling is similar as described by Smith et al. [13]. The potential of the ITP-CZE-MS coupling is demonstrated with the analysis of a mixture of anthracyclines.

Experimental

Isotachophoresis

ITP took place in a home-made apparatus consisting of Plexiglas electrode vials and a PTFE capillary of 150 x 0.32 mm. The terminating buffer consisted of 10 mmol/l histidine (HIS) pH 7.2 in 60 % (v/v) methanol (MeOH). Sodium phosphate (10 mmol/l pH 7.2) in 60 % MeOH was used as leading buffer. Injection of 5 µl analyte into the ITP was done by means of a 100 µl injection syringe. There was no detector used, the ITP zones of anthracyclines could be observed. For the determination of low concentrations one of the anthracyclines was used as marker and added in a high concentration. The voltage was supplied by a model RR100-1.5R power supply (Gamma High Voltage Research, Mt. Vernon, NY, USA) operating in the constant current mode at 60 µA. For injection of ITP zones in the CZE by means of electrical splitting an additional power supply (model RR40-1.5P, Gamma High Voltage Research) was used. The current was measured in series with the capillary using a micro-amperometer (model 134312, Goerz, Vienna, Austria).

Capillary electrophoresis

CZE was carried out in a 700 x 0.075 mm ID (for CZE-MS) or 700 x 0.040 mm ID (for CZE-MS and ITP-CZE-MS) fused silica capillary (SGE, Ringwood, Victoria, Australia) using an electrophoresis buffer that composed of 10 mmol/l sodium acetate at pH 7.5 and 60 % MeOH (for CZE-MS) or 10 mmol/l sodium phosphate at pH 7.2 in 60 % MeOH (for ITP-CZE-MS). The power supply was operated in the constant voltage mode at 20 kV for CZE. Samples were electrokinetically injected applying 6 kV for 6 s. On-capillary absorbance detection in CZE took place at 350 mm from the anodic end, using a Spectra 100 UV-Vis absorbance detector (Spectra-Physics Inc., Mt. View, CA, USA) at a wavelength of 210 nm.

Isotachophoresis - capillary electrophoresis

Coupling of ITP-CZE was done as previously described [19] by inserting the CZE capillary in the ITP capillary through a septum in the cathode compartment of the ITP (Fig. 1). As the ITP zones approached the CZE inlet injection took place by means of electrical splitting proportional to the current distribution over the CZE and ITP capillary. After injection the ITP capillary was carefully flushed with leading buffer and the CZE run was started. The CZE buffer was the same as the leading buffer.

A schematic representation of the ITP-CZE-MS coupling is given in Fig. 1. Injection took place through a silicon septum (1) by means of a syringe inserted up to valve 3b. The valves (3a-c) were used for flushing the ITP capillary with buffer. The terminating buffer vial (2) was connected to a positive voltage and the leading buffer (4) vial to earth during ITP and was raised to +2 kV at the time of injection. ITP takes place in a 150 x 0.320 mm capillary (6). The capillary was closed by a membrane (5) to prevent hydrodynamic flow. For the CZE run the electrode in vial 2 was disconnected and the electrode in vial 4 was set at a positive voltage. CZE takes place in either a 700 x 0.075 mm or 700 x 0.04 mm capillary (8) and was inserted in the ITP through a septum (7). The UV absorbance detector (9) was placed at 350 mm of the CZE capillary end. The sheath needle (10) for electrospray MS was always grounded. Arrow (a) points at the splitting point of ITP-CZE, arrow (b) at the inlet of the sheath liquid.

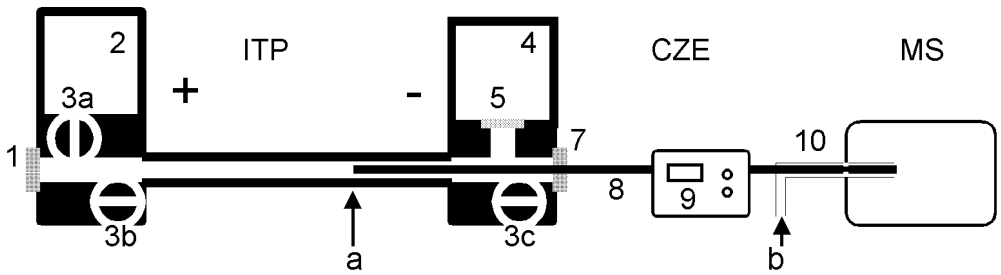

Fig. 1. Representation of the on-line coupling of ITP-CZE-MS. For explanation see text.

Capillary electrophoresis-mass spectrometry

A Finnigan MAT TSQ 70 triple-quadrupole mass spectrometer (Finnigan MAT, San Jose, CA, USA) equipped with an ESP (Finnigan MAT) was used in the positive ion mode. A sheath flow rate of 1 μl/min was applied by means of a syringe pump (model 2400, Harvard Apparatus, Edinbridge, UK). For the on-line coupling of CZE to the MS it is mandatory to make electrical contact between the ESP needle and the CZE capillary outlet. The sheath liquid consisted of 1 % glacial acetic acid in a mixture of ethanol-water (3:2, v/v). The current in the CZE capillary was monitored as described under the CZE conditions. The counter electrode of the electrospray was set at -4 kV, while the ESP needle was grounded. The distance of the outlet of the CZE capillary to the counter electrode was approximately 20 mm. Height differences between electrode vials and electrospray was omitted to prevent any hydrodynamic flow. All experiments were performed in multiple ion detection (MID) mode.

Chemicals

Doxorubicin (DOX), carminomicin (CAR) and epirubicin (EPI) were available as 1 mg/ml chlorohydrate solutions containing 5 mg/ml lactose and were purchased from Farmitalia, Carlo Erba S.A. (Nivelles, Belgium). Daunorubicin (DAU) was purchased from Rhone-Poulenc (Paris, France). Histidine, methanol, sodium hydrogenphosphate and sodium dihydrogenphosphate were purchased from Merck (Darmstadt, FRG). All further chemicals were of analytical grade. Throughout all experiments demineralised water was used.

Theory

Electrical splitting from ITP to CZE

The ITP-CZE coupling can be represented as an electrical circuit. When the influence of the electroosmotic flow is negligible, the split ratio between the CZE and the ITP capillary can be calculated by the current ratios I_2/I_3 (Fig. 2) [25].

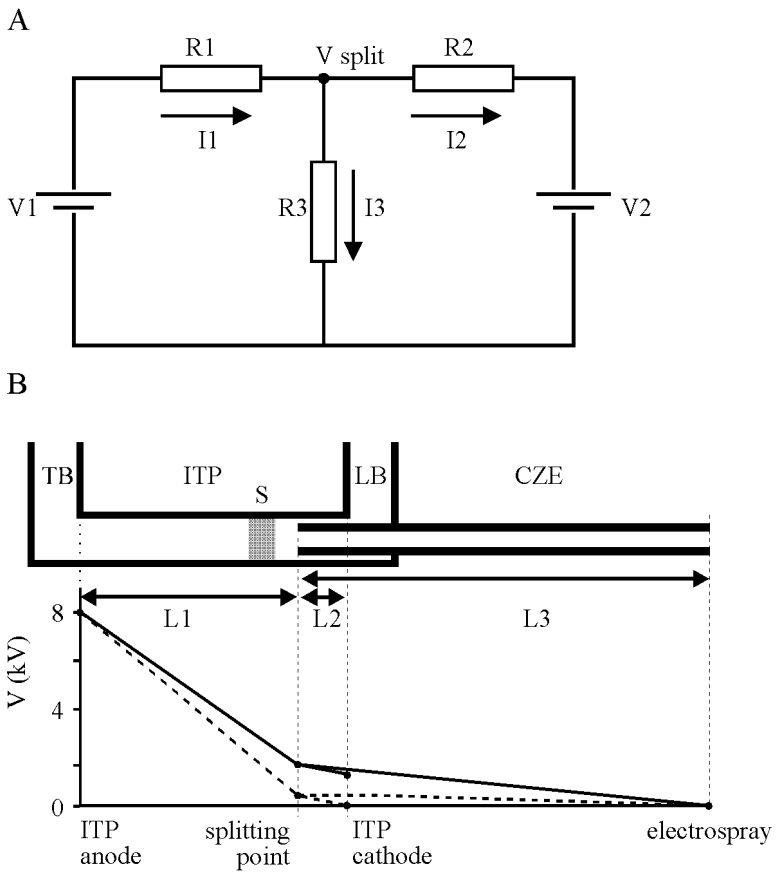

Fig. 2 (A). Schematic representation of the electrical circuit in ITP-CZE-MS at the time of injection. (B) The voltage distribution over the capillaries at the time of injection is given for V_2=0 kV (dashed line) and for V_2=2 kV (solid line) at a constant voltage V_1 of 8 kV. S is the sample zone, TB and LB are the terminating and leading buffer respectively. See text for further explanation.

In order to manipulate the splitting ratio it is convenient to know the parameters that are

influencing I_2 and I_3. Therefore an equation is derived giving the splitting ratio I_2/I_3 as a function of the capillaries dimensions using the resistance ratio R_3/R_2, and of the voltages applied at the time of injection. The currents I_2 and I_3 can be written as:

$$I_2 = (V_1 - I_1R_1 - V_2)/R_2 \qquad (2)$$

and

$$I_3 = (V_1 - I_1R_1)/R_3 \qquad (3)$$

and the ratio:

$$\frac{I_2}{I_3} = \frac{R_3}{R_2} \cdot \frac{V_1 - I_1R_1 - V_2}{V_1 - I_1R_1} \qquad (4)$$

V_1 and V_2 are respectively the potentials of the anode and cathode vial of the ITP at the time of injection. R_1, R_2 and R_3 are the electrical resistance of the ITP capillary from the anode to the splitting point and of the ITP capillary from the splitting point to the cathode and of the CZE capillary, respectively.

As $V_1 - I_1R_1$ represents the voltage at the splitting point at the time of injection (V_{split}) equation 4 becomes:

$$\frac{I_2}{I_3} = \frac{R_3}{R_2} \cdot \left(1 - \frac{V_2}{V_{split}}\right) \qquad (5)$$

When the cathode of the ITP is grounded at the time of injection (V_2=0) the equation is simplified and the splitting ratio is:

$$I_2/I_3 = R_3/R_2 \qquad (6)$$

In this case the splitting ratio is independent of V_{split} which means that the filling of the ITP capillary with terminating buffer is not influencing the splitting ratio. It should be noted that the current I_2 (Fig. 2a) can become negative. When V_2 approaches V_1 and $V_2 > V_{split}$ then the

direction of the current is reversed, the ions will migrate in the opposite direction and the ITP conditions no longer exist. Just before that, when $V_2 = V_{split}$, the current ratio $I_2/I_3 = 0$ which means that theoretically 100% of the analyte will migrate into the CZE. However, in this case small changes in the voltage will cause large differences in splitting ratio. In our experiments the splitting ratio is considerably lower to prevent overloading of the CZE system and to have a reproducible of the splitting ratio. The capillary resistance R can be calculated from:

$$R = L/\pi r^2 \kappa \qquad (7)$$

Where L is the capillary length, r is the capillary radius and κ is the conductivity of the buffer. As both the CZE capillary and the ITP capillary from the splitting point to the cathode are filled with the same leading buffer, the resistance ratio R_3/R_2 can be written as:

$$\frac{R_3}{R_2} = \frac{L_3}{L_2} \cdot \frac{r_{ITP}^2 - r_{CE,o}^2}{r_{CE,i}^2} \qquad (8)$$

where L_2 is the ITP capillary length from splitting point to cathode and L_3 the total CZE capillary length. The ITP capillary radius r_{ITP} is corrected for the inserted CZE capillary outer radius $r_{CZE,o}$, $r_{CZE,i}$ is the inner radius of the CZE capillary. The voltage at the splitting point at the time of injection is calculated from:

$$I_3 = I_1 - I_2 \qquad (9)$$

$$\frac{V_{split}}{R_3} = \frac{V_1 - V_{split}}{R_1} - \frac{V_{split} - V_2}{R_2} \qquad (10)$$

$$V_{split} = \frac{V_1 + \frac{R_1}{R_2} \cdot V_2}{1 + \frac{R_1}{R_3} + \frac{R_1}{R_2}} \qquad (11)$$

where resistance ratios are:

$$\frac{R_1}{R_2} = \frac{L_1}{L_2} \cdot \frac{\kappa_L}{\kappa_T} \cdot \frac{r_{ITP}^2 - r_{CE,o}^2}{r_{ITP}^2} \qquad (12)$$

and

$$\frac{R_1}{R_3} = \frac{L_1}{L_3} \cdot \frac{\kappa_L}{\kappa_T} \cdot \frac{r_{CE,i}^2}{r_{ITP}^2} \qquad (13)$$

The resistance ratios are corrected for differences in conductivities using the conductivity ratios κ_L/κ_T because at the time of injection the ITP capillary is filled up to the splitting point with terminating buffer. The conductivity ratio can easily be measured by the ratio of the voltage drop over the ITP capillary before the ITP run when the capillary is filled with leading buffer and at the end of the ITP run when the capillary is filled with terminating buffer at a constant current. The measured difference in voltage drop is caused by a proportional difference in conductivity of the leading buffer with respect to the terminating buffer. The influence of the electroosmotic flow and local temperature differences are considered negligible.

Results and discussion

CZE and ITP of anthracyclines

Several preliminary experiments are carried out for the optimisation of the capillary electrophoretic separation. Anthracyclines adsorb to the capillary wall, glassware and other laboratory materials introducing a source of irreproducibility especially at low concentrations [22]. One way to overcome this problem is the use of organic modifier in the stock solutions and the electrophoresis buffers [23]. Therefore, either acetonitrile (ACN) or MeOH is added to the electrophoresis buffer.

Although the use of volatile buffers is often preferred in MS to prevent contamination of the ion source by salt formation, it is possible to work for several days with a 10 mM sodium phosphate or sodium acetate buffer before crystallisation is notable and the ion source had to be cleaned.

The ITP separations of anthracyclines are performed in the cation mode because of their positive charge below pH 7.5. The ITP buffer system is a modification of the system described

by Akedo et al. [24] who used a leading buffer of sodium acetate at pH 6.0 and a terminating buffer of ß-alanine in 60 % MeOH for determination of doxorubicin and doxorubicinol in plasma. Under these conditions however, the mobility of some anthracyclines appeared to be higher than sodium. Therefore the pH is increased to 7.2 thus lowering the mobility of the anthracyclines. Histidine is chosen as the terminating buffer because its pI of 7.5 is close to the working pH resulting in the lowest mobility.

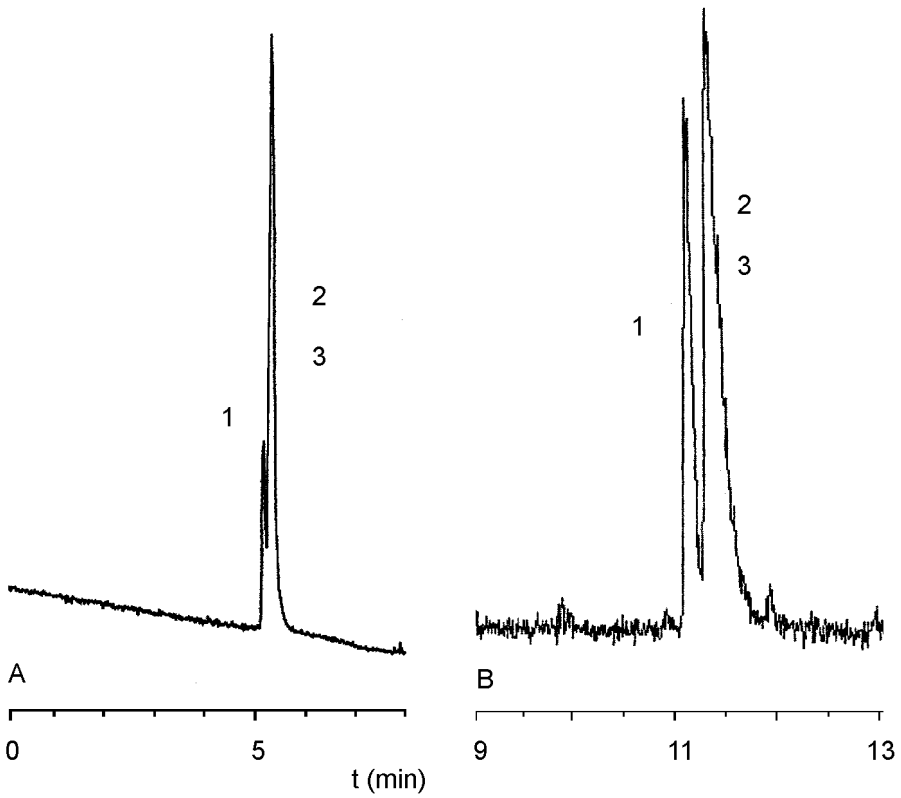

Fig. 3. Electropherograms of the UV absorbance (A) and mass spectrometric (B) detection of DAU(1), EPI(2) and DOX(3) (resp. 66, 83 and 83 µg/ml). CZE took place in a 0.075 x 700 mm capillary using a 10 mmole/l sodium acetate buffer pH4.6 in 70% ACN, and a voltage of 20 kV.

CZE-MS of anthracyclines

In the coupling of CZE with the MS the electrical contact between the electrospray needle and the capillary outlet appeared to be very important. Disruption of this contact could lead to electroperforation of the capillary because of the grounded stainless steel electrospray needle surrounding the CZE capillary over a length of 15 cm. By addition of 1% of glacial acetic acid to the sheath liquid this problem could be overcome, possibly due to improved wetting of the fused silica as well as the stainless steel ESP needle. Tuning of the mass spectrometer is done using a continuous flow of leading buffer containing 184 μmol/l DOX at a flow rate of 100 nl/min using the syringe pump.

Fig. 4. CZE-MS of the stereoisomers EPI(1) and DOX(2) (250 μg/ml each) in 10 mmole/l sodium acetate buffer pH 7.5 and 60% methanol using a 0.040 x 700 mm capillary and a voltage of 20 kV at the anodic end.

Fig. 3 shows the UV signal and the mass electropherogram of a mixture of DAU, EPI and DOX at a concentration of 66, 83 and 83 μg/ml, respectively. The UV trace shows no resolution

between the stereoisomers DOX and EPI. In the mass electropherogram a shoulder is formed on the peak at m/z 544 indicating a small difference in electrophoretic mobility. Also the resolution between the peak of DAU and the peak of DOX and EPI has improved compared to the UV signal. The efficiency calculated as the plate number from the mass spectrometric peak of DAU is approximately 120000.

In Fig. 4 the separation of the stereoisomers EPI and DOX is more pronounced. By changing the electrophoresis buffer from pH 4.6 to 7.2 the pH is closer to the pK_a of EPI and DOX which is 7.7 and 8.2 respectively. This enabled an almost baseline separation of both compounds.

ITP-CZE-MS of anthracyclines

The diameter of the CZE capillary in ITP-CZE-MS experiments is smaller than in CZE-MS experiments. It is necessary to use a 40 μm ID CZE capillary in the ITP-CZE mode in order to reduce a hydrodynamic flow in the CZE capillary when the ITP capillary is flushed with leading buffer. Flushing of the ITP capillary is done after injection of ITP zones in the CZE capillary. A syringe filled with leading buffer is connected to valve 3c (Fig. 1), valve 3c and 3b are opened and valve 3a is closed. A pressure is applied on the syringe and the ITP tube is flushed to establish a continuous buffer system during the CZE run. The pressure applied on the ITP system through valve 3c is distributed over the ITP capillary and the CZE capillary. This resulted in a hydrodynamic flow that is proportional to the capillary radius to the power 4 and to the reciprocal of the capillary length. This hydrodynamic flow is a major source of peak broadening of the CZE zones after ITP focusing when 75 μm CZE capillaries are used. By using 40 μm capillaries this peak broadening could be considerably reduced.

Injection of the ITP zones in the CZE capillary is done by electrical splitting [25]. The CZE inlet is positioned between the anode and cathode vial of the ITP, at approximately 3 cm from the cathode. The CZE capillary outlet is always grounded by means of the ESP interface. This means that during the ITP run a potential drop exists over the CZE capillary. By raising the cathode voltage of the ITP from 0 to +2 kV the split ratio is increased in favour of the CZE.

When in the described system the ITP cathode is grounded ($V_2 = 0$) the current ratio can be calculated from equation (6) and (8), using the capillary length L_3 ,L_2 and radius r_{ITP}, $r_{CZE,o}$ and r_CZE,i which are 70 cm, 3 cm, 160 μm, 100 μm and 20 μm respectively (Fig. 2). This results in a current ratio of 910, which means that 0.1 % of the total current is split to the CZE. Raising the voltage in the ITP cathode compartment appeared to be a convenient way to manipulate the splitting ratio. At a cathode voltage, V_2, of 2 kV, the splitting ratio is calculated to be 128

implying that 0.8% is split into the CZE (L_1 = 12 cm, κ_L/κ_T = 7, V_1 = 8 kV). This splitting ratio is used in further experiments. Although this split ratio is low, V_2 is not increased further because this would lead to overloading of the CZE capillary.

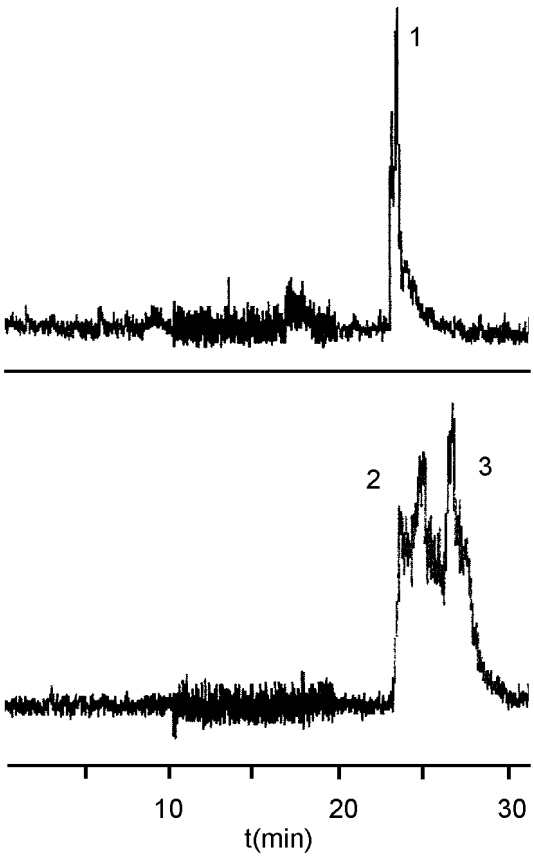

Fig. 5. Mass spectrometric electropherogram of ITP-CZE-MS of DAU(1), EPI(2) and DOX(3) (resp. 3, 8 and 8 μg/ml).

To study the potential of isotachophoretic analyte focusing in CZE-MS several ITP-CZE-MS experiments are performed. The standard mixture of anthracyclines is diluted to 5, 20, 50 and 200 times lower concentrations than in the CZE-MS experiments. Five microlitres of a mixture of DAU, EPI and DOX at concentrations of 3, 8 and 8 μg/ml respectively, are injected in the ITP system. CAR is added as a visible marker at a concentration of 10 μg/ml. The mass electropherogram after ITP-CZE separation (Fig. 5) shows considerable peak broadening due

to overloading of the CZE capillary after the ITP step.

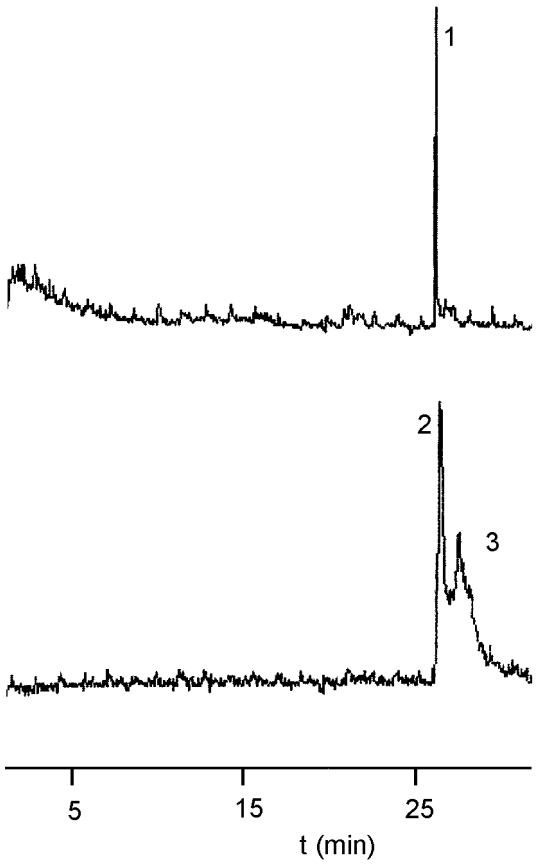

Fig. 6. Mass spectrometric electropherogram of ITP-CZE-MS of DAU(1), EPI(2) and DOX(3) (resp. 0.3, 0.8 and 0.8 μg/ml).

Lowering the concentration with a factor of 10 improved the peak shape considerably (Fig. 6). In this case the concentration of the marker CAR is 30 μg/ml. The improvement in detectability is clearly illustrated in Fig. 7. This figure shows the CZE-MS mass electropherogram of 66 μg/ml DAU (A) in comparison with a ITP-CZE-MS mass electropherogram of 0.3 μg/ml DAU (B). The improvement in detectability is at least a factor of 200.

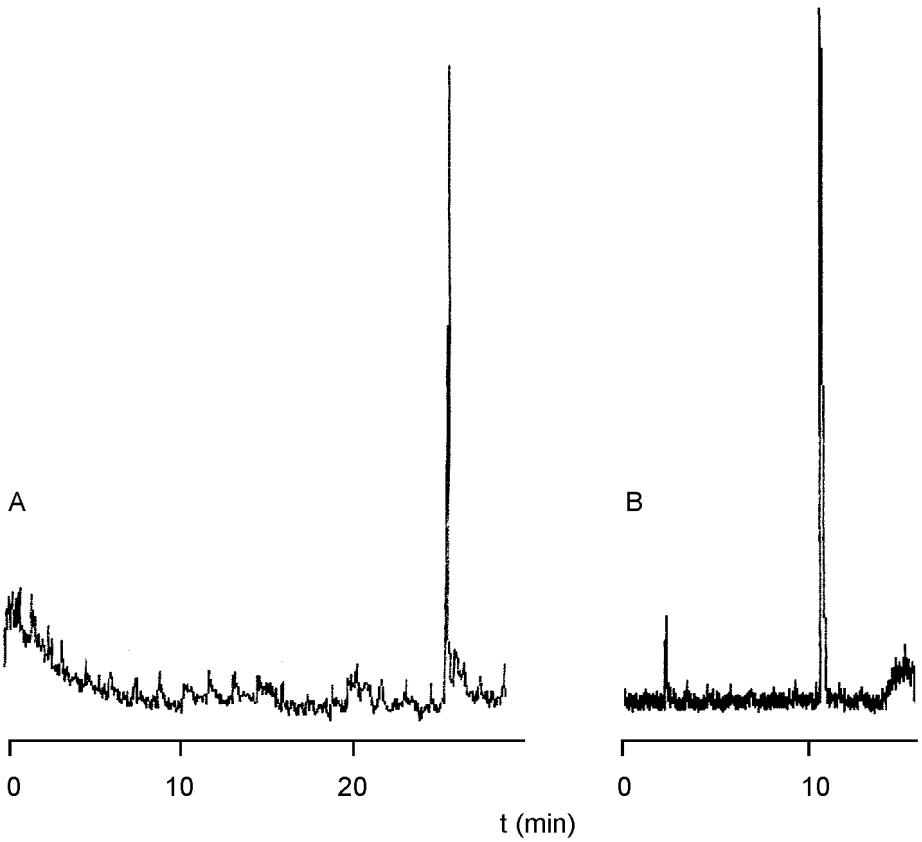

Fig. 7. Mass spectrometric detection of 0.3 μg/ml DAU by ITP-CZE-MS (A) and of 66 μg/ml DAU by CZE-MS (B).

Conclusion

The possibility of analyte focusing using on-line ITP-CZE-MS is demonstrated. Enenatiomer CZE separation and mass spectrometric confirmation in the analysis of DOX and EPI is realised. An improvement in detectability of at least a factor 200 is achieved in the analysis of DAU. Although in the ITP-CZE-MS mode the concentration of the anthracyclines is lowered a factor 5 - 200 still some overloading of the CZE could be seen.

References

1. R.D. Smith, J.A. Loo, C.J. Barinaga, C.G. Edmonds and H.R. Udseth, J. Chromatogr. 480 (1989) 211
2. R.M. Caprioli, W.T. Moore, M. Martin, B. DaGue, K. Wilson and S. Moring, J. Chromatogr. 480 (1989) 247
3. N.J. Reinhoud, E. Schroder, U.R. Tjaden, W.M.A. Niessen, M.C. ten Noever de Brauw and J. van der Greef, J. Chromatogr. 516 (1990) 147
4. M.A. Moseley, L.J. Deterding, K.B. Tomer and J.W. Jorgenson, Anal. Chem. 63 (1991) 109
5. I.M. Johansson, R. Pavelka and J.D. Henion, J. Chromatogr. 559 (1991) 515
6. P. Ferranti, A. Malorni, P. Pucci, S. Fanali, A. Nardi and L. Ossicini, Anal. Biochem. 194 (1991) 1
7. M.J.F. Suter, B.B. Dague, W.T. Moore, S.N. Lin and R.M. Caprioli, J. Chromatogr. 553 (1991) 101
8. I.M. Johansson, E.C. Huang, J.D. Henion and J. Zweigenbaum, J. Chromatogr. 554 (1991) 311
9. L.J. Deterding, C.E. Parker, J.R. Perkins, M.A. Moseley, J.W. Jorgenson and K.B. Tomer, J. Chromatogr. 554 (1991) 329
10. M.A. Moseley, L.J. Deterding, K.B. Tomer and J.W. Jorgenson, Rapid Comm. Mass Spectrom. 3 (1989) 87
11. N.J. Reinhoud, W.M.A. Niessen, U.R. Tjaden, L.G. Gramberg, E.R. Verheij and J. van der Greef, Rapid Comm. Mass Spectrom. 3 (1989) 348
12. R.D. Minard, D. Chin-Fatt, P. Curry and A. Ewing, Proc. 36th conf. on MS, San Francisco, ASMS 1988, p. 950
13. R.D. Smith, C.J. Barinaga and H.R. Udseth, Anal. Chem. 60 (1988) 1948
14. R.D. Smith, J.A. Loo, C.G. Edmonds, C.J. Barinaga and H.R. Udseth, J. Chromatogr. 516 (1990) 157
15. E.D. Lee, W. Muck, J.D. Henion and T.R. Covey, Biom. Env. Mass Spectrom. 18 (1989) 844
16. P. Thibault, C. Paris, and S. Pleasance, Rapid Commun. Mass Spectrom. 5 (1991) 484
17. S. Pleasance, S.W. Ayer, M.V. Laycock and P. Thibault, Rapid Commun. Mass Spectrom. 6 (1992) 14
18. D.S. Stegehuis, H. Irth, U.R. Tjaden and J. van der Greef, J. Chromatogr. 538 (1991) 393
19. D.S. Stegehuis, U.R. Tjaden and J. van der Greef, J. Chromatogr. 591 (1992) 341
20. D. Kaniansky and J. Marak, J. Chromatogr. 498 (1990) 191
21. F. Foret, V. Sustacek and P. Bocek, J. Microcol. Sep. 2 (1990) 229
22. U.R. Tjaden and E.A. de Bruijn, J. Chromatogr. 531 (1990) 235
23. N.J. Reinhoud, U.R. Tjaden, H. Irth and J. van der Greef, J. Chromatogr. 574 (1992) 327
24. H. Akedo and K. Shinkai, J. Chromatogr. 227 (1982) 262
25. M. Deml, F. Foret and P. Bocek, J. Chromatogr. 320 (1985) 159

Part 3

Capillary Isotachophoresis - Zone Electrophoresis

3.1

Automated Isotachophoretic Analyte Focusing for Capillary Zone Electrophoresis in a Single Capillary using Hydrodynamic Back-pressure Programming

Abstract

An automated isotachophoretic (ITP) analyte focusing procedure prior to capillary zone electrophoresis (CZE) is described. The ITP focusing step is carried out in the same capillary as the zone electrophoresis. Hydrodynamic backpressure programming results in a reduction of the effects of the electroosmotic flow rate during the ITP step and enables the removal of terminating buffer before the zone electrophoretic run is started. The characteristics of this on-line focusing procedure are studied for several anionic test compounds.

Introduction

Capillary electrophoresis (CE) has become an important separation technique complementary to high-performance liquid chromatography (HPLC). Several reviews have described the role of capillary electrophoretic separation methods in analytical chemistry [1-3]. Improvements in detection techniques resulted in detection of extremely low amounts of analyte. Nevertheless, owing to the small dimensions of the separation system and the small injection volumes, the corresponding concentration detection limits are relatively high.

Different on- and off-line methods to improve the determination limits in CE have been described. Off-line sample pretreatment and preconcentration, such as concentrating liquid-liquid or solid phase extraction, offers flexibility in the choice of buffers and the amount of sample to be pretreated. These procedures are laborious and time consuming. On-line sample pretreatment offers the possibility of automation but has some restrictions with respect to the following step in the analytical method. Examples of on-line sample pretreatment and/or preconcentration are the combination of LC-CE [4-6] and ITP-CZE [7-10].

An elegant way of lowering the detection limits that is typical for zone electrophoretic separations, is the application field amplified on-capillary sample concentration or stacking. This can be done in several ways, by using low conductivity sample buffers, by using sample self stacking, by addition of an electrolyte to the sample enabling a transient isotachophoretic preconcentration or by combining some of these methods [11-16].

In this paper we describe a procedure for the automated coupling of ITP with CZE using a single open capillary in a commercially available electrophoresis system without modification of the system. By using hydrodynamic backpressure programming during the focusing step the terminating buffer could be removed before the CZE step resulting in highly efficient separations.

Experimental

Untreated fused silica (100 µm ID, SGE, Ringwood, Victoria, Australia) and UV transparent (75 µm ID, Polymicro Technologies Inc., Phoenix, AZ, USA) capillary was used. A programmable injection system for capillary electrophoresis (PRINCE, Lauerlabs, Emmen, The Netherlands) equipped with a reversible polarity power supply and possibility for pressurised and/or electrokinetic injection was used for the analyte focusing process.

On-capillary LIF detection took place using a water-cooled argon-ion laser (2025-03, Spectra-Physics Inc., Mt. View, CA, USA) lasing at multiple wavelengths of 351.1 and 363.8 nm at 20 mW for excitation. The excitation wavelengths were filtered through a 350 nm bandpass filter (10 nm bandwidth). Fluorescence light was transported to the photomultiplier tube (PMT) through a liquid light guide (1000 x 5.0 mm ID, #77556 Oriel, Stratford, CT, USA) equipped with a plano convex fused silica lens (D 11 mm, focal length 19 mm, Oriel, model 41210) at each end. The fluorescence light was directed onto a 450 nm band pass interference filter (10 nm bandwidth, type 53830 Oriel) for ortho-phthaldialdehyde derivatives or onto a 525 nm interference filter (10 nm bandwidth) for fluorescein and analogues. The PMT (Model 9635A, Thorn EMI, Ruislip, Middlesex, UK) was operated at 800 V (power supply model 244, Keithley Instruments Inc., Cleveland, OH, USA).

The signal was amplified by a current amplifier (model 427, Keithley Instruments Inc.) and registered on a chart recorder (Kipp & Zn, Delft, The Netherlands) or digitised using a custom-made 12-bit A/D converter operating at a frequency of 20 Hz. The A/D converter was connected to a computer (Atari Mega ST4, Atari Corp., Sunnyvale, CA, USA) controlling the sampling frequency of the converter and the data handling.

Chemicals

Phosphoric acid, bariumhydroxide, glutamic acid (Glu), aspartic acid (Asp), and bromophenol blue were from Merck (Darmstadt, FRG). Sodium cacodylate and fluorescein (F) was purchased from Janssen Chimica (Beerse, Belgium). Hydroxypropylmethylcellulose (HPMC) came from Sigma (St. Louis, MO, USA). The viscosity of a 2% aqueous HPMC solution was

4000 cP. Fluoresceinisothiocyanate isomer I (FITC), ortho-phthaldialdehyde (OPA) and mercaptoethanol (ME) were from Aldrich Chemie (Steinheim, Germany). In all experiments deionised water was used (Milli-Q system, Millipore, Bradford, MA, USA).

OPA derivatives of amino acids were made by adding 1 ml of amino acid dissolved in leading buffer to an OPA solution of 1 mg/ml in leading buffer containing 0.1% ME. Unless mentioned otherwise the OPA derivatives were analysed after 5 min. Sample solutions of fluoresceins were made in leading buffer unless mentioned otherwise.

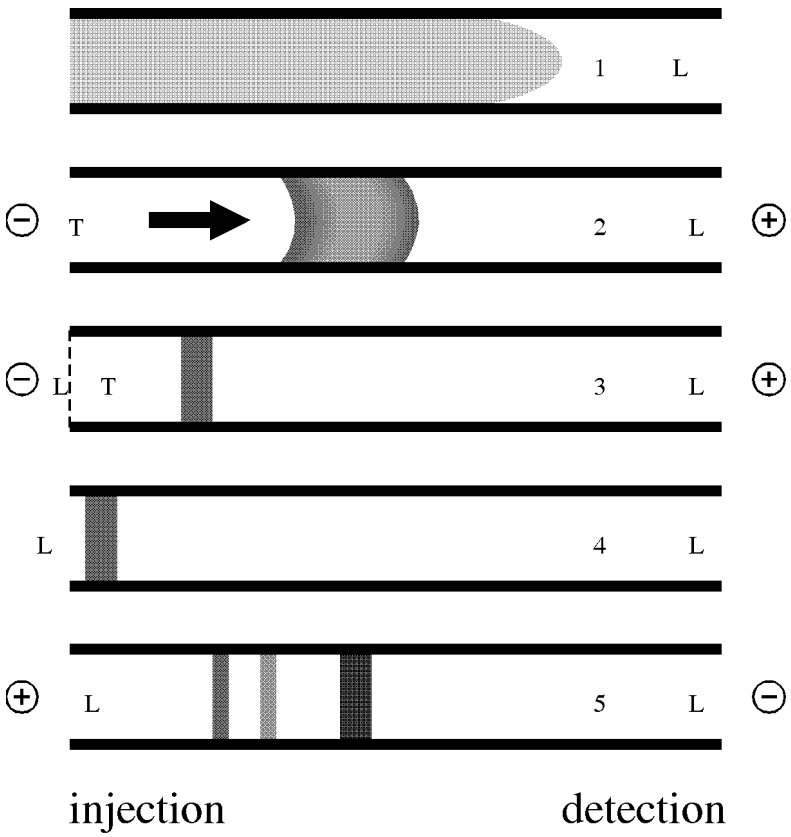

Fig. 1. Schematic representation of ITP-CZE in a single capillary. The leading buffer (L) is also used as electrophoresis buffer in the CZE step. The terminator buffer (T) is removed from the capillary in step 3. See text for further details.

Results and discussion

Analyte focusing after hydrodynamic sample introduction

A discontinuous buffer system is used to enable isotachophoretic sample preconcentration (Fig. 1). The capillary and ITP anode vial (which is also the CZE cathode vial) are filled with leading buffer consisting of 10 mmol/l sodium phosphate at a pH of 9.4.

To the leading buffer 0.05% (w/v) of HPMC is added. The HPMC only reduced the electroosmotic flow in the fused silica capillary to such an extent that acceptable preconcentration runs could be made. The leading buffer is also used as CZE buffer.

Step 1. Injections are made hydrodynamically at a pressure of 10 - 600 mbar. After injection a terminating buffer vial with 10 mmol/l sodium cacodylate buffer of pH 8.2 containing 0.05% HPMC (w/v) is placed at the capillary inlet. For the analysis of OPA derivatives the pH is raised to 9.4 using $Ba(OH)_2$.

Step 2. The analyte focusing started by applying a voltage of -25 kV in conjunction with a hydrodynamic backpressure of 40 mbar. This negative voltage resulted in an electroosmotic flow in the direction of the capillary inlet. To prevent the analyte from migrating out of the capillary a hydrodynamic backpressure is applied. Because of the self correcting properties of the ITP zones the hydrodynamic backpressure did not result in peak broadening. This is in contrast to field-amplified injection techniques where electroosmotic convections are a major source of peak broadening for large injection plugs [11].

Step 3. After 5 - 20 min of focusing, depending on the injected volume, the cacodylate buffer vial is replaced for the CZE buffer vial. A voltage of -20 kV is applied without a hydrodynamic backpressure. Since the capillary still contains cacodylate buffer, this step is carried out under real isotachophoretic conditions, although a vial with phosphate buffer is placed at the terminator end. The sample zones are sandwiched between the anodic leading buffer and terminating buffer plug which is in the capillary. The electroosmotic flow rate is higher than the mobility of the phosphate ions in the vial at the terminator end thus preventing these ions from entering the capillary. Simultaneously the plug of terminating buffer is removed out of the capillary. It is important for the next step that the CZE buffer vial is already in position.

Step 4 and 5. At the time that the sample zone is approaching the capillary inlet the voltage is reversed and the CZE run is started at a positive voltage of 30 kV. The correct timing of the voltage switching is important. When the ITP process is continued too long, the sample zones will migrate out of the capillary into the inlet buffer vial. If the voltage is switched too early a plug of terminating buffer is still in the capillary and will disturb the homogeneity of the electric

field necessary for CZE resulting in peak broadening. Initially bromophenol blue is used as a visible marker. When reproducible ITP run times are measured automated programming is applied and the marker could be omitted. When the use of a visible marker is inconvenient because of hardware incompatibility, timing can be done by monitoring the current. Applying a constant voltage the current increases as long as the terminating ions leave the capillary.

In principle all terminating ions and sample ions with mobilities below that of the analyte ion can be removed by the described procedure. This is an important difference from transient-like isotachophoretic preconcentration [12, 15]. Another advantage of focusing under isotachophoretic conditions using a hydrodynamic backpressure is that the time needed for focusing can be in principle as long as necessary for a given analysis without peak broadening or loss of analyte. An optimum can be found between the determination limit of an analyte for a given injection volume and the time needed for focusing.

The analyte focusing is studied for OPA derivatives of Glu and Asp derivatised before injection. The derivatives have an excitation maximum at 340 nm fitting with the 351.1/363.8 nm lasing wavelengths of the argon ion laser. The laser beam is filtered with a 350 nm bandpass filter before focusing onto the capillary. This reduced the background at 450 nm, the emission maximum of the OPA derivatives, considerably. Because OPA derivatives are not stable in time [17], some characteristics of the system are investigated with F and FITC. These compounds are native fluorescent with an excitation maximum around 490 nm. Although this excitation maximum fits perfectly with the 488 nm lasing wavelength of the argon ion laser, a good signal is obtained using the 351.1/363.8 nm lasing wavelengths for excitation. For convenience reasons the laser optics are not changed and all experiments are done using the same laser system, except for the emission wavelength which is 525 nm for the fluoresceins. The effect of analyte focusing is compared with CZE runs without focusing.

Loadability and linearity for OPA derivatives

When analyte focusing is carried out for injection volumes similar as for CZE runs, the improvement in detectability is limited (Fig. 2A and B).

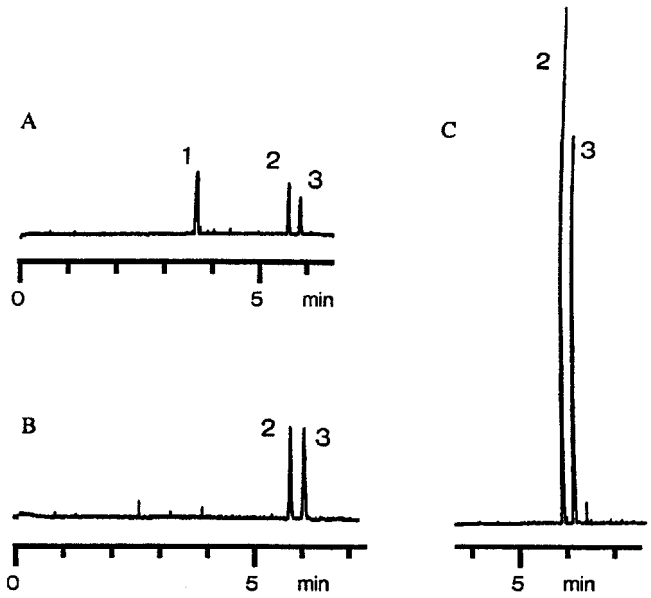

Fig. 2. Electropherograms of a mixture of 200 ng/ml OPA derivatives of Phe (1), Glu (2) and Asp (3). An injection volume of 70 nl using CZE (A) compared with 70 nl (B) and 350 nl (C) using ITP-CZE. A 700 x 0.1 mm fused silica capillary is used. The derivative of Phe had a lower mobility as the terminator and is removed from the capillary in ITP-CZE.

An explanation for this effect is that in CZE the analytes migrate through a background electrolyte while in ITP the analytes are sandwiched as distinct zones between a leading and terminating electrolyte. In ITP-CZE when the focusing procedure has been completed and the CZE is started a mixing of the analyte zones with the background electrolyte occurs. This results in some band broadening and dilution. In Fig. 2B the ITP preconcentration of analyte is levelled by this mixing process resulting in comparable peak heights. Fig. 2C shows that increasing the injection volume with a factor 5 results in an increase of signal with a factor 5.

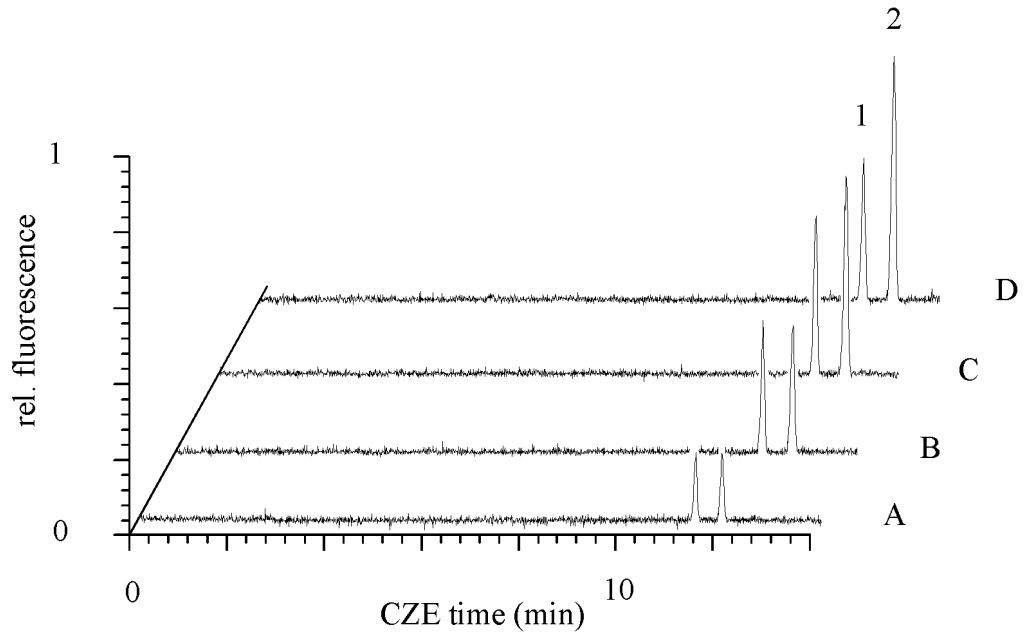

Fig. 3. Effect of the injection volume on the analysis of a derivatization mixture of 1 µg/ml Glu (1) and Asp (2) with OPA. The injection volume is increased from 0.2 µl (A), 0.7 µl (B), 1.4 µl (C) to 2.4 µl (D). A 700 x 0.1 mm fused silica capillary is used.

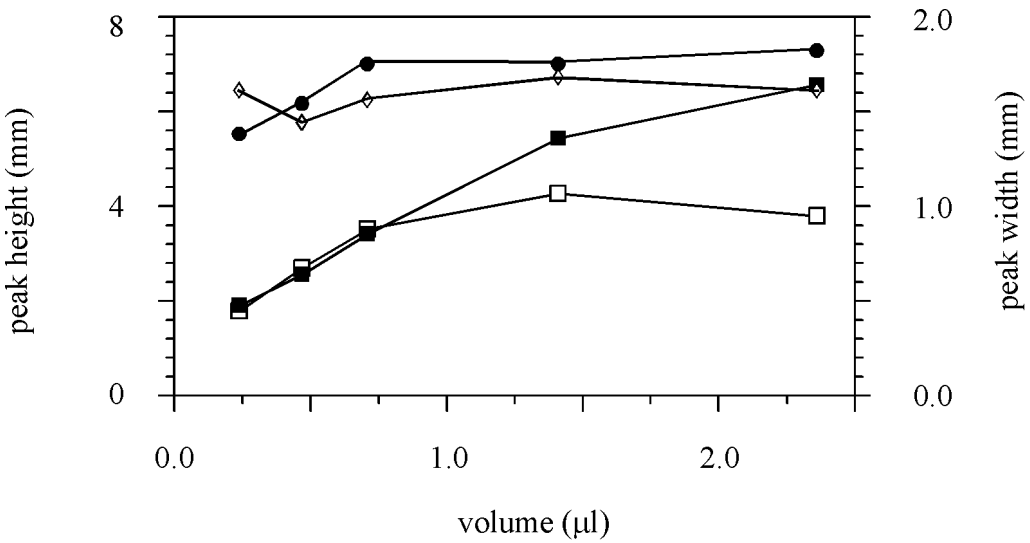

Fig. 4. The peak height of Asp (closed box) increases while the peak widths of Asp (closed dots) and Glu (open dots) remain the same at increasing injection volume. The peak height of Glu (open box) shows an optimum. The peak width is given as half the peak width measured

at 60% of the peak height. The corresponding electropherograms are shown in Fig. 3.

Fig. 3 and 4 show that the capillary can be filled for 50% (2.4 µl) without band broadening. For the OPA derivative of Glu there is an optimum in the loadability with respect to peak height, while the peak height of the Asp derivative does not increase linearly with the injection volume. At larger injection volumes longer focusing times are necessary resulting in degradation of the unstable derivatives. The focusing time increased from 4 min for 0.2 µl to 20 min for 2.4 µl injection volume. To eliminate these effects we studied the loadability, linearity and reproducibility with F and FITC.

Loadability, linearity and reproducibility for fluoresceins

F and FITC are more stable than OPA derivatives under alkaline conditions. FITC is a well known fluorescent probe for the derivatization of amines. The reaction products are usually anionic because of the charges on FITC. It is therefore expected that reaction products can be analysed in a similar way using ITP-CZE.

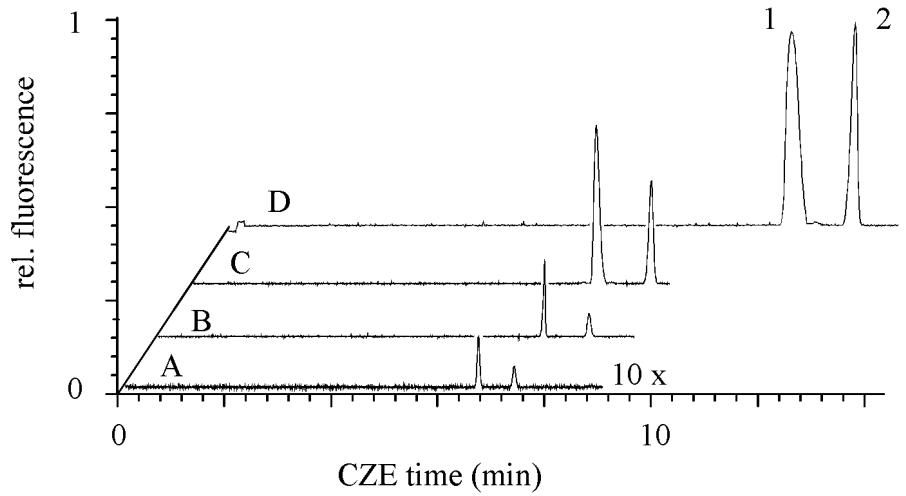

Fig. 5. Loadability in ITP-CZE of a mixture of FITC (1) and F (2) at a concentration of 500 ng/ml in leading buffer. Injection volume is 14 nl (A), 140 nl (B), 750 nl (C) and 1500 nl (D). The peak height of F and the peak area of F and FITC showed a linear increase with the injection volume. A 700 x 0.075 mm fused silica capillary is used.

As can be seen from Fig. 5 the increase of detectability of F corresponds to the increase of injection volume. The total analysis time for the CZE run is 10 min, while the ITP-CZE run took 20-24 min. This included a flush of 1 min with 10 mmol/l KOH, 1 min with leading buffer and an ITP focusing step of 10 min. The flushing is necessary to get reproducible migration times.

Loading of the capillary with large sample plugs changes the condition of the capillary wall especially when a dynamic coating of HPMC is used. In case of relatively clean samples and constant injection volumes this resulted in a small shift in the migration time. However, when the injection volumes are increased the effects on the capillary wall are more severe.

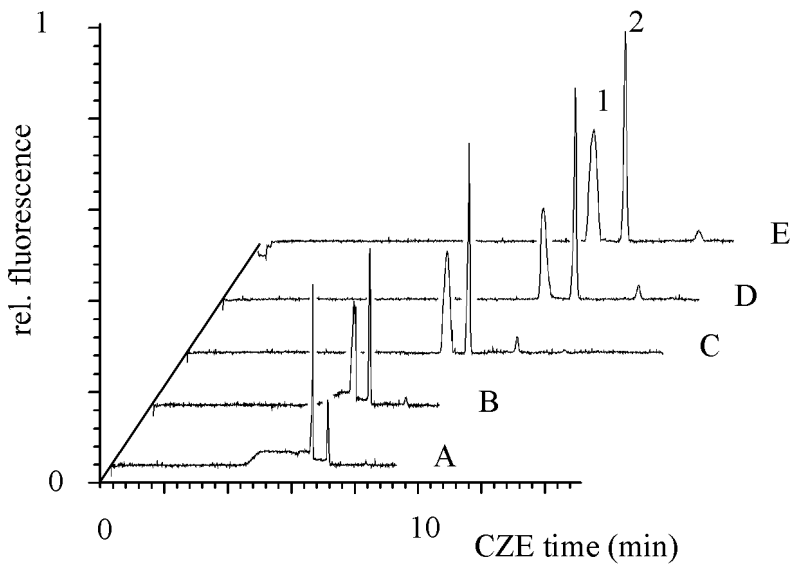

Fig. 6. The effect of the focusing time on the performance in ITP-CZE of a mixture of 50 ng/ml FITC (1) and F (2). Injection volume is 1.5 µl. A 700 x 0.075 mm fused silica capillary is used. The focusing time is increased from 1.8 min (A), 4.5 min (B), 10 min (C), 18 min (D) to 34 min (E).

In Fig. 5 the migration times in the CZE step increased with ca. 65% for both analytes. In the study of fluoresceins a buffer of pH 8.1 is used implying that at longer focusing times the pH in the capillary decreases. As a result the electroosmotic flow in the CZE decreased resulting in increased migration times. This shift is not seen for the OPA derivatives (Fig. 3). For the OPA derivatives a terminator buffer at the same pH as the leading buffer (pH 9.4) is used. The use of a buffering counter ion (i.e. Tris) is therefore advisable. However, for our test compounds the CZE performance is better with sodium phosphate buffer.

In Fig. 6 the effect of the focusing time on the performance in ITP-CZE is demonstrated. A focusing time of less than 5 min results in a loss in signal because of incomplete focusing. Increasing the focusing time from 10 to 34 min did not result in a change in resolution or efficiency. This is an important observation because it demonstrates that band broadening is

independent of time in the focusing procedure although a hydrodynamic backpressure is used. Everaerts et al. used a counterflow of electrolyte in ITP to increase the effective length of the separation system [18]. They measured a considerable disturbance when the counterflow is higher than 30% of the mobility of the sample zones is applied. They concluded that the optimal counterflow depended on amongst other things on the capillary diameter, the viscosity and the temperature in the capillary. In our ITP-CZE system no peak broadening is seen at a backpressure which is 100% of the analyte mobility. In principle this means that the effective length of our ITP system has been increased to infinity. However, the analysis time increases similarly. Therefore, an optimum has to be found between the injection volume, the complexity of the sample, the determination limit and the time needed for focusing of large injection plugs.

Table 5. Reproducibility of peak heights and areas of 5 CZE runs and 5 ITP-CZE runs. Hydrodynamic injections of 30 nl and 1.7 μl are used for CZE and ITP-CZE respectively. CZE concentrations are 1.0 and 0.5 μg/ml for F and FITC respectively. The concentrations in ITP-CZE are a factor of 100 lower.

	height RSD (%)		area RSD (%)	
	CZE	ITP-CZE	CZE	ITP-CZE
F	8.4	9.8	3.5	6.5
FITC	8.6	18	5.3	5.3
ratio F/FITC	-	-	4.6	4.8

The reproducibility in CZE and ITP-CZE is studied for a mixture of FITC with F. The peak areas gave better results than peak heights in both CZE and ITP-CZE (Table 5). The relative standard deviation (RSD) in peak areas for CZE is 3.5% and 5.3% for F and FITC respectively, the RSD in peak heights is 8.4% and 8.6% respectively. For ITP-CZE a RSD in peak areas of 6.5% and 5.3% is measured, these values are 9.8% and 18% for the peak heights of F and FITC respectively. When the ratio of peak areas is used an RSD of 4.6% in CZE and of 4.8% in ITP-CZE is found. The improvement in RSD's for peak area ratios demonstrate the necessity of the use of an internal standard in quantitative analysis with ITP-CZE.

The linearity of the method is studied at a concentration level just above the detection limit. Calibration plots are made for FITC between 0.2 and 18 ng/ml. F is used as internal standard at a concentration of 25 ng/ml. The peak area ratios are used for linear regression.

Table 6 shows the linear regression data calculated as described by Miller [19].

Table 6. Regression data for ITP-CZE of FITC using F as an internal standard. A 700 x 0.075 mm fused silica capillary is used with an injection volume of 1.7 µl. Weighting factors are not used. Calibration is carried out with 5 different concentrations with constant concentration intervals of 0.4 ng/ml for the low concentration range and 4.0 ng/ml for the higher concentration range.

Range (ng/ml)	Slope	SD	Intercept	SD	Correlation coefficient
0.2 - 1.8	0.137	0.010	-0.012	0.01	0.985
2.0 - 18.0	0.142	0.015	0.020	0.15	0.965

Practical considerations

Several practical aspects are of importance for the applicability of the method to analyses in complex matrices such as urine or plasma samples.

First, a separation window exists in the ITP step within which the analyte of interest is focused. This separation window is an important tool in sample cleanup and can be tuned by the choice of the leading and terminating buffer. In literature numerous ITP systems have been described [18].

The anions that are faster than the leading buffer ions are migrating into the separation capillary already during the ITP step. Ions with lower mobilities than the terminator ions, including neutrals and cations, are removed from the capillary in the ITP step resulting in a considerable sample cleanup. It is therefore important to choose a favourable set of buffers i.e. a leading buffer with a high mobility to reduce the number of matrix anions with a higher mobility. The electrophoretic mobility of the terminator buffer should be as close to the mobility of the analyte as possible. The pH of the buffers is often an important parameter for fine tuning the mobilities of the analytes and the buffer ions.

Secondly, the separation order of anions in ITP is reversed with respect to CZE. Anions with a high electrophoretic mobility migrate after focusing and reversal of the voltage, through the analyte zones with a lower electrophoretic mobility. In the analysis of for instance urine samples the possibility exists that a zone of matrix ions migrates as a spacer between two analyte zones. Depending on the zone length of the matrix ions the migration times in CZE may change. In case of clean samples as described above, no difference in migration times in ITP-CZE with respect to CZE has been observed.

Due to the fact that a low concentration of analyte (i.e. nanomolar range) is concentrated in

the ITP step approximately to that of the leading buffer ions (i.e. millimolar range), the starting zone length will be reduced from decimeters to micrometers. A mixing of zones occurs as soon as the ITP has been ended and the CZE has been started, which is caused by diffusion, convection and of dilution with background electrolyte. As a result, although strongly concentrated the analyte ions start in the CZE process more or less as one mixed zone. In biological samples, however, a number of ions is present in a much higher concentration. Depending on their mobilities and of the separation window these matrix ions may act as spacers for analyte ions. After switching from the ITP to the CZE mode the analytes start the CZE run at different positions in the capillary resulting in different migration lengths. In these cases a sample pretreatment might be necessary to obtain reproducible results. On the other hand, an excess of spacer ions can be added deliberately to the sample to improve the resolution in ITP-CZE separations.

Finally, in the ITP step a hydrodynamic backpressure is levelling the electroosmotic flow rate. If switching takes place on a time basis, fluctuations in either one of them would result in decreased reproducibility. It is therefore of crucial importance that the pressure can be monitored and controlled accurately during the process, which is the case in the described system. Furthermore, the electroosmotic flow should not change from run to run. A constant pH is important with respect to the electroosmotic flow rate and it is therefore advisable to use a buffering counter ion. Injection of large sample plugs of a different pH may cause local changes in the electroosmotic flow. In these cases the samples should be brought at pH or pretreated. The same accounts for samples with large differences in salt concentration. As a consequence the method will be suitable especially for analysis in a well-defined, constant matrix with respect to pH and salt concentration, such as plasma.

It is expected that if instead of timing, the current is monitored to determine the moment to switch from the ITP to the CZE step, the reproducibility will improve (Chapters 3.2 - 3.4).

Conclusion

An automated procedure is described for the isotachophoretic preconcentration of low concentrations of analyte using ITP-CZE in a single capillary in combination with hydrodynamic backpressure programming. The described method is reproducible and linear at low concentrations. An improvement in determination limit of more than a factor of 100 with respect to CZE has been demonstrated. The increase of loadability is only limited by the capillary volume. An optimum has to be found between the injection volume, the determination limit and the time needed for focusing of large injection plugs.

References

1. W.G. Kuhr, Anal. Chem., 62 (1990) 403R
2. W.G. Kuhr and C.A. Monnig, Anal. Chem., 64 (1992) 389R
3. R.A. Wallingford, A.G. Ewing, Adv. in Chromatogr., 29 (1989) 1
4. N.A. Guzman, M.A. Trebilcock and H.P. Advis, J. Liq. Chromatogr., 14 (1991) 997
5. M.M. Bushey and J.W. Jorgenson, Anal. Chem., 62 (1990) 978
6. J. Cai and Z. Elrassi, J. Liq. Chromatogr., 15 (1992) 1179
7. F. Foret, V. Sustacek and P. Bocek, J. Microcolumn Sep., 2 (1990) 229
8. D.S. Stegehuis, H. Irth, U.R. Tjaden and J. van der Greef, J. Chromatogr., 538 (1991) 393
9. D. Kaniansky and J. Marak, J. Chromatogr., 498 (1990) 191
10. V. Dolnik, K.A. Cobb and M. Novotny, J. Microcolumn Sep., 2 (1990) 127
11. R.L. Chien and D.S. Burgi, Anal. Chem., 64 (1992) A489
12. F. Foret, E. Szoko and B.L. Karger, J. Chromatogr., 608 (1992) 3
13. R.L. Chien and D.S. Burgi, Anal. Chem., 64 (1992) 1046
14. D.S. Burgi and R.L. Chien, Anal. Chem., 63 (1991) 2042
15. C. Schwer and F. Lottspeich, J. Chromatogr., 623 (1992) 345
16. F.E.P. Mikkers, F.M. Everaerts and T.P.E.M. Verheggen, J. Chromatogr., 169 (1979) 11
17. J.F. Stobaugh, A.J. Repta, L.A. Sternson and K.W. Garren, Anal. Biochem., 135 (1983) 495
18. F.M. Everaerts, J.L. Beckers and T.P.E.M. Verheggen, *Isotachophoresis: Theory, Instrumentation and Practice*, Elsevier, Amsterdam, 1976
19. J.N. Miller, Analyst, 116 (1991) 3

3.2

Strategy for Setting Up Single Capillary Isotachophoresis - Zone Electrophoresis

Abstract

A strategy is described for the optimisation of capillary zone electrophoresis (CZE) with isotachophoretic (ITP) preconcentration in a single capillary set-up. CZE with indirect UV absorbance detection is used as a tool in setting up ITP-CZE. The electropherograms obtained with indirect detection give immediate insight in the migration order of possible leading and terminating ions and of the analyte ions. Furthermore, information is obtained on the ionic composition of the sample matrix. The separation window in the ITP step can be chosen in such a way that a sample cleanup is achieved before zone electrophoresis is started. The described approach is applicable for setting up an ITP-CZE analysis in the cationic as well as in the anionic mode. The usefulness of the strategy is illustrated by setting up ITP-CZE of three cationic antimuscarinic drugs. Applying the developed strategy, combined with a liquid-liquid extraction, concentrations of homatropine and scopolamine down to 100 ng/ml could easily be determined.

Introduction

One of the challenges in the application of CZE separations in the analysis of biological samples is to reach for relevant determination limits. For a number of drugs this means that concentrations in the nanomolar range or lower have to be measured. To take full advantage of the separation power of CZE for trace analysis in biological samples two approaches are considered to improve the determination limits. One of the approaches is to increase the detection sensitivity. Several highly sensitive detection systems such as laser induced fluorescence detection and electrochemical detection have been described [1-3]. However, these detection systems are only applicable to those analytes showing the proper detection characteristics or can be applied after a derivatisation procedure. Especially for analyte concentrations at or below the nanomolar level derivatisation procedures are liable to involve artefact formation [4].

Another approach to improve the determination limits in CZE is to increase the sample loadability of the system. For reasons of separation efficiency injection volumes in CZE are usually not higher than 1% of the total volume of the separation system. This means that the

injection volumes are in the range of 0.1 - 70 nl. Although absolute detection limits of femtomoles seem very impressive, the corresponding sample concentration detection limits are in the micromolar range which is at least a factor 1000 away from trace analysis. One way to increase the loadability of the CZE system is to apply off-line concentrating sample pretreatment methods such as the use of extraction procedures in combination with an evaporation step. In these procedures millilitres of sample can be pretreated, concentrated and analysed.

Electrophoretic analyte focusing techniques provide an elegant way to increase the loadability in CZE. These focusing techniques such as the coupling of ITP with CZE and field amplified injection procedures are based upon the application of local differences in electrical field strength during the injection or the focusing step to enable stacking of the analyte ions [5-14]. The coupling of ITP with CZE has been described by several authors [5-10]. Improvements in determination limits up to a factor of 1000 have been reported. In a recent publication we described the possibility of automated ITP-CZE for anionic separations in a single capillary using backpressure programming [15]. Sample volumes up to 55% of the total capillary volume are focused isotachophoretically and analysed in the CZE step. A hydrodynamic pressure is used for removal of the terminator buffer before the zone electrophoresis is started. The isotachophoretic conditions prevented excessive zone broadening. The procedure is reproducible, quantitative and automated.

In this Chapter a strategy is described for anionic and cationic separations using ITP-CZE in a single capillary. A total of four focusing procedures are described, two for each ionic mode. In both ionic modes the CZE run can take place either in the leading or in the terminating buffer, depending on the configuration used. The choice of the leading and terminating buffer ions, which defines the actual separation window, is made after analyte and matrix analysis by CZE using indirect detection. Three antimuscarinic (atropinic) drugs, neostigmine, homatropine and scopolamine [16] are used as test compounds.

Experimental

Apparatus

Untreated fused silica (100 µm ID, SGE, Ringwood, Victoria, Australia) capillary was used. A programmable injection system for capillary electrophoresis (PRINCE, Lauerlabs, Emmen, The Netherlands) equipped with a reversible polarity power supply and possibility for pressurised and electrokinetic injection was used for the analyte focusing process.

On-capillary UV absorbance detection took place using a Spectra 100 UV/VIS detector (Spectra-Physics Inc., Mt. View, CA, USA). The signal was registered on a chart recorder (BD 40, Kipp & Zn, Delft, The Netherlands).

Chemicals

Scopolamine hydrobromide, homatropine hydrobromide and neostigmine bromide came from Sigma (St. Louis, MO, USA). Crystal violet, triethylamine (TEA) (99%), diethanolamine (DEtOHA) (99%), triethanolamine (TEtOHA) (97%), 2,4,6 collidine (2,4,6 trimethylpyridine) (99%), and pyridine (99%) were from Janssen Chimica (Beerse, Belgium). Phosphoric acid, tri(hydroxymethyl)aminomethane (TRIS), lithium hydroxide, sodium hydroxide, potassium hydroxide, ammonium acetate were obtained from Merck (Darmstadt, FRG). Dichloromethane (99%) came from Baker BV (Deventer, The Netherlands). In all experiments deionised water was used (Milli-Q system, Millipore, Bradford, MA, USA).

Extraction of spiked plasma and urine samples

The extraction procedure used was similar to the procedure described for atropine [17]. Stock solutions of 1 mg/ml scopolamine hydrobromide, homatropine hydrobromide and neostigmine bromide were made in water and kept frozen (253 K) until use. Dilutions of the drugs were added to 225 µl of untreated blank plasma and urine from healthy volunteers until a final volume of 250 µl. The pH was increased by adding 50 µl of 1 mol/l lithium hydroxide. The samples were extracted by adding 600 µl of dichloromethane followed by 1 min vortex mixing. The samples were centrifuged for 5 min at 1000 x g. Then the upper layer was discarded, 500 µl of the lower layer was transferred to another vial and evaporated to dryness under reduced pressure using an evaporation centrifuge (Speedvac SVC 100H, Savant Instruments Inc., Farmingdale, NY, USA). After evaporation the samples were dissolved in 500 µl of terminating buffer for ITP-CZE or CZE buffer for CZE analysis.

Analyte focusing

The analyte focusing procedure of the three antimuscarinic drugs consisted of five steps (Fig. 1A).

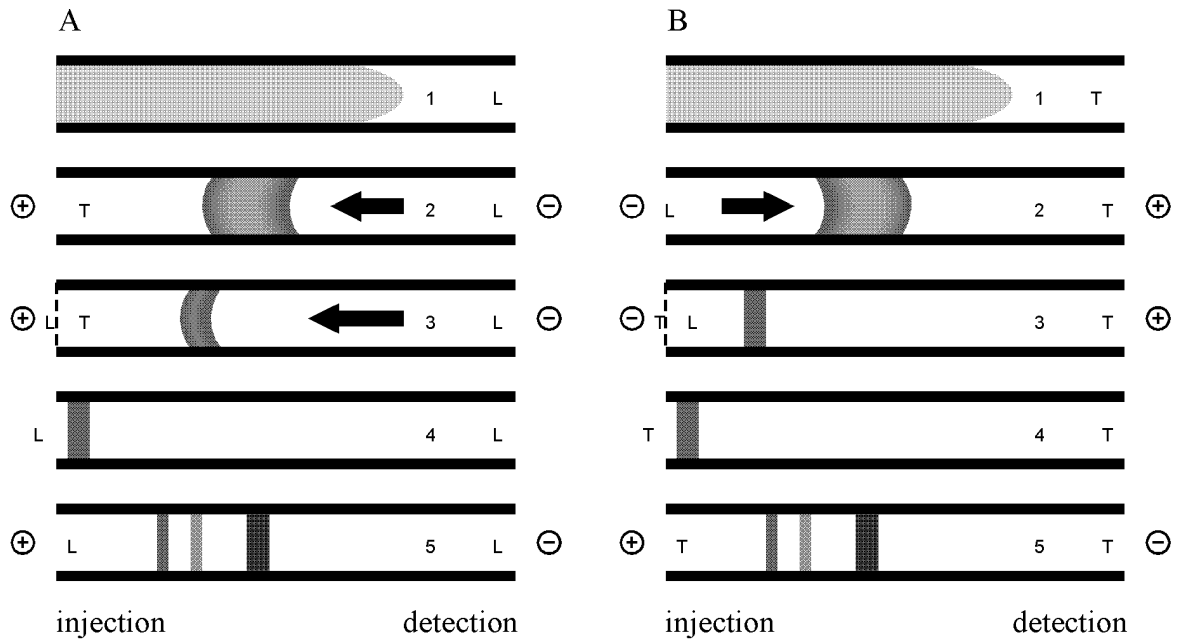

Fig. 1. Schematic representation of the ITP-CZE procedure for cations (A) using the leading buffer (L) as CZE background electrolyte in combination with a negative backpressure (arrows), and (B) using the terminating buffer (T) as CZE background electrolyte and a positive backpressure. A reversal of the voltage is necessary in procedure (B).

Step 1. After filling the capillary and the ITP cathode vial with leading buffer, the capillary was loaded with sample.

Step 2. The sample vial was replaced by the anode vial containing terminating buffer. The ITP was started and a hydrodynamic backpressure was applied to counterbalance the migration velocity of the analyte ions.

Step 3. When the focusing process was completed the voltage was switched of and the vial with terminating buffer was replaced for a vial with CZE buffer which was the same as the leading buffer. The voltage was turned on with a similar hydrodynamic backpressure but with a lower voltage than used in step 2. As a result the highly concentrated plug of analyte cations was moving into the direction of the capillary inlet.

Step 4. When the concentrated analyte ions approach the capillary inlet the hydrodynamic backpressure was switched off and the CZE (Step 5) was started.

Results and discussion

In each ionic mode of ITP-CZE the CZE step can take place in either the leading or the terminating buffer resulting in four analyte focusing procedures (Fig. 1 and 2). The ITP-CZE procedure which will be applied for the cationic test compounds as given in Fig. 1A, will now be discussed. The differences with the other three procedures will be indicated rather than discussing all procedures in detail. The procedure for ITP-CZE of anions as given in Fig. 2B has been described in detail elsewhere [15].

Analyte focusing

When during the focusing step (step 2) a positive voltage is applied at the capillary inlet the analyte cations will migrate in the direction of the cathode because of the electrophoretic and electroosmotic mobility.

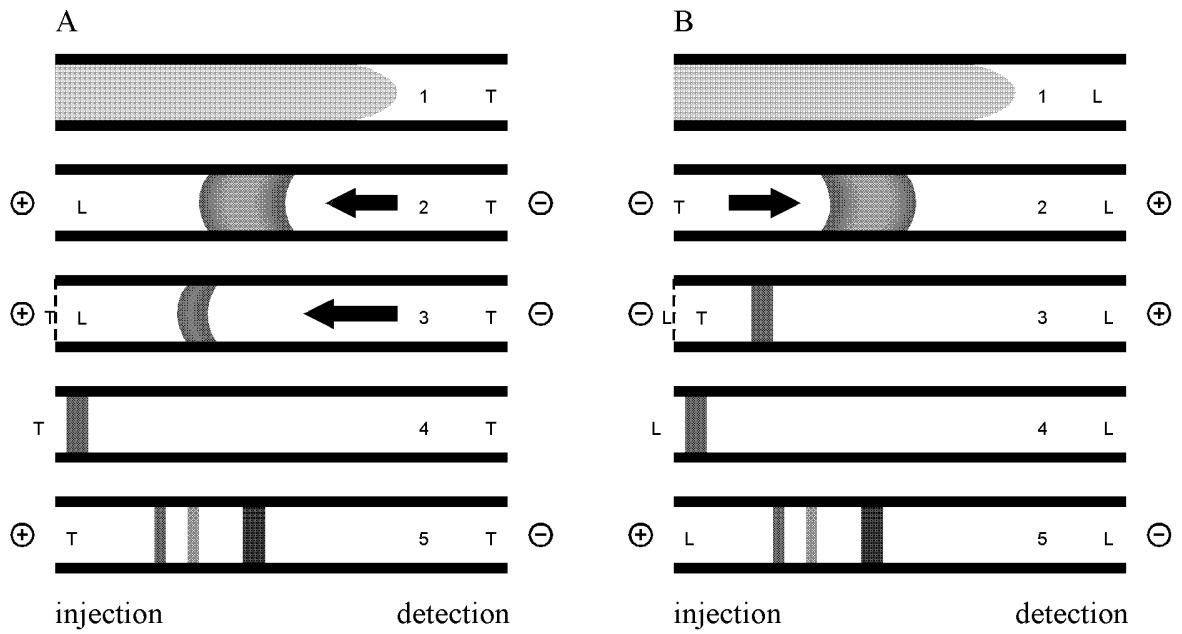

Fig. 2. Schematic representation of the ITP-CZE procedure for anions (A) using the terminating buffer (T) as CZE background electrolyte in combination with a negative backpressure (arrows), and (B) using the leading buffer (L) as CZE background electrolyte and a positive backpressure. A reversal of the voltage is necessary in procedure (B).

A hydrodynamic pressure is applied to counterbalance the migration velocity of the analyte ions. In contrast to conventional ITP the analyte ions are not moving into the capillary during the focusing step but they are concentrated and fixed on a position in the capillary by the hydrodynamic backpressure. The terms positive and negative backpressure have been used to describe the direction in which the hydrodynamic backpressure is applied. A positive backpressure induces a flow into the direction of the detector and a negative backpressure results in a flow in the opposite direction.

In step 3 the highly concentrated plug of analyte cations is moving hydrodynamically into the direction of the capillary inlet. Zone broadening is counteracted by the isotachophoretic conditions that still exist. The plug of terminating buffer which is still in the capillary is removed at the capillary inlet.

A critical point in the procedure is the timing of the moment to switch off the hydrodynamic backpressure (step 4) and to start the CZE (step 5). This is done at the moment the analytes are about to exit the capillary. When the CZE step is started too early the remaining plug of terminating ions causes an inhomogeneous electric field and influences the efficiency and migration times in the CZE step. When the CZE step is started too late the analyte ions have left the capillary. In the first few runs a visible dye is used for precise timing of the moment that the sample ions are near the capillary inlet. When reproducible migration times in the focusing step are obtained the procedure can be automated and the dye is not longer needed. Timing is also possible by monitoring the increase of current during step 3. The plug of terminating buffer raises the total resistance of the capillary which means that at constant voltage the current increases until the terminating buffer has left the capillary.

The procedures for ITP-CZE using negative backpressure (Fig. 1A and 2A) differ from those using positive backpressure (Fig. 1B and 2B) in that in step 3 the backpressure is increased to mobilise the focused sample zone in the direction of the capillary inlet. In step 4 the backpressure is reduced to zero and the CZE run is started *without reversal of the voltage.* This means that the migration order of ions is the same in the ITP and CZE step. In the procedures with reversal of the voltage also a reversal of the migration order of the analyte ions takes place when switching from ITP to CZE. This phenomenon did not affect the efficiency or resolution in ITP-CZE with respect to CZE separations of relatively clean samples [15].

ITP as sample cleanup for CZE

The choice of the buffer system determines to what extent the ITP focusing step can be used in sample cleanup for the CZE analysis. In Fig. 3 a summary is given of the different focusing steps in ITP-CZE. The migration direction of the ions with a lower mobility than the terminating ions is either in the direction of the capillary inlet or in the direction of the detector. Obviously, with respect to sample cleanup, the cationic mode with negative backpressure (Fig. 1A, 3A) and the anionic mode with positive backpressure (Fig. 2B, 3C) are favourable. In both cases the ions with a lower mobility than the terminating ions, including the neutrals and the counter ions, are removed and diluted in the inlet vial during the focusing step.

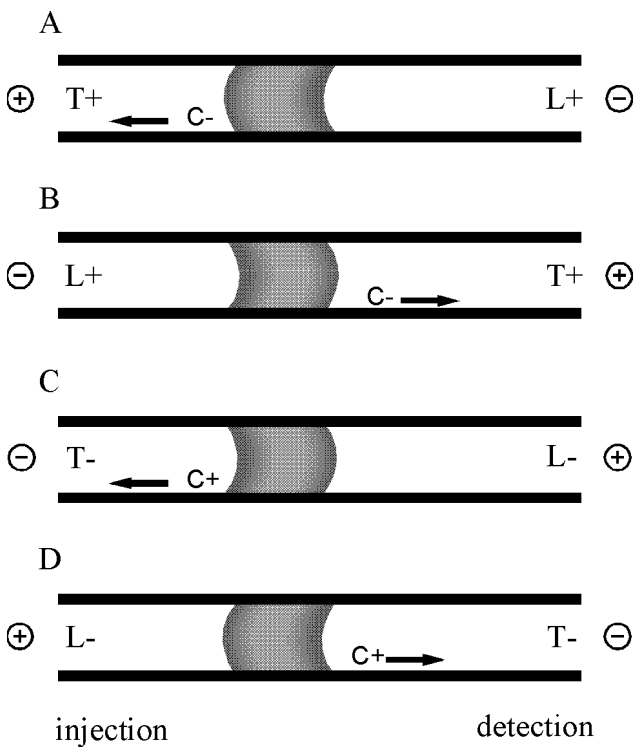

Fig. 3. The migration direction of the neutrals and counter ions (C^+, C^-) in the focusing step (Fig. 1 and 2, step 2) of the ITP-CZE procedure. Situation (A) and (C) are favourable with respect to sample cleanup.

The focusing step is completed when all ions move isotachophoretically under steady state conditions [18]. The more complex a sample is with respect to ion composition and ionic

strength the more time it takes to reach a true isotachophoretic state. Therefore, a sample pretreatment before the ITP-CZE step that results in a decrease of ionic strength of the sample matrix, will reduce the focusing time in ITP-CZE. In case of large variations in the composition of sample matrix (i.e. urine) a pretreatment step is likely to improve both the reproducibility and the efficiency in ITP-CZE. These aspects will be demonstrated below where a strategy is given and discussed for setting up an ITP-CZE system for the three cationic test compounds.

Choice of the CZE buffer

The first step in the optimisation procedure for ITP-CZE will always be the optimisation of the CZE step. Several papers are available describing CZE separations and methods for optimisation [1-3]. However, in ITP-CZE the CZE buffer will also be a leading (or terminating) buffer. This will influence the choice of the background electrolyte for CZE.

With respect to sample cleanup it is favourable to use the leading buffer as background electrolyte in CZE. Another aspect in favour of using the leading buffer is concerning the band broadening caused by conductivity differences between the sample zones and the background electrolyte [19].

When a highly concentrated sample zone after the focusing step is switched to zone electrophoresis, band broadening takes place because of differences in conductivity of the sample zone and the background electrolyte [15]. The sample zone itself is disturbing the homogeneity of the electric field in the electrophoresis tube. Zone broadening because of differences in conductivity is described by equation (1):

$$dz = L/\kappa \, d\kappa \qquad (1)$$

where $d\kappa$ is the conductivity difference between the sample zone and the background electrolyte, κ is the conductivity of the background electrolyte, L is the electrophoretic migration distance and dz is the zone broadening because of the conductivity difference [19].

From eqn. (1) it can be seen that when the sample zone has approximately the same conductivity as the terminator zone, using the terminating buffer as background electrolyte will result in less electromigration dispersion. The same holds for the leading buffer. Using the leading buffer as background electrolyte will result in less electromigration dispersion when $(\kappa_S - \kappa_L) / \kappa_L < (\kappa_S - \kappa_T) / \kappa_T$ which is the case when

$$\kappa_S > \frac{\kappa_L}{\kappa_L + \kappa_T} \cdot 2\,\kappa_T \qquad (2)$$

where κ_S, κ_T and κ_L are the absolute values of the conductivity of the sample zone, terminating buffer and leading buffer respectively. When $\kappa_L >> \kappa_T$ eqn. (2) becomes $\kappa_S > 2\kappa_T$ which implies that in many cases the leading buffer will be favourable as background electrolyte.

Addition of selectivity enhancing compounds to the background electrolyte is allowed as long as those additives are non-ionic (i.e. non-ionic detergents, non-ionic complex forming agents, organic modifiers). In case of ionic additives care must be taken that those additives do not disturb the isotachophoretic conditions.

The ionic strength of the CZE buffer should be chosen so that the concentrating properties in the ITP step are high, but not so high that the analyte precipitates (e.g. 5 - 100 mmol/l). The pH of the CZE buffer affects the electroosmotic flow rate which influences the efficiency of the ITP step. A high electroosmotic flow rate will result in a mixing of zones in ITP. Therefore, at high pH additives are used that reduce the electroosmotic flow rate such as hydroxypropyl-methylcellulose (HPMC).

In conventional CZE the background electrolyte should have buffering capacity to maintain a constant pH during separation. In ITP and ITP-CZE the counter ion should have this buffering capacity. In the steady state conditions in ITP the analyte ions are focused between the leading and terminating ions. The counter ions are present throughout the separation tube. This means that the best way to buffer the system is by means of the counter ions.

The most important parameters in the initial conditions of the CZE background electrolyte will be the choice of pH, the buffering counter ions and the additives used. The choice of the leading and terminating ion can be made after studying the ITP separation window. In the ITP-CZE analysis of the cationic test compounds the migration order of analyte, leading and terminating ions is not changed by switching from triethylamine to sodium as leading ion. However, changing the pH, the percentage of organic modifier or buffering counter ion might affect the migration order.

The ITP separation window

One of the advantages in ITP-CZE is that the majority of the matrix constituents can be removed in the focusing step. When maximum sample cleanup is desired a system is chosen where the CZE step takes place in the leading buffer (Fig. 1A, 2B, 3A and 3C).

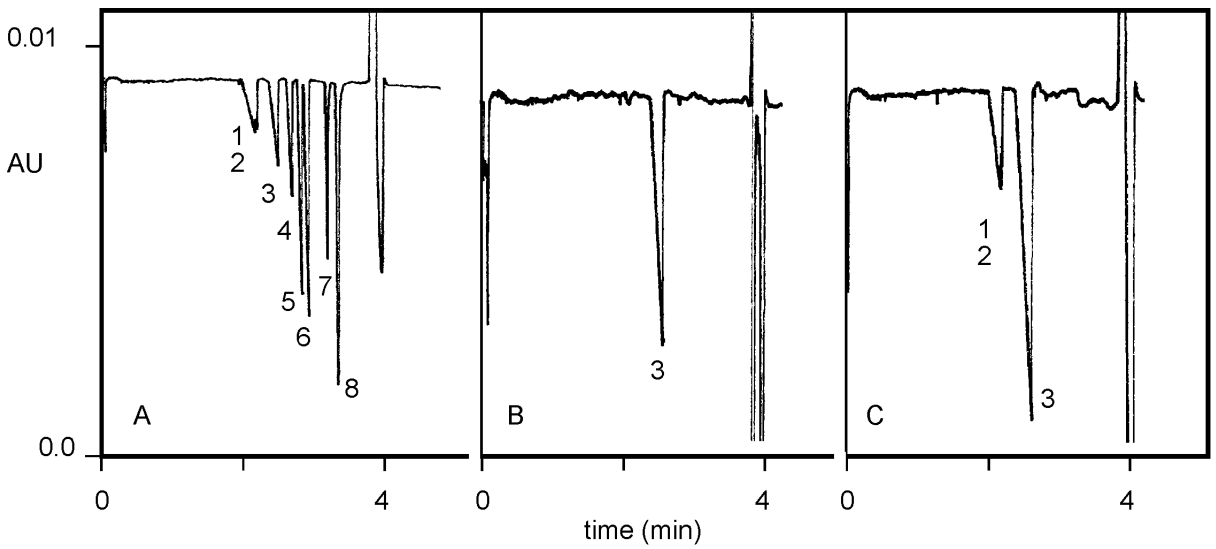

Fig. 4. Electropherograms of (A) a mixture of cations (2.5 mmol/l in background electrolyte), (B) human plasma (1:19 diluted in background electrolyte) and (C) human urine (1:19 diluted in background electrolyte). A voltage of 25 kV (4.7 µA) is applied over the 900 x 0.1 mm separation capillary. Indirect UV absorbance detection took place at 550 mm from the injection end at 200 nm using a 10 mmol/l collidine buffer brought at pH 8.0 using phosphoric acid. Injection is performed hydrodynamically using 10 mbar for 6 s (A) or electrokinetically at 6 kV for 6 s (B, C). The cationic mixture consisted of ammonium (1), potassium (2), sodium (3), lithium (4), TEA (5), DEtOHA (6), TRIS (7) and TEtOHA (8). At 4 min a system peak appeared together with the electroosmotic flow marker (acetonitrile).

Matrix ions with a higher mobility than that of the leading ions are in this case migrating into the separation capillary, already during the focusing step. When such ions are present in the matrix at a high concentration then it is advisable to use them as leading ions. Otherwise they may cause an inhomogeneity in the electrical field during the CZE run. When these ions give a strong signal in the detection system they usually cannot be used as leading ions and should be trapped within the ITP separation window.

For the optimisation of the ITP-CZE it is necessary to have information on the ionic com-

position of the sample matrix. A conventional CZE system with indirect UV absorbance detection [20] is particularly suitable as a screening method for the main matrix components (Fig. 4).

With respect to sample cleanup the terminating ion should be chosen so that the mobility is just below that of the analyte ion with the lowest mobility.

Choice of the leading and terminating buffer

Several reviews on ITP are available containing buffer systems and ionic mobilities of compounds which are most helpful in setting up an ITP-CZE separation [18, 21]. The ionic mobility of a compound is defined as the electrophoretic mobility of the compound when it is fully ionised. For ionic compounds such as sodium and chloride tabulated values can be used without correction for pH. For weak acids and bases the effective electrophoretic mobility ($\overline{m}$) can be calculated using the relationship between the ionisation fraction and the ionic mobility [21]. This relationship is given by:

$$\overline{m}_{HA} = \alpha_{A^-} m_{A^-} \qquad (3)$$

for compounds with one pKa, where m_{A^-} is the ionic mobility and α_{A^-} the molar fraction of HA that is in the ionic form. For dibasic acids eqn. (3) becomes:

$$\overline{m}_{H_2A} = \alpha_{HA^-} m_{HA^-} + \alpha_{A^{2-}} m_{A^{2-}} \qquad (4)$$

The ionic mobilities are given by m_{A2-} and m_{HA-}.

Equations (3) and (4) correct for the fraction of the compound that is not in the ionic form. Only the ionised fraction contributes to the electrophoretic mobility of an ion. Using the conditions in Fig. 4A for TRIS the effective mobility is calculated to be 1.55 10^{-8} m^2 V^{-1} s^{-1} (migration time 3.40 min, electroosmotic flow marker 4.05 min, the electrical field strength of 25 kV per 90 cm, at pH 8.0). According to eqn. (3) an effective mobility of 1.48 10^{-8} m^2 $V^{-1}s^{-1}$ is expected, which is close to the measured effective electrophoretic mobility (tabulated value for the ionic mobility of TRIS of 2.95 10^{-8} m^2 V^{-1} s^{-1} [21], pKa of TRIS is 8.0). In the same system sodium which is always fully ionised, has an effective electrophoretic mobility of 5.05 10^{-8} m^2 V^{-1} s^{-1} which is approximately the same as the ionic mobility [18] as expected.

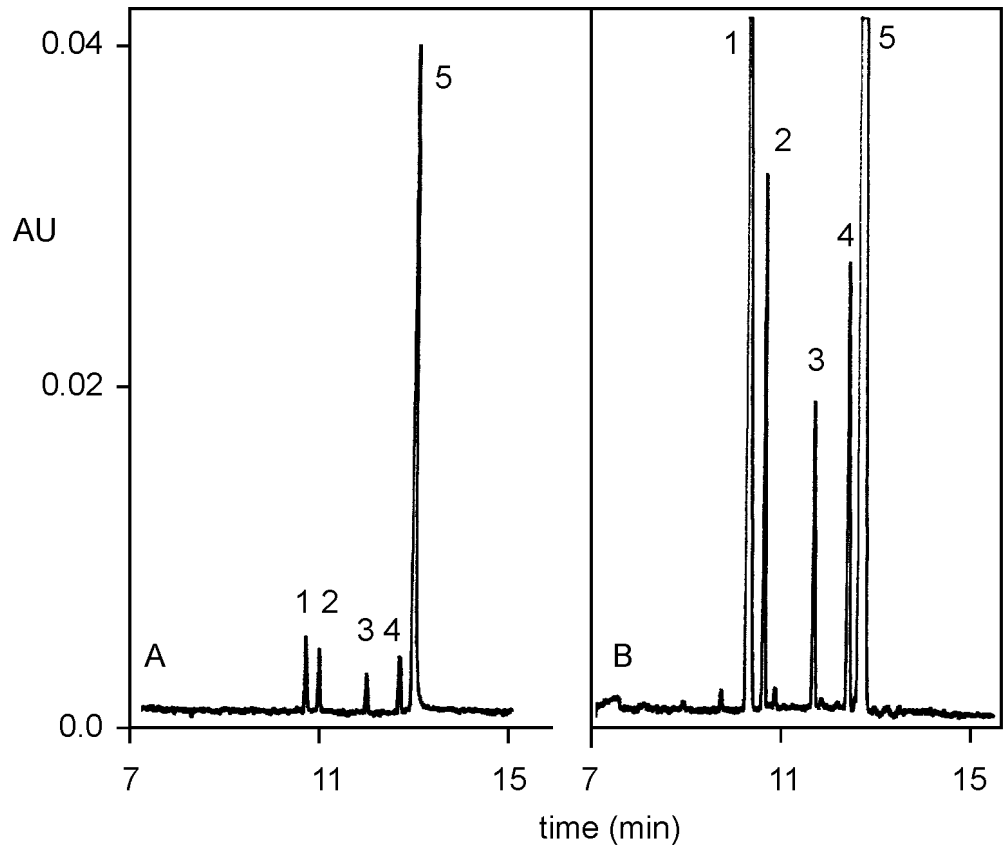

Fig. 5. (A) ITP-CZE of 280 nl and (B) CZE of 28 nl of the three test compounds neostigmine (2), homatropine (3), scopolamine (4) and of the dye crystal violet (5). Peak (1) is an unidentified system peak. In both cases a concentration of a 1 µg/ml of the test compounds and 10 µg/ml for the dye is injected. Leading buffer is 10 mmol/l TEA in 50% methanol brought at pH 5.0 with acetic acid. The terminating buffer consisted of 10 mmol/l β-alanine in 50% methanol brought at pH 5.0 with acetic acid. UV absorbance detection took place at 550 mm from the injection end at 200 nm. The detector settings are the same for both electropherograms. The ITP-CZE is performed as described in Fig. 1A.

As shown in Fig. 6 a CZE system applying indirect detection can be used for selecting the proper leading and terminating ions in ITP-CZE. Especially in those cases where additives to the buffer are used, tabulated values are not always available. The electropherogram gives a good insight in the migration order of the leading, the terminating and the sample ions. To make a good comparison possible it is necessary that the indirect detection system is similar to the chosen CZE buffer in the ITP-CZE analysis with respect to additives, counter ion and pH.

Based on data obtained by the indirect detection system the final choice of leading and terminating ions can be made. For plasma and urine samples sodium is most likely the main cationic compound (Fig. 4) and is preferably used as leading ion.

Application of ITP-CZE to spiked plasma and urine samples

The first step in the ITP-CZE analysis of the three antimuscarinic test compounds in spiked plasma and urine is the optimisation of the CZE system. At pH 5.0 the compounds are baseline separated (Fig. 5). Therefore, an acetate buffer is chosen as background electrolyte for CZE.

To enable a high loadability of the system a separation capillary of 900 x 0.1 mm is used. To reduce the CZE run times the detector is placed at 550 mm from the capillary inlet. This offered the additional advantage of enabling the application of a negative hydrostatic backpressure by raising the electrode vial at the capillary outlet.

The second step is the selection of the ITP separation window. An indirect detection system is used to study the main matrix components in urine and plasma (Fig. 4). Conditions for indirect detection of urine and plasma are chosen so that semi-quantitative information is obtained rapidly. Electropherograms of urine and plasma are compared with an electropherogram of a mixture of cations. The main cationic component in urine and plasma is sodium, as expected. Therefore, sodium is chosen as a leading ion in the ITP-CZE method. Especially urine contains a considerable concentration of cations with a higher mobility such as potassium or ammonium ions (Fig. 4C). These ions did not disturb the final ITP-CZE analysis.

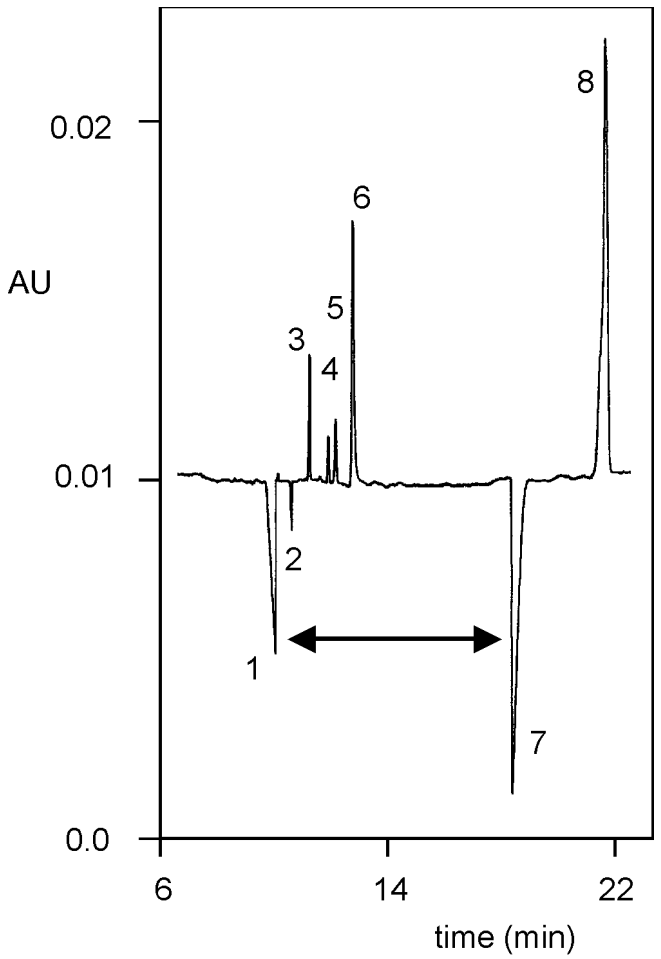

Fig. 6. Representation of the ITP separation window (arrow) using CZE with an indirect detection system. The background electrolyte consisted of 10 mmol/l pyridine in 50% methanol brought at pH 5.0 using acetic acid. The migration order of neostigmine (3), homatropine (4), scopolamine (5) and of crystal violet (6) can be easily determined with respect to possible leading (1, TEA) and terminating (7, β-alanine) ions. Peak (2) is an unidentified system peak and (8) is pyridine. For electrophoretic conditions see Fig. 4.

The choice of β-alanine as terminating ion is made in a similar way using indirect detection. However, to make a good comparison with the migration order in ITP-CZE possible, the conditions of the indirect system are carefully chosen. The buffer consisted of acetate at pH 5.0 in 50% methanol. The only difference to the conditions of the CZE background electrolyte in the final ITP-CZE system is the use of pyridine as UV absorbing co-ion instead of sodium. Fig. 6 demonstrates the separation window between leading and terminating ions.

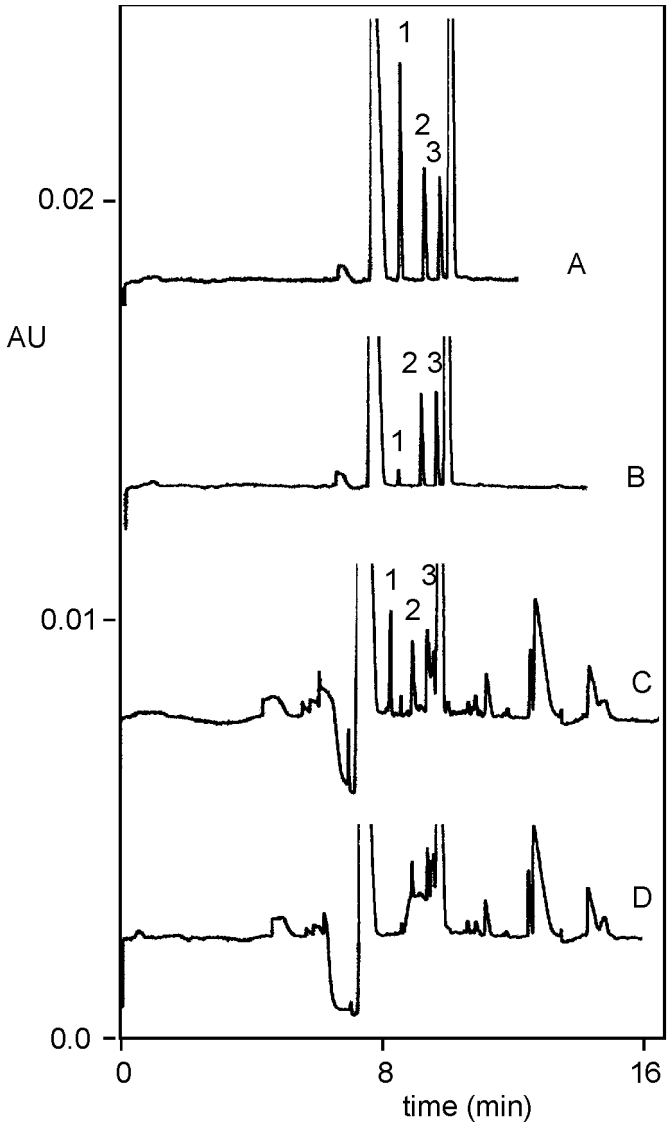

Fig. 7. ITP-CZE of 92 nl (10 µg/ml) neostigmine (1), homatropine (2) and scopolamine (3) in buffer (A), in urine after dichloromethane extraction (B) and in urine without any pretreatment (C) in comparison with (D) blank urine. The ITP-CZE is described in Fig. 1A. Sodium acetate (10 mmole/l) at pH 5.0 in 50% methanol is used as leading buffer and as CZE background electrolyte. The terminating ion is β-alanine. During the focusing step (Fig. 1A, step 2) a voltage of 10 kV and a backpressure of 22 mbar is applied. For the hydrodynamic mobilisation of the sample zones (Fig. 1A, step 3) the backpressure is increased to 30 mbar at the same voltage. The focusing step took 5.5 min for run (A) and (B) and 15 min for (C) and (D).

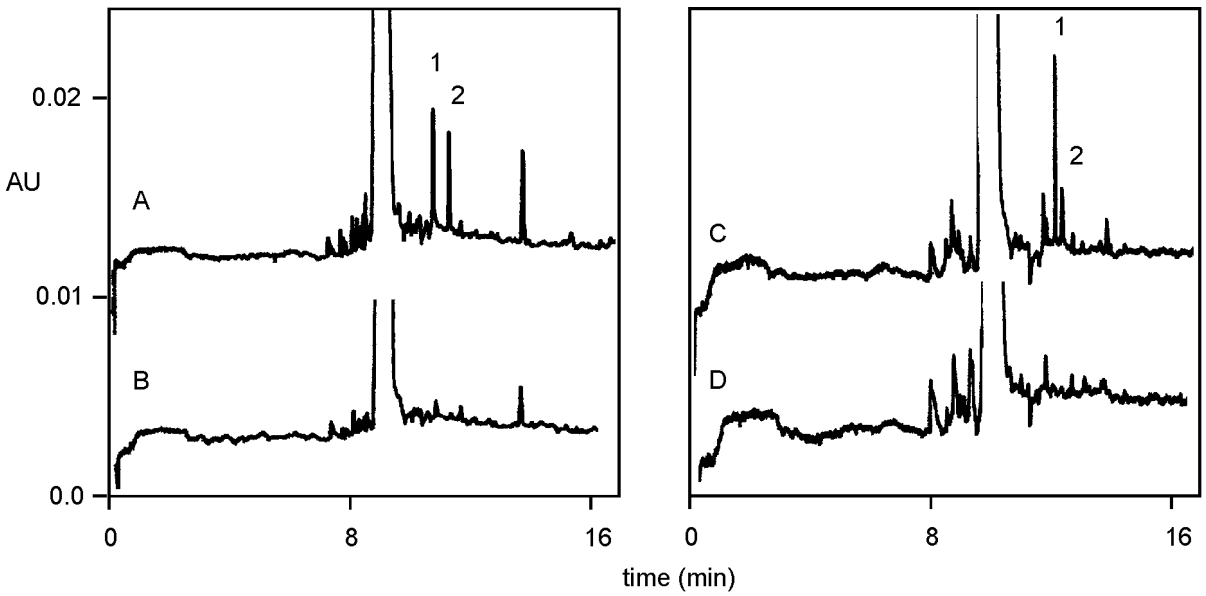

Fig. 8. ITP-CZE of 1.8 µl of 100 ng/ml homatropine (1) and scopolamine (2) in urine (A) and plasma (C) and of blank urine (B) and plasma (D) after dichloromethane extraction. ITP-CZE conditions are the same as in Fig. 7 except for the backpressure in the focusing step (Fig. 1A, step 2) which is 30 mbar at a voltage of 15 kV. The voltage is decreased to 10 kV at a constant backpressure to mobilise the focused analyte zones (Fig. 1A, step 3) towards the capillary inlet. The focusing step took 25 min before the CZE step is started at 25 kV. Crystal violet is no longer used as dye. The current in step 3 increased from 0.1 to 3.1 µA.

Depending on the complexity of the matrix and the analyte concentration, ITP [22-24] and ITP-CZE can be used for the analysis of plasma and urine samples without any or with minor pretreatment (i.e. filtration). In Fig. 7 the electropherograms after ITP-CZE of 10 µg/ml anti-muscarinic drugs in urine with and without pretreatment are shown. For trace analysis it is unlikely that the selectivity in ITP-CZE without an additional pretreatment will be sufficient. Interferences in the CZE analysis will by definition migrate within the separation window in the ITP step because the separation principle in both electrophoretic modes is the same. The use of spacer ions in the ITP step may enhance the selectivity of the final analysis, especially when large differences in analyte concentration occur. In case of co-migrating zones in CZE the ITP step will not give additional selectivity.

The selectivity is considerably enhanced by using a liquid/liquid extraction with dichloro-methane prior to the ITP-CZE step (Fig. 7-8). As can be seen in Fig. 7B the extraction recovery

for neostigmine is low. Scopolamine and homatropine can be measured at a concentration level of 100 ng/ml in plasma and urine (Fig. 8) after extraction. Although it is likely that the determination limits can be lowered using a concentrating step by dissolving the evaporated extract in a smaller volume, there are no attempts made to optimise the method.

Conclusions

Two ITP-CZE procedures for cationic and two ITP-CZE procedures for anionic separations are given. A strategy is described for setting up an ITP-CZE analysis. Information on the migration order of leading ions, terminating ions and analyte ions can be obtained using CZE with indirect UV absorbance detection. Furthermore, information on the ionic composition of the matrix can be obtained. Indirect detection enables tuning of the ITP separation window when ITP is used as sample cleanup for CZE.

The applicability of the described strategy is demonstrated for the optimisation of ITP-CZE of homatropine, scopolamine and neostigmine in spiked urine and plasma samples. Depending on the analyte concentrations plasma and urine samples can be determined without pretreatment. However, because the separation mechanism in both ITP and CZE are based upon the same principle an additional sample pretreatment will be needed in case of co-migrating matrix interferences. The coupling of a sample pretreatment based on another separation mechanism than electrophoresis in combination with the tremendous concentrating properties in ITP makes the highly efficient separation power of CZE applicable for trace analysis.

Literature

1. R.A. Wallingford, A.G. Ewing, Adv. Chromatogr., 29 (1989) 1
2. W.G. Kuhr, Anal. Chem., 62 (1990) 403R
3. W.G. Kuhr and C.A. Monnig, Anal. Chem., 64 (1992) 389R
4. C.M.B. van den Beld, U.R. Tjaden, N.J. Reinhoud, D.S. Stegehuis and J. van der Greef, J. Controlled Release, 13 (1990) 129
5. F. Foret, V. Sustacek and P. Bocek, J. Microcol. Sep., 2 (1990) 229
6. D.S. Stegehuis, H. Irth, U.R. Tjaden and J. van der Greef, J. Chromatogr., 538 (1991) 393
7. D. Kaniansky and J. Marak, J. Chromatogr., 498 (1990) 191
8. V. Dolnik, K.A. Cobb and M. Novotny, J. Microcolumn Sep., 2 (1990) 127
9. R.L. Chien and D.S. Burgi, Anal. Chem., 64 (1992) A489
10. F. Foret, E. Szoko and B.L. Karger, J. Chromatogr., 608 (1992) 3
11. R.L. Chien and D.S. Burgi, Anal. Chem., 64 (1992) 1046
12. D.S. Burgi and R.L. Chien, Anal. Chem., 63 (1991) 2042
13. C. Schwer and F. Lottspeich, J. Chromatogr., 623 (1992) 345
14. F.E.P. Mikkers, F.M. Everaerts and T.P.E.M. Verheggen, J. Chromatogr., 169 (1979) 11

15. N.J. Reinhoud, U.R. Tjaden and J. van der Greef, J. Chromatogr., 641 (1993) 155
16. I.R. Innes and M. Nickerson, In *The pharmaceutical basis of therapeutics*, L.S. Goodman and A. Gilman, Eds., Fourth ed., Chpt. 25, Collier-MacMillan Ltd., London, 1970.
17. T. Okuda, M. Nishida, I. Sameshima, K. Kyoyama, K. Hiramatsu, Y. Takehara, K. Kohriyama, J. Chromatogr., 567 (1991) 141
18. F.M. Everaerts, J.L. Beckers and T.P.E.M. Verheggen, *Isotachophoresis: Theory, Instrumentation and Practice*, Elsevier, Amsterdam, 1976.
19. S. Hjerten, Electrophoresis, 11 (1990) 665
20. E.S. Yeung and W.G. Kuhr, Anal. Chem., 63 (1991) 275A
21. J. Pospichal, P. Gebauer and P. Bocek, Chem. Rev., 89 (1989) 419
22. P. Oefner, R. Häfele, G. Bartsch and G. Bonn, J. Chromatogr., 516 (1990) 251
23. T. Hirokawa, H. Takemina, Y. Kiso, R. Takiyama, M. Morio, K. Fujii and H. Kikuchi, J. Chromatogr., 305 (1984) 429
24. V. Dolnik and P. Bocek, J. Chromatogr., 225 (1981) 455

3.3

Correlation between Zone Velocity and Current in Automated Single Capillary Isotachophoresis - Zone Electrophoresis

Abstract

In single capillary isotachophoresis - zone electrophoresis (ITP-CZE) the sample zone velocity is varying with its position in the capillary during the focusing step. When the voltage is kept constant, the current changes to the same extent. Correlation between the current and the sample zone velocity can therefore be used to calculate the velocity of the hydrodynamic flow that is needed to counterbalance the sample zone velocity. Measured data are in agreement with calculations implying that current monitoring can be used in an automated feedback system to regulate the hydrodynamic flow velocity during the focusing step. Conditions are described where automated anionic single capillary ITP-CZE can be performed without application of a hydrodynamic counterflow, extending its applicability to any commercially available CZE system.

Correlation between the ITP current and the sample zone position in the capillary is used to determine the moment for automatic switching from ITP to CZE. The reproducibility of the corresponding CZE migration times is investigated in addition to the effect of the remaining ITP terminator zone length on the CZE separation. A remaining terminator zone length of 10% of the total capillary length still resulted in an acceptable CZE performance.

Introduction

Capillary electrophoresis in combination with trace enrichment procedures has been proven to be a powerful analytical technique capable of high efficient separations at low analyte concentrations [1, 2]. Several methods of lowering determination limits in CZE have been described [3]. Classical off-line sample pretreatment and preconcentration techniques, such as liquid-liquid extraction or solid phase isolation, have been used in a number of bioassays. Although these procedures can be laborious and time consuming they offer flexibility [4]. On-line sample pretreatment offers the possibility of automation but has some restrictions with respect to the following step in the analytical method [5].

Electrophoretic analyte focusing procedures are a convenient way of lowering the determination limits that are typical for zone electrophoretic separations. Several modes have been described and successfully applied. A common feature of procedures such as stacking and sample self stacking or transient isotachophoretic preconcentration, is that the analyte is concentrated at the boundary over which a difference in the electric field strength exists [3, 6].

The combination of ITP with CZE has been successfully applied by several groups in a dual capillary mode. In this mode the sample ions are transferred from the ITP system to the CZE capillary. In the single capillary mode the process of ITP and CZE takes place in the same capillary, only the buffer vials are switched [7, 8]. Large sample volumes are injected, typically 10 - 90% of the total capillary volume. A hydrodynamic counterflow is used during the focusing step to keep the sample zones inside the capillary. The discontinuous ITP buffer is removed before the CZE step is started resulting in highly efficient separations. The method is automated, reproducible and takes place in a commercially available CZE apparatus without any modifications of the hardware. Determination limits are at least a factor hundred better than for conventional CZE. Similar results have been obtained in combination with electrospray mass spectrometry of β-agonists [9].

In this Chapter an equation is derived giving the correlation between the current and the sample zone velocity during the focusing step in single capillary ITP-CZE. With this linear relationship the pressure needed to counterbalance the sample zone velocity can be calculated. The position of the sample zone in the capillary is calculated from the current, compared with experimental data and applied in automated ITP-CZE procedures. The reproducibility is investigated for ITP-CZE using current monitoring for automated switching from the ITP to the CZE mode.

Experimental

Chemicals

Acetic acid (HAc) was from Merck (Darmstadt, FRG). Fluorescein (F) and triethanolamine (TEtOHA) (97%) were purchased from Janssen Chimica (Beerse, Belgium). Fluoresceinisothiocyanate isomer I (FITC) was from Aldrich Chemie (Steinheim, Germany). The food colorant brilliant acid green (E142) was from Morton (Amersfoort, Netherlands). Hydroxypropylmethylcellulose (HPMC) and 4-(2-Hydroxyethyl)-1-piperazine ethanesulphonic acid (HEPES)

came from Sigma (St. Louis, MO, USA). The viscosity of a 2% aqueous HPMC solution was 4000 cP. In all experiments deionised water was used (Milli-Q system, Millipore, Bradford, MA, USA).

Conditions used in calculations

Zone velocity, current and counterflow (Fig. 2, 3 and 6) were calculated for an untreated fused silica capillary with 100 µm ID and 500 mm length. An electroosmotic mobility of 60.0 10^{-9} $m^2V^{-1}s^{-1}$ was used for the leading buffer and 70.5 10^{-9} $m^2V^{-1}s^{-1}$ for the terminating buffer. The leading buffer consisted of 10 mmol/l HAc set at pH 8.0 with TEtOHA and was also used as CZE background electrolyte. In the ITP step 7.25 mmol/l HEPES at pH 8.0 was used as terminating buffer. The effective and ionic electrophoretic mobilities used in calculations were -42.0 and -42.0 10^{-9} $m^2V^{-1}s^{-1}$ for acetate, -16.5 and -22.0 10^{-9} $m^2V^{-1}s^{-1}$ for HEPES and 11.0 and 30.1 10^{-9} $m^2V^{-1}s^{-1}$ for TEtOHA. The ITP took place at a voltage of 10 kV. The calculated conductivities were 0.070 and 0.027 Sm^{-1} in respectively the leading and the terminating zone. The equations used for calculation of these parameters will be given in Theory.

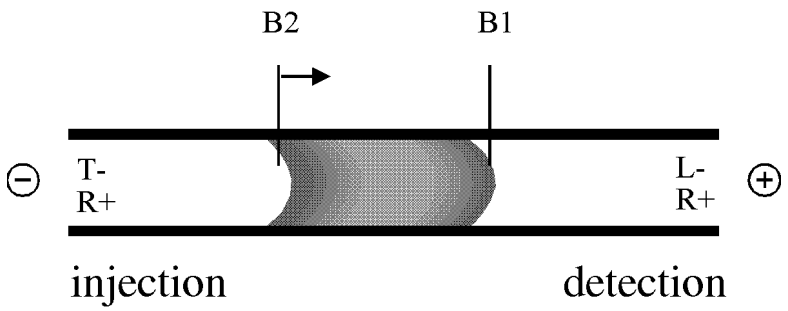

Fig. 1. Schematic representation of an anionic sample zone in the focusing step of ITP-CZE. The sample was dissolved in terminator buffer (T^-, R^+). The leading buffer (L^-, R^+) was also used as background electrolyte in the CZE step. The hydrodynamic flow velocity counterbalances the electroosmotic and electrophoretic velocities of a sample zone at the front boundary (B1). The rear boundary (B2) migrates to B1 resulting in a concentration of the analyte.

In most commercially available apparatus the pressure is applied at the capillary inlet. An increased pressure at the inlet is always considered a positive pressure and the resulting hydro-

dynamic flow has therefore a positive sign. A reduced pressure at the inlet results in a hydrodynamic flow in the opposite direction and has, according to our notation a negative sign.

During the ITP of anions the cathode was at the capillary inlet (Fig. 1), therefore the sign of the electrophoretic velocity of an anion A ($v_{el,A}$) in the direction of the anode was positive, analogous to the sign of a hydrodynamic flow. The sign of the electroosmotic velocity (v_{eof}) in the direction of the cathode was negative for the same reason. The total velocity of the anion (v_A) in cases where the electroosmotic velocity predominates, was thus negative.

Experimental conditions

The conditions in Fig. 4 and 5 were similar to the conditions as given above with exception of the following. The capillary (520 x 0.100 mm ID, SGE, Ringwood, Victoria, Australia) was pretreated by standing overnight with a solution of 0.05% HPMC and as a result the electroosmotic mobility was 30 and 35 10^{-9} $m^2V^{-1}s^{-1}$ in the leading and the terminating zone, respectively. The effective mobility of acetate was -39.7 10^{-9} $m^2V^{-1}s^{-1}$ which value was also used as the ionic mobility. A voltage of 15 kV was used and the current was respectively 13.1 and 6.0 µA for the leading and terminating buffer. Corresponding conductivities of 0.058 and 0.0265 Sm^{-1} were used in calculations in Fig. 4 and 5.

For the counterflow and current monitoring experiments the food colorant brilliant acid green (E142) was used as visible test compound. For the reproducibility measurements and the variation of the terminator zone length (Fig. 7) fluoresceins were used with laser induced fluorescence detection (LIF). The LIF detection system has been described in detail elsewhere [7]. A programmable injection system for capillary electrophoresis (PRINCE, Lauerlabs, Emmen, Netherlands) equipped with a reversible polarity power supply and possibility for pressurised and electrokinetic injection was used for the automated ITP-CZE procedures.

Analyte focusing

The analyte focusing procedure consists of five steps [7, 8]. In step 1 the injection takes place hydrodynamically at a pressure of 100 mbar. In the focusing step (step 2), the analyte focusing was started by applying a voltage in conjunction with a hydrodynamic pressure. The hydrodynamic pressure was used to prevent the sample zone from leaving the capillary. After 5 - 20 min. of focusing, depending on the injected zone length, the focusing was completed. Step 3 was the isotachophoretic removal of the terminator buffer zone from the capillary. A voltage of 20 kV was applied without a hydrodynamic pressure. At the time that the sample

zone was approaching the capillary inlet the terminator buffer vial was replaced for a vial containing the CZE background electrolyte (step 4), the voltage was reversed and the CZE run was started (step 5).

The current was monitored for precise timing of the moment to switch from the ITP to the CZE mode. When a constant voltage was applied the current increases as long as the terminating zone length decreased. The CZE equipment could be programmed so that at a defined threshold of the current the switching took place automatically. In principle, all terminating ions and sample ions with mobilities below that of the terminating ion, including the counter ions, were removed by the described procedure.

Theory

The coupling of ITP with CZE using a single capillary set-up has been described for both anions and cations [7, 8]. In both cases either the leading or terminating buffer can be used as background electrolyte for CZE, resulting in four modes of ITP-CZE. The focusing step is started after injection of a large sample zone in terminator buffer, typically 10 - 90 % of the total capillary length. A counterflow is used to keep the sample zones in the capillary during the focusing process (Fig. 1). The front of the sample zone which forms a boundary with the leading buffer, is kept at a fixed position in the capillary by balancing the electrophoretic leading ion velocity with the hydrodynamic velocity. The rear boundary of the analyte zone is migrating in the direction of the front boundary resulting in a concentration of the analyte. After focusing the discontinuous buffer is removed isotachophoretically by either increasing or decreasing the hydrodynamic counterflow depending on the ITP-CZE mode that is used.

Theoretical model

For the calculation of the zone velocity during the focusing step an isotachophoretic state is assumed. This assumption has been made to enable calculations of the local electric field strengths and the electrophoretic and electroosmotic velocities. In the isotachophoretic state the velocities of all ions are the same with exception of the counter ion velocity [10]. For the analyte ions during the focusing step this assumption is not true, only when the focusing is completed they migrate with the same velocity as the leading and terminating ions. However, when low analyte concentrations in terminator buffer (i.e. <0.1% of the terminator buffer concentration) are considered the contribution to the local electric field strength and conductivity

in the terminator zone is negligible. Therefore, the velocity of the leading ions can be calculated without consideration of the migration of sample ions.

The terminator buffer is prepared at the isotachophoretic concentration. This concentration is given by:

$$\bar{c}_T = \frac{m_T}{m_L} \cdot \frac{m_L + m_R}{m_T + m_R} \cdot \bar{c}_L \qquad (1)$$

where m_i is the absolute value of the ionic mobility of i. The subscripts L, T and R refer to the leading, terminating and counter ions respectively. Because in buffer systems weak electrolytes are involved the analytical concentration of an analyte A is notated as $\bar{c}_A$ ([HA] + [A^-]) and the ionic concentration is notated as c_A ([A^-]). Analogous, the mobility of the fully ionised analyte A is written as m_A and the effective mobility as $\bar{m}_A$. The relationship between the ionic and effective mobility is then given by $c_A m_A = \bar{c}_A \bar{m}_A$. An anionic system with univalent buffer ions will be considered consisting of only one type of cation and anion (i.e. leading buffer L^- and R^+, terminating buffer T^- and R^+). The leading buffer is also used as CZE background electrolyte.

In our model the temperature in the leading and terminating zone is considered to be the same and constant. Most of the considered parameters are dependent on temperature. This means that the model is only applicable for systems where the Joule heat is efficiently dissipated. When the terminator zone is removed from the capillary, the local electrical field strength in the terminator zone increases considerably resulting in an increased heat development. Therefore, at a small terminating buffer zone length a deviation of the measured velocities from the calculated velocities may occur. However, in ITP-CZE usually large injection volumes are applied. After the focusing step, when the terminator buffer is removed, the accurate magnitude of the velocity is usually no longer relevant. In Results and Discussion the assumption of a constant axial temperature is verified.

The hydrodynamic counterflow

The counterflow to keep the boundary of the sample zone with the leading buffer zone on a fixed position in the capillary (Fig. 1) is given by:

$$v_L + v_{hd} = 0 \qquad (2)$$

where v_L is the velocity of the leading ions and v_{hd} is the hydrodynamic flow velocity in the opposite direction. The velocity of the leading ions is given by the sum of the electrophoretic velocity ($v_{el,L}$) and the bulk electroosmotic velocity (v_{eof})

$$v_L = v_{el,L} + v_{eof} \qquad (3)$$

The electrophoretic velocity of the leading ions is given by

$$v_{el,L} = \overline{m}_L E_L \qquad (4)$$

where $\overline{m}_L$ is the effective electrophoretic mobility of the leading ions and E_L is the electric field strength in the leading buffer zone.

The electroosmotic velocity is weighted over the fraction of capillary filled with leading buffer (x) and with terminating buffer (1 - x) [6]

$$v_{eof} = x\, v_{eof,L} + (1 - x)\, v_{eof,T} \qquad (5)$$

where v_{eof} is the bulk electroosmotic velocity, $v_{eof,L}$ is the electroosmotic velocity in the leading zone and $v_{eof,T}$ is the electroosmotic velocity in the terminating zone. Combination of (5) and (3) gives for the velocity of the leading ions

$$v_L = x\, v_{eof,L} + (1 - x)\, v_{eof,T} + v_{el,L} \qquad (6)$$

The hydrodynamic flow velocity caused by a pressure difference over a capillary is given by the Poiseuille equation:

$$v_{hd} = \frac{d^2}{32 \eta L_0} \cdot \Delta p \qquad (7)$$

where L_0 is the total capillary length, η is the viscosity ($9.93\ 10^{-4}$ $kgm^{-1}s^{-1}$), d the capillary

diameter and p the pressure difference. Combination of (2), (6) and (7) gives the pressure difference that results in a hydrodynamic velocity that counterbalances the velocity of the boundary between the leading and analyte zone

$$\Delta p = \frac{32\eta L_0}{d^2} \cdot [\, x v_{eof,L} + (1-x) v_{eof,T} + v_{el,L} \,] \qquad (8)$$

where the electrophoretic velocity ($v_{el,L}$) has a negative value for anions. The fraction of the capillary that is filled with leading buffer (x) depends on the injected volume and changes when the focusing procedure proceeds. When the capillary is filled for 75% with sample in terminating buffer, the value of x is 0.25. This fraction will increase to 1.0 when the terminating buffer is removed from the capillary.

From equation (3) it can be seen that when the electroosmotic velocity is smaller than the velocity of the leading ions ($v_{el,L}+v_{eof}>0$) the direction of the leading zone velocity reverses. Therefore, the counterflow velocity balancing the leading zone velocity (eqn. 1) is also reversed. This means that in stead of an increased pressure a reduced pressure is needed for complete removal of the anionic ITP buffer. The four ITP-CZE procedures as described previously [8] can all be performed in absence as well as in presence of electroosmotic flow using the appropriate pressure difference given by equation (8).

When the electrophoretic mobility is approximately the same as the electroosmotic mobility, there will be one value of x for which the leading zone velocity (v_L) is zero. Without applying a hydrodynamic flow, the boundary of the sample zone and leading zone will migrate in the electric field until this particular leading zone length is reached and the velocity is zero. When all parameters are kept constant, the position of this boundary will not change in time. When the position of this boundary is close to the capillary inlet, the ITP step can be stopped and the CZE step can be started without removing the remaining terminator zone. For untreated fused silica with an electroosmotic mobility of the buffer of ca. 60 10^{-9} $m^2V^{-1}s^{-1}$ this may be the case when chlorate (m=-63 10^{-9} $m^2V^{-1}s^{-1}$) or chloride (m=-75 10^{-9} $m^2V^{-1}s^{-1}$) is used as leading ion.

Determination of parameters

In the isotachophoretic steady state the electric field strength in the leading buffer zone (E_L) is by definition lower than in the terminating buffer zone (E_T). The local electric field strength

depends on the total electric field applied over the capillary (E_0), the conductivities of the buffers and the length over which the capillary is filled with leading or terminating buffer. The total electric field strength is given by the running voltage (V_0) divided by the total capillary length (L_0). The electric field strength in the leading zone is given by [6]

$$E_L = \frac{\gamma E_0}{\gamma x + (1 - x)} \qquad (9)$$

and in the terminating zone

$$E_T = \frac{E_0}{\gamma x + (1 - x)} \qquad (10)$$

where γ is the conductivity ratio of the terminating and the leading zone (κ_T/κ_L) and x is the fraction of the capillary that is filled with leading buffer (L_L/L_0). The fraction that is filled with terminator buffer (1 - x) is equal to L_T/L_0. When the sample is dissolved in terminator buffer at the isotachophoretic concentration (eqn. 1) the length of the injection zone is considered to be L_T.

The conductivity (κ_i in Sm^{-1}) can be measured in a capillary filled with buffer i using equation 11:

$$\kappa_i = \frac{I}{\pi r^2 E} \qquad (11)$$

where I is the electric current and r is the capillary radius. Alternatively, when the electrophoretic mobilities are known, the conductivity for weak univalent electrolytes can be calculated by [11]

$$\kappa_i = F\ \bar{c}_A\ (\ |\bar{m}_A| + \alpha_A\ |m_R|\ ) \qquad (12)$$

where F is the Faraday constant (96485 $Cmol^{-1}$) and α_A the mole fraction of A that is in the

ionic form. In case of univalent buffer ions the conductivity ratio (γ) is given by

$$\gamma = \frac{\kappa_T}{\kappa_L} = \frac{\bar{c}_T}{\bar{c}_L} \cdot \frac{|\bar{m}_T| + \alpha_T |m_R|}{|\bar{m}_L| + \alpha_L |m_R|} \qquad (13)$$

The concentration $\bar{c}_T$ is calculated via the isotachophoresis equation (1). The ionic mobility m_R is assumed to be the same in the leading and terminating zone. Although the ionic mobility depends on the ionic strength which differs in the leading and terminating zone, for the conductivity ratio this is negligible.

The electroosmotic flow velocities are calculated using

$$v_{eof,L} = m_{eof,L}\, E_L \qquad (14)$$

and

$$v_{eof,T} = m_{eof,T}\, E_T \qquad (15)$$

where m_{eof} is the electroosmotic mobility ($m^2V^{-1}s^{-1}$). The bulk electroosmotic mobility is the same in both zones, however, local differences in the electroosmotic mobility in the leading and terminating zone exists. The electroosmotic mobility decreases as the ionic strength of the buffer increases. Because of a lower buffer concentration in the terminator zone, the electroosmotic mobility will be higher than in the leading buffer zone. The local difference in flow rate with respect to the bulk flow rate, is compensated for by a convective flow in the buffer zones. The electroosmotic velocity ($v_{eof,L}$) can be measured in the CZE mode, when the leading buffer is used as background electrolyte. The electroosmotic velocity of the terminator zone $v_{eof,T}$ can be measured in the capillary filled with terminating buffer, using the buffer concentration calculated using the isotachophoresis equation (1).

From equations (9) and (10) it follows that the electric field strength is considerably influenced by the length of the leading zone, which results in varying electrophoretic and electroosmotic velocities during the focusing procedure. Substituting equations (9), (10), (14) and (15) in (8) gives the full impact of the fractional leading zone length (x) on the pressure difference.

$$\Delta p = \frac{32\eta L_0}{d^2} \cdot \frac{\gamma E_0}{\gamma x + (1-x)} \cdot [\, x\, m_{eof,L} + \frac{(1-x)}{\gamma} \cdot m_{eof,T} + \overline{m}_L \,] \qquad (16)$$

where the effective mobility of the leading ions ($\overline{m}_L$) has a negative value for anions. Both equations (16) and (8) can be used to calculate the pressure difference that results in a hydrodynamic flow that counterbalances the velocity of the boundary between the leading and analyte zone. Equation (16) gives insight in all the parameters that are affecting the pressure difference.

When the conductivities of the leading and terminating buffer are measured or calculated (eqn. 12), the conductivity ratio γ (eqn. 13) can be calculated. Via experimentally determined electrophoretic and electroosmotic mobilities the corresponding velocities can be calculated using equations (4), (14) and (15). The total velocity of the boundary of the leading buffer zone with the sample zone (v_L) is then calculated with eqn. (6). The pressure that results in a hydrodynamic flow velocity that counterbalances v_L is then given by eqn. (8).

When it is not possible to apply a pressure during the focusing procedure, a height difference can be used. The calculated pressure difference can be converted to a height difference using

$$\Delta h = \Delta p / \rho\, g \qquad (17)$$

where Δp is the pressure difference (bar), ρ is the buffer density (1000 kg m^{-3}), and g is the gravitational force (9.8 ms^{-2}). A pressure difference of 20 mbar corresponds to a height difference of approximately 20 cm. This conversion is independent of the capillary diameter.

Current monitoring

When a constant voltage is applied during the focusing step, and the leading buffer is used as background electrolyte in the CZE step, the current will increase as more leading buffer enters the capillary. Just before a complete removal of the terminator buffer the ITP is stopped and the CZE is started. Monitoring of the current can be used to determine the moment for automated switching from ITP to CZE.

The total current in an isotachophoresis process is determined by Ohm's law as the ratio of the applied voltage and the electrical resistance of the liquid in the capillary. The total resistance

in the ITP capillary is given by the sum of the resistances of the leading, terminating and sample zones. For the isotachophoresis of low concentrations of analyte the contribution of the sample zones to the total resistance of the capillary will be negligible so that

$$I = V_0/(R_L + R_T) \qquad (18)$$

The electrical resistance of zone i (R_i) depends on the capillary radius (r), the length (L_i) and the conductivity (κ_i) of the zone.

$$R_i = L_i/(\pi\, r^2\, \kappa_i) \qquad (19)$$

Substituting (19) in (18) gives

$$I = V_0 \pi r^2 \left[\frac{L_L}{\kappa_L} + \frac{L_T}{\kappa_T} \right]^{-1} \qquad (20)$$

When the conductivities are known the variation of current during the focusing step can be calculated using equation (20) for a given leading and terminating zone length. The current after removal of the terminator zone in single capillary ITP-CZE is given by (20) for L_T=0, i.e. when the capillary is filled with leading buffer only. In practice always a small zone of terminator will remain in the capillary when switching from ITP to CZE.

In isotachophoresis the composition of the leading zone also determines the composition of the terminating zone. Thus when the composition of the leading zone is known and the mobilities of the leading and terminating ions and of the counter ions are known, the change in current can be calculated. The conductivity in a zone is given by the sum of the product of concentration, mobility and charge of all ionic species. Combining (12) and (20) for a system with univalent ions gives

$$I = V_0 \pi r^2 F \left[\frac{L_L}{\bar{c}_L \left(|\overline{m}_L| + \alpha_L |m_R| \right)} + \frac{L_T}{\bar{c}_T \left(|\overline{m}_T| + \alpha_T |m_R| \right)} \right]^{-1} \qquad (21)$$

When in single capillary ITP-CZE a given remaining zone length of the terminator buffer is

allowed, the corresponding ITP current is then calculated using (20). This is the threshold of the current that can be used to program the CZE apparatus to switch automatically from the ITP step to the CZE step. Although equation (21) gives a better insight in all parameters that are affecting the change in current, for precise determination of the current profile during the ITP step it is advisable to use equation (20) in conjunction with conductivity measurements of the leading and terminating buffers.

Counterflow and current

The hydrodynamic flow velocity needed to counterbalance the sample zone velocity depends on the position of the sample zones in the capillary (eqn. 16). This position can be calculated from the current (eqn. 20 and 21). Combining these equations makes it possible to calculate the hydrodynamic flow velocity for a given current. The current is measured during the analysis and will be constant as long as the sample zones are not moving. Using equation 20, $L_L=xL_0$ and $L_T=(1-x)L_0$, the relative leading zone length x can be written as

$$x = \frac{\pi r^2 E_0 \kappa_T}{I(\gamma - 1)} - \frac{1}{(\gamma - 1)} \qquad (22)$$

Substituting the expression for the current density $I/(\pi r^2)=E_L\kappa_L$ (eqn. 11) in equation 9 gives

$$\frac{\gamma E_0}{\gamma x + (1 - x)} = \frac{I}{\pi r^2 \kappa_L} \qquad (23)$$

Substituting 22 and 23 in 16 results in the linear equation

$$\Delta p = a + b\,I \qquad (24)$$

which gives the pressure difference for a given current. The slope b and intercept a are given by

$$a = \frac{32\eta V_0}{d^2} \cdot \left[\frac{\kappa_T m_{eof,L} - \kappa_L m_{eof,T}}{\kappa_T - \kappa_L} \right] \qquad (25)$$

and

$$b = \frac{128\ \eta\ L_0}{d^4\ \kappa_L\ \pi} \cdot \left[\left(1 + \frac{1}{\gamma - 1} \right) \cdot \frac{m_{eof,T}}{\gamma} - \left(\frac{1}{\gamma - 1} \right) \cdot m_{eof,L} + \overline{m}_L \right] \qquad (26)$$

where the effective mobility of the leading ions ($\overline{m}_L$) has a negative value for anions. Equation 24 implies that with current monitoring not only the moment to switch from ITP to CZE can be determined, but also the pressure needed in single capillary ITP-CZE.

The focusing step

An important aspect in the focusing step is the focusing time of the analytes. The time to focus the injection zone is given by the sample zone length divided by the total velocity of the slowest analyte ion in the ITP separation window, $t=L_{inj}/v_{A,f}$. The subscript f refers to focusing conditions. The analyte velocity under focusing conditions is given by:

$$v_{A,f} = v_{el,A} - v_{el,T} = (\overline{m}_A - \overline{m}_T)\ E_T \qquad (27)$$

The focusing time is then given by:

$$t = L_{inj} / [(\overline{m}_A - \overline{m}_T)E_T] \qquad (28)$$

The focusing time is thus independent from the electroosmotic and hydrodynamic velocity. When the effective electrophoretic mobility of the analyte and the terminator ion are similar the focusing time will increase to infinity.

In practice the focusing step and the isotachophoretic removal of the terminator buffer can be combined thus reducing the analysis time. The focusing step is started at the appropriate pressure, given by (8) and after a few minutes the pressure is lowered. As a result the terminating zone length decreases slowly and the electrical field strength E_T increases. This can be repeated several times, thus increasing E_T and reducing the focusing time.

The described focusing procedure as illustrated in Fig. 1 offers several alternatives. In stead of counterbalancing the sample zone boundary with the leading buffer (the front boundary) the

boundary of the slowest sample ion with the terminator zone (rear boundary) can be counterbalanced. Analogous to (8) the pressure needed to induce an appropriate counterflow is given by

$$\Delta p = \frac{32\eta L_0}{d^2} \cdot [\, x v_{eof,L} + (1-x)\, v_{eof,T} + v_{el,A} \,] \qquad (29)$$

where $v_{el,A}$ is given by the effective electrophoretic mobility of the slowest analyte A and the electric field strength in the terminator zone (eqn. 4).

Dissolving the sample in leading buffer is another option. When the boundary of the terminator buffer with the sample zone in leading buffer (rear boundary) is counterbalanced (using eqn. 8), the focusing time is given analogous to eqn. (28) by

$$t = L_{inj} / [(\overline{m}_L - \overline{m}_A) E_L] \qquad (30)$$

In most cases it is unlikely that this will reduce the analysis time because the electrical field strength in the leading buffer is always lower than in the terminating buffer. However, when $\overline{m}_A$ approaches $\overline{m}_T$ the focusing time can be reduced by dissolving the sample in leading buffer.

Another possibility in reducing the focusing time is focusing under unsteady state conditions by dissolving the sample in a lower terminator concentration than given by eqn. (1) which results in an increased E_T. However, under unsteady state conditions care must be taken that no analyte is lost.

Composition of the sample

For the calculation of the velocities at the start of the focusing procedure, it is assumed that low concentrations analyte are dissolved in terminating buffer. The terminating buffer is at the isotachophoretic concentration (eqn. 1) and the sample zone length is considered to be L_T. The conductivity of the sample is considered to be the same as the terminating buffer. In that case all equations can be used immediately from the start of the focusing procedure. Another advantage of working under these well defined conditions is that the velocities of analyte ions are known and by using the appropriate counterflow no loss of analyte occurs.

When the analyte is dissolved in a matrix other than the terminator buffer or when high concentrations of matrix constituents are present in the sample, the applicability of the derived equations is limited to the ITP steady state. Only the zone velocity at the start of the focusing step can be calculated with the sample zone conductivity. The focusing step then proceeds under unsteady state conditions. The sample zone velocity is not only changing with its position in the capillary but also because of local changes in electric field strength as a result of the migration of matrix ions. Under unsteady state conditions the possibility exists that analyte ions migrate out of the capillary. A full discussion on unsteady state migration is given by Foret et al. [12].

One way to overcome incompatibility of the sample matrix with the ITP conditions is a sample pretreatment where an excess of matrix components is removed and the analytes are transferred to a well defined matrix. In trace analysis (nanomolar sample concentration range and lower) of analytes in complex matrix it is unlikely that ITP-CZE or CE in general can be used without an additional pretreatment step. An additional sample pretreatment usually improves the performance of ITP-CZE with respect to reproducibility, selectivity and ITP focusing time [7, 8].

Results and discussion

Equation 16 gives insight in all parameters that are affecting the zone velocity and the linear related counterbalancing pressure difference in the focusing and ITP step. Several of these parameters will now be discussed and compared with experimental data. Then the applicability of current monitoring for automated switching from ITP to CZE will be investigated in addition to the effect of the terminator zone length on the CZE performance.

Parameters affecting the sample zone velocity

In Fig. 2 the leading zone velocity is given for several electroosmotic flow rates. As can be seen from eqn. (3) for a high electroosmotic flow rate the zone velocity is always negative. However, when the electroosmotic mobility is similar or lower than the electrophoretic mobility the velocity v_L increases or becomes positive (increases in the opposite direction).

As an example an injection zone length of 60% of the total capillary length will be considered. The leading zone velocity is counterbalanced so that the rear boundary is moving to the fixed front boundary. As already mentioned in Theory alternatives are possible.

Under conditions as illustrated in Fig. 2 line A, the focusing procedure is started at a pressure

of 15 mbar (for conditions see Experimental). The front boundary of the sample zone is then focused at 60% terminator zone length. When the focusing step is completed the pressure is reduced to zero and the analyte zones migrate to the cathode. The analyte zones remain focused because of the isotachophoretic conditions and the terminator zone is removed from the capillary. The velocity of the sample zone as a function of the terminator zone length is described by line A. Just before complete removal of the terminator zone the voltage is reversed and the CZE is started.

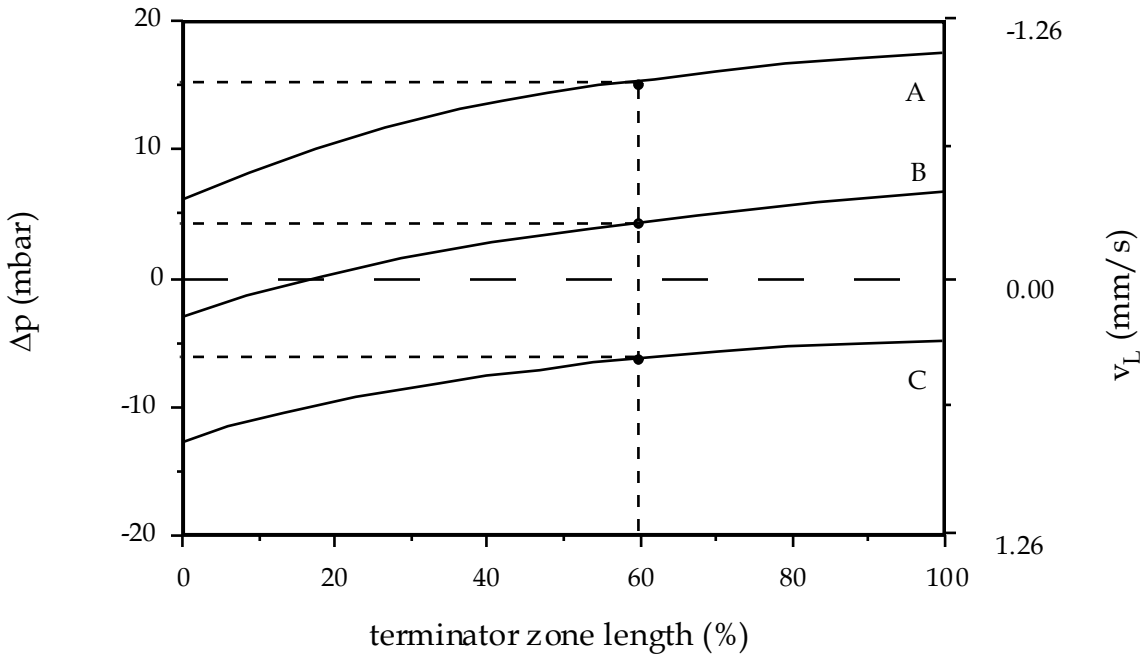

Fig. 2. The effect of the electroosmotic flow rate on the leading zone velocity and the counterbalancing pressure in ITP-CZE. The lines are calculated values for an electroosmotic mobility in the leading zone of 60.0 (A), 30.0 (B) and 1.0 (C) 10^{-9} $m^2V^{-1}s^{-1}$. All further parameters are given in Experimental.

For a similar injection under the conditions in Fig. 2 line B, the focusing procedure is started at a pressure of 4 mbar. After the focusing step the pressure is reduced to zero and the analyte zones will move to the point of 18% terminator zone length. At this point the electrophoretic mobility of the leading ions is counterbalanced by the electroosmotic mobility of the bulk. A

reduced pressure (i.e. $\Delta p<-4$ mbar) is needed to remove the remaining terminator zone from the capillary.

Under the conditions in Fig. 2 line C, the focusing procedure is started at a pressure of -7 mbar to focus the analyte front boundary at 60% terminator zone length. After focusing the pressure is reduced (i.e. $\Delta p<-14$ mbar) to remove the remaining terminator zone from the capillary. All constants and variables used for Fig. 2 are given in Experimental.

Another parameter that is affecting the counterflow needed in the focusing procedure is the electric field strength. Increasing the electric field strength linearly increases all velocities (eqn. 4, 9, 10, 14 and 15) and shortens the focusing time in ITP-CZE. As a result a linear increase of the counterflow velocity is needed. When the focusing voltage is doubled, a doubling of the pressure is needed to counterbalance the leading zone velocity. The time to complete the focusing will be reduced by a factor two (eqn. 28 and 30).

High electric field strengths are not always favourable with respect to zone broadening. Increasing the electric field strength will increase the heat generation in the capillary, especially in the terminator zone where the electrical resistance is higher. When the terminator zone is almost removed from the capillary the electric field strength in the terminator zone increases to E_0/γ (eqn. 10, x=1). At the same time, at a constant voltage the current through the capillary increases as more leading buffer is entering the capillary. The power in the terminator zone (W_T) increases with $W_T=V_T I$ resulting in a corresponding increase of heat development. Furthermore, the laminar flow profile that exists because of a mismatch of the electroosmotic velocities in the leading and the terminating zone [6] will be increased at higher electric field strengths. This is usually compensated for by the self correcting properties of the isotachophoretic zones [7, 8, 10] but at high electric field strengths problems may arise. In order to avoid zone distortion or even disruption of the electrical current, it may be necessary to reduce the voltage when the length of the terminating zone is getting smaller.

The ratio of mobility of the leading and terminator ions is important for the focusing time (eqn. 28 and 30). When a weak electrolyte is used as terminator buffer a low conductivity can be obtained, resulting in a small value of γ. The electroosmotic velocities in the leading and terminator zone change with the local electric field strengths E_T and E_L (eqn. 9, 10, 14 and 15). A lower conductivity of the terminating zone results in an increase of E_T, especially at small terminator zone length. This results in a reduction of the focusing time. However, as mentioned, a high electrical field strength may lead to excessive heat development in the terminating zone.

The sample zone velocity is independent from the capillary diameter. However, the pressure

(and height) difference is inversely dependent on the square of the capillary diameter. Capillaries with smaller inner diameters have better heat dissipating properties and therefore higher electric field strengths are allowed. Because of a decreased loadability and detectability at small inner diameters an optimum can be found with respect to electric field strength, analysis time, capillary diameter and determination limits.

Single capillary ITP-CZE without a hydrodynamic counterflow

During the ITP step the electric field strength in the terminator (E_T) and leading buffer zone (E_L) and the corresponding zone velocities can be calculated. From (9) and (10) it follows that when x (relative leading zone length) approaches unity, the terminating electric field strength increases to E_0/γ and the electric field strength in the leading zone increases to E_0. For the focusing step this means that during the removal of the terminating zone the electric field strength and the corresponding electrophoretic and electroosmotic velocities in the leading zone and in the terminating increase. For anionic separations the electroosmotic and electrophoretic velocities increase of opposite directions.

Under certain conditions the possibility exists that at a certain terminator length the electrophoretic velocity is counterbalanced by the electroosmotic velocity, without application of a pressure.

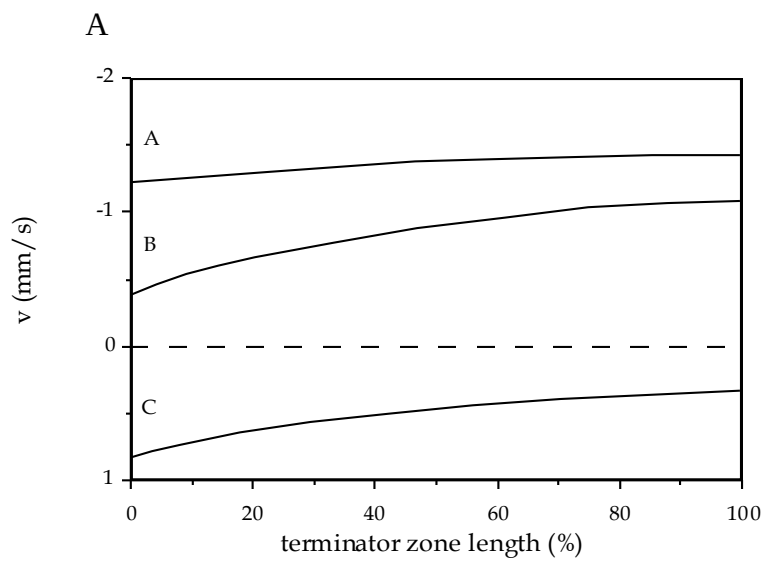

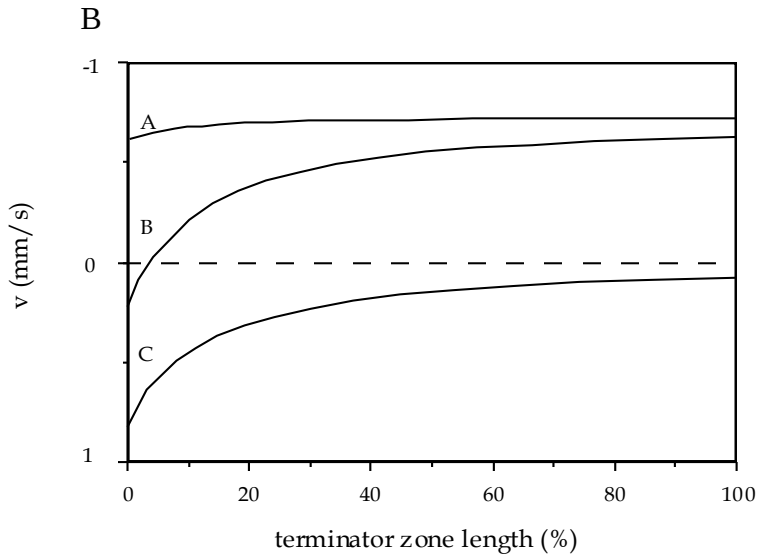

Fig. 3 (A). Variation in the bulk electroosmotic (A, v_{eof}) and the electrophoretic (C, $v_{el,L}$) flow velocity for a given position in the capillary. The total sample zone velocity (B, v_L) decreases during the removal of the terminator zone. All further parameters are given in Experimental. (B) The same velocities as in 3A are calculated for an electroosmotic and electrophoretic mobility of respectively 30 and -42 10^{-9} $m^2V^{-1}s^{-1}$ and a γ of 0.1. At 4% terminator zone length the electrophoretic velocity is counterbalanced by the electroosmotic velocity. This implies that in principle anionic ITP-CZE can be carried out without a hydrodynamic counterflow.

In Fig. 3A the calculated electrophoretic and electroosmotic velocities during the focusing procedure are shown for a given position in the capillary. Although the local electroosmotic velocities in the leading ($v_{eof,L}$) and terminating zone ($v_{eof,T}$) vary during the focusing procedure, the bulk electroosmotic flow velocity (v_{eof}, line A) is more or less constant. The electrophoretic velocity ($v_{el,L}$, line C) of the anionic leading ions increases in the opposite direction (gets more positive). This means that the total sample zone velocity (v_L, line B) reduces as the terminating buffer is removed from the capillary using a constant voltage.

When the electroosmotic mobility in the leading zone is approximately equal to the electrophoretic mobility of the leading ions, there is one value of x where the zone velocity is zero. A reduced pressure is necessary to remove the remaining terminator buffer. The sample zone velocity will be reversed as the terminator zone length is getting smaller. Under these conditions (i.e. $-m_L \sim m_{eof,L}$) in principle the complete ITP-CZE procedure can be carried out without the application of a hydrodynamic counterflow.

Under the conditions in Fig. 3B the leading zone velocity in is zero at 4% terminator zone length. This means that when ITP-CZE is carried out without application of a counterflow the sample zones will be focused at 4% terminator zone length. Under these conditions the velocity of the front boundary of the sample zone is not counterbalanced by a hydrodynamic flow. As a result the terminator zone length containing the analyte ions is reduced to 4% already during the focusing step. As mentioned in Theory, this means that a loss of analyte may occur. Therefore the sample should be dissolved in leading buffer so that the rear boundary of the sample zone is the boundary between leading and terminating buffer. During focusing this boundary moves to the 4% position and remains there. The front boundary will migrate to the rear boundary without loss of analyte. The boundary velocity and the focusing time are then given by respectively eqn. (6) and (30). After the focusing step the CZE can be started without the additional step of the removal of the terminator buffer, providing that the 4% zone does not disturb the CZE separation. Fine tuning of the leading ion velocity with respect to the electroosmotic flow velocity is one way of optimising such an ITP-CZE procedure. This broadens the applicability of automated anionic single capillary ITP-CZE to all commercially available systems that are not capable of fine adjustment of a pressure.

Verification of sample zone velocity

To verify the derived equation (16) a counterflow experiment is carried out using height differences for focusing a zone of coloured dye on a fixed position in the capillary. The height difference is measured at two points, where the sample zone is slowly moving forward and where the sample zone is slowly moving backward. The mean value is considered the height difference where the sample zone velocity is zero. At height differences close to zero, where the direction of the sample zone velocity reversed, it is not possible to obtain reliable results. A hysteresis in the zone velocity is observed when counterbalancing it with a hydrodynamic velocity. Different results are obtained depending from which direction the height difference is changed. At height differences of 5 cm or more the data became reproducible. In Fig. 4A the calculated line and measured data points are shown. The deviation of the measured data points from the calculated line may be due to temperature effects which become more pronounced at small terminator zone lengths.

In Fig. 4B the calculated current is plotted against the pressure difference needed for a proper counterflow which is a straight line (eqn. 24). The same data points as in Fig. 4A are

used in 4B. The regression line of the calculated data is p = 18.4 - 1.76 I, the line of the measured data is p = 18.5 - 1.92 I. The measured intercept is approximately similar to the calculated intercept. The calculated slope is 9% below the value of the measured slope. Using the regression line for p=0 the current at zero sample zone velocity (i.e. $-v_{el,L} = v_{eof}$) is calculated. For the calculated line this is at 10.5 µA, for the measured data this is 9.63 µA.

Fig. 4B demonstrates that relatively small differences in the used parameters may result in considerable differences in the calculated and the actually needed pressure, especially near the point of reversal of the pressure. However, it should be kept in mind that current monitoring will be a convenient tool in compensating for these differences. Only when the appropriate pressure is applied under isotachophoretic conditions the current will be constant. In Experimental all parameters and those used for calculations are given.

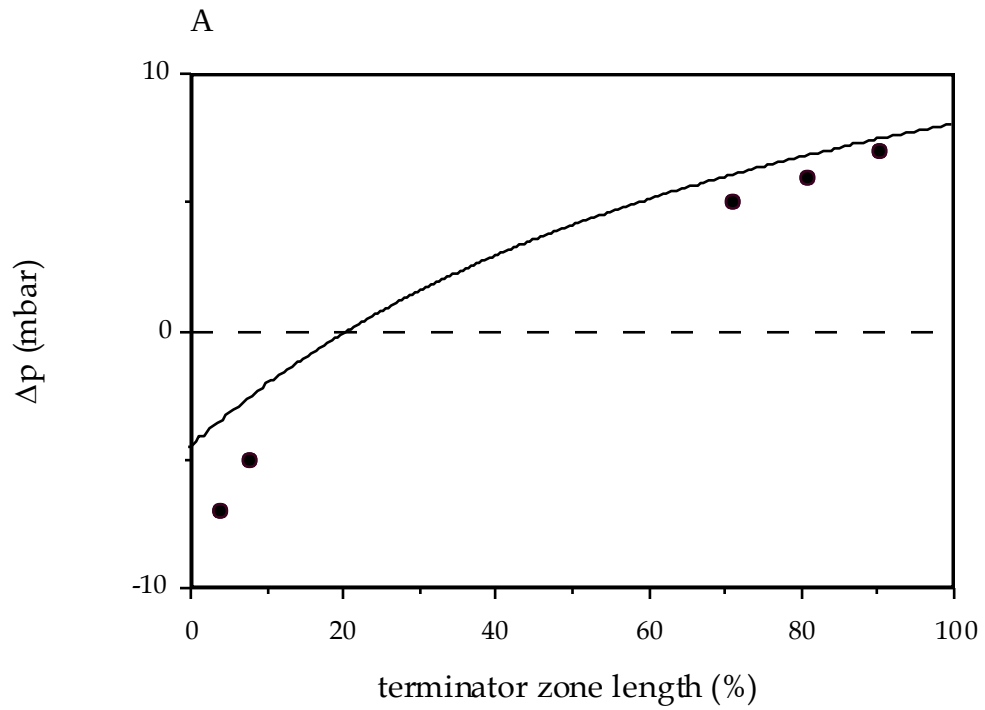

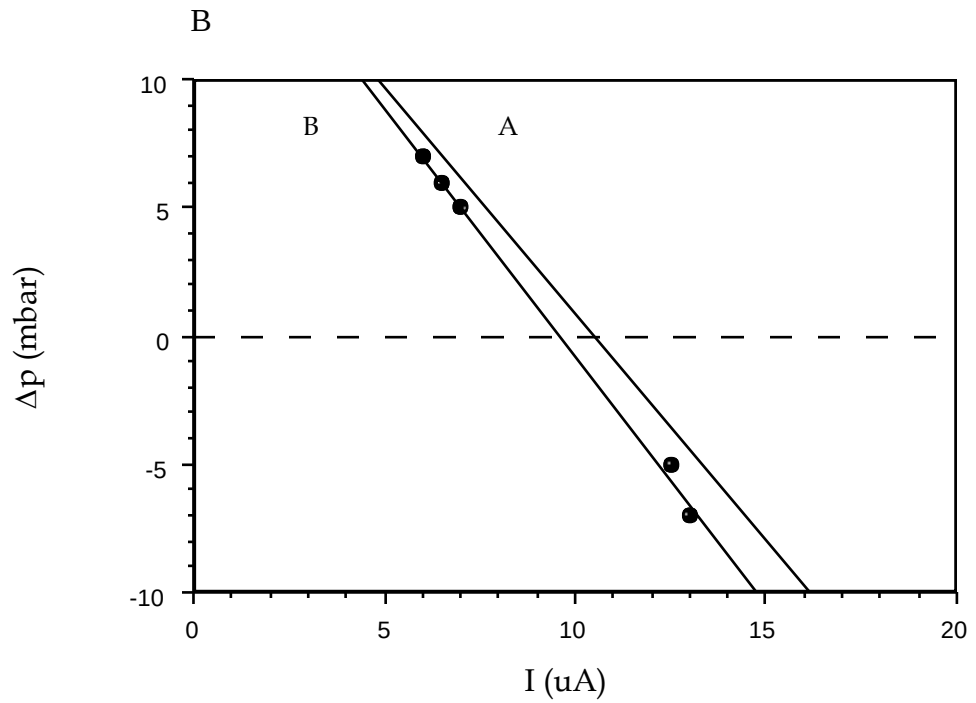

Fig. 4 (A). Calculated counterbalancing pressure difference in ITP-CZE (line) and the measured data points at several positions in the capillary. A negative pressure difference is needed for complete removal of the terminator buffer from the capillary. All parameters are given in Experimental.
(4B). For several positions of a sample zone in the capillary the running current is plotted against the counterbalancing pressure. Calculated (A) and measured (B) data results in a straight line as predicted by eqn. 24. The same data points as in 4A are used.

Temperature effects

One of the assumptions in the described model is that the temperature in the leading and terminating buffer zone is the same and constant. For isotachophoresis this is not true because the electrical field strength in the leading buffer is lower than in the terminating zone. However, in systems with efficient dissipation of the Joule heat the effects of axial temperature differences will be negligible. The temperature inside the capillary can be calculated using [13]

$$T = T_a + \frac{E^2 d_1^2 \kappa}{8} \cdot \left[\frac{1}{k_1} \ln \frac{d_2}{d_1} + \frac{1}{k_2} \ln \frac{d_3}{d_2} + \frac{2}{h d_3} \right] \qquad (31)$$

where d_1, d_2 and d_3 are the inside capillary diameter, the outside fused silica diameter and the outside polyimide diameter, respectively. T_a is the working temperature and h is the heat transfer coefficient to the surroundings. The thermal conductivities k_1 and k_2 are respectively 1.5 $Wm^{-1}K^{-1}$ for silica and 0.16 $Wm^{-1}K^{-1}$ for polyimide. For example, the temperature in the leading and terminating zone is calculated for a terminating zone length of 60% and 10% of the total capillary length under conditions as described for Fig. 2.

When the capillary is filled for 60% with sample in terminating buffer, the temperature inside the leading and terminating zone is 293.3 K and 293.8 K respectively (T_a=293, E_L=10.4 kVm^{-1}, E_T=26.4 kVm^{-1}, κ_L=0.070 Sm^{-1}, κ_T=0.027 Sm^{-1}, d_1=100 µm, d_2=340 µm, d_3=355 µm, h=180 $Wm^{-2}K^{-1}$, for other conditions see Experimental). The viscosity and electrophoretic mobility decrease 2.6% per degree K, which means a difference of 1.3% in viscosity and mobility is expected under these conditions. The effects on the calculated counterbalancing pressure will be negligible.

After the focusing step the terminator buffer is removed from the capillary. When the length of the terminating zone is 10% of the total capillary length the temperature inside the leading and terminating zone is respectively 293.8 and 295.1 K (E_L=17.3 kVm^{-1}, E_T=44.1 kVm^{-1}). When the running voltage is reduced to 6 kV (E_0=12 kVm^{-1}) the temperature in the leading and terminating zone becomes 293.3 K and 293.8 K respectively (T_a=293, E_L=10.4 kVm^{-1}, E_T=26.5 kVm^{-1}). As the terminating zone gets smaller the temperature will increase. In our experience, the corresponding decrease of viscosity does not interfere with automated ITP-CZE procedures.

Current monitoring

The calculated change in current (eqn. 20) is in good agreement with the measured data (Fig. 5). The change in current at constant voltage during the focusing procedure is calculated for several other conductivities of the terminator buffer (Fig. 6). The larger the difference in conductivity, the larger the change in current. In practice large differences in conductivity will make automated switching from ITP to CZE using current monitoring easier.

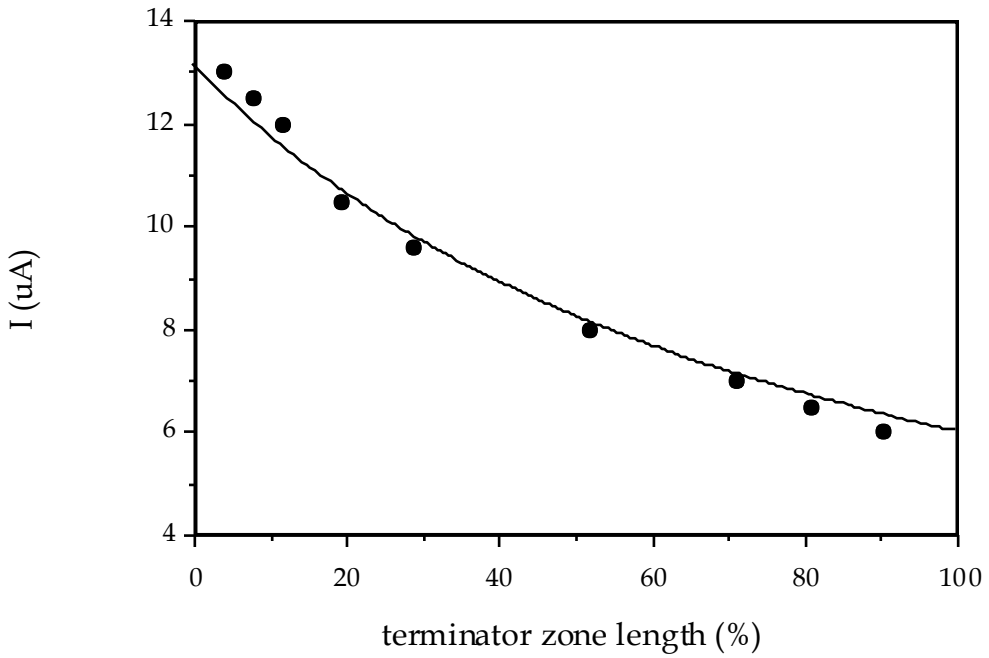

Fig. 5. Calculated change in current at a constant voltage during the focusing step in ITP-CZE (line) and the measured data points at several positions in the capillary. All parameters are given in Experimental.

When the zone length of terminator buffer is 5% of the total capillary length, the current is at 95% of I_0 for a conductivity ratio of 0.48 (line A). Where I_0 is the maximum current when the capillary is completely filled with leading buffer. For the same terminator zone length the current is at 50% of I_0 for a conductivity ratio of 0.048 (line C). In practice this means that at large differences in conductivities smaller terminator zone length will remain after automated switching from ITP to CZE. However, in case of similar conductivities of leading and terminator buffer, somewhat larger remaining terminator zone lengths are allowed. The effect on zone broadening in the CZE step caused by conductivity differences will consequently be less.

In Fig. 7 the effect of the length of the remaining terminator zone on the CZE separation is shown. When the current at the moment of switching is lower than 92% of I_0 zone broadening occurs. The corresponding remaining terminating zone length is 10% of the total capillary length.

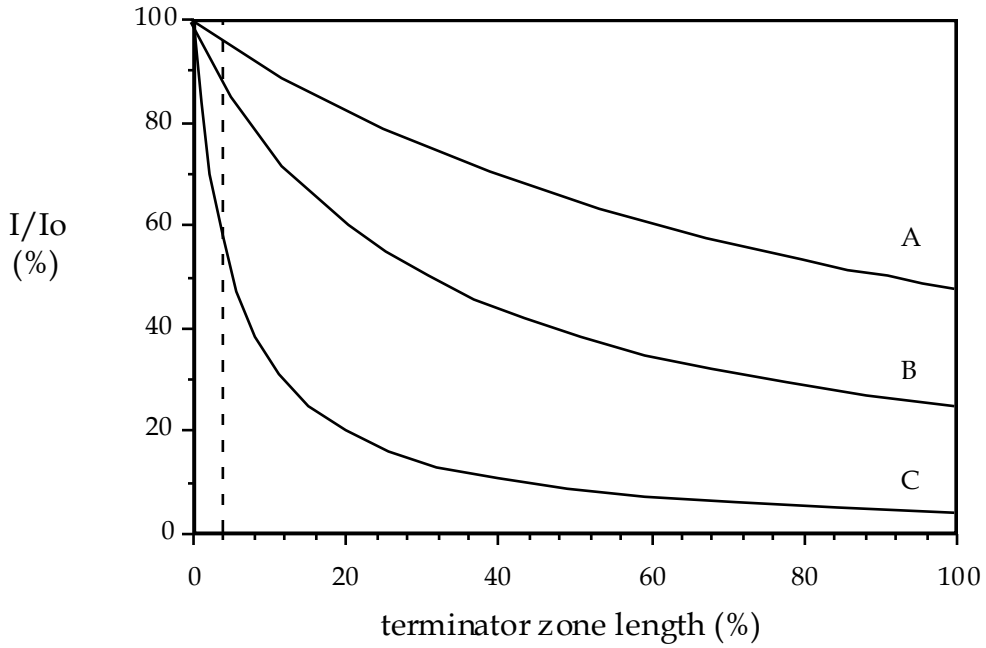

Fig. 6. The calculated change in current at a constant voltage during the focusing step in ITP-CZE. A conductivity ratio of terminating and leading buffer (γ) of 0.48 (A), 0.24 (B) and 0.048 (C) is used for calculation. The conductivity of the leading buffer (κ_L) is kept constant. The ionic mobility of the terminator ions is -22.0 10^{-9} $m^2V^{-1}s^{-1}$. All other parameters are given in Experimental.

Although the 10% seems like an overload of the CZE, the effect on the peak shape is relatively small. Because of the conductivity ratio of 0.48 the disturbance of the homogeneity of the electric field by the remaining terminator zone is limited. A larger difference in conductivity would result in more peak broadening, but the consequently smaller conductivity ratio would make precise switching with small remaining terminator zones easier (Fig. 6, C: γ = 0.048).

The reproducibility of CZE migration times in ITP-CZE with automated switching using current monitoring is investigated for six ITP-CZE runs. The current is programmed at 99% of I_0 at the switching time. The RSD in migration times is 1.4%. This is approximately three times higher in comparison with CZE in a bioassay of anthracyclines where a RSD of the migration times of 0.5% has been reported by our group [4].

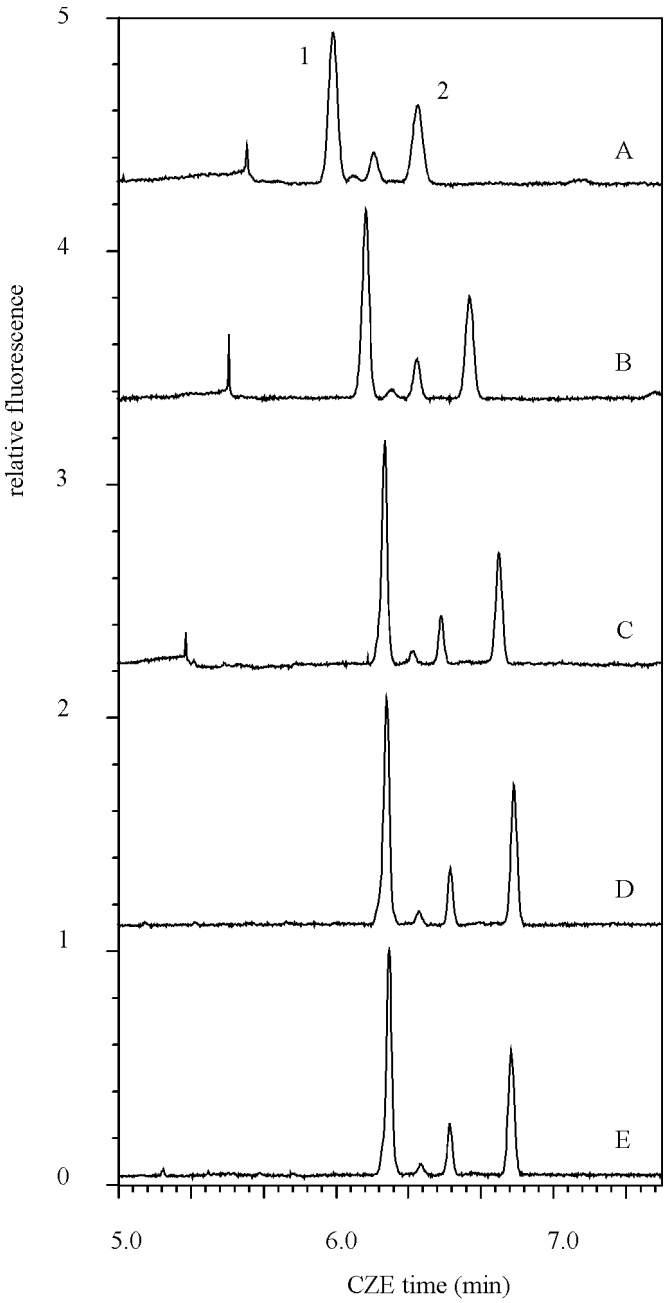

Fig. 7. The effect of the remaining terminator buffer zone length on the CZE separation of FITC (1) and F (2) in ITP-CZE. Other peaks are unknown degradation products of FITC. Automated switching using current monitoring is used at 88.2 (A), 90.9 (B), 93.6 (C), 96.3

(D), and 99.0 (E) percent of the maximum current I_0. Because of a decrease of the migration length in CZE a decreased migration time is notable as the remaining terminating zone gets larger.

Conclusions

Equations have been derived giving the zone velocity and the current for a given terminator zone length in single capillary ITP-CZE. Monitoring the current offers the possibility to calculate the hydrodynamic flow velocity that is needed to counterbalance the leading zone velocity. It is therefore expected that current monitoring can be used in an automated feedback mechanism to control the applied pressure. Correlation between current and the position of the sample zones in the capillary can be used for automated switching from ITP to CZE. This results in reproducible CZE migration times and will make the implementation of automated focusing procedures in bioassays easier.

Under certain conditions ITP-CZE separations can be carried out even without the application of a hydrodynamic counterflow. This extends the applicability of this procedure to equipment that is not capable of applying a hydrodynamic pressure during the focusing step.

References

1. W.G. Kuhr, Anal. Chem., 62 (1990) 403R
2. W.G. Kuhr and C.A. Monnig, Anal. Chem., 64 (1992) 389R
3. M. Albin, P.D. Grossman and S.E. Moring, Anal. Chem., 65 (1993) A489
4. N.J. Reinhoud, U.R. Tjaden, H. Irth and J. van der Greef, J. Chromatogr., 574 (1992) 327
5. A.J.J. Debets, M. Mazereeuw, W.H. Voogt, D.J. Vaniperen, H. Lingeman, K.P. Hupe and U.A.T. Brinkman, J. Chromatogr. 608 (1992) 151
6. R.L. Chien and D.S. Burgi, Anal. Chem., 64 (1992) A489
7. N.J. Reinhoud, U.R. Tjaden and J. van der Greef, J. Chromatogr., 641 (1993) 155
8. N.J. Reinhoud, U.R. Tjaden and J. van der Greef, J. Chromatogr. A, 653 (1993) 303
9. M.H. Lamoree, N.J. Reinhoud, U.R. Tjaden, W.M.A. Niessen and J. van der Greef, Biol. Mass Spectrom., 23 (1994) 339
10. P. Bocek, M. Deml, P. Gebauer and V. Dolnik, *Analytical Isotachophoresis*, (Electrophoresis Library, Vol. 1), B.J. Radola (Editor), 1988, VCH, Weinheim, Switzerland.
11. V. Sustacek, F. Foret and P. Bocek, J. Chromatogr., 545 (1991) 239
12. F. Foret and P. Bocek, in A. Chrambach, M.J. Dunn, B.J.Radola (Editors) *Advances in Electrophoresis*, Vol. 3, VCH Weinheim, 1989, p. 271-347
13. E. Grushka, R.M. McCormick and J.J. Kirkland, Anal. Chem., 61 (1989) 241

3.4

Automated On-Capillary Isotachophoretic Reaction Cell for Fluorescence Derivatization of Small Sample Volumes at Low Concentrations Followed by Capillary Zone Electrophoresis

Abstract

An automated on-line reaction cell is described combining the concentrating properties of isotachophoresis (ITP), the separation efficiency in capillary zone electrophoresis (CZE) and the detection sensitivity of laser induced fluorescence detection (LIF). The applicability of the reaction cell is demonstrated for an automated derivatization procedure of glutathion (GSH) and several amino acids with ortho-phthaldialdehyde (OPA) and naphthalene-2,3-dicarboxaldehyde (NDA). Nanolitres analyte, at nanomolar concentration level, are concentrated and derivatised in capillary ITP. The derivatives are analysed by CZE with LIF detection. The entire procedure is automated and takes place in the same capillary using single capillary ITP-CZE. Furthermore, an easy applicable on-capillary OPA derivatization is described for CZE without ITP step.

Introduction

The on-line coupling of CZE with other analytical separation techniques has resulted in increased selectivity and separation power. Improvements in detection techniques has resulted in detection of extremely low amounts of analyte [1-3]. In combination with electrophoretic stacking or isotachophoretic preconcentration methods the corresponding determination limits are impressive [4].

Small injection volumes, typically in the nanolitre range, are characteristic for CZE. However, in most analytical sample pretreatment procedures the smallest volumes that can be handled are in the microlitre range. This implies that in most cases more than 99% of the sample is wasted. In situations where analytes are chemically modified before analysis a more efficient use of reagents is achieved by reduction of the reaction cell volume. This is especially relevant in cases where expensive reagents are involved such as enzymes or antibodies. The reaction cell described in this paper has at least a factor 100 lower reagent consumption compared to a conventional 100 microlitre reaction vial. The applicability of the reaction cell is demonstrated

for a fluorescence introducing derivatization reaction.

The use of on-line fluorescence derivatization procedures puts several demands on the analytical method. Fluorophoric derivatization reagents, which show fluorescent properties similar to that of the derivatization product, are difficult to apply in an on-line procedure because the reagent has to be separated from the derivative before detection takes place. Therefore, fluorophoric derivatization reagents are usually applied in the pre-column mode, sometimes in combination with an additional step for removal of the excess of reagent. Fluorogenic reagents, which do not have fluorescent properties similar to that of the derivatization product, are considerably easier to apply in on-line procedures [5-7].

Several applications of CZE with LIF and precolumn derivatisation have been described [1-3, 7]. Recently, Houben et al. [8] described an automated derivatization procedure for absorbance detection of amino acids. Combination of CZE with an on-capillary enzyme reactor has been described by Avila et al. [9]. Chang et al. described an on-column protein digestion with pepsin followed by CZE with native LIF detection [10].

In this paper the applicability of the capillary reaction cell is demonstrated for an automated on-capillary derivatization of low concentrations of analyte in single capillary ITP-CZE. The analyte is concentrated in the focusing step, derivatized in the ITP step and analysed in the CZE step. The method takes place in a commercially available CZE system without any hardware modifications. In previous papers we have described automated procedures for ITP-CZE in a single capillary for cationic and anionic separations [11-13]. Furthermore, an on-capillary OPA derivatization is described for CZE without an ITP step of amines at higher analyte concentrations.

Experimental

Untreated fused silica capillaries (SGE, Ringwood, Victoria, Australia) were used. A programmable injection system for capillary electrophoresis (PRINCE, Lauerlabs, Emmen, The Netherlands) equipped with a reversible polarity power supply and possibility for pressurised and electrokinetic injection was used for the analyte focusing process. The LIF detection system has been described previously [11]. Excitation of OPA derivatives took place at 351.1 and 363.8 nm, for emission a 450 nm bandpass filter (10 nm bandwidth, type 53830 Oriel, Stratford, CT, USA) was used. The NDA derivatives were detected using the 457.9 nm laser line for excitation and a 515 nm long pass filter (Oriel) for emission.

Chemicals

Sodium cacodylate, triethanolamine (TEtOHA) (97%) and 4-(2-Hydroxyethyl)-1-piperazine ethanesulphonic acid (HEPES) were purchased from Janssen Chimica (Beerse, Belgium). Hydroxypropylmethylcellulose (HPMC) with a viscosity for a 2% aqueous HPMC solution of 4000 cP, came from Sigma (St. Louis, MO, USA). Acetic acid (HAc), sodium borate, phosphoric acid, barium hydroxide, potassium cyanide (KCN), glutamic acid (Glu), aspartic acid (Asp), arginine (Arg), lysine (Lys), tryptophan (Trp), phenylalanine (Phe), threonine (Thr), serine (Ser), 3,4-dihydroxyphenylalanine (Dopa) and bromophenol blue were from Merck (Darmstadt, FRG). OPA and β-mercaptoethanol (ME) were from Aldrich Chemie (Steinheim, Germany). NDA came from Molecular Probes (Eugene, OR, USA). In all experiments deionised water was used (Milli-Q system, Millipore, Bradford, MA, USA).

Analyte focusing with on-capillary derivatization

The ITP-CZE procedures were used as described previously [11, 12], with exception of the first step (Fig. 1). In step 1 the capillary was filled with leading buffer containing the derivatization reagent. Then the injection of sample takes place hydrodynamically at a pressure of 100 mbar. In step 2 the analyte focusing starts by applying a voltage in conjunction with a hydrodynamic pressure. After 5 - 20 min of focusing and derivatization, depending on the injected volume, a voltage of -20 kV was applied without a hydrodynamic pressure (step 3). The zone of terminating buffer was removed isotachophoretically out of the capillary. At the time that the sample zone was approaching the capillary inlet the terminator buffer vial was replaced for a vial containing the CZE background electrolyte (step 4), the voltage was reversed and the CZE run was started (step 5).

The current was monitored for precise timing of the moment to switch from ITP to CZE. When a constant voltage was applied the current increases as long as the terminating ions leave the capillary. The CZE equipment can be programmed so that at a defined threshold of the current the switching takes place automatically. In principle all ions with mobilities below that of the terminating ion, including the counter ions, were removed by the described procedure.

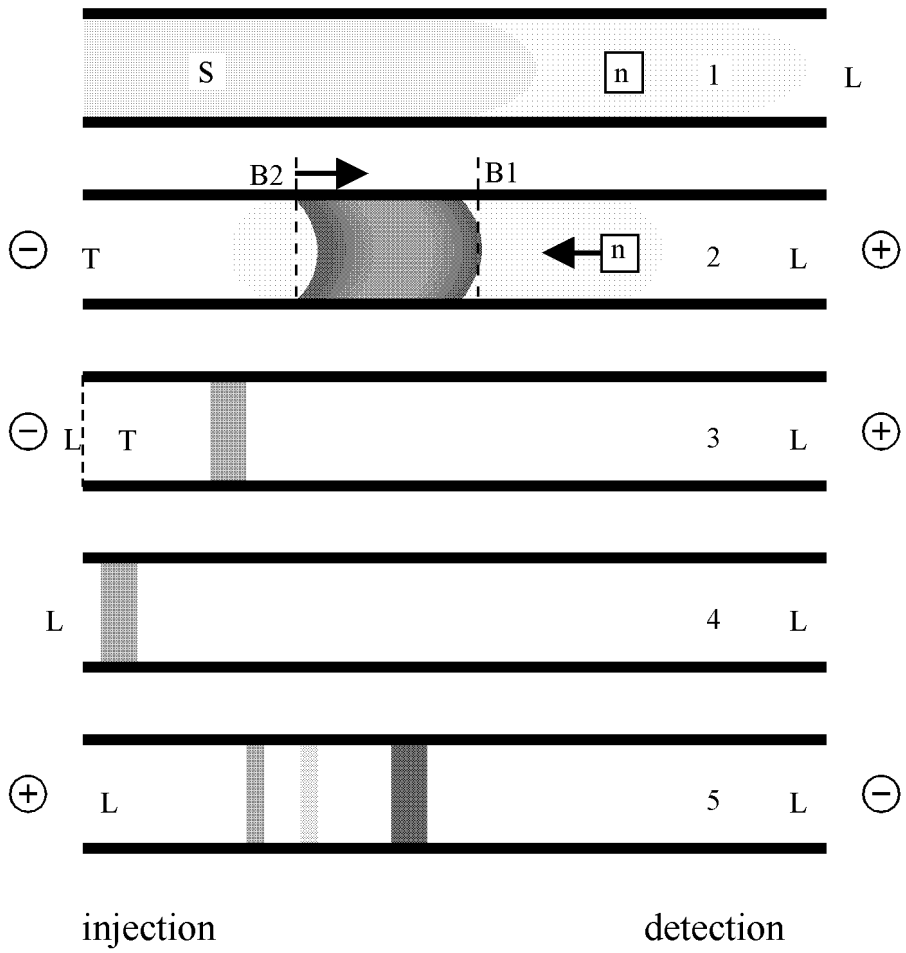

Fig. 1. Schematic representation of the on-capillary derivatization during the ITP step in single capillary ITP-CZE. In step (1) the neutral reagent (n, in leading buffer) was injected before the sample (S, in terminating buffer). In the focusing step (2) electrophoretic and hydrodynamic velocities were balanced so that the boundary (B1) was kept on a fixed position in the capillary. Boundary (B2) moves to boundary (B1). The neutral derivatization reagent was moving through the sample zones into the direction of the cathode and the derivatization takes place. The reagent was supplied by injection as a zone with a defined length or continuously supplied by addition to the leading buffer vial. See Experimental for further explanation.

ITP-CZE buffer systems

System I: The leading buffer consisted of 10 mmol/l HAc set at pH 8.0 with TEtOHA and was also used as CZE background electrolyte. The terminating buffer was 10 mmol/l HEPES set at pH 8.0 with TEtOHA. The capillary dimensions were 590 x 0.100 mm, detection took place at 520 mm from the inlet.

System II: The leading buffer was a 10 mmol/l sodium phosphate buffer at pH 9.4 and was also used as CZE background electrolyte. To the leading buffer 0.05% (w/v) of HPMC was added. The terminating buffer consisted of 10 mmol/l sodium cacodylate set at pH 9.4 with $Ba(OH)_2$ and contained 0.05% HPMC (w/v). The capillary dimensions were 700 x 0.100 mm, detection took place at 600 mm from the inlet.

System III: The CZE buffer consisted of a 40 mmol/l borate buffer at pH 9.5 and contained 0.1 mg/ml OPA and 0.1% (v/v) ME. In initial experiments 1.0 mg/ml OPA was used. The capillary dimensions were 730 x 0.075 mm, detection took place at 665 mm from the inlet.

Derivatization

Pre-column OPA derivatives were made by 1:1 addition of the analyte in leading buffer to an OPA solution of 1 mg/ml in leading buffer containing 0.1% ME. The NDA derivatives were made by 1:1 addition of the analyte in leading buffer to a NDA solution of 2 mmol/l in leading buffer containing 1 mmol/l potassium cyanide. The NDA reagent was diluted from a stock solution of 100 mmol/l in MeOH and mixed with KCN in leading buffer just before the derivatization was started.

For on-capillary derivatization reactions in ITP-CZE the reagent was added to the leading buffer. The OPA reagent was used at a concentration of 0.1 mg/ml and 0.01% ME and was added to the leading buffer vial. This buffer vial was used during the entire ITP-CZE procedure. The NDA and KCN concentration was 0.1 mmol/l. The NDA reagent was supplied by injecting a zone of leading buffer containing the derivatization reagent before sample injection for immediate start of the derivatization during the focusing step. For NDA derivatization with continuous supply of reagent only during the ITP step the leading buffer vial was switched for a leading buffer vial containing the NDA reagent. Glutathion is unstable under alkaline conditions and was added to the terminator buffer just before injection.

Theory

Derivatization reactions

The OPA reagent in combination with a nucleophile such as β-mercaptoethanol (ME) forms N-substituted 1-alkyl-isoindole derivatives. The derivative is formed within one minute and slowly decomposes (Fig. 2A). Therefore, it is important that the reaction times are kept constant.

This makes the OPA reagent only suitable for pre-capillary derivatization if the procedure is automated so that the derivatization times are kept constant as is the case in the described on-capillary derivatization methods. Derivatization of peptides with the OPA reagent is only possible if the peptide contains lysine, due to the high reactivity of the ε-amine function [14, 15].

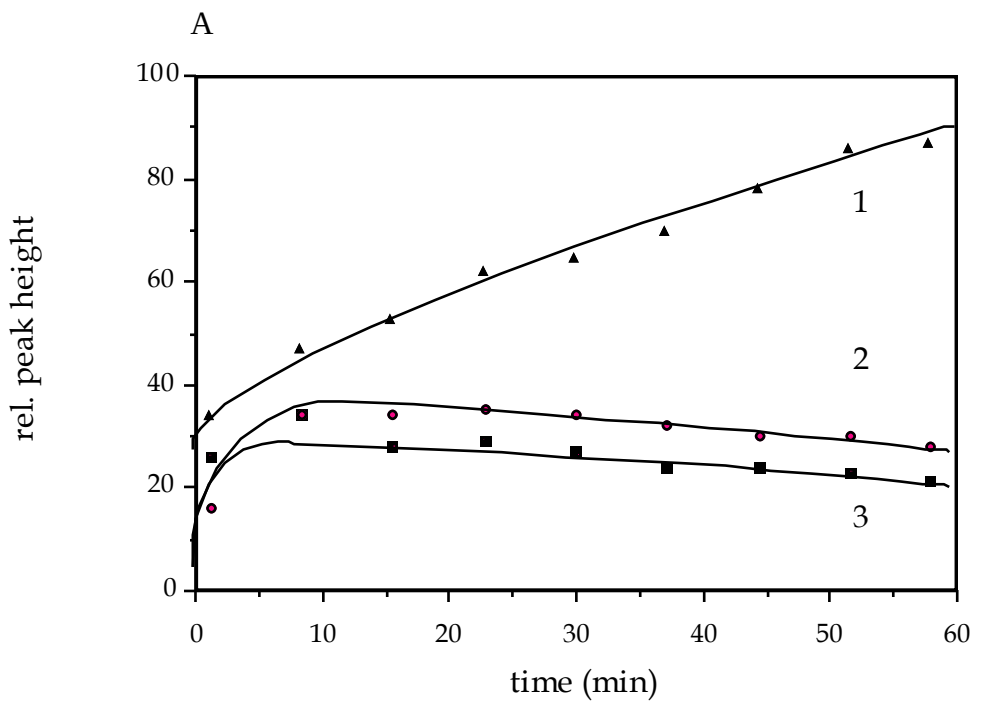

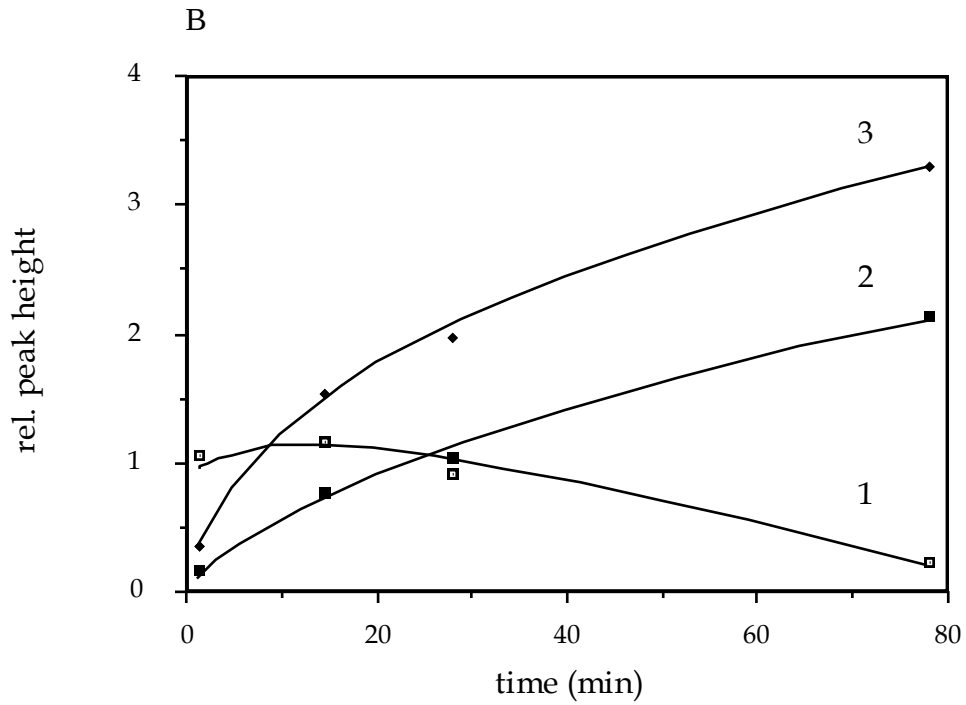

Fig. 2. Relative peak height measured at different times after derivatization of GSH (1), Asp (2) and Glu (3) with (A) OPA/ME and (B) NDA/CN reagent. Concentrations analyte are respectively 100, 100 and 200 ng/ml for the OPA derivatization and 1.0 µmol/l each for the NDA derivatization.

The NDA reagent in presence of a nucleophile such as cyanide forms stable derivatives with primary amines, including the terminal amine function of peptides. As a result of the formation of side products and the derivatization time needed (10 min for peptides, Fig. 2B) it is mainly used as pre-capillary derivatization reagent. NDA in combination with ME forms a less stable product but in combination with fast reaction times (1 min for peptides) it is suitable as post-capillary derivatization reagent [16].

OPA and NDA are also used in derivatization procedures for electrochemical detection [17], for NDA derivatives a selective peroxyoxalate chemiluminescence detection procedure has been described [18]. Certain analytes such as histidine [19], histamine [19], spermidine [20], serotonin [21] and glutathione [22, 23] react with OPA without addition of a nucleophile which increases the selectivity of the derivatization reaction considerably.

ITP-CZE

Capillary zone electrophoresis (CZE) has become an important separation technique complementary to high-performance liquid chromatography (HPLC). One of the challenges in the application of CZE separations in the analysis of biological samples is to reach for relevant determination limits. Electrophoretic analyte focusing techniques provide a way to increase the loadability and concentration detection sensitivity in CZE. The coupling of ITP with CZE has been described by several authors [4]. Improvements in determination limits by a factor of 1000 have been reported.

In ITP a discontinuous buffer is used and only anions or cations can be analysed in one run. In anionic separations the capillary and the anode vial is filled with leading buffer. The leading buffer contains anions with a mobility higher than the mobility of the analyte ions. The cathode vial is filled with terminating ions which have the lowest mobility. The pH is set with the buffering counterions. In the steady state, when the analytes are separated, they migrate as consecutive zones ordered by their electrophoretic mobilities. A characteristic of ITP is its concentrating property. The concentrations of analyte ions are adapted to the concentration of the leading ions according to the Kohlrausch regulation function [13]. The analyte concentrating property makes the technique attractive as preconcentration technique for CZE.

On-capillary reactions in ITP-CZE

An on-capillary reaction cell in ITP-CZE puts several demands on the system that is used. The reagent is added to the ITP buffer, therefore it should not be reactive to buffer components and the buffers should be of a high purity. In case of reactions with primary amines the number of buffers that can be used is limited. When the reagent is ionic, care must be taken that the isotachophoretic conditions are not disturbed and that mixing of the reagent with sample zones takes place. The analyte is derivatized under ITP conditions. To maintain sharp analyte zones the analyte and derivative should be within the ITP separation window. These conditions are all fulfilled with the OPA and NDA derivatization of primary amines.

The combination of single capillary ITP-CZE and an on-capillary reaction offers several advantages. Reaction conditions such as the temperature can be chosen easily, most of the commercially available CZE equipment offer the possibility of temperature control. The reaction time can be chosen as long as necessary. We already demonstrated that the ITP time does not influence the efficiency in single capillary ITP-CZE [11]. When the analyte zone is concentrated and fixed on a certain position in the capillary it stays there until the hydrodynamic

pressure is reduced. In an automated ITP-CZE procedure the reaction time will be constant which is important in case of unstable reaction products.

Using single capillary ITP-CZE adds an interesting feature to reaction kinetics. Not only the initial concentrations of reactants can be set but also the supply of fresh reagent can be varied while the analyte concentration is kept constant. In principle only the length of the underivatised analyte zone will reduce under ITP conditions until the derivatization is complete. The mixing of the reacting species is done in a very controlled way. The velocity of the neutral reagent is precisely known and can be manipulated by the applied electrical field strength during the ITP step. The velocity of the analyte is zero and because of the concentrating properties of ITP the analyte concentration will be high resulting in favourable reaction kinetics. The excess of reagent will automatically be removed before the CZE is started. All reaction products that are outside the separation window with a mobility lower than the terminator ions, are discarded during the ITP step. Another aspect is that in ITP-CZE using narrow bore capillaries, reactions in picolitre volumes can be carried out.

The reagent molar mass flow

One of the attractive features of the on-capillary isotachophoretic reaction cell is the possibility of controlling the reagent molar mass flow in the analyte zone. The reagent molar mass flow is calculated by deriving an equation for the velocity of neutrals during the ITP step. A simple buffer system is assumed, consisting of only one type of univalent cations and anions (i.e. L^- and R^+, T^- and R^+ for leading and terminating buffer).

In single capillary ITP-CZE a hydrodynamic pressure is applied during the focusing and ITP step to keep the front boundary of the sample zone (Fig. 1, B1) on a fixed position in the capillary. The hydrodynamic flow velocity counter balances the velocity of the leading ions so that the total velocity of the leading ions is zero. In the focusing step the terminating boundary of the sample zone (B2) migrates towards B1 resulting in a concentration of the analytes until the ITP state is reached. Under isotachophoretic conditions the velocities of all anions are the same. This distinguishes the focusing step from the ITP step.

The molar mass flow of a neutral reagent in the ITP step (J in mol/s) is determined by the reagent velocity, the cross sectional area of the capillary and the reagent concentration and is given by

$$J = v \pi r^2 c \qquad (1)$$

where v is the velocity of the neutral reagent under ITP conditions with a counterbalancing pressure, c is the reagent concentration and r is the capillary radius.

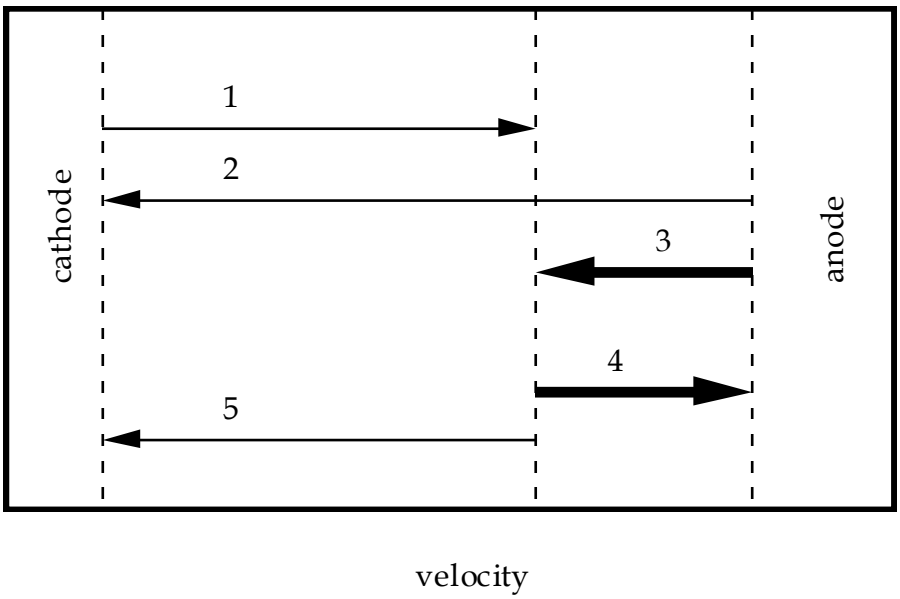

Fig. 3. Velocities during electrophoresis (1-3) and during electrophoresis under ITP conditions (4, 5). The vectors represent the electrophoretic velocity of the leading ions (1), the velocity of the electroosmotic flow (2), the net velocity of the leading ion (3) which is the sum of (1) and (2), the velocity of the counterbalancing hydrodynamic flow (4) and the velocity of the neutrals in presence of the counterbalancing hydrodynamic flow during the ITP step (5). For further explanation see Theory.

When the velocity of the leading ions is counterbalanced by a pressure induced flow, the electrophoretic velocity of the leading ions will be zero. Fig. 3 gives a schematic vector representation of the velocities during electrophoresis. Under ITP conditions the velocity of the neutrals is determined by the hydrodynamic and electroosmotic velocity. During electrophoresis a leading anion with an electrophoretic velocity (vector 1) will migrate to the cathode with a total velocity (vector 3) due to a high electroosmotic velocity (vector 2). Neutrals are carried with the electroosmotic flow and have a velocity (vector 2). When a counterbalancing pressure is applied (vector 4), the velocity of the anion (vector 3) is reduced to zero. Under these conditions

the velocity of the neutrals (vector 5) is also reduced. The velocity of neutrals under conditions with a counterbalancing pressure (vector 5) is the same as the electrophoretic velocity of the leading anions without a counterbalancing pressure (vector 1), in the opposite direction.

The velocity of the neutrals is then given by [13]

$$v = -v_{el,L} \qquad (2)$$

where $v_{el,L}$ is the electrophoretic velocity of the leading ions under ITP conditions without a counterbalancing pressure.

The supply of reagent can be manipulated by the electric field strength. Using $v_{el,L}=\overline{m}_L E_L$, the reagent molar mass flow is given by

$$J = \overline{m}_L E_L \pi r^2 c \qquad (3)$$

where $\overline{m}_L$ is the effective electrophoretic mobility of the leading ions and E_L is the electrical field strength in the leading buffer zone. Analogous to (3) the molar mass flow in the terminator zone is given by $J = \overline{m}_T E_T \pi r^2 c$. In the isotachophoretic steady state the electrical field strength in the leading buffer zone (E_L) is by definition lower than in the terminating buffer zone (E_T). In ITP it holds that $E_T\overline{m}_T=E_L\overline{m}_L$ which means that the molar mass flow of the neutral reagent in the terminator zone is the same as in the leading buffer zone. In a similar way it can be shown that in ITP the molar mass flow in the sample zones is the same as in the leading buffer zone.

The capillary reaction cell is not only restricted to neutrals. Charged reagents can be used as long as the focusing and ITP process are not disturbed. In case of anionic separations cationic reagents or anionic reagents with a low electrophoretic mobility can be used as well. Ampholytic reagents (enzymes, antibodies) can be used at a pH near the isoelectric point where the net charge is zero. For on-capillary NDA derivatization of amino acids cyanide is used which has a small anionic charge at the working pH (pK_a cyanide is 9.5). When a counter ion is used as a reagent the velocity and concentration in the leading and terminating zone can be calculated using the well known moving boundary equation.

Results and discussion

Several aspects of the on-capillary reaction cell are investigated. The linearity and reproducibility of the method is investigated for the selective derivatization of GSH with NDA at nanomolar analyte concentration levels. Supplying the reagent immediately after analyte injection is compared with supplying the reagent from the leading buffer vial after the focusing step, only during the ITP step. A less selective and more widely applicable derivatization procedure of amino acids with NDA in conjunction with CN is investigated.

The loadability and linearity over a large concentration range is investigated for the OPA/ME derivatization in ITP-CZE of some amino acids. Finally, the linearity and efficiency of a rapid on-capillary derivatization of amino acids in CZE without ITP step is investigated.

On-capillary isotachophoretic derivatization with NDA

In Fig. 4 the electropherograms are shown of the on-capillary reaction of GSH with NDA at nanomolar concentration level. System I is used for ITP-CZE (Experimental). The capillary is filled for 13.5% with leading buffer containing NDA, followed by a 27% injection of terminator buffer containing GSH.

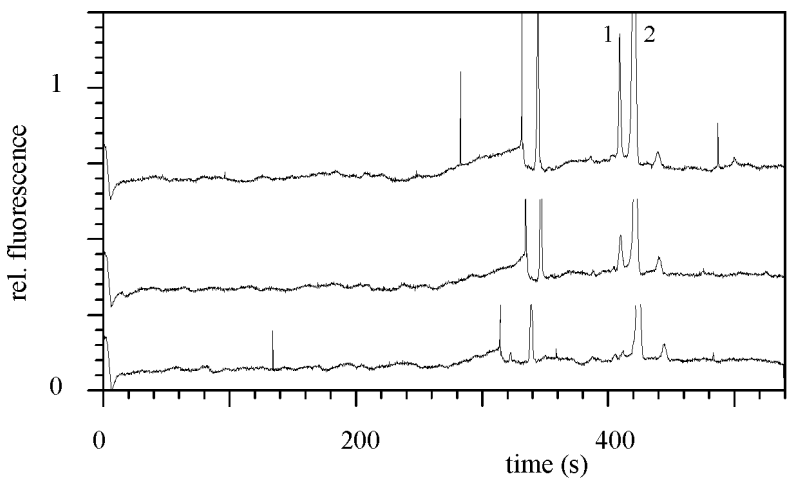

Fig. 4. On-capillary NDA derivatization and ITP-CZE of 3.0 (A) and 1.0 (B) nmol/l GSH (1) and the blank (C). Peak (2) is the internal standard fluorescein. Other peaks are system peaks.

The focusing step took place at a voltage of -10 kV, in the CZE step 25 kV is used. The

electrical field strength in the leading buffer zone under ITP conditions is -12 kV/m (for calculation see [13], conductivity ratio leading and terminating buffer is 0.39, fractional leading zone length 0.73). When an effective electrophoretic mobility of acetate of -42 10^{-9} $m^2V^{-1}s^{-1}$ is assumed, the velocity of the neutral NDA is 0.5 mm/s (eqn. 2). The reagent molar mass flow is 3,92 10^{-13} mol/s under these conditions (eqn. 3, c=0.1 mol/m^3, v=0.5 mm/s). The time for the NDA zone to leave the capillary is 372 s.

The linearity of the reaction of NDA with GSH is investigated at concentrations just above the detection limit from 1 to 11 nmol/l (Table I). The correlation is considerably improved by using fluorescein as internal standard. The relative standard deviation in CZE migration times of the ITP-CZE derivatization procedure is 1.4% (n = 5).

Table 7. Unweighted linear regression data of the on-capillary derivatization in ITP-CZE of GSH with NDA in the range 1 - 11 nmol/l. Six calibration points are used with concentration intervals of 2 nmol/l. Analyte injection volumes of 1.25 µl are used corresponding to 27% of the capillary volume. The intercept a and the slope b are given with the standard deviation. The correlation coefficient is r.

	a	SD	b	SD	r
height	248	152	151	22	0.960
height ratio	0.18	0.10	0.20	0.015	0.989
area ratio	-0.022	0.084	0.17	0.012	0.990

When in the ITP-CZE procedure, the capillary is filled with leading buffer containing the neutral reagent, the derivatization starts immediately after injection of the analyte. For the considered derivatization reaction this is convenient because it reduces the total analysis time. However, in cases where precise control of the reaction parameters are needed, the starting time of the reaction should be better defined. Therefore, the possibility of performing a derivatization reaction under ITP conditions is demonstrated in Fig. 5.

The same ITP-CZE buffers are used as in Fig. 4 except that the capillary is filled with leading buffer without NDA reagent. The underivatised GSH is focused for 10 minutes and then the leading buffer vial is replaced for a leading buffer vial containing the reagent. The GSH is

kept isotachophoretically at a fixed position in the capillary and the velocity of the neutral NDA reagent is 1.0 mm/s at an ITP voltage of -20 kV (E_L=-24 kV/m). After 10 minutes of derivatization under ITP conditions the CZE is started. The remaining NDA reagent migrates with the velocity of the electroosmotic flow which is seen as an increase of the baseline until t=400s. At 750s the derivative of GSH appears.

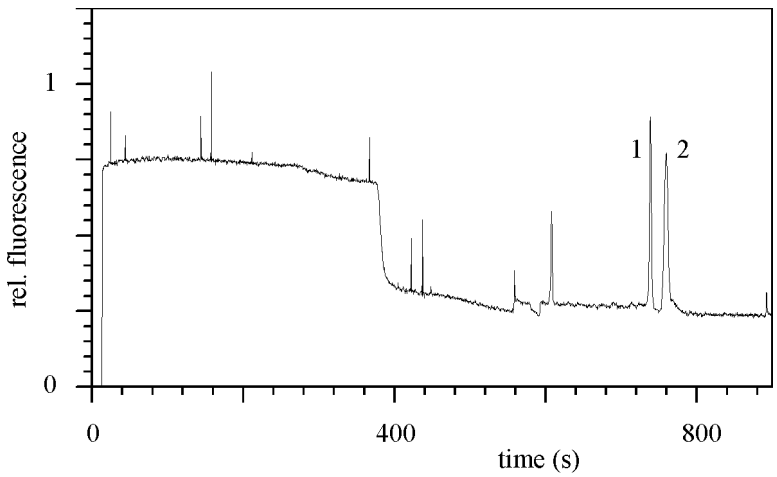

Fig. 5. ITP-CZE of 5 nmol/l GSH (1) with NDA reagent in the leading buffer vial. Derivatization of GSH occurred after focusing during the ITP step. The remaining NDA reagent caused an increased background in the CZE step. Peak (2) is fluorescein.

This example illustrates the flexibility of the on-capillary reaction cell. The analyte zones are kept isotachophoretically between the leading and terminating buffer. Using a hydrodynamic counter flow the position of the analyte zones along the capillary is fixed. By switching buffer vials cationic or neutral reagents can be supplied, as long as the ITP conditions are not disturbed the analyte zones remain concentrated. The reaction speed can be increased with the reagent molar mass flow. This can be done by choosing a leading ion with a high electrophoretic mobility, by increasing the electrical field strength during ITP or by using higher reagent concentrations (eqn. 3).

On-capillary isotachophoretic derivatization with NDA/CN

In the derivatization reaction of amines with NDA in presence of CN stable cyanobenz[f]isoindole (CBIs) adducts are formed. However, also several side products are formed, even when no amine containing analyte is present [18]. The on-capillary derivatization and ITP-CZE analysis of GSH, Glu and Asp is demonstrated in Fig. 6.

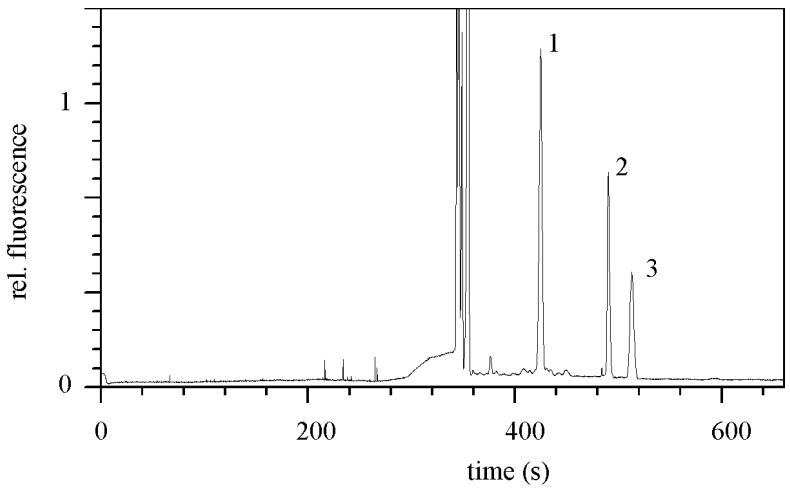

Fig. 6. On-capillary NDA/CN derivatization and ITP-CZE of 50 nmol/l GSH(1), Glu (2) and Asp (3). Other peaks are system peaks.

At low analyte concentrations the analysis is hindered by background peaks. Most of the background peaks appeared also in the blank electropherogram and are formed at the moment that KCN and NDA are mixed. Therefore, quantitative analysis with NDA/CN derivatization is difficult at low analyte concentration levels.

Table 8. Unweighted linear regression data of the on-capillary derivatization in ITP-CZE of Glu and Asp with OPA/ME in the range 50 - 2000 ng/ml. Six calibration points are used with concentrations 50, 100, 200, 500, 1000 and 2000 ng/ml. Analyte injection volumes of 0.53 µl are used corresponding to 9.6% of the capillary volume.

	a	SD	b	SD	r
Glu(height)	150	160	3.4	0.17	0.995
Asp(height)	-31	100	4.4	0.11	0.999
Glu(area)	137	1700	36	1.6	0.997
Asp(area)	-19	1500	54	1.6	0.998

On-capillary isotachophoretic derivatization with OPA/ME

The linearity in on-capillary ITP-CZE derivatization is investigated for the reaction of OPA/ME with Glu and Asp in the range of 50 - 2000 ng /ml. Although an internal standard is not used all correlation coefficients are higher than 0.99 (Table II).

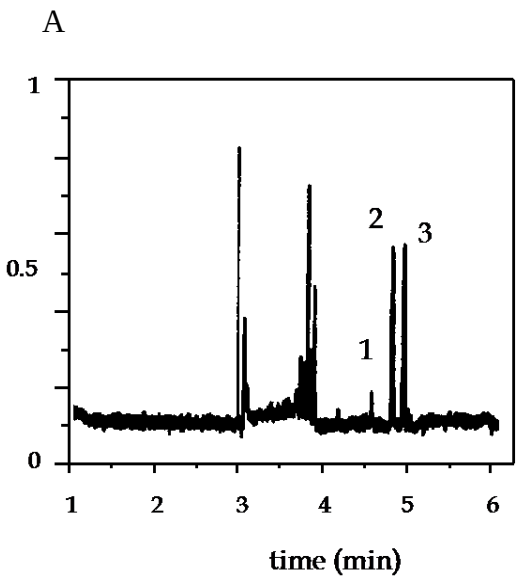

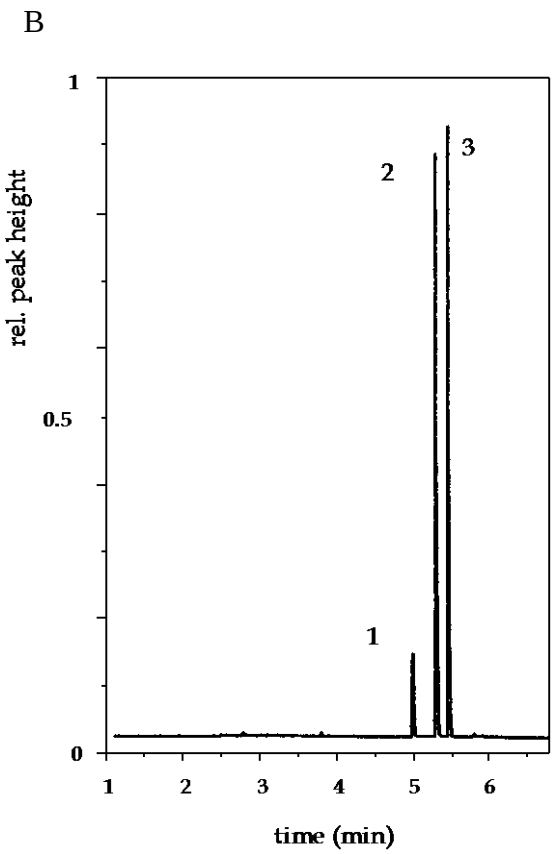

Fig. 7. Derivatization of 100 ng/ml GSH (1), Glu (2) and Asp (3) with OPA/ME with (B) on-capillary derivatization using ITP-CZE and with (A) CZE with conventional off-line derivatization. Injection volumes are (B) 1800 nl and (A) 13 nl. Improvement in S/N ratio in (A) is mainly due to the high loadability and the ITP concentration step.

The determination limit of Glu and Asp is 40 pg/ml based on 10 times the signal-to-noise ratio (Fig. 7B). The noise is calculated as one fifth of the peak-to-peak noise, measured at a high sensitivity. The determination limit of Glu and Asp in CZE with conventional pre-capillary derivatization is 7 ng/ml (Fig. 7A). In both cases a derivatization time of approximately 10 min is used. The improvement in determination limit by factor of 175 is mainly due to the concentrating ITP step. The analyte loadability in ITP-CZE is increased by a factor 135 in comparison with CZE. In CZE several system peaks resulting from the OPA reagent are visible

between 3 - 4 min (Fig. 7A). In ITP-CZE these side products migrate outside the ITP window and do not appear in the electropherogram (Fig. 7B).

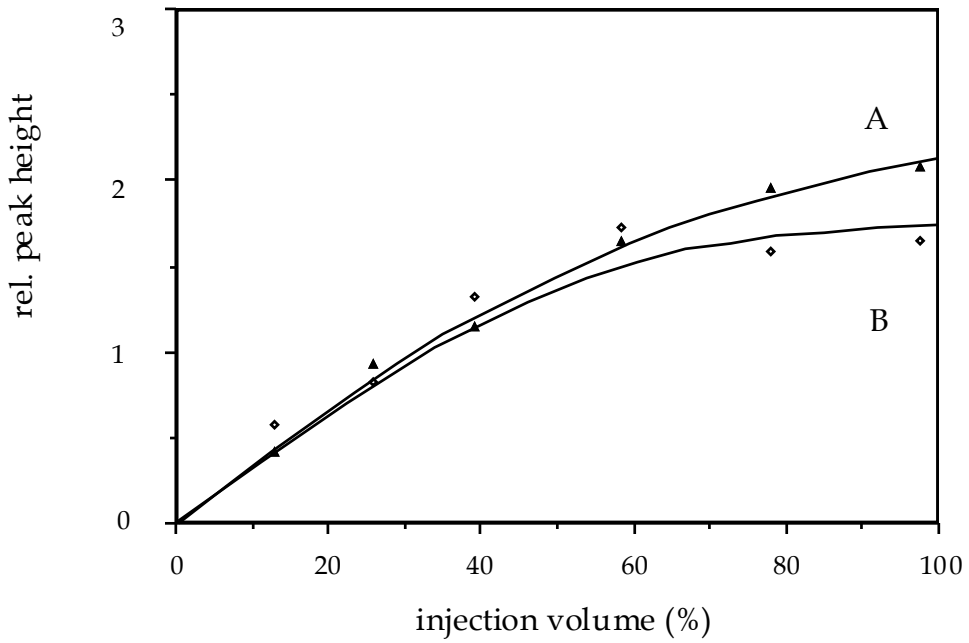

Fig. 8. Loadability in on-capillary derivatization of 100 ng/ml Glu (A) and Asp (B) with OPA/ME using ITP-CZE.

In Fig. 8 the effect of the loadability on the peak height is shown. The increase of peak height is linear with the loadability until the injection zone length is 60% of the total capillary length. At higher injection volumes, longer ITP and focusing times are used and degradation of the derivatives results in a decreased in signal. The zone width is the same at all injection volumes. Similar results have been obtained in ITP-CZE of these amino acids with pre-capillary derivatization [11].

At high sensitivity determinations precautions are taken to avoid memory effects. Because ITP-CZE takes place without waste of buffers, in principle all injected analytes maintain within the separation system until all buffers are refreshed. In conventional CZE this is not a problem because all analyte ions are migrating in the same direction from injection to detection. However, in ITP-CZE the voltage is reversed in the ITP step which makes it in principle possible for analyte ions to be concentrated several times within the ITP window resulting in an increase

of the background signal. In practice this means that the capillary is flushed between runs and that the buffers are refreshed several times a day.

On-capillary derivatization for CZE

In cases where the analyte concentrations are high enough the ITP step is not always necessary. In Fig. 9B and C an on-capillary OPA derivatization method for CZE without ITP step is demonstrated. Simply by adding the OPA reagent to the background electrolyte (system III, Experimental), a nanolitre (or picolitre, if smaller ID capillaries are used) reaction cell is created.

Table 9. Unweighted linear regression data of the on-capillary derivatization in CZE of amino acids with OPA/ME in the range 0.040 - 240 µg/ml. Seven calibration points are used with concentrations 0.040, 0.200, 0.800, 4.00, 20.0, 80.0 and 240 µg/ml. Electrokinetic injection is applied at 3kV for 3s, corresponding to 5-15 nl injection volume depending on the analyte mobility.

	a	SD	b	SD	r
Arg	200	150	0.149	0.002	0.9996
Lys	200	125	0.0048	0.0002	0.997
Trp	120	70	0.0746	0.001	0.9997
Phe	130	70	0.128	0.001	0.9999
Thr	150	100	0.121	0.001	0.9998
Ser	-170	250	0.145	0.003	0.9990
Glu	-250	320	0.039	0.002	0.997
Asp	-160	220	0.030	0.001	0.997

This is demonstrated in Fig. 9B. A mixture of underivatized amino acids is electrokinetically injected and the CZE is started within 20 seconds. Plate numbers in this on-capillary derivatization procedure (Fig. 9B) are varying from 1.5 10^5 to 2.5 10^5. This is approximately 15% lower than in CZE with conventional off-line derivatization (Fig. 9A). This indicates that the OPA derivatization takes place before the electrophoresis is started. Otherwise zone broadening would occur because of small differences in electrophoretic mobility of the amino acids

and the OPA derivatives of the amino acids.

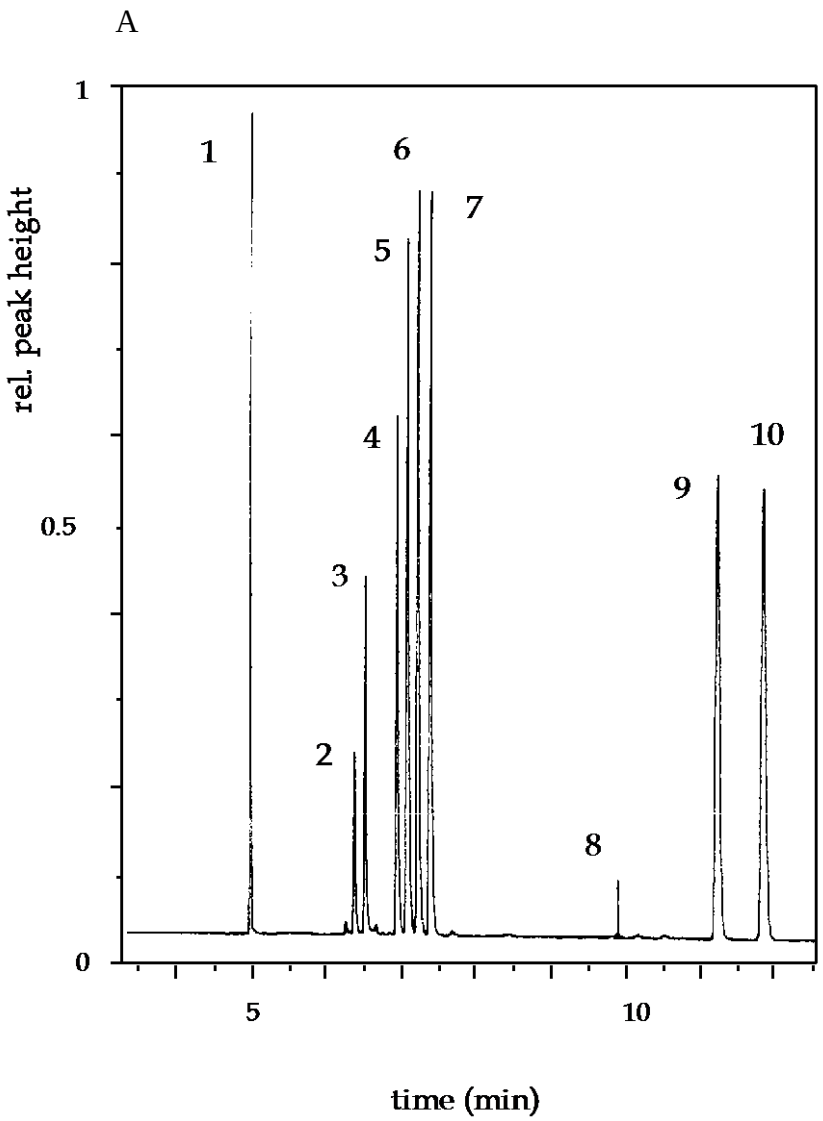

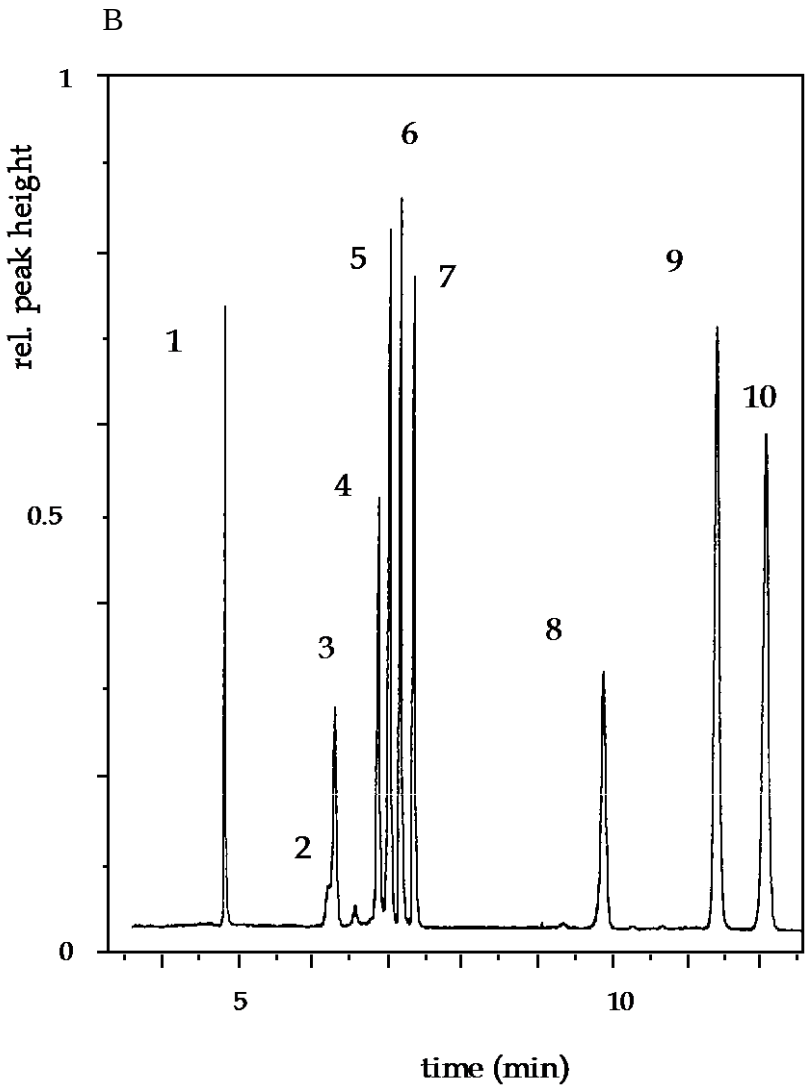
B
1
0.5
0
rel. peak height
1
2
3
4
5
6
7
8
9
10
5
10
time (min)

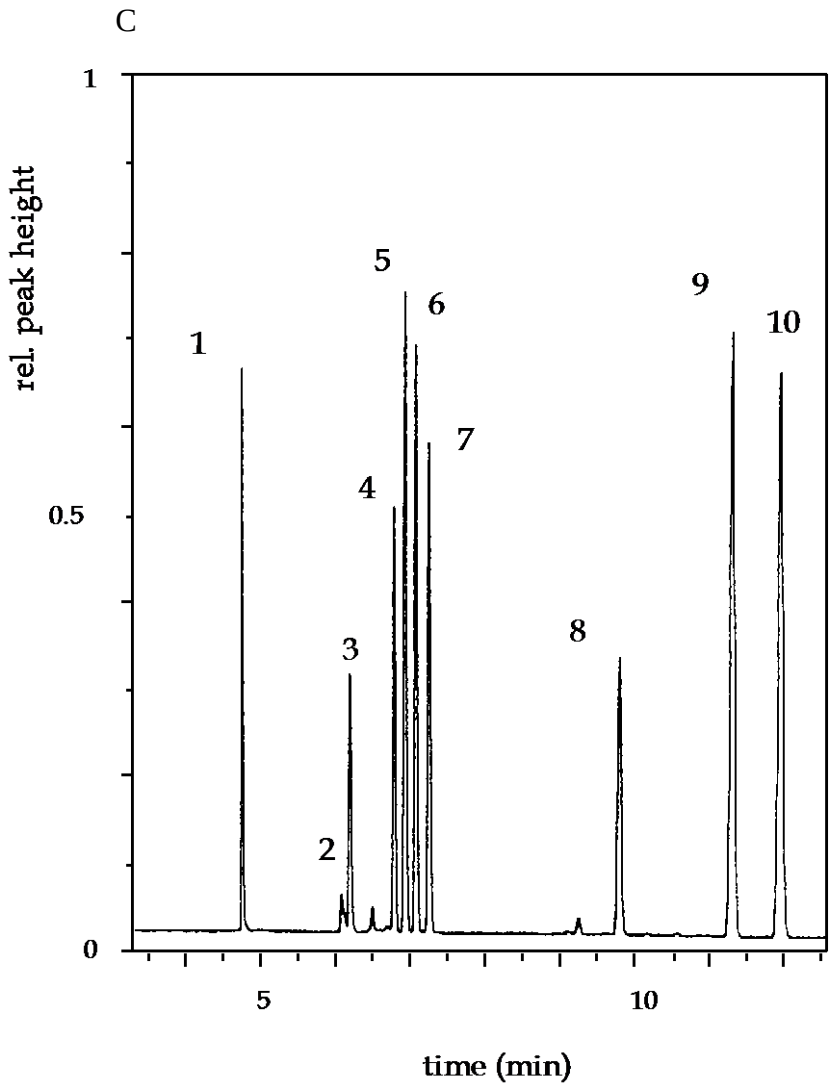

Fig. 9. On-capillary derivatization using CZE without ITP step. Separation of Arg (1), Lys (2, 3), Trp (4), Phe (5), Thr (6), Ser (7), L-Dopa (8), Glu (9), Asp (10). (A) CZE after 10 min off-line derivatization compared with (B) on-capillary derivatization using CZE immediately started after injection or (C) started 10 min after electrokinetic injection. All concentrations are 5 µg/ml except Lys (50 µg/ml), Asp and Glu (12 µg/ml).

The reaction times are easily kept constant in automated CZE procedures and can be increased if necessary, without zone broadening. In Fig. 9C the time between injection and the

start of the CZE is 10 min. Plate numbers are the same as in Fig. 9B. The fluorescence background signal increased by a factor 2 after addition of 1 g/l OPA and 0.1 % (v/v) ME to the background electrolyte. The detection limit for Phe is 10 ng/ml based on a S/N ratio of 3. This is 5 ng/ml for CZE with conventional off-line derivatization of Phe under similar CZE conditions. When a ten times lower reagent concentration is used in the electrophoresis buffer the derivatization reaction still takes place and the increase of fluorescence background is less than 20% compared to buffer only. Fluorescent reaction products, including contaminants in the buffer, decompose in time. Therefore, the OPA reagent is mixed with the electrophoresis buffer a day before use.

The linearity of the on-capillary derivatization method for CZE is studied in the range of 0.040 - 240 µg/ml for 8 amino acids. All correlation coefficients are higher than 0.99 (Table III).

Conclusions

An on-capillary reaction cell is described for nanolitre volumes at nanomolar concentration levels. When reactions with expensive reagents are involved the costs are reduced with the reduction of the reaction cell volume. The applicability is demonstrated for on-capillary fluorescence derivatization reactions. Requirements for the isotachophoretic reaction cell are described, including the equations necessary to calculate the electrophoretic supply of a neutral reagent.

The described procedure combines the concentrating properties of ITP, the separation efficiency of CZE and the detection sensitivity of LIF. The method is automated and quantitative at nanomolar concentration level for the reaction of GSH with NDA. Depending on the concentration of analyte and the required determination limit a choice can be made for on-capillary OPA/ME derivatization with or without ITP step before CZE.

References

1. R.A. Wallingford and A.G. Ewing, Adv. Chromatogr., 29 (1989) 1
2. W.G. Kuhr, Anal. Chem., 62 (1990) 403R
3. W.G. Kuhr and C.A. Monnig, Anal. Chem., 64 (1992) 389R
4. M. Albin, P.D. Grossman and S.E. Moring, Anal. Chem., 65 (1993) A489
5. Y. Ohkura and H. Nohta, Adv. Chromatogr. 29 (1989) 221 - 258.
6. J.A.P. Meulendijk and W.J.M. Underberg, In *Detection oriented derivatization techniques in liquid*

chromatography, (Chromatographic science series, vol. 48), H. Lingeman and W.J.M. Underberg (Editors), Chpt. 7, Marcel Dekker, New York, 1990.
7. M. Albin, R. Weinberger, E. Sapp and S. Moring, Anal. Chem. 63 (1991) 417
8. R.J.H. Houben, H. Gielen and S. van der Wal, J. Chromatogr. 634 (1993) 317
9. L.Z. Avila and G.M. Whitesides, J. Org. Chem. 58 (1993) 5508
10. H.T Chang, E.S. Yeung, Anal. Chem., 65 (1993) 2947
11. N.J. Reinhoud, U.R. Tjaden and J. van der Greef, J. Chromatogr., 641 (1993) 155
12. N.J. Reinhoud, U.R. Tjaden and J. van der Greef, J. Chromatogr. A, 653 (1993) 303
13. N.J. Reinhoud, U.R. Tjaden and J. van der Greef, J. Chromatogr. A, 673 (1994) 239
14. L.A. Sternson, J.F. Stobaugh, J. Reid and P. deMontigny, J. Pharm. & Biomed. Analysis, 6 (1988) 657
15. R.F. Chen, C. Scott and E. Trepman, Biochimica et Biophysica Acta, 576 (1979) 440
16. K.J. Dave, J.F. Stobaugh, T.M. Rossi and C.M. Riley, J. Pharm. & Biomed. Analysis, 10 (1992) 965
17. M.A. Nussbaum, J.E. Przedwiecki, D.U. Staerk, S.M. Lunte and C.M. Riley, Anal. Chem. 64 (1992) 1259
18. P. Kwakman, Ph.D. Thesis, Free University, Amsterdam, 1991
19. T. Yoshimura, T. Kamataki and T. Miura, Anal. Biochem., 188 (1990) 132
20. R. Håkanson and A.L. Rönnberg, Anal. Biochem., 54 (1973) 353
21. R.P. Maickel and F.P. Miller, Anal. Chem., 38 (1966) 1937
22. V.H. Cohn and J.L. Lyle, Anal. Biochem., 14 (1966) 434
23. P.J. Hissin and R. Hilf, Anal. Biochem., 74 (1976) 214

4

Conclusions and Perspectives

Capillary electrophoretic separations are widely applied in analytical methods. The technique is capable of highly efficient separations which has been demonstrated for a wide variety of applications. The commercial availability of automated systems makes CE in principle suitable for routine analysis. Especially in quality control CZE is already applied on a routine basis.

The limited loadability and the small optical path length, resulting in a lack of sensitivity are restraining the applicability of the technique for trace analysis. Combining automated pretreatment and derivatisation methods with sensitive detection systems will make the potential of capillary electrophoretic separation methods more widely applicable.

An important conclusion in this thesis is that an ITP step prior to CZE improves the detection limits, but when dealing with complex biological matrices also a selectivity improvement is required. Therefore, future research will focus on CZE-compatible, concentrating and preferably desalting, sample pretreatment methods based on a separation mechanism different from electrophoresis. An example is a recently developed method that combines a liquid-liquid electro-extraction with single capillary ITP-CZE [1].

Another research topic will be the development of sensitive detection systems for CZE. In particular the combination of CZE with electrochemical detection is promising as this detection method is in principle not restricted by capillary dimensions. Other research will focus on improvements in laser induced fluorescence detection and mass spectrometry.

References

1. E. van der Vlis, M. Mazereeuw, U.R. Tjaden, H. Irth and J. van der Greef, J. Chromatogr. A, 687 (1994) 333-341

5

Summary

Capillary electrophoresis (CE) is characterised by highly efficient separations in presence of a high electric field. The use of narrow bore capillaries provides an efficient way of dissipating the Joule heat. CE can be performed in several modes depending on the buffer system that is used. Switching between different modes is easy. Adding a chiral selector to the buffer enables enantiomer separations, adding a soluble gel enables the separation of macromolecules based on molecular mass. The poor detection sensitivity is the limiting factor in the applicability of CE in analytical methods. In this thesis several approaches are described of improving the loadability and the determination limits in CE.

Bioanalysis of some anthracyclines in human plasma is described with picomolar determination limits (Chapter 1.2). These low determination limits are achieved by combining a concentrating sample pretreatment, a concentrating analyte injection procedure and sensitive and selective laser induced fluorescence detection. An optimisation strategy is described for CZE with indirect detection (Chapter 1.3).

The coupling of C(Z)E with MS is considered one of the most promising developments in CE. The applicability of CE-MS is restricted to the higher analyte concentration range due to a combination of limited loadability and detection sensitivity. Several approaches are considered for improvements of the detection sensitivity. A liquid junction coupling of CZE with MS using a CF-FAB interface is described (Chapter 2.1). Excessive zone broadening in CZE-MS with a liquid junction coupling occurs in the transfer capillary. The CZE capillary was overloaded to improve the detection limits for peptides. The use of an array detection system in the MS resulted in a factor 100 increase of sensitivity in the scanning mode. In the coaxial coupling of CZE with electrospray MS the loadability was improved by a factor of 200 by using an on-line capillary isotachophoretic analyte focusing before the CZE-MS (Chapter 2.2).

Improvements in detection sensitivity of more than a factor of 100 were obtained by the coupling of ITP with CZE (Chapter 3.1). The described method is automated, reproducible and takes place in a commercially available CZE system without any hardware modifications. A strategy is described for setting up an ITP-CZE method (Chapter 3.2). CZE with indirect detection is used for determination of the migration order of leading, terminating and analyte ions. This information is needed to optimise the ITP separation window. The hydrodynamic pressure that is needed in ITP-CZE changes with the length of the leading buffer zone. The current also changes with the leading zone length and the correlation of the current and the

counter pressure is described by a straight line (Chapter 3.3). This may be used for an automated feed-back system for control of the hydrodynamic counter pressure. The application of completely automated systems will enable the implementation of ITP-CZE in routine analyses.

An automated on-line reaction cell is described in Chapter 3.4. The method combines the concentrating properties of isotachophoresis, the separation efficiency of capillary zone electrophoresis and the detection sensitivity of laser-induced fluorescence detection. The applicability of the reaction cell is demonstrated for an automated derivatisation procedure of glutamic acid, aspartic acid and glutathion with ortho-phthaldialdehyde (OPA) and naphthalene-2,3-dicarboxaldehyde (NDA). Small sample volumes (nanolitres) at nanomolar concentration level, were concentrated and derivatised in capillary ITP. The derivatives were analysed by CZE with LIF detection. The entire procedure was automated and took place in the same capillary using single capillary ITP-CZE.

6

Samenvatting

Capillaire electroforese (CE) wordt gekenmerkt door zeer efficiënte scheidingen onder invloed van een hoge elektrische veldsterkte. Het gebruik van capillairen met geringe diameter maakt een efficiënte warmtedissipatie mogelijk. CE kan in verschillende vormen worden uitgevoerd, afhankelijk van de buffer die gebruikt wordt. Overschakelen tussen de verschillende vormen is makkelijk. Wanneer een chirale selector wordt toegevoegd aan de buffer kunnen chirale scheidingen worden uitgevoerd. Het toevoegen van een vloeibare gel maakt scheidingen mogelijk op grond van molecuulgrootte. Momenteel is de ongunstige detectiegrens een beperkende factor in de toepasbaarheid van CE in analytische methoden. In dit proefschrift worden verschillende mogelijkheden beschreven om belaadbaarheid en detectiegrenzen in CE te verbeteren.

Bioanalyse van enkele anthracyclines in humaan plasma met een detectiegrens op picomolair niveau, wordt beschreven in hoofdstuk 1.2. Kwantitatieve analyse op deze lage detectiegrens is mogelijk door combinatie van een concentrerende monstervoorbewerking, een concentrerende injectiemethode en gevoelige en selectieve laser-geïnduceerde fluorescentie (LIF) detectie. Een optimalisering voor CZE met indirecte detectie is beschreven in hoofdstuk 1.3.

De koppeling van CZE met MS wordt beschouwd als één van de meest veelbelovende ontwikkelingen in CE. De toepasbaarheid van CE-MS is beperkt tot hogere monsterconcentraties door beperkingen ten aanzien van belaadbaarheid en detectiegrens. Verschillende manieren voor verbetering van de detectiegrens worden beschreven. Een open vloeistofverbinding van CZE met CF-FAB-MS is beschreven in hoofdstuk 2.1. De piekverbreding in CZE-MS met een open vloeistofverbinding vindt hoofdzakelijk plaats in het transportcapillair. Het CZE capillair werd overbeladen om de detectiegrens voor peptiden te verbeteren. Een array detectiesysteem in MS leidt tot een factor 100 betere gevoeligheid in de scanmode. In de coaxiale koppeling van CZE met electrospray MS wordt de belaadbaarheid een factor 200 verbeterd door een isotachoforetische monsterconcentrering toe te passen (hoofdstuk 2.2).

De detectiegrens in CZE verbetert met meer dan een factor 100 door koppeling met ITP (hoofdstuk 3.1). De beschreven methode is geautomatiseerd, reproduceerbaar en kan toegepast worden met een commercieel verkrijgbaar CZE systeem zonder dat de apparatuur hiervoor gemodificeerd hoeft te worden. Een strategie is beschreven voor het opzetten van ITP-CZE methodes (hoofdstuk 3.2). CZE met indirecte detectie wordt gebruikt voor de bepaling van de migratie volgorde van leading, terminating en monsterionen. Deze informatie wordt

gebruikt om de ITP-scheiding te optimaliseren. De hydrodynamische druk die nodig is in ITP-CZE verandert met de lengte van de leading zone lengte. De elektrische stroomsterkte verandert ook met de lengte van de leading zone, en de relatie tussen de elektrische stroomsterkte en de tegendruk wordt beschreven door een rechte lijn (hoofdstuk 3.3). Dit gegeven kan gebruikt worden voor een terugkoppelsysteem voor de regeling van een hydrodynamische tegendruk. De toepassing van volledig geautomatiseerde systemen zal de toepasbaarheid van ITP-CZE in routineanalyse bevorderen.

Een geautomatiseerde derivatiseringsreactie cel is beschreven in hoofdstuk 3.4. De methode combineert de concentrerende eigenschappen van ITP, de scheidingsefficiëntie van CZE en de detectiegevoeligheid van LIF detectie. De toepasbaarheid van de reactiecel wordt gedemonstreerd voor een geautomatiseerde derivatiseringsprocedure voor glutaminezuur, asparaginezuur en glutation. De ITP-concentrering en derivatisering wordt uitgevoerd met kleine monstervolumes (nanoliters) en lage monsterconcentraties (nanomolair niveau). De reactieproducten worden geanalyseerd met CZE met LIF detectie. De gehele procedure is geautomatiseerd en vindt plaats in één capillair met ITP-CZE.

7

Curriculum vitae

Nicolaas Jan Reinhoud werd geboren op 17 juni 1963 in Woerden. In 1979 en 1981 werden respectievelijk het MAVO en HAVO diploma behaald aan de scholengemeenschap de Driestar te Gouda. Aansluitend werd de militaire dienstplicht vervuld. In 1987 werd met succes het HLO examen afgelegd aan het van ‘t Hoff Instituut te Rotterdam. De eindexamen scriptie betrof onderzoek verricht aan het Rudolf Magnus Instituut voor Farmacologie van de Rijksuniversiteit Utrecht naar receptoren van het neuropeptide des-enkefaline-γ-endorfine (DEγE). In juni van dat jaar trad hij als analist in dienst bij de Sectie Analytische Chemie van het Centrum voor Bio-Farmaceutische Wetenschappen te Leiden. Het onderzoek betrof het ontwikkelen van een fluorescentiederivatisering in de bioanalyse van DEγE. Op 1 september 1989 werd begonnen aan een promotieonderzoek op het gebied van capillaire electroforese onder begeleiding van dr. U.R. Tjaden (co-promotor) en prof. dr. J. van der Greef (promotor). Sinds 1 december 1993 is hij werkzaam bij Antec Leyden B.V. als hoofd van de afdeling Research and Development.

8

Nawoord

Aan de totstandkoming van dit proefschrift hebben velen een bijdrage geleverd waarvoor ik eenieder zeer erkentelijk ben. Op deze plaats wil ik enkele mensen met name noemen. In het bijzonder alle medewerkers van de sectie Analytische Chemie van de BFW (LACDR) voor de goede sfeer en de vele diepgaande gesprekken. Met name Cas van den Beld voor de vele verhelderende en stimulerende discussies, met de juiste 'stimmung' wist hij het werken in de kernkamer te veraangenamen. Désirée Stegehuis voor de vele gesprekken over alles wat met promoveren te maken heeft, en voor haar doorzettingsvermogen bij het introduceren van ITP-CZE. Bea Reeuwijk voor al haar hulp, beginnende bij het inleidend programma. Arjen Tinke, die met enthousiasme en groot doorzettingsvermogen de ITP-CZE electrospray MS aan de praat wist te krijgen en te houden. Elwin Verheij en Marja Lamoree voor de prettige samenwerking op gebied van CZE-MS. De mensen bij de centraal electronische afdeling (CEA), met name Ben Ouwehand, hebben mij regelmatig op weg geholpen met diverse hard- en software problemen.

De medewerkers van de afdeling Instrumentele Analyse (TNO, Zeist) ben ik zeer erkentelijk voor de goede werksfeer en samenwerking gedurende de CZE-CFFAB-MS experimenten. Met name Laurens Gramberg voor zijn onverstoorbare geduld en voor het bedienen en optimaliseren van de MAT 90.

Wat begon met een eenvoudig idee (Rineke) kon uiteindelijk worden gerealiseerd in een sfeer van vertrouwen waarin eigen creativiteit volop de ruimte kreeg. Onmisbaar waren daarbij de vele, niet alleen wetenschappelijke, discussies met mijn dagelijkse begeleider en het onuitputtelijk enthousiasme van de begeleiding in het algemeen.

Met haar luisterend oor en voortdurende interesse heeft Greet een belangrijke bijdrage geleverd aan de totstandkoming van dit proefschrift.

9

List of publications

C.M.B. van den Beld, U.R. Tjaden, N.J. Reinhoud, D.S. Stegehuis and J. van der Greef
Determination of some β-endorphin fragments in human plasma by high-performance liquid chromatography with laser-induced fluorescence detection
J. Controlled Release, 13 (1990) 129-139

N.J. Reinhoud, W.M.A. Niessen, U.R. Tjaden, L.G. Gramberg, E.R. Verheij, J. van der Greef
Performance of a liquid - junction interface for capillary electrophoresis mass spectrometry using continuous-flow fast atom-bombardment
Rap. Commun. Mass Spectrom., 3 (1989) 348

N.J. Reinhoud, E. Schröder, U.R. Tjaden, W.M.A. Niessen, M.C. ten Noever de Brauw, J. van der Greef
Static and scanning array detection in capillary electrophoresis-mass spectrometry
J. Chromatogr., 516 (1990) 147

N.J. Reinhoud, U.R. Tjaden, H. Irth and J. van der Greef
Bioanalysis of some anthracyclines in human plasma by capillary electrophoresis with laser-induced fluorescence detection
J. Chromatogr., 574 (1992) 327

A.P. Tinke, N.J. Reinhoud, W.M.A. Niessen, U.R. Tjaden and J. van der Greef
On-line isotachophoretic analyte focusing for improvement of detection limits in capillary electrophoresis electrospray mass spectrometry
Rap. Commun. Mass Spectrom., 6 (1992) 560

N.J. Reinhoud, A.P. Tinke, U.R. Tjaden, W.M.A. Niessen and J. van der Greef
Capillary isotachophoretic analyte focusing for capillary electrophoresis with mass spectrometric detection using electrospray ionisation
J. Chromatogr., 627 (1992) 263

N.J. Reinhoud, U.R. Tjaden and J. van der Greef
Automated isotachophoretic analyte focusing for capillary zone electrophoresis in a single capillary using hydrodynamic back pressure programming
J. Chromatogr., 641 (1993) 155

N.J. Reinhoud, U.R. Tjaden and J. van der Greef
Strategy for setting up single capillary isotachophoresis - zone electrophoresis
J. Chromatogr. 653 (1993) 303

N.J. Reinhoud, U.R. Tjaden and J. van der Greef
Correlation between zone velocity and current in automated single capillary isotachophoresis - zone electrophoresis
J. Chromatogr. A, 673 (1994) 239

N.J. Reinhoud, U.R. Tjaden and J. van der Greef
Automated on-capillary isotachophoretic reaction cell for fluorescence derivatization of small sample volumes at low concentrations followed by capillary zone electrophoresis
J. Chromatogr. A, 673 (1994) 255

M.H. Lamoree, N.J. Reinhoud, U.R. Tjaden, W.M.A. Niessen and J. van der Greef
On-capillary isotachophoresis for loadability enhancement in capillary zone electrophoresis - mass spectrometry of β-agonists
Biol. Mass Spectrom., 23 (1994) 339